Methods of rapid bruise assessment and the formulation of robust bruise indices for potatoes

Stephen David Evans

PhD. Thesis

University of Edinburgh

1995

I declare that I am the author of this thesis and that the work contained herein was carried out by myself unless otherwise stated.

Stephen David Evans

24 February 1995

Since the measuring device has been constructed by the observer . . . we have to remember that what we observe is not nature itself but nature exposed to our method of questioning.

Physics and Philosophy (1958)
Werner Karl Heisenberg 1901-1976

Contents

Abstract

When potato tubers are subjected to impacts, the sub-surface tissue may become discoloured as damaged cells produce the blue-black pigment melanin. Bruising caused during harvesting and handling can lead to downgrading of potatoes for the processing industry and quality retail trade. The two aims of this thesis were to reduce the time to detect bruising, and to develop a non-subjective method for the quantification of bruising.

Reflectance spectrophotometry was investigated as a rapid, non-subjective and non-invasive way of detecting bruising. Wavelengths from ultraviolet to near infrared were selected by discriminant analysis to separate unbruised and bruised tubers. Neural nets were trained with these wavelengths to identify bruised tubers in a sample of unbruised and bruised tubers. The detection of bruising gave inconsistent results in unpeeled tubers, but proved to be reliable in peeled tubers.

The rate of bruise development at air pressures up to 10 bar was measured by reflectance spectrophotometry and by a visual rating. The production of dopachrome, an orange pre-cursor pigment of melanin, was used as an early indication of bruising. Dopachrome is visible to the human eye and the time for bruise detection can be reduced to approximately 3 hours when compressed air is used.

Infrared and microwave thermography were used to measure possible rises in bruised tissue temperature. Thermography was used in conjunction with scanning laser Doppler imaging to detect changes in the biological zero of bruised tissue. No significant differences could be detected between unbruised and bruised tubers using these techniques.

Reflectance spectrophotometry was also used in combination with a colour digital camera to automatically measure bruise area in peeled tubers. While the camera alone could measure bruise area with precision, constant adjustments were needed. Reflectance spectrophotometry was faster but less precise than the camera for measuring bruise area.

A new bruise index was formulated by taking measurements of the volume of a tuber removed per peeler stroke for the variety Record, and using the data to model the percentage volume lost for any variety. By counting the number of peeler strokes to remove a bruise an estimate of the tuber volume lost could be derived. This method can accommodate any type and size of bruise and results in an index that can be easily interpreted.

Acknowledgements

I would like to thank everyone at the Scottish Centre of Agricultural Engineering for their help in this project. I particularly appreciate the assistance from my supervisor Eur. Ing. Douglas McRae, from Calum Dewar, John Fleming, Bill Lamond, Mary Lightbody, Harry Melrose, Fraser Milne, Andrew Muir, David Ross and the director of the SCAE Prof. Brian Witney.

I am indebted to Dr. Neil Abbot from the Institute of Biomedical and Life Sciences, University of Glasgow for his help and advice and providing the materials for thermography and laser Doppler imagery. I would also like to thank Dr. Joan Cotterel for providing the opportunity to conduct biochemical experiments at the Scottish Agricultural College, Edinburgh.

I would like to express my gratitude to the Potato Marketing Board who provided the studentship and to Dr. Mike Storey, Dr. Mary Miller and Karla Michalski for their interest in this project.

I am also grateful to my faithful research assistant, Moss the Border Collie, who always enjoyed 'going for more potatoes'. Lastly, I would like to give a special thankyou to my wife Carol, for her patience and support. This thesis is dedicated to her.

Chapter 1

Introduction and aims

Bruising is the production of melanin, a blue-black pigment, in the sub-surface tissue of a potato tuber. The internal discolouration is initiated when a potato tuber receives an impact that leads to disruption of cell membranes. The damaged membranes then allow the enzymatic oxidation of phenols which forms melanin. Impact damage can occur when tubers collide with soil clods, stones, other tubers, or parts of machinery during mechanical handling, or when they are subjected to careless manual treatment. Bruising is a particular problem where potato crop production is highly mechanised from harvesting to retail or processing outlets.

The blue-black discolouration, which is often only visible when the tubers are peeled, is considered an undesirable quality and producers and processors are under constant pressure from consumers to keep bruising levels to a minimum. In the UK, bruising is thought to be one of the biggest problems in the potato industry with an annual loss of many millions of pounds (Potato Producers Association 1994). There are several reasons for the financial loss.

- The price obtained for a potato crop is greatly influenced by the extent of mechanical damage. However, impacts can never be eliminated in potato harvesting because potatoes have to be physically separated from the soil. The force needed to separate tubers from soil include a number of factors, such as the soil type and the amount of soil moisture (Timm 1989). Therefore, a compromise has to be made between the force needed to separate tubers from the soil and the need to reduce bruising levels. Harvester settings can be adjusted to vary the force of impacts, but due to the delay between an impact occurring and the development of a bruise, typically 24 hours under ambient conditions (Li 1985) harvester settings can never be truly optimised. The longer the time taken to detect bruising, the greater the proportion of the crop that can be harvested with potentially high bruising levels. When operating a two-row harvester, every hour that elapses before bruising is discovered can lead to a loss of over £700 (personal communication Eur. Ing. D.C. McRae).

- Unfortunately there is no simple correlation between a tuber receiving an impact and the development of a bruise. Different varieties, and individual tubers within a variety, differ in their susceptibility to bruising. There may be many genetic and environmental factors involved in bruising susceptibility, but the reasons for this

are not yet clear. The unpredictability of a tuber developing a bruise after impact complicates the optimisation of harvesting machinery.

- The discolouration of bruised tissue is often only visible when a tuber is peeled so tubers can pass unnoticed through quality control. Bruised tubers reaching the processor and consumer can then result in potato wastage or in a loss of confidence in the producer.

- Quality assessment can be time consuming and costly because of the need to peel or slice a tuber first to detect bruising.

- There are no national or international standards, or indices, for quantifying bruising. If the assessment of the amount of bruising in a crop is inaccurate, this could result in unnecessary financial loss. Consistent bruise indices need to be evolved if different grades of potatoes are to be sold to specific markets, if results are to be compared between producers and if potato breeders world-wide are to properly select for varietal characteristics that may be involved in bruise resistance.

- In storage, bruised tubers can encourage the infection of soft rot bacteria (*Erwinia* spp.) that can then spread to healthy tubers (Perombelon and Kelman 1980). Bruised tubers also lose water at a faster rate in storage than healthy tubers, becoming flaccid and unmarketable (Hughes 1980a).

The potato industry has invested a considerable amount of money on research in an attempt to minimise the financial losses associated with bruising, but three main areas of enquiry remain largely unanswered.

1. Primarily there is a need to understand the factors that affect the susceptibility of a tuber to bruising. If tuber susceptibility could be manipulated by genetic or environmental means before harvesting, this would reduce the need to monitor harvester settings.

2. Bruise development time needs to be reduced to a minimum. At present, the shortest time interval before a bruise can be detected is about five hours when compressed oxygen is used to speed the process. However, compressed oxygen is potentially dangerous so compressed air has been suggested as an alternative. Research needs to establish the optimum atmospheric conditions for bruise development.

3. At present there are no national or international standards for quantifying bruising. An evaluation of the present methods needs to be given and proposals for an alternative method put forward.

The first of these, bruising susceptibility, is multi-factorial and it will probably be many years before its elements are fully determined. However, the reduction in bruise development time and the standardisation of bruise quantification are likely to be achievable and are the aims of this thesis. The following methods have been used in an attempt to achieve these aims.

- Evaluation of reflectance spectrophotometry as a non-invasive way of detecting changes in sub-surface tissue colour associated with bruising (Chapters 6, 7, 8 and 9). If bruising could be detected in unpeeled tubers this would reduce the need to peel a tuber before bruise assessment.

- Evaluation of reflectance spectrophotometry as a non-invasive method for detecting pre-cursor pigments to melanin (Chapters 12 and 13). If pre-cursor pigments can be detected then this may reduce the time for bruise detection.

- Evaluation of scanning laser Doppler imaging and microwave thermography as a non-invasive method for detecting and quantifying possible rises in tuber temperature associated with a rise in respiration in bruised tissue (Chapter 10).

- Evaluation of compressed air as a method for accelerating bruise development (Chapter 14). Different pressure and temperature combinations need to be investigated to determine if this method can give the optimum bruise development.

- Evaluation of reflectance spectrophotometry and image analysis techniques for measuring the severity of bruising (Chapter 11). If this method is successful, then assessment of bruising could be objective, non-invasive and rapid.

- Evaluation of a mathematical model to predict the percentage volume removed per peeler stroke (Chapter 15). By counting the number of peeler strokes to remove a bruise, a stepless index could be derived and directly related to possible losses due to bruising.

Before discussing these aims in greater detail, it is first necessary to understand the anatomy of the potato tuber, the cascade of events that occur in damaged tuber tissue upon impact, and the factors affecting the susceptibility of a tuber to bruising.

Chapter 2

Anatomy of the potato tuber and overview of the bruising process

The potato tuber is a modified stem possessing leaves and axillary buds that are much reduced. Potato tubers originate from stolons that are lateral shoots borne generally at the basal node of the plant. Stolons have elongated internodes, scale leaves and a recurved apical portion usually referred to as a hook. A radially expanded stolon apex is the bud end, while the site of attachment to the stolon is the heel or stem end. At the bud end are 'eyes' which are stem nodes and consist of a main axillary bud and a subtending scale leaf. The buds in the eyes have the same anatomy as a normal shoot apex; they have leaf primordia that are simple in structure, with a few stomata on the surface of an epidermal layer (Cutter 1977).

The initiation of tubers is a shift from elongation to radial growth in the stolon as a result of a stimulus produced in the leaves in response to short days (Burton 1989). The structure of mature tubers reflects their stem origin but is influenced dramatically by extensive radial growth. The epidermis of the stolon forms the periderm, a protective layer to prevent rapid water loss and to impede soil pathogens. The periderm consists of phellem (cork) and phellogen (cork cambium). The extent of phellogen activity determines the thickness of phellem and is dependent on cultivar and environment. In some cultivars there may be pigment deposition in the phellem cells (Burton 1989). Lenticels within the phellem cells allow gas exchange between the external environment and the tuber and are initiated by parallel divisions in cortical cells subtending the substomatal cavity (Artschwager 1924, Cutter 1977). The cortex is a narrow area of parenchymatous tissue separating the periderm from the vascular ring (Fig. 1.1). The cortex contributes considerably to the volume of stolon tissue, but it increases in size rather than cell number during tuber expansion. In some cultivars there may be pigments in the outer cortical cells (Reeve *et al.* 1969a).

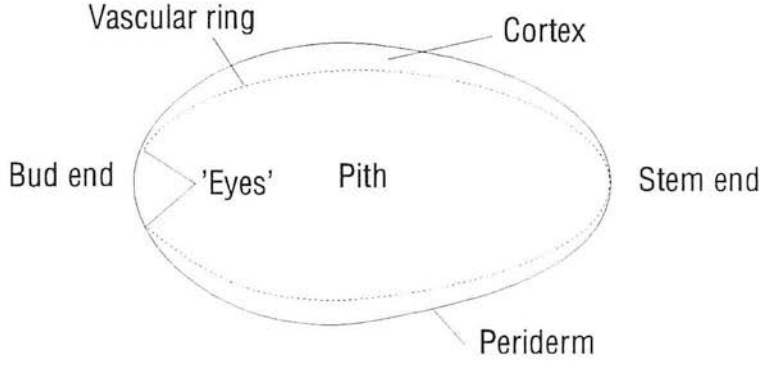

Fig. 1.1 Anatomy of a potato tuber.

The vascular tissue is composed of phloem and xylem strands that are involved in the transport of metabolites within the tuber. There is internal and external phloem that is developed from procambial tissue and constitutes a larger proportion of the tissue than xylem. There is more xylem at the stem end reflecting that developmentally the stem end is the oldest part of the tuber (Reeve *et al.* 1969a).

The pith is derived from ground meristem and contributes to the early enlargement of the tuber. The pith radiates outward and is continuous with the axillary buds in the eyes. In more mature tubers, the pith cells are polyhedral and these form the 'water core' of the tuber (Reeve *et al.* 1969b).

In the context of this thesis, the portion of tuber anatomy of most importance is the area immediately below the periderm in the most superficial cortical tissue. It is here that bruising develops and from here that the modifications to surrounding tissues are initiated (Pratt 1980).

2.1 Overview of the bruising process

Bruising can appear in many different forms depending on whether the cell walls (internal crushing or shattering) or the cell contents have been damaged. Internal crushing refers to zones of damaged tissue a few millimetres under the skin, which may discolour and rapidly dry out to give hollow areas similar to those seen in blackspot. Such tubers may appear unblemished as the skins are not always damaged (Hughes 1981). Internal shattering is caused by impacts of short durations and high loading velocities (Noble 1985) and can appear as cracks or striations in the sub surface tissue that may penetrate deeply into the tuber. Shatter bruising does not damage the skin (Thornton 1979).

Blackspot is often the result of impacts with low loading velocities which cause the disruption of the cell contents without cell damage (Hughes 1975). In blackspot, the skin is unbroken, and the discolouration is not normally visible until affected tubers are peeled (Li 1985). The discolouration may have diffused edges (Noble 1985).

Pressure bruises occur only in storage where the weight of tubers causes tubers below to be crushed. This type of bruising is difficult to distinguish from blackspot, except when the external surface is flattened (Meyer *et al.* 1985).

Whatever the type of bruising, each is the consequence of complex biochemical changes beginning with cell membrane degradation and ending with the production of melanin. The following sections briefly summarise each stage of the bruising process.

2.1.1 Cell membrane degradation

The production of melanin, the dark pigment seen in bruised tissue, begins when the cell membranes are damaged as a result of a potato tuber receiving an impact. The cell membranes may be damaged directly on impact, or indirectly by activation of degradative enzymes such as patatin.

Patatin is a group of glycoproteins that account for approximately 40% of the soluble proteins in the potato tuber. Patatin is stored in the vacuole (Sommewald *et al.* 1989) and has enzymatic activities involved in the autolysis of damaged cell membranes (Racusen 1984). The enzyme activities are more specifically known as lipolytic acyl hydrolase (LAH).

It is thought that LAH is contained within the vacuole where it is inactive and is released upon mechanical damage to the membranes (Sommewald *et al.* 1989). Alternatively, it has been suggested that LAH is present as an inactive enzyme (Racusen 1984) which becomes activated when the cell membranes are stressed. Changes in cell membrane permeability could cause calcium to enter the cytosol where it then causes calmodulin to form a complex that results in LAH being activated (Lesham 1987). In either case, LAH activity degrades phospholipids from cell membranes to produce polyunsaturated fatty acids, mostly linoleic and linolenic acid, for use in the production of suberin and cytoxic waxes (Bostock *et al.* 1981). The fatty acids also provide a substrate for lipoxygenases (LOX). LOX activity then generates oxygen free radicals, ethylene, endogenous calcium ionophores, and jasmonic acid (Lesham 1987). The products of lipid peroxidation may then cause further membrane breakdown. The consequences of such cell membrane degradation are many but involve mainly the following.

- The release of electrolytes (ions) is among the indicators of membrane damage and the rate of leakage has been directly related to the disruption of the membranes (Fortunati and Bianchi 1990). The electrolyte release may enhance further cell degradation and increase the susceptibility to soft rotting by *Erwinia* spp. (Lewosz *et al.* 1985).

- The conversion of starch to sugars (Sowokinos *et al.* 1987). This effect has particular relevance to potato processors because of its influence on storage potential and chip frying colour (Pisarczyk 1982).

- The induction of melanin formation. Peroxisomes, cell organelles within the cytoplasm of the potato tuber cell, contain a large protein crystal incorporating o-

diphenol oxidase, the principle enzyme involved in the production of melanin. This enzyme is nuclear coded but is inactive until incorporated into the peroxisome. When the membranes around the peroxisome degrade, they allow the o-diphenol oxidase to react with phenols to produce melanin in the peroxisome (McIlroy 1976). O-diphenol oxidase has been shown to have maximum concentration in the peripheral 2 mm of the tuber and to decrease to a minimum 5 mm from the surface (Mulder 1949).

2.1.2 Biochemistry of melanin formation

The overall reaction in bruising can be divided into enzymatic and non-enzymatic reactions (Lerner and Fitzpatrick 1950). The first part of the reaction is enzymatic and involves o-diphenol oxidase catalysing the oxidation of tyrosine and chlorogenic acid to 3,4-dihydroxyphenylalanine (dopa) and then the oxidation of dopa to dopaquinone with atmospheric oxygen.

Through non-enzymatic reactions, dopaquinone forms the reddish-orange pigment, dopachrome with maximum light absorption at 305 and 475 nm (Muneta 1948). Non-enzymatic oxidation then rearranges dopachrome to form the purple pigment 5,6 dihydroxy-indole with maximum light absorption at 305 and 475 nm (Mason 1948). The 5,6 dihydroxy-indole then undergoes repeated condensation, polymerisation and interactions with proteins to give brown, and finally black melanin pigments. Bu'Lock and Harley-Mason (1951) suggested that extensive connections of long chains of molecules in melanin could account for light absorption over a wide range of wavelengths.

Melanin is relatively unreactive and is only soluble in strong alkalis (Thomas 1955). In vitro, melanin is bound to a protein by sulphydryl groups (Lerner 1950) making extraction difficult in its natural form (Nicolaus and Piattelli 1965). Thus, once formed, melanin cannot be metabolised further or broken down by the cell. Under the electron microscope, melanin is seen in bruised cortex tissue as round granules 0.5-1.5 μm in diameter on intracellular surfaces of the protoplasts and inner cell wall surfaces. Such granules are not seen in undamaged tissue (McIlroy 1976).

The extreme insolubility of melanin has made the determination of its final structure difficult. However, it is known that this structure can vary according to source, substrate and manner of preparation (Singleton 1972). In this respect, melanin resembles lignin, a substance that also seems to be of variable composition and is formed from phenolic precursors (Mason 1967).

2.1.3 Effects of bruising on cell structure

The production of melanin occurs in the cortex and is rarely deeper than the vascular ring (Pratt 1980). Scanning electron microscope pictures (Hartmans and Van Es 1974) have shown that in bruised tissue there is a greater degree of cell separation compared with tissue that has been damaged without the development of bruising. Bruised tissue shows differences in cell wall composition: hemicellulose and pectin content are higher than normal, but lignification is usually absent except when bruises are large (Reeve 1968).

When the periderm is wounded, suberin is produced. Suberin is composed of phenolic and aliphatic compounds and has an important role in wound healing, physically separating damaged from undamaged tissue (Dean and Kolattukudy 1977). Wound phellogen (a secondary skin) may also be formed at the site of a bruise, but there is some disagreement whether suberin and wound phellogen are produced as a result of bruising. Horne (1913) found no evidence of suberin formation in bruised tissue, but it is not clear if he was referring to blackspot or to the disorder known as black heart (Reeve 1968). Artshwager (1924) discovered wound phellogen (secondary skin) formation underlying the site of a bruise, whereas Boyd (1951) found cell wall suberisation but no wound periderm (secondary skin) associated with blackspot. Reeve (1968) observed the production of suberin in bruised tissue in cases where the original periderm had been broken and internal cells were crushed (shatter bruising). However, these were cases of splitting damage whereas in true bruising the epidermis remains unbroken.

2.1.4 Responses to bruising at the gene level

Ilker *et al.* (1977) showed that there is a prompt increase in messenger RNA (mRNA) and protein synthesis two hours after injury in damaged tissue. The most important mRNA produced is a proteinase inhibitor II messenger RNA (Pena-Cortes *et al.* 1988).

Proteinase inhibitor II is a small protein that is encoded by a small gene family of three to five copies per haploid genome (Sanchez-Serrano *et al.* 1987). It is thought that the production of proteinase inhibitor II reduces the nutritive value of the tissue to invading pests (Richardson 1977).

Wounding triggers the induction of proteinase inhibitor II genes in tissues far from the actual site of injury. The induction of genes that produce proteinase inhibitor II in non-damaged tissue is thought to be caused by a hormone synthesised or released

at the wound site, possibly abscissic acid (Pena-Cortes *et al.* 1989). The accumulation of proteinase inhibitor II causes other genes to produce enzymes or new compounds that are involved in repairing the cells, or protecting against further damage (Sanchez-Serrano *et al.* 1990).

In blackspot (Reeve 1968) as well as in ageing excised slices (Kahl 1974) of potato tuber, chlorogenic acid and other phenolics accumulate. Rickey *et al.* (1989) showed that the accumulation of phenolics in bruised tissue is induced by changes in enzyme activity and gene expression. Phenylalanine ammonia lyase (PAL) an enzyme required for the synthesis of phenolic compounds, showed a transient 200-fold increase, while other enzymes examined (chorismate mutase, tyrosine ammonia-lyase, and polyphenol oxidase) showed either modest or no activation.

The PAL activity reached a maximum 48 hours after the start of bruising, when discolouration reactions were complete. The change in PAL activity was associated with a transient increase in mRNA coding for PAL. In addition, mRNA encoding for two stress-induced genes, ubiquitin and a heat shock protein were transiently induced by bruising (Belknap *et al.* 1990).

Physical impact also induced a marked decrease followed by recovery in the mRNA for patatin, a primary storage protein in the tuber (Belknap and Rickey 1990). Different forms of physical stress (cutting, bruising) did not induce identical changes in the levels of transcripts analysed. The stress-induced changes are not coupled suggesting that the levels of these transcripts are regulated independently.

2.1.5 Effects of bruising on metabolism and ethylene production

There is also a rise in respiration after bruising which may be caused by the production of ethylene (Hunter and Reeves 1983). Plants respond to physical stress by increasing the rate of ethylene synthesis (Pratt and Goeschl 1969). Ethylene acts as a hormone, initiating wound healing and repair, and increasing the rate of aerobic respiration (Solomos and Laties 1975).

Reid and Pratt (1972) found that tubers exposed to ethylene have a 5 to 10 times higher respiration rate, with a peak after 32 hours, and that respiration may remain high for several days.

The rise in respiration due to bruising is important for potatoes in storage for two reasons. Firstly, the increase in respiration leads to the hydrolysis of starch to form sucrose, thereby sweetening the potatoes. Sugar content is an important element of

the colour of fried chip potatoes. Secondly, there is a loss of water accompanied by the rise in respiration. This water loss, aided by the degradation of cell membranes, results in a reduced turgor pressure (flaccid tubers) which increases the susceptibility of the tuber to bruising during handling after storage (Hughes 1980a) and increases the susceptibility of the tuber to infection by bacteria and fungi. After four months in storage, the weight loss due to rises in respiration can be more than 16% in severely damaged potatoes (Specht 1981).

Timm *et al.* (1976) demonstrated that the severity of blackspot in harvested Russet Burbank potatoes could be reduced by fumigating the tubers with air containing 1ppm ethylene, 48 hours before damage. The effect persisted for about 96 hours after removal of the ethylene. Exposure of potatoes to ethylene does not prevent blackspot development but induces uninjured cells to rapidly develop callus around injured cells, thereby confining the area of damaged tissue (Ilker *et al.* 1977).

In ethylene treated tissue there is also a reduced accumulation of polyphenols, and a larger increase in mRNA and protein synthesis after wounding. It is likely that the increase in protein is at the expense of amino acids such as tyrosine, reducing the amount of substrate for oxidation to melanin (Ilker *et al.* 1977).

2.1.6 Glycoalkaloid formation

Glycoalkaloids are normally present in potatoes at low levels but can accumulate to high levels in greened or damaged potatoes. Glycoalkaloids are potentially toxic compounds and are found in all parts of the potato plant, with the highest levels in flowers and actively growing parts. Tubers have much lower levels, with the highest concentration in the skin. In low concentrations they enhance potato flavour but a content greater than $150\mu g.g^{-1}$ fresh weight causes a bitter taste (Sinden *et al.* 1974) though this can be reduced by salt or oils in cooking.

The consumption of potatoes with high glycoalkaloids can cause poisoning and even death (Morris and Lee 1984) and the upper safety limit is $200\mu g.g^{-1}$ fresh weight. At least 95% of the total content of glycoalkaloids in tubers consist of α- solanine (~40% of total) and α-chaconine (~60% of total) and solanidine may be present. Neither of these glycoalkaloids are destroyed by cooking (Bushway and Ponnampalam 1981).

Glycoalkaloid levels vary considerably between potato genotypes (Coxon and Jones 1981)and small, immature tubers have higher levels than larger, mature specimens. The levels are strongly influenced by the environment during the growing season,

storage period and exposure to daylight. Wounding also increases glycoalkaloid content, and levels as high as 2000 $\mu g.g^{-1}$ have been reported (Wu and Salunke 1976) ten times higher than the toxic limit. Wu and Salunke (1978) considered the increase in glycoalkaloid content due to mechanical damage to tubers, to be more important than exposure to light.

Olsson (1986) analysed the effects of impact damage on the accumulation of glycoalkaloids in 21 cultivars over two years. Bruising resulted in increased glycoalkaloid levels that sometimes exceeded the toxic limit, and large differences were seen in levels between genotypes.

2.1.7 Possible functions of bruising in the potato

Potato tubers are attractive to a variety of pests and diseases due to the large amounts of polysaccharides. Plants can have passive reactions, that is, preformed barriers acting as deterrents, or plants can react to pathogen attack by actively synthesising new compounds either toxic or repellent to the pathogen (Sanchez-Serrano *et al.* 1990).

There is evidence that the physiological and biochemical reactions in bruising, may be a by-product of the defence mechanisms evolved by the tuber to guard against fungal, or bacterial invasion of damaged tissue (Richardson 1977).

The production of melanin is thought to be a mechanism for reducing the nutritive value of the tissue, or it may be a way of strengthening bruised tissue against further damage (McIlroy 1976).

Glycoalkaloids are toxic to insects, fungi and nematodes as well as to humans and animals, and protection against pathogens could well be the major function of glycoalkaloids in the plant (Morris and Lee 1984). However, some pathogenic fungi are not sensitive to glycoalkaloids and have developed the ability to metabolise glycoalkaloids, for example, *Phytophthora infestans* can break down α-solanine (Holland and Taylor 1979). The toxic effect on nematodes has also been examined but is only toxic under certain conditions (Allen and Fieldmesser 1971).

Parasitic infection also leads to the production of polyphenols in the infected tissue. Phenolic compounds can be associated with plant disease resistance and immunity in at least three ways: they can be present in the plant tissue before infection; they can be present but need to be oxidised to form quinones to inhibit the spread of a

pathogen, or they can accumulate in sound tissue adjacent to a mechanical or disease induced injury (Johnson and Schaal 1957).

Thus, while bruising is usually seen as a physiological and economic problem, it must be remembered that it also probably represents an evolutionary adaptation to physical assault or infection. Therefore, if future research offers the potential to genetically engineer bruise resistant potatoes, it could also significantly increase the susceptibility of a tuber to disease.

2.2 Summary

Chapter 2 has described the events of the bruising process from several, but complementary angles. As cell membranes degrade on impact, a cascade of events begins: biochemical changes induce melanin formation, the cell structure alters, there is activity at gene level, cell respiration increases, and the concentration of glycoalkaloids increase. These processes are part of the potato tubers defensive mechanism for initiating repair of damaged tissue, and preventing further damage and infection by pathogens.

However, as melanin in bruised tissue gives the potato an undesirable appearance, consumers demand a high quality product with low levels of bruising. Unfortunately there is no consistent correlation between a tuber receiving an impact and the production of melanin. There are many factors that affect the susceptibility of a tuber to bruising and these will be discussed in the next chapter.

Chapter 3

Factors affecting the susceptibility of a tuber to bruising

Susceptibility to bruising is not well understood, but since the trait is highly heritable (Pavek *et al.* 1989) genetic factors must play an important role. Growing conditions and storage environments also affect bruising susceptibility (for example; Hughes 1974, Peterson and Hall 1975, Stark *et al.* 1985) and so the influence of the physical environment cannot be overlooked.

Researchers use various tests to evaluate the susceptibility of a tuber to damage. This is particularly valuable for potato breeders who try to select for characteristics that may be involved in bruise resistance. In addition, the assessment of bruise susceptibility before harvest, could help determine the optimum time to harvest and the suitability of the tubers for storage and processing.

Susceptibility tests have involved many different methods; dropping a weight from a constant height onto a tuber (Maas 1966); dropping a potato from a constant height (McRae 1976); hitting a tuber with a pendulum and recording the rebound height (Gall and Lamprecht 1967); placing a tuber under a flat metal plate, with weights placed on top (Finney *et al.* 1964a); the depth that a weighted plunger will enter a tuber, or the static load required to penetrate the tissue (Blight and Hamilton 1974).

Additional methods include; peeling a tuber and measure the resulting enzymatic discolouration (Pavek *et al.* 1985); mathematical models to predict the occurrence of bruising (Peterson and Hall 1974, Sherif and Segerlind 1977); and finite stress analysis (Pitt and Davis 1984, Zhang *et al.* 1989).

However, there are no national or international methods for inflicting a standard impact, nor is there an agreed method for quantifying bruising. The lack of consistent standards does not help to determine the multitude of possible genetic and environmental influences affecting bruising susceptibility. Despite the varying standards, researchers have investigated a wide variety of possible genetic and external factors that may affect bruise susceptibility. This chapter describes some of the more important influences, but it is not an exhaustive description of them.

3.1 Genetic factors

The genetic composition of a potato affects all its physiological components and this includes its response to bruising. The following factors that are controlled genetically have been studied to try and establish their contribution, if any, to bruising susceptibility.

3.1.1 Variety

A radiation induced mutant of Russet Burbank has been recovered that is more susceptible to blackspot bruising than the original cultivar. Compared to Russet Burbank the mutant had slightly lower tuber yield, higher percentage tuber dry matter, similar total tuber dry matter yield, lower tuber protein and higher free tyrosine content. This mutant will be used as a tool to gain a better understanding of tuber characteristics that may affect bruising susceptibility (Love *et al.* 1994).

3.1.2 Size and shape of tuber

As bruising is highly heritable it might be thought that tuber size and shape would be good predictors of potential damage. However, Skrobacki *et al.* (1989) found that blackspot indices did not correlate well with tuber mass, and Hughes and Grant (1985) also found that size did not influence the intrinsic susceptibility to fracture damage. Tuber shape is characteristic of the potato variety and there is a wide variation in shape between and within varieties. While tubers with small radii of curvature (long varieties) are particularly prone at their bud and stem ends (Hughes 1980b) there is little additional evidence that shape is important. Thus, the external appearance of a variety gives little indication of bruising susceptibility.

3.1.3 Skin thickness

It seems likely that a thicker skin will reduce the chances of impact induced damage to underlying tissue. Combrink and Prinsloo (1976) found that the amount of mechanical damage was indeed reduced when the haulm was cut two weeks before maturity, and where the harvesting time was delayed up to four weeks after maturity. This may be due to the suberisation of the phellogen, and or, to a thickened phellem since formation of phellem cells seem to continue for some weeks after maturity. On the other hand, Roztropowicz and Czernik (1985) found that neither the number of periderm layers nor the maturity of the tuber was related to resistance to damage.

3.1.4 Vascular tissue

Genotypes that failed to show a relationship between dry matter and bruising had a relatively thin cortical layer and a relatively high degree of vascular ring lignification (Weber *et al.* 1980) and so it may be that the vascular ring has a role in bruising resistance.

3.1.5 Cell size

Cell size and the extent of intracellular spaces between cells could be important factors in bruising susceptibility. Hudson (1975) who compared depth of bruising to cell size and intracellular space of 11 varieties found that tissue with large cells and high intracellular spaces were more susceptible to bruising.

3.1.6 Dry matter content

The dry matter of the potato tuber is composed of many inorganic and organic components which can be broadly divided into cell wall materials, starch, lipids, proteins and acids (Burton 1989). The percentage of dry matter is usually determined by weighing the fresh weight of sub-samples and oven drying them at 90° C for 24 hours and re weighing (Jefferies *et al.* 1989). Alternatively, the percentage dry matter can also be determined in a less destructive way by immersing whole tubers or sub-samples in a range of salt solutions with different specific gravities. The specific gravity of a tuber is the ratio of dry matter to water in the tuber and is taken as being that of the salt solution in which it just sinks. Due to the close linear correlation between specific gravity and dry matter (+0.912 according to Schippers 1968) the percentage dry matter can be estimated as:

$$\text{Percentage dry matter} = 24.181 + 211.04 \cdot (\text{specific gravity of tuber} - 1.0988)$$

A specific gravity of 1.050 corresponds to about 14% dry matter and 1.100 to about 24% dry matter (Cole 1975).

The percentage dry matter increases from the periphery inwards, as far as the inner cortical tissue and outer vascular tissue, and decreases from there inwards to the centre. The bulk of dry matter is contained in storage parenchyma associated with the phloem. Small tubers have more dry matter than large ones, because the wetter vascular tissue forms a smaller proportion in small tubers than in larger ones. However, the trend is erratic. There is also a gradation in each zone, except for the

inner pith, from the heel to the rose end, which has the higher percentage dry matter (Burton 1966).

Weber *et al.* (1980) studied 23 genotypes grown over three sites and found that tuber dry matter content was correlated with the incidence of bruising; tubers with a high percentage of dry matter were more susceptible than those with a low dry matter. Other workers have reported similar, but less clear-cut results (Anon. 1977).

The percentage of dry matter is important not only in its relation to bruising, but also to the potato processor. High dry matter potatoes yield a higher mass of processed product per unit of raw product, have less fat absorbed in frying and accumulate less reducing sugars in storage than low dry matter potatoes. Therefore, a compromise is necessary between the percentage dry matter required for processing and the susceptibility to bruising. The nature of dry matter is of such importance to the problem of bruising that a description of its constituent parts and the relation of each to the bruising process is required.

3.1.7 Constituents of dry matter and their possible relationship to bruising

a) Structural materials

Each cell is surrounded by a wall consisting of interwoven hemicellulose and cellulose fibres that are 'glued' together into a matrix by pectin substances and some proteinaceous and phenolic compounds. The pectin substances are first formed between two adjacent cells at the time of cell division and is the source of adhesion between them (Burton 1989). It has been suggested that pectin substances may be involved in bruise resistance as they affect the structural properties of cell walls and contribute to firmness and coherence of the tissues (Keijbets and Pilnik 1973). In analysis of tubers, the cell wall material is called 'crude fibre' and the amounts vary from 1 to 10% of the dry matter. However, little is known about the proportions of cell wall materials present in different varieties, or about factors that may affect the amount (Burton 1989).

b) Starch

Starch is the most important storage substance within the cells, constituting 75% of the carbohydrates present, and is stored as grains. The distribution, size and number of starch grains determine in part the density and texture of the tuber (Burton 1966).

The starch grains are synthesised from the products of photosynthesis within specialised plastids called amyloplasts. Most starch grains located in the tuber are simple with an eccentric hilum and distinctive striations. Large grains (over 60 μm diameter) are flattened ellipsoids or are egg shaped. Compound starch grains with more than one hilum are occasionally present. These differ from simple grains only in that the crystallisation process is initiated at more than one nucleus (Burton 1966).

The size and number of starch grains are extremely variable and are partly dependent on tuber age and position within the tuber, and is not a varietal characteristic (Li 1985). It has been proposed that the effect of percentage dry matter on bruise susceptibility is through the starch grain content of the cells. Tuber tissue of high dry matter would consist of cells that were more densely packed with starch grains, than those with low percentage dry matter. On receiving a physical shock, densely packed starch grains would be more liable to push against the tonolplast (vacuolar membrane) thereby causing it to be damaged or stressed (McIlroy 1976).

It has also been suggested that discrepancies in the relationship between percentage dry matter and bruising could be due to differences in starch grain size distribution. For a given starch content per cell, a very few large starch grains would be more likely to damage the cytoplasm on deformation than would a large number of small starch grains (McIlroy 1980). To date, however, there has been little experimental evidence to support these suggestions, and Baumgartner *et al.* (1983) found no correlation between bruising and the size and shape of the starch grains among eight cultivars.

c) Lipids

The lipids constitute less than 1% of the dry matter (Burton 1966) but, intriguingly, Mondy and Mueller (1977) discovered that low lipid tubers are more susceptible to bruising. Lojkowska (1988) found that potato cultivars differed markedly in their lipid content and in their susceptibility to degradation by lipolytic acyl hydrolase (LAH) during the post wounding period. Tissues from cultivars susceptible to membrane degradation showed higher LAH activities than those from resistant cultivars.

The importance of varietal variation in lipid degradation is not clear as there is not yet sufficient evidence to explain the cellular regulation of LAH (Racusen 1984, Lesham 1987). However, because lipids in potato tuber tissues are mainly membrane

lipids, even small changes in their composition may alter membrane stability and increase susceptibility of the tissue to physiological disorders (Lulai *et al.* 1987).

Varieties resistant to mechanical damage, showed low electrolyte release, while low damage resistance cultivars showed high electrolyte release. It is thought that the variability in electrolyte release and susceptibility to mechanical damage in individual cultivars is related to environmental factors influencing the susceptibility of cell membranes to auto degradation (Lewosz and Lojkowska 1985).

d) Phenols

The most abundant phenols in the potato are the monophenol tyrosine (0.1%-0.3% tissue dry weight) and the o-diphenol chlorogenic acid (0.025-0.15% dry weight). In the variety Russet Burbank, chlorogenic acid is more concentrated in the epidermis and outer tissue, especially in the phloem and phloem parenchyma. Tyrosine is more evenly distributed but with higher concentrations in the stem end, and in the central rather than peripheral tissues (Reeve *et al.* 1969b). Other phenolic substances such as flavones and anthocyanin are either negligible or are present only in the epidermis (Talburt *et al.* 1975).

Mapson *et al.* (1963) found that chlorogenic acid content was not correlated with the susceptibility to bruising. However some evidence was obtained from *in vitro* experiments to show that the rate of enzymatic browning was reduced in the absence of chlorogenic acid. If the concentration of chlorogenic acid was increased to between 0 to 200μg/ml the reaction rate was significantly enhanced. This indicates that in most potatoes there is sufficient chlorogenic acid to give the maximum rate of oxidation.

Corsini *et al.* (1992) found differences in free and protein-bound tyrosine among potato tubers with relationship to bruise resistance. Mature tubers of all genotypes contained 26 ± 1μmole.g^{-1} dry weight total tyrosine. Partitioning of tyrosine between tuber protein and free amino acid pool varied with genotype and appeared to be an important determinant of blackspot resistance. Tubers with free tyrosine levels below 4μmole.g^{-1}.dry weight consistently showed a resistant blackspot response. Bud end samples had lower tyrosine levels and a reduction in susceptibility compared to stem ends. Phenols other than tyrosine showed no consistent relationship to blackspot reaction.

e) Proteins

About 8-10% of total proteins are present as insoluble proteins and are often visible under the electron microscope as large cubic crystals 12-25 μm in diameter. The crystals contain lysine, RNA and iron and show little substructure (Hoff 1971). Protein crystals are found mostly in cortical cells adjacent to the periderm, but are also present in other tissues where they are often closely associated with the nucleus (Li 1985).

Soluble protein present in the cell sap is composed of 70% tuberin, a storage protein. Soluble protein distribution patterns in highly resistant and highly bruise susceptible varieties have been compared. There were large quantitative differences in some major protein bands, particularly the glycoproteins. However, there were no specific proteins that could be used as markers for blackspot resistance, and the association between blackspot resistance and soluble proteins appeared to be indirect. It is suggested that this may be due to the depletion of free aromatic amino acids during protein synthesis, thereby minimising the pool of substrates available for melanin formation (Corsini *et al.* 1988).

Enzymes are complex proteins, and there are many studies on their role in bruising susceptibility. Although polyphenol oxidase is the primary enzyme responsible for bruise discolouration, studies of the enzyme's direct influence on varietal differences in blackspot susceptibility have been inconclusive. Some have found a positive correlation between polyphenol oxidase activity of different clones and blackspot susceptibility, while others have not (Mapson *et al.* 1963).

These inconsistencies in experimental findings may be due, not to varietal susceptibility and enzymatic discolouration being linked, but to the characteristic properties of polyphenol oxidase that may differ among potato clones (Stark *et al.* 1985). It is also probable that the main factor that controls bruising is the concentration of tyrosine, and not the concentration of the enzyme. This was confirmed by the fact that a solution of homocatechol (a substance readily oxidised by phenol oxidase to form a brown colour) when painted on the cut surface of a potato, showed the same rate of browning inside the vascular ring as outside it. This emphasises that the concentration of the enzyme is not limiting browning (Mapson 1963).

The activity of enzymes depends not only on the presence and perhaps the amount of enzymes, but also on the presence or absence and concentration of specific activators

and inhibitors. In the case of polyphenol oxidase, the inhibitor is chlorogenic acid, and the activator is calcium (Li 1985).

Polyphenoloxidase is usually abundant in potato tubers (Stark *et al.* 1985). However, in blackspot resistant clones selected from the wild species *Solanum hjertingii*, polyphenoloxidase activity is much lower than *S. tuberosum*. Therefore, reduced polyphenoloxidase activity may be a mechanism for bruise resistance in some tuber bearing Solanums (Gubb *et al.* 1989, Woodwards *et al.* 1985).

3.2 Environmental factors

3.2.1. Nutrients

In addition to carbon, hydrogen and oxygen that form part of most organic compounds in the potato there are additional macro and micro-nutrients that are essential for growth. The macro-nutrients (> 1 $mg.g^{-1}$ F.W) are nitrogen, potassium, phosphorous, calcium, magnesium and sulphur. The micro-nutrients ($\leq$ 100 $\mu g.g^{-1}$ F.W.) are iron, chlorine, copper, magnesium, zinc, molybdenum, and boron (Burton 1989). The presence of nutrients is dependent on the type and amount of fertiliser applied and the availability of nutrients to the plant is dependent on timing, soil type and precipitation levels. Therefore, when studying the influence of different nutrients on bruise susceptibility there are many interacting factors which complicate the determination of possible influences on bruising susceptibility. The following nutrients have been the main focus of attention in trying to determine the influence on bruise susceptibility, but are by no means an exhaustive treatise.

a) Potassium (K)

Potassium is necessary for osmotic regulation, stomatal opening and is an essential component of several enzyme systems. Potato plants deficient in K show increased susceptibility of the tubers to blackspot (Mulder 1949) and thus blackspot susceptibility decreases with sufficient K in the tissue. Increasing K fertiliser has two effects; it increases the K content of the tuber (Vertregt 1968) and decreases the percentage dry matter (Kunkel and Gardner 1965, McIlroy 1980). Vertregt (1968) estimated that a level of 2.6% of K in the dry weight is necessary for resistance to bruising.

Shotton (1978) found that sulphate of potash was more effective than muriate, and that it increased yield, reduced specific gravity and reduced blackspot when K levels

were limiting. On plots with adequate soil K, potash had no effect on bruise development. The application of potash on low K soils reduced blackspot to levels observed on soils with adequate K in four cultivars (Dwelle *et al.* 1977).

It been suggested that K may influence bruise susceptibility by its effect on cell wall elasticity or upon osmotic regulation of the tuber (Burton 1989). Kunkel *et al.* (1973) and White *et al.* (1974) found that high K content in the tuber produces greater hydration (lower specific gravity) which also seems to be associated with reduced blackspot development. Alternatively, the effect may not be directly associated with K. With an increase in K there are other changes that may be relevant. For example, the content of citric acid may be increased and that of sugars, amino acids and phenolic substrates decreased, as may polyphenoloxidase activity (Mulder 1949, Mondy *et al.* 1967, Burton 1989).

b) Nitrogen (N)

It is known that high N delays tuber maturity and slows dry matter accumulation (Swiniarski and Ladenberger 1970) increases tuber size and sucrose content (Voogd 1963) and reduces the specific gravity (Rogers-Lewis 1980). However, the effects of N fertilisers on bruising susceptibility are not clear. Mulder (1949) thought that large amounts of N fertilisers may increase the plants' potassium requirements, thereby decreasing the susceptibility to bruising. It has also been suggested that a reduction in specific gravity through the application of high N may decrease bruise susceptibility but there is a wide varietal response (Thornton and Timm 1990). In contrast, Mapson *et al.* (1963) found that supplying N in the form of urea induced a three fold increase in the rate of discolouration and in the concentration of tyrosine compared with controls; phenoloxidase activity was similarly increased (Mapson *et al.* 1963).

c) Calcium (Ca)

Ca is an important cell messenger mediating various physiological processes that are initiated by extra cellular signals such as light, gravity and hormones. Ca is also essential for the structural integrity of both the plasma membrane and cell wall. In potato tubers, approximately 60% of the cellular calcium is present in the cell wall. The Ca maintains cell adhesion and tissue coherence primarily through the formation of calcium pectate that stabilises intermolecular bonds in pectin protein complexes (Poovaiah and Reddy 1987).

Increases in Ca concentration in nutrient solutions supplied to Superior and Russet Burbank potatoes resulted in an increased Ca concentration in the tuber. Electrolyte leakage from sections of potato with high Ca concentration was lower than tubers with a low Ca concentration. The higher Ca concentration enhanced the structural integrity of cell walls and membranes (McGuire and Kelman 1986).

Timm (1989) found that an insufficient supply of soluble Ca can lead to the weakening of the vacuole membrane of the cells in the cortical tissue. The weakened vacuole membrane would then be more prone to rupture when subjected to impacts.

Calcium deficiency is confined to acid soils in which it may be aggravated or induced by high K applications. It is most prevalent in areas with a high rainfall which can lead to excessive leaching. Calcium deficiency can reduce K uptake because in the absence of adequate membrane Ca, K and Na ions compete for entry into the cell, which does not occur in a fully functioning cell membrane (Burton 1989).

d) Copper (Cu)

The supply of Cu is necessary for the formation of melanin since o-diphenol oxidase contains Cu and for other oxidative pathways. As a result, tubers from plants deficient in both potassium and Cu have a decrease in polyphenoloxidase activity (Mulder 1949) and are therefore generally free of blackening. However, Cu deficiency is rare, mainly occurring on newly reclaimed peat (Burton 1989). It is therefore unlikely that Cu is involved in bruise susceptibility although Weaver *et al.* (1968) have noted that the average Cu content of bruise resistant varieties were higher than in susceptible varieties.

3.2.2 Temperature

Temperature has been shown to have a significant effect on bruising susceptibility before, during and after harvest. More discolouration was observed in tubers grown at intermediate soil temperatures (15 to 20°C) than those at higher (28 to 32°C) or lower soil temperatures (8 to 12°C). Microscopic examination of tubers grown at intermediate temperatures showed that the cells around the phellogen and phelloderm stained more deeply, than tubers grown in the lowest and higher temperature. This may have been the result of the presence of more phenols (Yamaguchi *et al.* 1964).

Several workers have shown that the temperature of tubers when they are handled, either at harvesting or in store, has a bearing on damage levels (for example Ophuis *et al.* 1958). Tubers impacted at a temperature of 4°C had a 77% chance of splitting

when dropped from 110 cm. Under the same conditions tubers had a 38% chance of damage at 8°C tuber temperature (McRae 1976).

Johnson and Wilson (1969) found a linear relationship between soil temperature and bruising at harvest time. A 0.5°C increase in soil temperature would tend to increase the force necessary to bruise by about 2%: when these potatoes were dropped 30 cm onto metal rods, the proportion receiving bruises reduced from 44 to 11%. In contrast, Thornton (1979) found a non-linear response to temperature variations and suggested that the response to temperature varied with the level of turgidity.

The rapid ability of membranes to react to temperature suggests a physical rather than a biochemical change. Studies indicate that low temperatures cause the membranes to decrease in fluidity and increase in permeability (Shekhar *et al.* 1978). The decrease in membrane fluididy may reduce the ability of the cell to absorb energy from an impact, and the increase in membrane permeability may allow LAH to be more easily activated or to be released from the vacuole.

3.2.3 Water

Hughes (1974) observed that there was a very fine balance in the water relationship of potatoes when tubers are most resistant to damage; too turgid and they will crack and split, too flaccid and they will suffer from blackspot. Thornton (1979) found that at a given temperature there is a tuber hydration level at which bruise damage is at a minimum (Fig. 3.1).

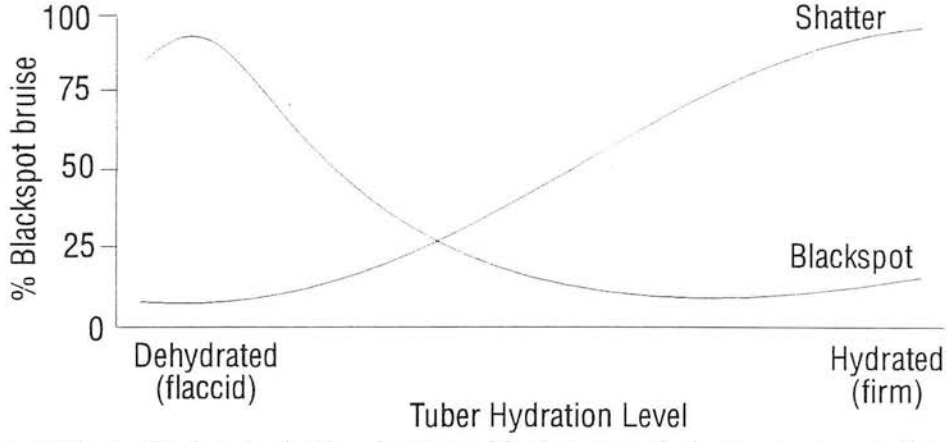

Fig 3.1 Effect of tuber hydration level on blackspot and shatter bruise at 7 to 10°C (after Thornton 1979).

When the temperature changes, the amount of shatter bruise or blackspot that results from a force changes. Shatter bruise is the primary bruise problem with cold

potatoes and blackspot is the main problem with warm potatoes at harvest time (Thornton and Timm 1990).

Experiments using a pendulum to inflict a standard impact, showed that hydrated potatoes are very susceptible to shatter bruise, and are quite resistant to blackspot. Dehydrated potatoes are resistant to shatter bruise but are highly susceptible to blackspot (Bland *et al.* 1987).

The role of turgor in bruise susceptibility may be explained by the mechanical and rheological properties of the cell. When the turgor pressure is low, the cells deform more readily for a given force (Nilsson *et al.* 1958). Therefore, when flaccid tubers are subjected to an impact, the limit of cell wall and membrane deformation may be reached which would then result in cell damage. However, it has been shown that the various rheological properties of tubers, for example, modulus of elasticity, force to rupture point, deformation to rupture point, differ within varieties (Finney *et al.* 1964b). Hughes (1974) suggested that the reason for the inconsistent correlation between turgor and variety may be due to differences in biochemical properties and factors that affect the amount of deformation that tissue can withstand before cell damage occurs.

3.2.4 Soil

The soil influences the susceptibility of tubers to bruising through the content of nutrients (Mulder 1956, Vertregt 1968) and its physical and atmospheric condition (Howard *et al.* 1962, Yamaguchi *et al.* 1964, Kunkel *et al.* 1970).

The texture of the soil also determines the ease with which the potatoes are separated from the soil on the webs (rods that form a vibrating conveyor belt on the harvester). Clay soil adheres to tubers more readily than sand. In clay soil, the potatoes are shielded from damage by a protective layer of soil (Hesen and Kroesbergen 1960).

However, potatoes from clay soil are more susceptible to bruising than potatoes grown in sand, possibly because of higher dry matter content and the lower potassium content of potatoes grown in clay (Schippers 1968).

The planting depth of tubers is also an important factor. Blackspot tends to be worst in shallow tubers and tubers from drier soil, and has been linked to the soil carbon dioxide (CO_2) concentration (Thornton and Timm 1990). The diffusion of CO_2 into the soil under plastic sheets slightly increases the intensity of spot discolouration (Kunkel *et al.* 1970).

3.2.5 Storage

Most potatoes are stored before being processed or distributed to retail outlets. If tubers are bruised before storage it can lead to the infection of soft rot, and this can spread to undamaged tubers (Perombelon and Kelman 1980). In addition, during storage, the potato's susceptibility to bruising can be significantly affected by storage itself.

Tubers are often treated with a sprout suppressant before being stored. Tubers of the variety Katahdin treated with the sprout inhibitor CIPC (5 min dip in 1% aqueous emulsion) discoloured significantly more and had a higher phenolic content than controls. Crude lipid and phospholipid contents were reduced by CIPC treatment; low lipid tubers are more susceptible to bruising (Mondy 1983).

In storage, water loss from the tubers can be a problem, especially if the tubers are damaged and the respiration rate is increased. Water loss decreases turgidity so that tubers deform under low impact forces (Hughes and Grant 1985). Collin (1961) noted that susceptibility to bruising increased with depth of storage. Jacob (1959) claimed that nearly all bruising after storage results from pressure bruising.

Potatoes that are kept in extended storage have higher water losses, tyrosine levels and polyphenoloxidase activity, producing tubers that are very sensitive to handling. For example, after storage for 33 weeks at 6°C, the force needed to produce a given deformation was half that required after 7 weeks, and the amount of blackspot doubled (Hughes 1981).

The concentration of ascorbic acid is also known to decrease in storage. Workman and Holm (1984) found that among 11 clones the mean ascorbic acid content ranged from 13 to 27 mg per 100g (F.W.) at harvest to 8 to 16 mg after 6 months in storage at 3.9°C. The decrease in ascorbic acid content occurs irrespective of storage temperature (Kida *et al.* 1991). Ascorbic acid is of potential significance in relation to bruising susceptibility because of its role as a strong reducing agent. Thomas (1955) reported that oxidation of dopa *in vitro* could be inhibited by ascorbic acid and suggested that polyphenol oxidase activity may be inhibited its presence. However, the concentration of ascorbic acid in the tuber has not been correlated with bruise susceptibility (Johnson and Schaal 1957, Workman and Holm 1984, Thornton and Workman 1987).

3.3 Engineering for bruise prevention

It is outside the scope of this thesis to elaborate on the many ways in which harvesting and potato handling equipment can be modified and adjusted to minimise impacts. In addition to minimising impacts, it is also important that the machine operators are aware of the factors that cause bruising, so that the machines can work optimally (McRae and Fleming 1994).

3.4 Summary

Genetic and environmental factors that may be involved in bruising susceptibility are complex and inter linked. In addition to variety, the environment can modify the growth and bruising response to a very large degree. Due to unpredictability of the environment it is difficult to alter the susceptibility of tubers to bruising in the field.

At present, the best way to remedy the problem is to reduce impacts to tubers. This can be aided by detecting bruising quickly and non-invasively, and quantifying bruising consistently and accurately. The methods that have been used up to the present time for bruise detection and quantification will be outlined in the next chapter.

4.2.1 Hotbox

One of the most widely used methods for speeding up the biochemical processes in bruising is to place the tubers in a hotbox. This is a large box that is heated to 37°C and is kept humid by a water container and capillary matting in the base. The tubers will show bruising within 12 hours of being damaged, but this can only be detected by peeling the tubers (McRae *et al.* 1976).

4.2.2 Hot water soak method

Iritani and Weller (1985) investigated the practicality of using hot water to accelerate bruise development as heat is more easily transferred in water than in air. Water temperatures of 40, 50 and 60°C and soak times after bruising of 5, 10 and 20 minutes were used. After soaking the tubers in hot water they were left at room temperature for 7 hours before assessing blackspot bruise development. Approximately 88% of blackspot bruising appeared after the tubers had been dipped in hot water at 60°C for 10 minutes, compared to 38% of tubers left at room temperature for 7 hours. This is the percentage of total bruised tubers obtained after 24 hours at room temperature. If the tubers were peeled after bruising and prior to the hot water treatment, the time for maximum bruise development was reduced to 5.5 hours.

Higher water temperatures or a longer period in hot water did not increase the rate of bruise development due to the possible inactivation of enzymes. The time taken for a tuber to warm to the optimum temperature for bruise development was affected by tuber size and initial tuber temperatures. Large tubers and lower initial tissue temperatures take longer to achieve a desirable tuber temperature with the hot water soak method. Iritani and Weller's preliminary results suggest that the use of hot water for short periods of time may be superior to high room temperatures for bruise development.

4.2.3 Tetrazolium Chloride

In this method bruised tubers are peeled and soaked in a warm solution of 0.1% tetrazolium chloride for up to 45 minutes. Tetrazolium chloride reduces in competition with oxygen at the terminal electron transport chain in mitochondria, to produce a pink colouration. Due to the rise in respiration in injured tissue, the tetrazolium chloride highlights the areas of tissue that are undergoing repair (Beaver and DeVoy 1985).

The tetrazolium chloride method is relatively simple but there are several disadvantages; the tubers have to be peeled evenly; fresh solutions need to be made each time the method is used; the substance is toxic; and the colour change can be difficult to detect in bruised tissue (Beaver and DeVoy 1985). In addition, Melrose and McRae (1985) found that the success of revealing bruising depended on the type of surface on to which the tubers were dropped and the period since harvest.

4.2.4 Conductivity

Bruising results in the release of electrolytes, particularly potassium, from the cell membranes. An increase in potassium content, or conductivity of cell washings, has occasionally been used as an indicator of membrane damage or cell death (McIlroy 1976).

Wilson *et al.* (1987) took 4mm intact cores of potato tissue from the site of impact. The aim was to use conductivity measurements across the core to give an immediate indication of the kind of impact damage that would lead to a bruise. With only one tuber at each time interval the results were erratic. It was found that there was a general rise in conductivity in bruised tissue but not in controls about 6-8 hours after impact.

Wilson *et al.* (1987) also investigated the tetrazolium chloride method in conjuction with conductivity experiments. Despite attempts, they could not find a faster method than tetrazolium, nor could this test be modified to make it faster. The conductivity experiments suggest that a substantially faster method would be difficult to find, since membrane damage that precedes the other symptoms of bruising does not occur immediately on impact.

It seems likely that the tetrazolium test does not detect part of the sequence of events leading to bruising, but measures something more superficial that correlates with blackspot. The closeness of the correlation depends on the surface onto which the potatoes are dropped. Conductivity experiments raise some doubts whether oxygen is required for the subsequent polyphenol oxidation (Wilson *et al.* 1987).

4.2.5 Compressed air

Duncan (1973) showed that bruise development accelerated to occur in approximately five hours with compressed oxygen at 1.7 bar. Dwell and Stallknecht (1976) exposed tubers to combinations of various temperatures and gas pressures of

0.3 to 2 bar using air, oxygen, carbon dioxide and nitrogen to try and find the optimal combination for blackspot development. Pressurised air slightly enhanced the temperature effect at 40°C, pressurised oxygen had no significant effect upon blackspot development, while carbon dioxide and nitrogen inhibited blackspot formation. Increasing the incubation temperature accelerated blackspot formation, with an optimum response at 36 to 40°C. At 40°C, tubers reached maximum discolouration within 6 hours. Bruises incurred in the field during harvesting required a longer incubation period at a lower temperature, than impacts on tubers held in storage for 1 to 5 months.

Compressed oxygen is hazardous and compressed air has been suggested as a safer alternative (Melrose 1991). A prototype compressed air tank was built at the Scottish Centre of Agricultural Engineering (SCAE) in which pressure could be raised to 3 bar at high humidity. Results showed that bruise development was accelerated, but that a higher pressure is likely to be necessary to obtain the same results as for compressed oxygen (Melrose and McRae 1987, Melrose 1991). A new tank has been commissioned that can be compressed to 10 bar and can hold large sample sizes. The compressed gas method clearly has potential for accelerating bruising but the precise combination of gases, pressure and temperature require greater attention. Experiments involving the new tank will be discussed in chapters 13 and 14 of this thesis.

4.2.6 Nuclear Magnetic Resonance (NMR)

The previous methods have attempted to speed up the biochemical processes that are involved in producing the melanin reaction. A method that could detect physical changes in the cells before the discolouration processes begins would enable faster bruise detection.

One method is NMR, based on the resonant absorption and emission of very low magnetic energy by certain atomic nuclei when subjected to a magnetic field (Fukushima and Roeder 1981). It provides an accurate and non destructive technique of determining chemical structures in liquid and solid materials (Martin *et al.* 1980). NMR has been used to evaluate the internal quality of fruits and vegetables such as bruising, pits and seeds, worm damage, dry regions, void space, maturity and ripeness (Chen *et al.* 1989). However, the method is expensive, requires specialist knowledge and is not widely available.

4.2.7 Ultrasound

Ultrasonics is the name given to the study and application of sound waves with a frequency greater than 18 kHz. A transmitting and a receiving transducer are placed either side of a sample. The main obstacle to the ultrasonic testing of fruits and vegetables has been very high attenuation coefficients of nearly all tissues examined and this has prevented the technique being used on whole fruit and vegetables (Javanaud 1988). Increasing the power of the transmitter could reduce the attenuation but could also damage plant cells (Sarkar and Wolfe 1983).

Ultrasound has been used to detect hollow heart in potatoes (Cheng and Haugh 1994) but the detection of bruising in potatoes has not been successful (personal communication Mr A.Y. Muir).

4.2.8 Infrared gas analysis

Field and laboratory experiments show that damage to potato tubers increases the tuber respiration which declines over time. Measurements of tuber respiration with an infrared CO_2 analyser can be a sensitive indicator of the amount of damage (Pisarczyk 1982). It is suggested that this technique may be useful in evaluating the bruise damage caused by harvesting and handling systems (Burton and Schulte-Pason 1987). However, this method measures the total respiration of a tuber and cannot locate areas of tissue on a tuber that may be respiring more than others due to bruising.

4.2.9 Spectrophotometry

Spectrophotometry measures the colour and intensity of transmitted or reflected light from a sample. When light is incident on biological materials some of the light will be reflected, some will be absorbed, and some will be transmitted. By measuring the intensity of the transmitted or reflected light, many useful biological molecules can be quantified.

Birth (1960) used transmission spectrophotometry to detect 98% of Irish Cobbler potatoes with hollow heart. Hollow heart is the term used to describe the internal death of tuber cells, resulting in a hollow cavity and melanin production. It was also found that this technique could detect with 81% certainty the discolouration associated with blackspot and greening.

Reflectance spectrophotometry has been used to study bruising in apples (Brown *et al.* 1974, Reid 1976, Kucynski *et al.* 1994) but to date, reflectance spectrophotometry has only been used to detect surface defects on tubers (Porteous *et al.* 1981, Muir *et al.* 1982) and not sub-surface defects such as bruising. Therefore, this method needs further investigation as a non-invasive way of possibly detecting bruising. The principles and application of this technique for detecting sub-surface bruising will be developed further in Chapter 5.

Chapter 5

Principles of sub-surface bruise detection by reflectance spectrophotometry

5.1 Introduction

Quality assessment of unpeeled or peeled potatoes is largely based on the visual appearance of a tuber. However, the human eye is subject to fatigue, lack of colour memory, and variations in colour discrimination between individuals can influence the decision determining the quality of a product. In addition, the human eye is limited to detecting a narrow band of the electromagnetic spectrum from about 400 to 700 nm. To overcome the deficiencies of the human eye, optical methods of quality assessment have been developed. Optical methods have the advantage of being non-invasive and can detect regions of the electromagnetic spectrum outside the visible range.

Optical methods involve illuminating a sample with a light source and measuring the light reflected or transmitted. When light is incident on biological materials some of the light will be reflected, some will be absorbed, and some will be transmitted (Fig. 5.1). The transmitted light encounters randomly orientated internal surfaces and is reflected back. The phenomenon of random reflection and refraction at the numerous internal surfaces is called 'light scattering', or body reflectance. In biological materials, the body reflectance is of greatest interest as it can be used to quantify many useful factors determining quality (Gunasekaran *et al.* 1985).

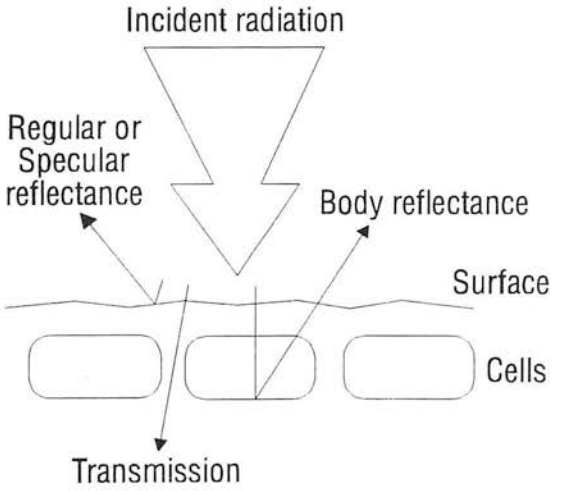

Fig. 5.1 Pathways of light in biological materials (after Birth 1976).

Body reflectance can be quantified from a sample with reflectance spectrophotometry which measures the intensity of each wavelength present to create a spectrum.

Reflectance spectrophotometry has been used to detect a wide variety of surface defects in agricultural products including potatoes (Porteous *et al.* 1981). However, until now, there has been no published research on the application of reflectance spectrophotometry for detecting sub-surface defects in potatoes such as bruising.

To understand how it may be possible to detect sub-surface bruising, it is first necessary to outline the ways that light interacts with matter, and how these interactions can be measured.

5.2 The electromagnetic spectrum

When electrons within an atom are caused to oscillate they result in a changing electric and magnetic field. The oscillation of electrons can be caused by thermal, electrical or chemical excitation, or with high frequency radiation. Depending on the bonding of an electron to an atom, the electrons can oscillate at different resonant frequencies to produce electromagnetic radiation.

Electromagnetic radiation is one of the basic physical processes by which energy is transferred from one place to another. This energy is transferred as waves and particles and the physical laws governing their motion and interaction with matter are called quantum mechanics. Quantum mechanics associates a wave property such as frequency, wavelength, and amplitude, with 'particles' known as photons. The photon has no mass and is the 'quantum' of electromagnetic energy and momentum absorbed or emitted in a single process by a charged particle (Mohsenin 1984).

Electromagnetic radiation with the highest frequency and shortest wavelengths are cosmic rays. The radiation with lowest frequency and longest wavelengths are radio waves (Fig. 5.2).

Ultraviolet (UV) rays are produced by molecules and atoms in electric discharges. The wavelength range of sunlight is from 350 to 950 nm and is a very powerful source of UV radiation.

Radiation in the visible part of the spectrum is produced by rearrangement of the outer electrons of atoms. The typical human eye detects energy within the visible spectrum from approximately 390 to 780 nm, with a peak detection at 555 nm (Fig. 5.3). Colour is not a property of the light itself but a manifestation of the electrochemical sensing system of eye, nerves and brain. A variety of different frequency mixtures can cause the same colour response from the eye-brain sensor. For example, a beam of red light overlapping a beam of green light will result in the

perception of yellow light, even thought there are no wavelengths present in the so-called yellow band. This is the reason for a television screen producing a range of colours with only three phosphors; red, green and blue (Mohsenin 1984).

Infrared (IR) radiation is subdivided into four regions; the near infrared (NIR; 780 to 3000 nm) the intermediate infrared (3000 to 6000 nm) the far infrared (6000 to 15000 nm) and the extreme infrared (15000 nm to 1 mm). Any material will radiate and absorb IR through via thermal agitation of its constituent molecules. The human body radiates IR weakly, starting at 3000 nm and peaking at 10000 nm (Hecht 1989).

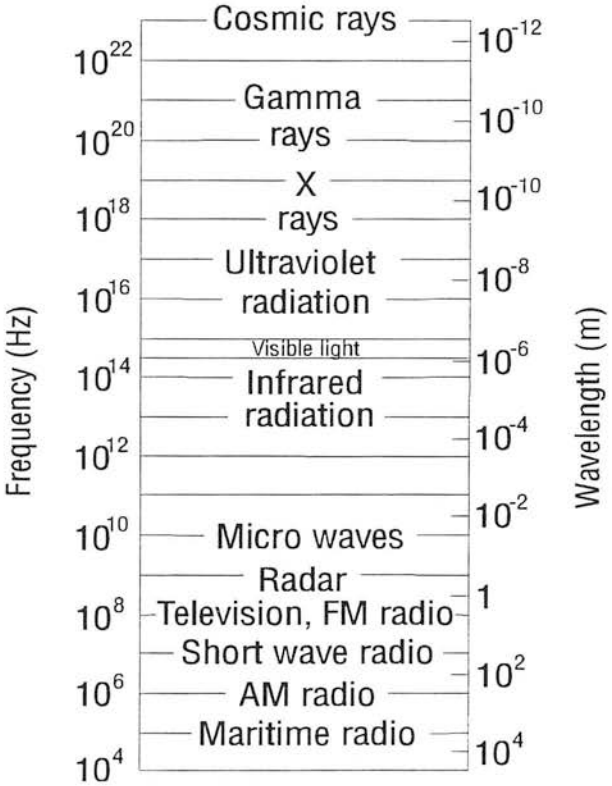

Fig. 5.2 The electromagnetic spectrum (after Shortley and Williams 1971).

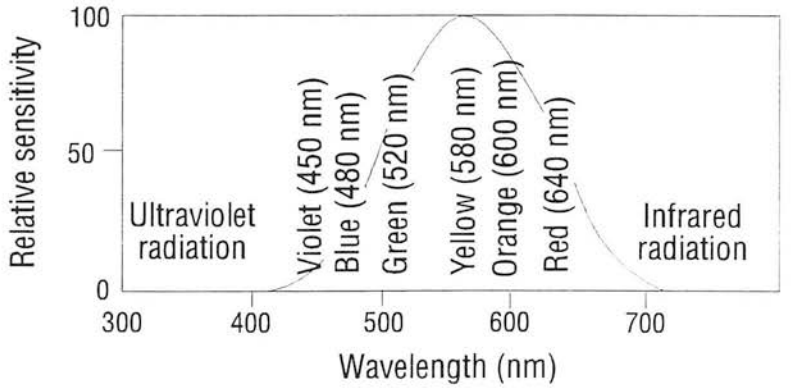

Fig. 5.3 The visible spectrum of the human eye (after Shortley and Williams 1971).

5.3 Interaction of electromagnetic radiation and matter

All electromagnetic radiation travels through a vacuum at the speed of light, but the way in which different types of radiation interact with matter can vary considerably across the electromagnetic spectrum. For example, radiation having photons with an energy equal to that of electrons in atoms or of atoms in molecules will interact more strongly with atoms and molecules. This is the case for UV, visible and NIR radiation. At wavelengths less than 290 nm, UV radiation results in the ionisation and dissociation of molecules that will destroy micro-organisms.

Radiation with longer wavelengths, carrying photons with less energy, in general interacts less with matter. This is the case with radio waves. Radiation that has high energy or very short wavelengths, such as x and gamma rays, is absorbed very little in matter, but they produce atomic and molecular ionisation, and nuclear break-up (Mohsenin 1984).

The effects of electromagnetic radiation on food materials have been known for a long time. However, the technological implications for processing, preservation, quality evaluation and quality control have been known and applied only in recent decades. Because of its practical importance and numerous applications in food production and processing, the physical laws of light and matter for the visible spectrum of electromagnetic radiation will be considered. These laws are generally applicable over the entire range of the electromagnetic spectrum.

5.3.1 Interaction of light and matter

Birth and Law (1977) considered two fundamental factors in the interaction between light and matter as follows:

a) Geometric factors

The geometry of interaction is affected by the dimensions of the matter and the wavelength of radiation to which the matter is subjected. For example, if a rough surface is polished, a point is reach when the surface appears smooth. This is the point at which the scratches on the surface have a smaller dimension than the wavelength of light.

b) Absorption factors

Molecules absorb radiation in discrete amounts and are excited to specific vibrational states, depending on the energy levels of the exciting radiation. The absorbed portion of radiation can be transformed into other forms of energy. For the infrared, the energy is usually transformed into heat. For the UV, the energy may be converted to chemical changes or to other forms of radiation such as fluorescence or phosphorescence.

According to quantum theory, molecules absorb light in the visible and UV because their electrons can move to higher energy states. Infrared light does not carry enough energy to excite electrons in molecules. Instead, molecules absorb IR radiation by vibrating or rotating. Rotational absorption bands are those which involve the far infrared bands. The vibration absorption bands are those which involve NIR.

The complex phenomenon of molecular absorption can be simplified by saying that particles as small as molecules, according to quantum theory, can only vibrate at fixed frequencies when energised by radiation, and therefore absorb light of that particular frequency. Since the speed of light is constant, it follows that each molecule of a given chemical compound can absorb light at only particular wavelengths and frequencies. If these wavelengths and frequencies are known, then optical methods can be optimised to detect particular molecules (Mohsenin 1984).

The geometric and absorption factors of a material affect the proportions of light that will be reflected, transmitted and absorbed. As the body reflectance is of greatest interest in biological materials, the factors affecting the reflection and transmission of light will be discussed in more detail.

c) Reflection

The radiation reflected at the initial interface is termed regular or specular reflection. This type of radiation gives a glossy appearance to smooth surfaces and a diffuse appearance to rough surfaces. In diffuse reflectance, light is reflected from a surface at all angles. In regular or specular reflection, light is reflected more strongly at a specific angle. The law of specular reflection states that the angle at which a light ray is reflected from a surface must equal the angle at which it is incident to the surface (Guneskeran *et al.* 1985).

The law of conservation of energy states that the sum of the reflected (R) transmitted (T) and absorbed (A) radiation should equal the total incident (I) radiation.

$$I = R + T + A$$

This equation can be used to calculate the percentage of light reflected or transmitted or absorbed, when the incident radiation and two of the other parameters are measured (Birth 1976).

d) Transmission

If the angle of the incident light is less than then 60°, then only about 4% of the incident light striking a biological material is reflected off the surface. The remaining radiation, about 96%, is transmitted into the object (Mohsenin 1984).

The forward transmission of light in tissue depends both on the absorption in the tissue and on the scatter. At very short UV wavelengths and for transmission in the infrared, tissue absorption may be significantly greater than scatter. On the other hand, for most optical wavelengths, scattering makes a substantial contribution to the forward transmission. The scattering is also dependent on the size of the scatterer relative to the wavelength.

Rayleigh scattering, where the scattering particles are very much smaller that the wavelength gives weak nearly uniform scatter that varies with the fourth power of the wavelength. When scattering occurs from particles whose size greatly exceeds the wavelength, so called Mie scattering, it is highly forward directed and independent of frequency. Scatter from structures of intermediate size, equal to the wavelength, shows frequency and direction dependence between these limits (Hecht 1989).

e) Body reflectance

Birth (1976) recognised that light must be transmitted through the pigments within cells to produce a coloured appearance. The light so transmitted through the object encounters randomly oriented internal surfaces. Depending on the size and nature of the internal surfaces, a fraction of this reflected radiation is transmitted back through the initial interface. This reflected radiation is called body reflectance and radiates from the material in a hemisphere (Mohensin 1984).

The body reflectance signal is not directly measurable as it is combined with the diffuse and regular reflectance. To minimise the regular reflectance, the detector and

light source can be placed in direct contact with the sample using a bifurcated fibre optic light guide (chapter 7) or an integrating sphere (chapter 8) can be used to ensure that all the reflected radiation is collected.

In biological materials it is the body reflectance that is of significance because it provides information about the nature of the sub-surface tissue. In potato tubers, it is hoped that bruising can be detected non-invasively in the sub-surface tissue by measuring the body reflectance. The next section outlines the principles of quantifying body reflectance.

5.4 Spectrophotometry

A spectrophotometer measures the intensity of light across a spectral region by splitting the light into its constituent wavelengths, and measuring the intensity of each wavelength. In this way, a spectral signature of a sample can be composed. Spectrophotometry is a very versatile technique and has been used in many different ways to measure the light reflected or transmitted through a sample (Mohsenin 1984).

The two basic components of any spectrophotometer are the scanning monochromator and the detector. These are normally chosen to optimise the overall sensitivity of the system in a particular wavelength region.

5.4.1 The monochromator

Spectrophotometers split light into its constituent wavelengths with a diffraction grating (also called a monochromator). A diffraction grating is a glass or metal plate with very fine parallel grooves etched in it. When a light wave is incident onto a grating with grooves similar to the wavelength of incident light, it undergoes interference and is spatially separated by a process called diffraction (Fig. 5.4).

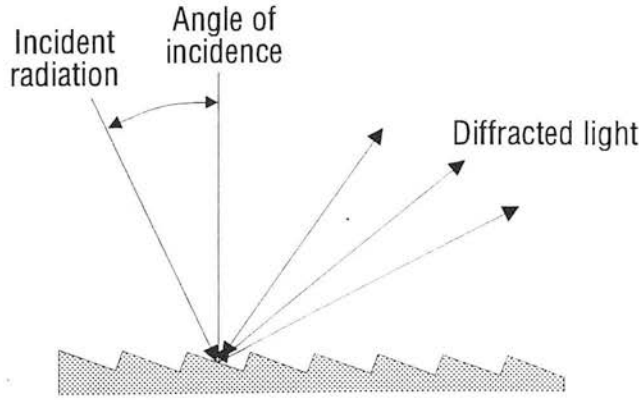

Fig. 5.4 Schematic of a diffraction grating (after Mohensin 1984).

Modification of the groove width or profile causes a 'blaze' effect, that is, the efficiency of production of a discrete wavelength is increased. Depending on the blaze effect and angle of incident light, a beam of light at one wavelength (monochromatic light) is produced. By altering the angle of incident light, the entire spectrum of the incident light may be viewed. The smaller the angle of incident light, the shorter the wavelength for a given blaze.

One of the most important specifications of the grating is the wavelength blaze. This is the wavelength at which the grating is most efficient and the operating range is nominally from two thirds to twice the wavelength blaze. For example, a grating with a blaze wavelength of 500 nm would therefore be suitable for operation over the 330 to 1000 nm region. The actual useful range also depends on the wavelength range of the detector used and the spectral characteristics of the source being examined (Hecht 1989).

5.4.2 Detectors

Photon detectors produce, under perfect conditions, a single response element for a single photon. The response is very rapid so these detectors have the potential of following fast changing radiation levels.

The single response elements can be classified as photoemissive or semiconductors. In either case, the net result is either a change in current flow or voltage level that can then be processed by amplifiers and other electronics into a display or for recording.

a) Photoemissive detectors

A commonly used photoemissive detector is photomultiplier tube (PMT) in which light interacts directly with the electrons in the detector material. An absorbed photon frees an electron and the surplus energy gets converted into kinetic energy of an electron. Electrons with sufficient kinetic energy will escape from the surface of the detector material. The electrons emitted in this way produce a cathode photocurrent in the PMT. An applied voltage causes the electrons to flow towards the anode, creating a voltage that is proportional to the light intensity over 6 to 8 orders of magnitude. The electron multiplier part of a PMT amplifies the photocurrent by secondary emission (Fig. 5.5). This is a low noise process that produces currents that are orders of magnitude larger that the initial photocurrent. Photomultpliers are more sensitive that any other detector in the 200 to 800 nm regions (Fig. 5.8).

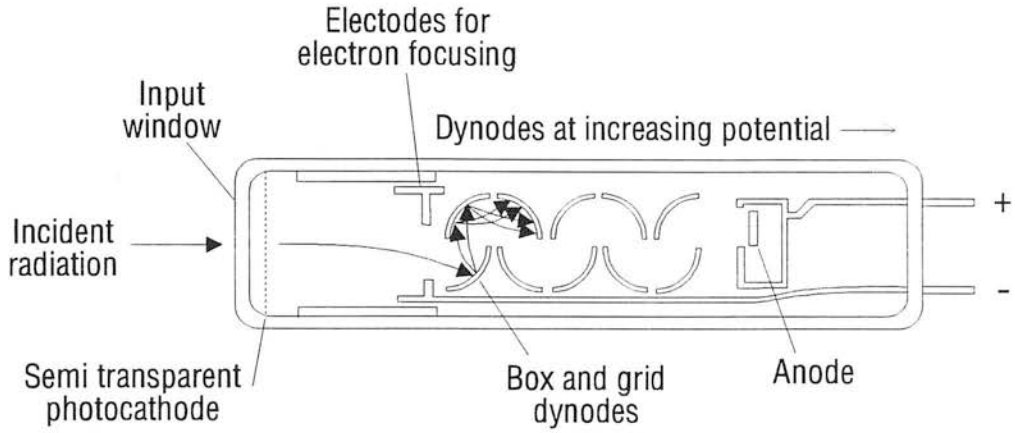

Fig. 5.5 Schematic diagram of a photomultiplier tube (connections and resistor network omitted for clarity). After Oriel Corp. 1994.

b) Semiconductor detectors

Silicon photodiodes are the most common detectors of light used in instrumentation. The spectral response extends from 400 to 1100 nm (Fig. 5.8). Figure 5.6 shows the typical structure of a silicon photodiode. Photons pass through the thin top layer to generate electrons and holes near the junction. The junction is a region depleted of current carriers, both electrons and holes, by the gradients of the potentials associated with the energy bands. It is formed between the p and n type silicon. The junction drives holes into the p material and the electrons into the n material. This results in a voltage difference between the two regions, and if they are connected by external circuitry, a current. This form of junction is called a photovoltaic detector.

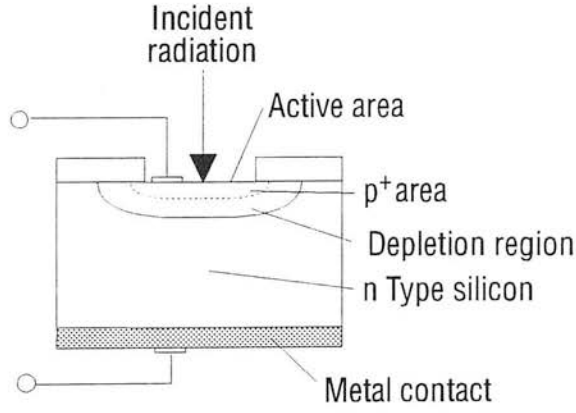

Fig. 5.6 Model of a silicon photodiode (after Oriel Corp. 1994).

The junction detector can also be used in photoconductive mode. In photoconductive detectors, absorbed incident photons produce free charge carriers. These change the electrical conductivity of the detector. An applied voltage, or bias, causes a current to flow which is proportional to the photon irradiance (Fig. 5.7).

Germanium is an example of this type of detector and has a spectral response from 600 to 1900 nm (Fig. 5.8).

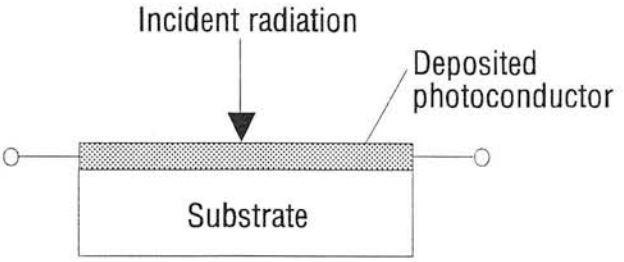

Fig. 5.7 Schematic of a photoconductive detector (after Oriel Corp. 1994).

Photon detectors produce at most one response element, before any amplification, per incoming photon. The energy carried by individual photons is inversely proportional to their wavelength. Therefore, for the same radiant power, the photon flux is much lower in the UV than in the IR. Accordingly, the response of a photon detector is significantly lower in the UV part of the spectrum than in the IR. Detector performance is evaluated by the spectral response and the quantum efficiency; the percentage of the incoming photon flux that is being converted into electrical signals. One hundred per cent quantum efficiency is never obtained, and efficiency is lost at short wavelengths. Some of the reasons are outlined below (Oriel Corp. 1994).

1. All the detection mechanisms are wavelength dependent; that is, there is a peak in responsivity with a fall off at both long and short wavelengths. The long wavelength (low photon energy) cut-off occurs because there is a certain minimum photon energy required to cause photo emission, to produce charge carriers or to generate hole-electron pairs.

2. The short wavelength cut-off is a function of two effects.

a) The responsitivity, in terms of power, drops off because there are fewer short wavelength photons per watt.

b) At the extreme short wavelength end, the energetic photons may no longer be absorbed in the sensitive region. Detector windows, or surface coatings on semiconductors are strong absorbers of UV.

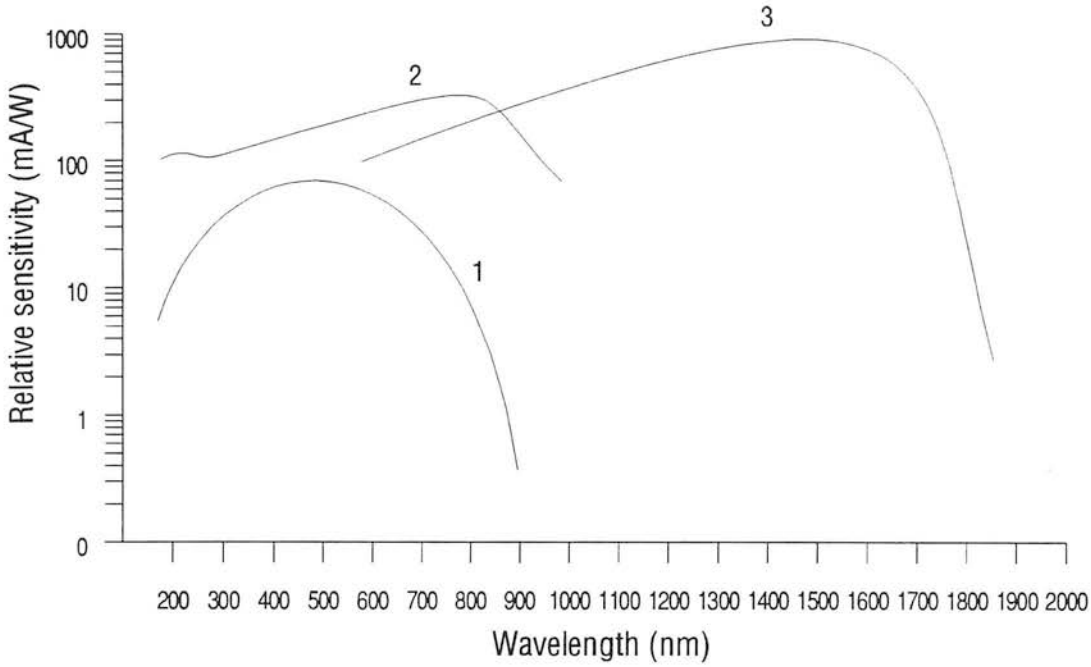

Fig. 5.8 Spectral responses of PMT (1) uncooled silicon photodiode (2) and uncooled germanium photodiode (3). Note that while the PMT appears to be less sensitive than silicon or germanium the graph shows PMT with no gain, the silicon photodiode with a gain of $15 \cdot 10^6$ V/A and the germanium photodiode with a gain of $2 \cdot 10^6$ V/A.

5.4.3 Fibre optic light guides

The first spectrophotometers to be developed relied on fixed lenses to focus light onto a sample and to measure the intensity of reflected or transmitted light. The use of fixed lenses have been largely superseded by flexible fibre optic light guides that are more versatile than lenses for transmitting light.

Fibre optic light guides consist of a large number of transparent fibres bound together in bundles large enough to transmit a usable quantity of light. Fibres are available in diameters from about 2 μm to 6 mm, but are seldom used in sizes much smaller than about 10 μm (a human hair is roughly 50 μm in diameter). Light incident on the end of the fibres is internally reflected along it. As long as the wavelength of the ray does not exceed the diameter of the fibre, the ray will pass along the fibre according to the law of specular reflection (Fig. 5.9). A light ray may undergo several thousand reflections per metre before exiting at the other end (Hecht 1989).

The smooth surface of a single fibre must be kept clean of moisture, dust, etc. if there is to be no leakage of light. Similarly if large numbers of fibres are packed in proximity, light may leak from one fibre to another in what is known as cross-talk.

For these reasons it is customary to enshroud each fibre in a transparent sheath of lower refraction index called a cladding (Hecht 1989).

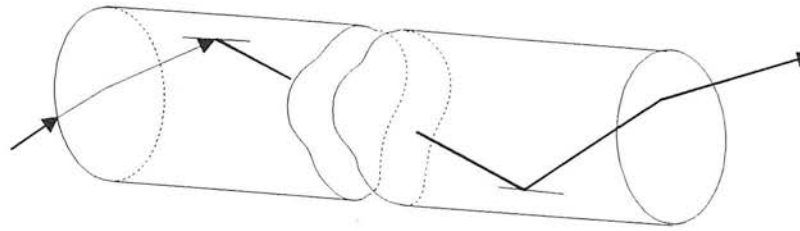

Fig. 5.9 Light rays reflected within a fibre optic light guide (after Hecht 1989).

If no attempt is made to align the fibres in an ordered array they form an incoherent bundle. For example, the first fibre in the top row of a bundle at the entrance face may have its terminus anywhere in the bundle of the exit face. These flexible light carriers are relatively easy to make and inexpensive. Their primary function is simply to conduct light from one region to another (Hecht 1989).

The composition of the fibres needs to be chosen according to the wavelength range under investigation as different optical materials have different transmission characteristics. For the collection of UV spectra, quartz or UV grade fused silica has to be used as glass attenuates light below 400 nm (Appendix A).

Fibre optics can be used in a variety of ways to transmit light to a sample and return reflected light to a monochromator. One of the simplest methods is a bifurcated fibre optic light guide that has the transmitting and collecting fibres combined into a single unit (Fig. 5.10). The transmitting and collecting fibres can be randomly distributed, or the transmitting fibres may form a central core with the collecting fibres around it.

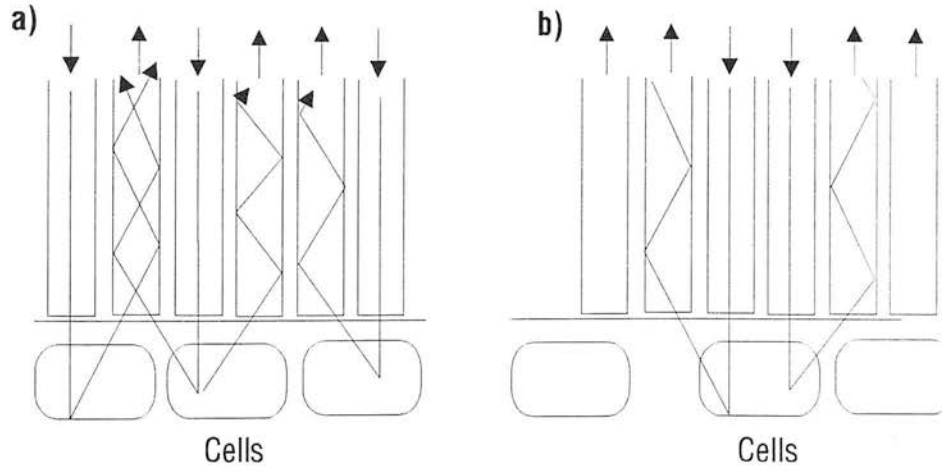

Fig. 5.10 Two common bifurcated fibre optic light guides: a) Randomly distributed transmitting and receiving fibre optic fibres and b) transmitting fibres in centre with receiving fibres at periphery. In reality, a fibre optic cable is composed of hundreds of fibres.

5.4.4 Light sources

Light sources are chosen according to whether the UV, visible or NIR is to be investigated. Deuterium lamps emit radiation from 180 to 400 nm and are the preferred source for UV spectroscopy because it ensures the best signal to noise ratio for UV measurements, and has negligible visible to NIR output (Oriel Corp. 1994).

Quartz tungsten halogen lamps emit radiation from 240 to 2700 nm and have the advantage of being easy and inexpensive to operate and use. They also have a stable and high visible output (Oriel Corp. 1994).

Both of these light sources will be used in this thesis to capture spectral signatures from 250 to 1850 nm.

5.4.5 The Monolight spectrophotometer

In this thesis, a Monolight spectrophotometer (Rees Instruments Ltd., UK) is used to collect reflectance spectra. The monochromator and optical detector in the system can be optimised to detect a broad band of the electromagnetic spectrum from 200 to 15000 nm, although for the detection of bruising, wavelengths from 250 to 1850 nm will be used. The spectrophotometer can also acquire spectral signatures very quickly and with a high degree of precision.

The monochromator uses a continuously rotating diffraction grating driven by an electronically controlled d.c. motor. Light from a sample is transmitted to an input slit, dispersed into its component wavelengths by the diffraction grating and then sequentially passed to an output slit, where a photo sensitive detector converts the optical signal into a corresponding electrical signal. The signal is amplified and then sent to the system controller for processing. An IBM AT computer with Spectral Analysis software controls the configuration of the system controller and saves spectral data. As can be seen in Fig. 5.11 the scanning monochromator also generates a pulse train that is used by the 6800 system controller to produce an accurate wavelength measurement scale.

The slit plate controls the wavelength resolution for a given grating and detector. The slit plate has slits of 0.09, 0.18, 0.45 and 0.9 mm wide. The smaller the slit width the greater the wavelength resolution, but it also gives the lowest light input to the monochromator.

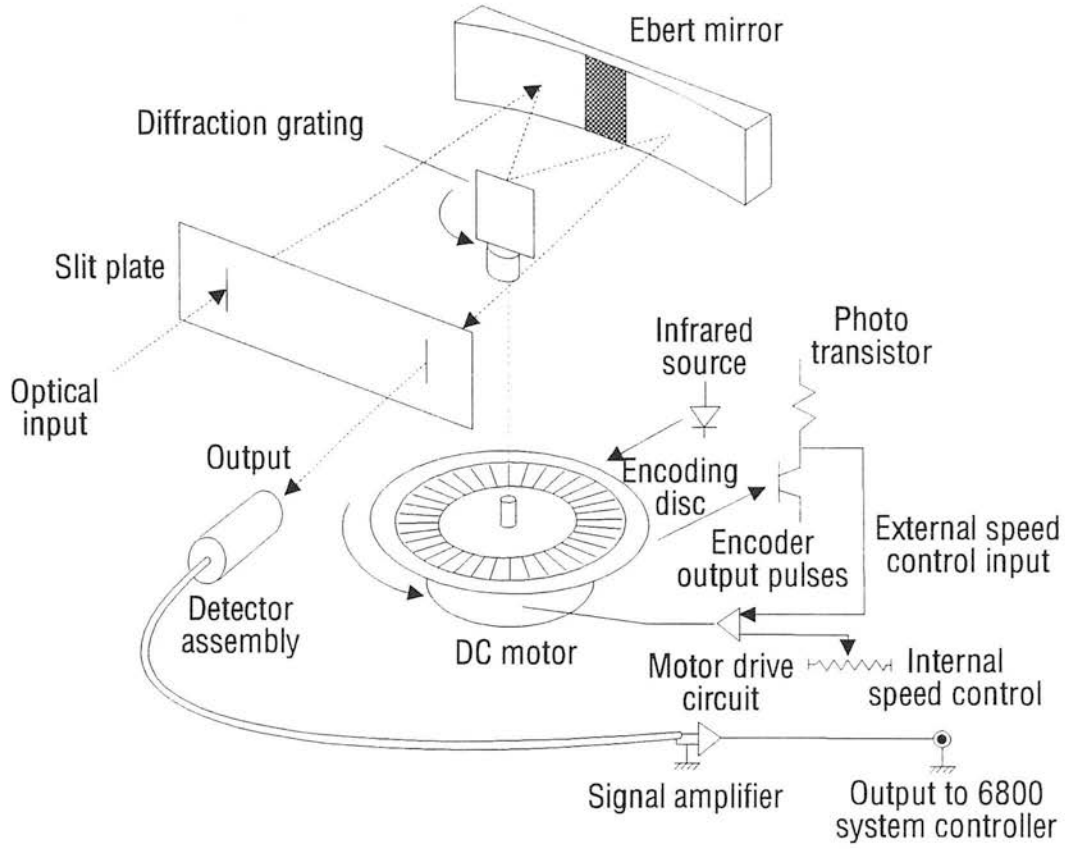

Fig. 5.11 Schematic block diagram of the Monolight scanning monochromator (after Rees Instruments Ltd. 1992).

The Monolight spectrophotometer was used in the next few chapters to determine if the production of pigments and other cellular changes associated with bruising could be non-invasively and rapidly detected.

Chapter 6

Determination of light penetration depth in potato tuber tissue

Before taking reflectance spectra from unpeeled and peeled tubers its was necessary to determine the depth that light might pass into potato tissue and be reflected back to the surface. Until this depth is known then the hypothesis that bruising could be detected non-invasively with reflectance spectrophotometry is unfounded.

The Monolight spectrophotometer was used to measure the intensity of transmitted light in a sample of potato tissue from 400 to 700 nm. By varying the thickness of potato tissue, the point at which the transmission became undetectable was determined. This point is the maximum depth of light penetration for this combination of light source, fibre optics and detector. The depth of tissue from which the body reflectance is reflected is assumed to be half the maximum depth of transmitted light. This assumption is based on the idea that if there was a perfect reflector in the potato tissue, a transmitted beam of light would pass through the tissue until it reached the reflector and then pass out of the tissue at the initial interface. This is a simplified model of what happens in reality, but it may indicate that body reflectance can come from the cortical tissue where bruising occurs.

6.1 Methods

Tubers of the varieties Desiree, Pentland Dell and Record were hand dug, washed and stored at 4°C. These varieties were chosen to give a comparison between the red skin of Desiree and the yellow-brown skin of Pentland Dell and Record. Record and Pentland Dell were selected as these are widely used in the processing industry for chip and crisp manufacture. Record was selected because of its susceptibility to bruising.

Sections of unpeeled and peeled tissue were taken from the cortical tissue and cut into cubes. A Vernier gauge was used to measure the thickness of tissue.

Wavelengths from 400 to 700 nm were collected with a Monolight 6112 monochromator and 6118 photo multiplier tube (Rees Instruments Ltd., UK). A fibre optic light guide (4 mm diameter) transmitted light from a 150 watt halogen light source (FOT 150; All Inspection NDT. Ltd., UK) to a sample of potato tissue. Another fibre optic light guide (4 mm diameter) was placed on the other side of the sample to collect the transmitted light and relay it to the monochromator. The fibre

optic light guides and tissue sample were held in an adjustable clamp that allowed different thicknesses of tissue to be inserted (Fig. 6.1).

A reference reading was taken of the air gap without the tissue sample, and then a transmission measurement was taken of a sample to create a spectrum. The ratio of sample to air gap measurements constitutes the 'normalised' or relative transmission spectrum. The maximum depth of light penetration in potato tissue is measured at the point where the percentage transmission is zero or close to zero.

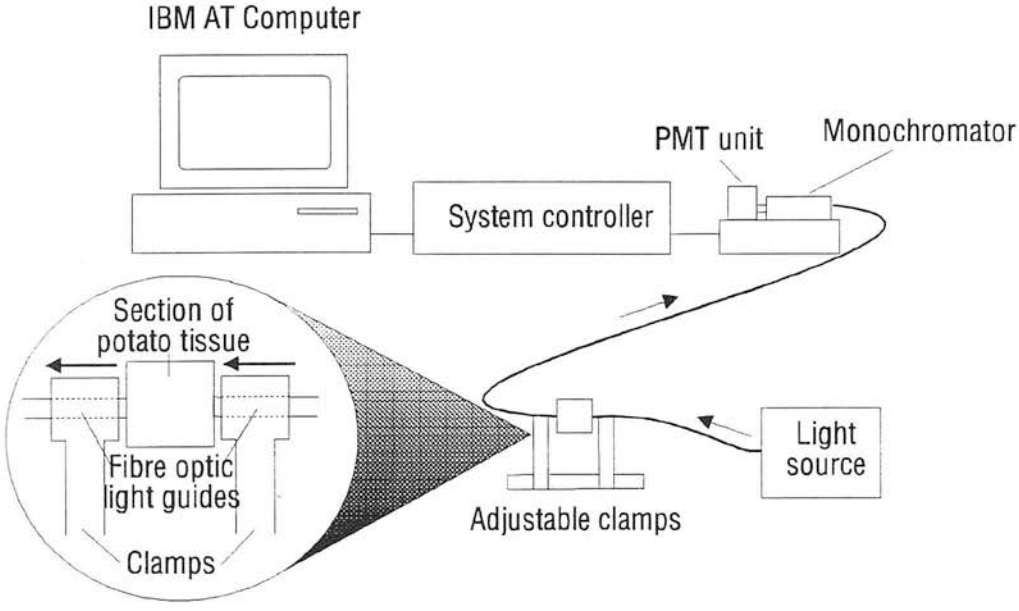

Fig. 6.1 Schematic diagram of experimental set-up for transmission measurements.

6.2 Results

The relationship between percentage light transmission and depth of tissue is non-linear for unpeeled and peeled tubers. In unpeeled Desiree, Pentland Dell and Record tubers the maximum transmission depth of light is approximately 9 mm at 700 nm and 3 mm at 400 nm (Fig. 6.2).

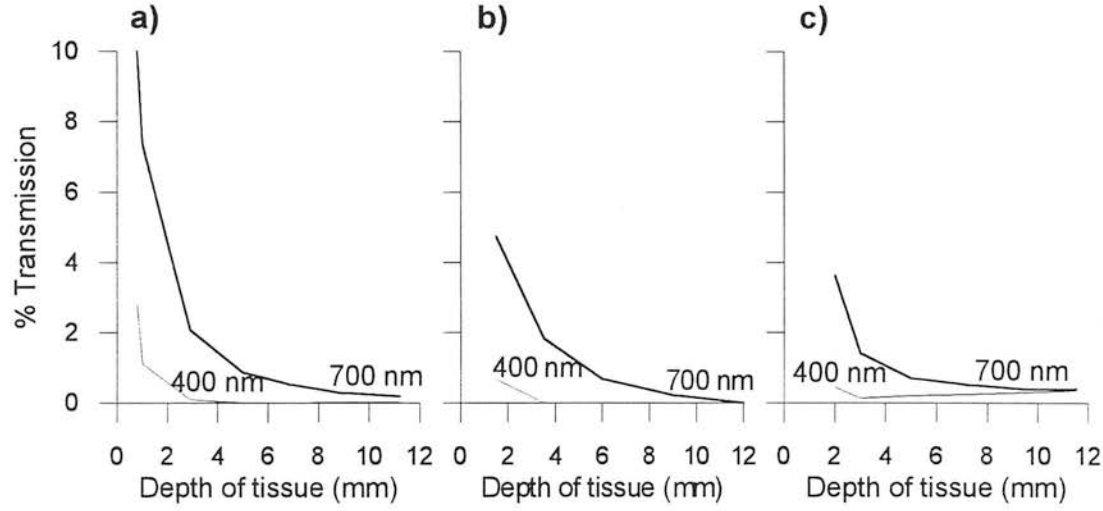

Fig. 6.2 Percentage light transmission in unpeeled a) Desiree b) Pentland Dell and c) Record tubers at 400 and 700 nm.

In peeled tubers, the maximum transmission depth is greater than unpeeled tubers, particularly at 400 nm. In Desiree, Pentland Dell and Record tubers the depth is approximately 12 mm at 700 nm, and 8 mm at 400 nm (Fig. 6.3).

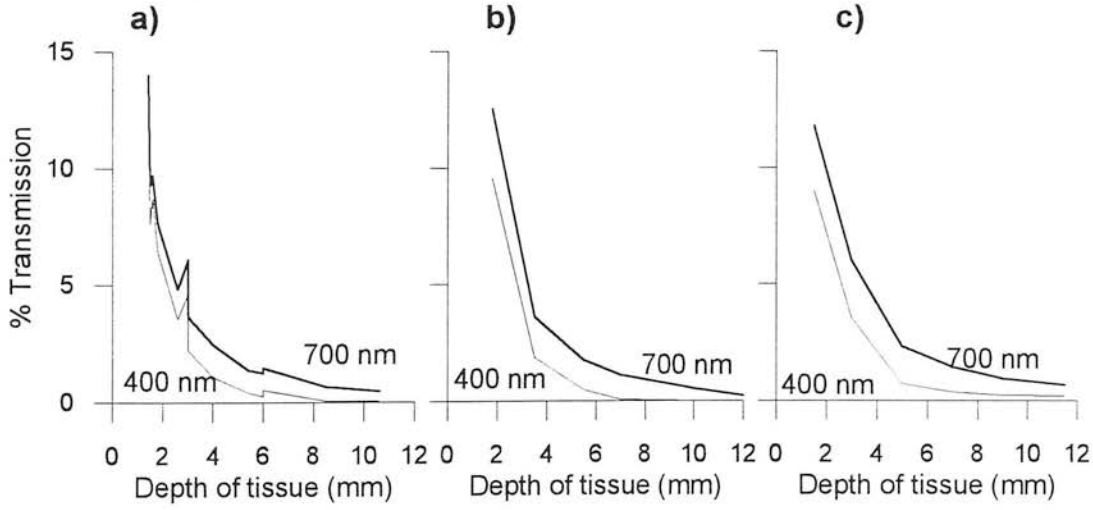

Fig. 6.3 Percentage light transmission in peeled a) Desiree b) Pentland Dell and c) Record tubers at 400 and 700 nm.

If the depth of body reflectance is taken to be half the maximum transmission depth, then body reflectance can be assumed to detect tissue approximately 1.5 to 4.5 mm deep in unpeeled tubers, and 3.5 mm to 6 mm in peeled tubers.

6.3 Discussion

The distance that visible light is transmitted through potato tissue has been measured in unpeeled and peeled tubers. The relationship between percentage transmission and depth of tissue is non-linear and appears to follow an exponential decrease with an increased depth of tissue. In unpeeled and peeled tubers the longer the wavelength, the greater the depth of tissue through which light can be transmitted.

However, the estimate of depth may be optimistic as the reflection of remitted light involves scattering through a 360 degree angle and thus results in greater light losses at the detector. An experiment was conducted in which reflectance measurements were taken of unpeeled and peeled tubers with a piece of blue coloured card embedded at different depths from the surface. Spectra were taken with the card present and absent to try and determine the depth at which the card could no longer be detected. While this experiment imitated the principles of reflectance spectrophotometry more accurately than the transmission method, it was difficult to determine the maximum depth of light penetration. It was found that the blue card absorbed light across a broad wavelength band and that the deeper the card was in the tuber, the harder it became to detect. However, in general it was observed that the longer the wavelength the greater the depth of penetration, and that the depth of light penetration was slightly less than those obtained with transmission spectrophotometry.

Depth of tissue penetration with either transmitted or reflected light must depend on several factors, for example, whether the skin has been washed, or if there is disease present. For washed, healthy tubers, these results suggest that bruising might well be detected by body reflectance techniques if the bruising is not greater than 3 mm deep for unpeeled samples and not greater than 6 mm deep in peeled samples. This hypothesis will be tested further in the next chapter, when reflectance spectrophotometry will be used to determine if bruising can indeed be non-invasively detected in the sub-surface tissue.

Chapter 7

Non-invasive detection of bruising in potato tubers using reflectance spectrophotometry

7.1 Introduction

The use of reflectance spectrophotometry to quantify bruising would be a powerful technique because it would be non-invasive and non-subjective. It could reduce the financial loss associated with bruising in two ways.

- At present, bruised tubers usually pass unnoticed through quality control. Bruised tubers reaching the processor and consumer can then result in potato wastage or more seriously in a loss of confidence in the producer. If bruised tubers could be detected non-invasively with reflectance spectrophotometry, they could be automatically rejected before going to market.

- Quality assessment can be time consuming and costly because of the need to peel or slice tubers before detecting bruising. In addition, because of its destructive nature, this procedure can only be done on a small sample of tubers. The non-invasive technique of reflectance spectrophotometry could reduce the need for peeling and make quality assessment less subjective.

Reflectance spectrophotometry from ultraviolet (UV) to near infrared (NIR) was used to non-invasively measure the body reflectance of unbruised and bruised tubers. The aim was to find regions of the electromagnetic spectrum that are sensitive to the changes in pigmentation and cell structure associated with bruising. These regions were defined using Stepwise Discriminant Analysis which selects wavelengths that best separate bruised and unbruised tubers. Discriminant analysis also generates linear regression equations that can predict if a tuber taken from an unknown sample is bruised.

7.2 Methods

7.2.1 Spectral data acquisition

The Monolight spectrophotometer (section 5.4.5) was used to acquire relative reflectance spectra. Wavelengths from 250 to 700 nm were collected with a 6112 monochromator and 6118 photo multiplier tube. Wavelengths from 700 to 1850 nm were collected with a 6102 monochromator and 6111 germanium detector.

For visible to NIR wavelengths a randomly distributed bifurcated fibre optic light guide (4 mm diameter) transmitted light from a 150 watt halogen light source (FOT 150; All Inspection NDT. Ltd., UK) to the sample, and returned reflected light to the monochromator). An aluminium holder was placed on the measuring end of the fibre optic cable to ensure that for each sample the incident radiation was 90° to the surface of a sample (Fig. 7.1). For spectral acquisition in the UV, the fibre optic light guide had to be 1 mm from the surface of the sample. If the fibre optic light guide was in direct contact with the sample, the light was attenuated too strongly.

For ultraviolet spectral acquisition, a bifurcated fibre optic light guide with UV grade synthetic fused silica and deuterium lamp (Rees Instruments Ltd, UK) was used.

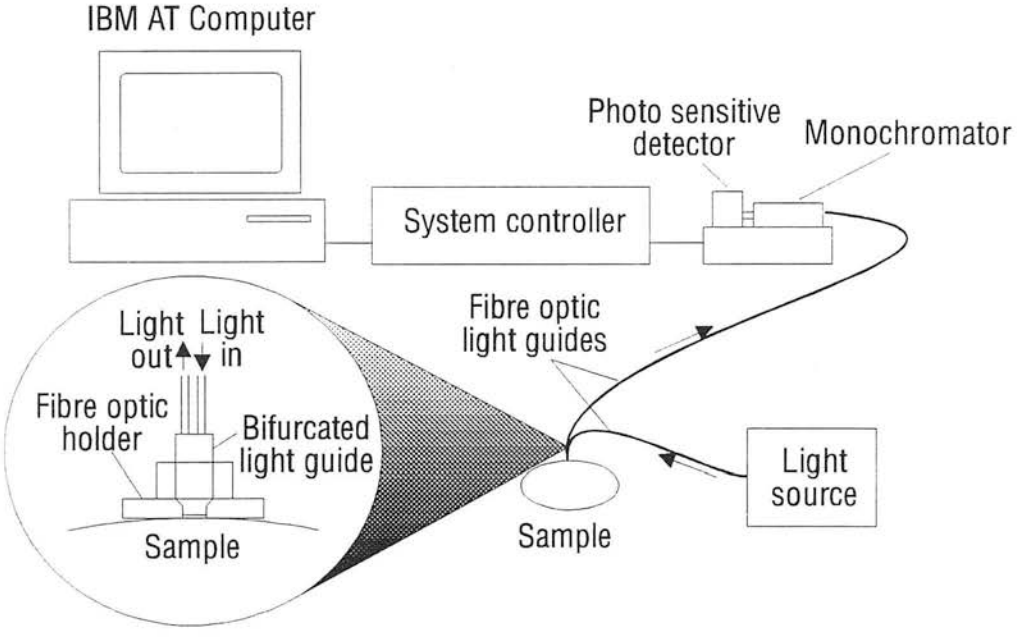

Fig. 7.1 Schematic diagram of experimental set-up.

The spectrophotometer was used in reflectance relative mode to take the average percentage reflectance of 200 spectra per sample. To create a spectrum, a reference reading was taken from a white surface (Spectralon; Labsphere, North Sutton, UK) and then a measurement was taken of a sample. The ratio of sample to reflectance measurements then constitutes the 'normalised' or relative reflectance spectrum. A reference reading was taken for every set of thirty spectra.

7.2.2 The SCAE drop tester

The SCAE drop tester (Fig. 7.2.) was used to give a consistent impact to tubers (McRae *et al.* 1976). The operation of this instrument is simple. Tubers are placed

onto a handle and held there by three spikes. When the handle is lifted, the spikes are retracted from the tuber and it drops onto the base of the apparatus. The height of the handle can be adjusted to vary the force of impact. For **all experiments in this thesis** a height of 200 mm was used which gave a sufficiently large impact to initiate bruising but did not usually cause a tuber to split or crack. This height is measured from the bottom of the dropper to the base of the handle.

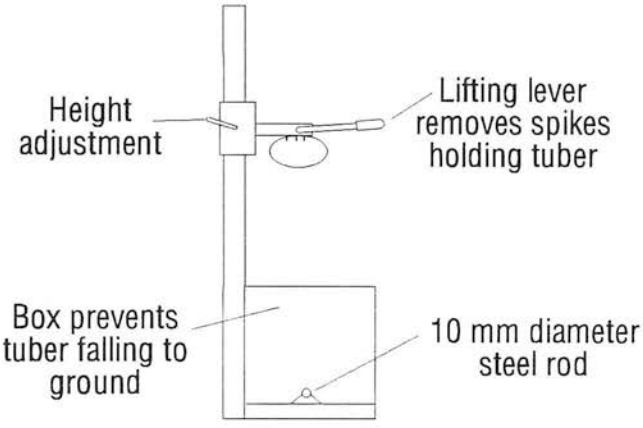

Fig. 7.2 Cross section of SCAE drop tester for impacting tubers.

A 10 mm diameter steel rod at the base of the apparatus simulated a web rod (a conveyor of web rods separates tubers from soil on a potato harvester). By dusting the steel rod with chalk, the site of impact was known. The site of impact is marked with a waterproof marker and the chalk wiped from the tuber with a damp cloth.

The temperature of tuber tissue at the time of impact is an important factor affecting the susceptibility of a tuber to bruising (section 3.3.5). Prior to impact, a temperature probe was used to ensure the temperature of a tuber was below 9°C.

7.2.3 Samples

Tubers of the varieties Desiree, Pentland Dell and Record were hand dug, washed and stored at 4°C. After impacting with the SCAE drop tester the samples were placed in a 'hot box' at 40°C, relative humidity 95%, for 16 hours.

A sample was classified as bruised if there was any discoloration visible after peeling. These bruises were further classified as shatter and blackspot bruising (section 2.1).

A spectrum was first taken from an unpeeled tuber and then the tuber was peeled and another spectrum taken. One hundred tubers per variety and per wavelength region were used. For three wavelength regions and three varieties, this gave a total of 900 tubers and 1800 spectra.

7.2.4 Data analysis - the use of first derivatives

Spectral data were converted into ASCII format and the first derivatives calculated using a program written in BASIC (Appendix B). The first derivative is a measurement of the slope of the spectrum, or the rate of reflectance change:

$$\frac{R\lambda_1 - R\lambda_2}{\lambda_1 - \lambda_2}$$

where; $R\lambda_1$ and $R\lambda_2$ denote the percentage relative reflectance values at two adjacent wavelengths, and λ_1 and λ_2 are the respective wavelength values. First derivative spectra are quantified as reflectance per nm (O'Haver 1979).

Analysis of derivative spectra has several advantages over analysing the untransformed spectra. Since derivative spectra measure spectral slope they are uniquely insensitive to uncontrollable baseline shifts in the untransformed spectrum (Fig. 7.3). Shifts in the baseline can occur due to varying angles of incident light and surface defects (O'Haver 1979).

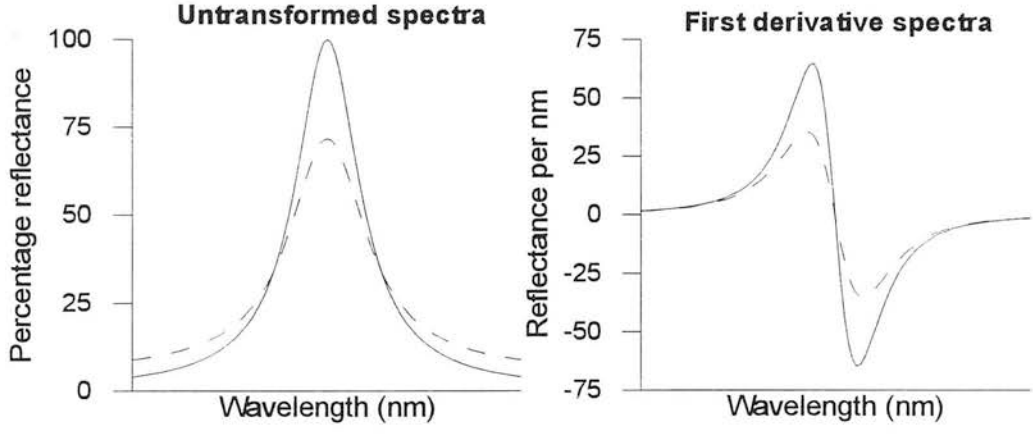

Fig. 7.3 Hypothetical symmetrical spectrum and its first derivative (after 'O'Haver 1979). Note that in the first derivative spectra the point at which the spectrum crosses the x-axis corresponds to the peak seen in the untransformed spectrum. In addition, note that a shift in the baseline in the untransformed spectra is eliminated in the first derivative spectra.

7.2.5 Discriminant analysis

The untransformed and first derivative spectra were analysed using BMDP program 7M, Stepwise Discriminant Analysis (BMDP Statistical Software, Inc., California). Program 7M (Appendix C) finds the combination of variables that best predicts the group category to which a case belongs. The combination of predictor variables is called a classification function. The classification function is linear and can be used in the classification of new cases whose group membership is not known (Dixon 1992).

In this experiment, the aim was to find the best combination of wavelengths that predicted whether a tuber was bruised or unbruised. Half of the spectra from bruised and unbruised tubers were used to determine the classification function (denoted as 'known' tubers) and the remainder (denoted as 'trial' tubers) used to determine the success of the classifying a tuber as bruised or unbruised when the classification of a tuber was unknown to the discriminant program.

Program 7M selects the variables used in computing the linear classification functions in a stepwise procedure. At step zero, before any variable is entered into the classification function, the 'F-to-enter' for a variable corresponds to the F-statistic computed from a one-way analysis of variance (ANOVA) for the groups used in the analysis. The variable with the largest 'F-to-enter' at step zero enters the classification function.

After step zero, the conditional F ratios are computed for each variable. The conditional F ratio is the ratio of the between groups sums of squares and the within groups sum of squares, associated with a particular variable. It tests the difference between the group means and measures how much a given variable contributes to the group differences, given the variables already entered the equation. Large values of F correspond to well-separated groups (James 1985).

Therefore, at each step the variable that adds the largest change to the F ratio is entered into (or the variable that adds the least is removed from) the discriminant function. Any variable that enters at one step because it produces a maximum change in the F-ratio, could be removed at a later stage because it is non-significant. The variable selection procedure is stopped when none of the remaining variables have an F value greater than four (Hahn and Muir 1993).

For each group, the corresponding function is the linear combination of variables that best discriminates that group from the rest of the cases. In order to understand how the linear classification separates groups it is necessary to understand the multivariate distribution.

The normal distribution describes the probability density distribution for a single variable and is specified by its mean μ and its standard deviation σ:

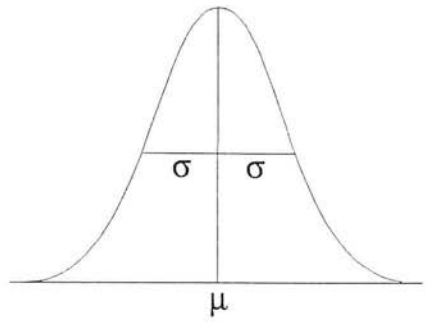

When more than one variable is involved then the multivariate generalisation of the normal distribution has to be used - the multivariate normal distribution. Instead of a single mean controlling the location of the distribution there is now one mean for each variable making up a 'mean vector' (James 1985). The description of the way the distribution spreads is also more complex. The multivariate equivalent of the standard deviation is the 'covariance matrix'. For two variables X_1 and X_2, the mean vector and covariance matrix are:

$$\text{mean} = \begin{bmatrix} \mu_1 \\ \mu_2 \end{bmatrix} \qquad \text{covariance} = \begin{bmatrix} \sigma_{11}^2 & \sigma_{12}^2 \\ \sigma_{21}^2 & \sigma_{22}^2 \end{bmatrix}$$

From this information it is possible to draw a diagram (Fig. 7.4) of the distribution. It is centred on the mean vector and 'spreads' by $2 \cdot \sigma_{11}$ in the X_1 direction and $2 \cdot \sigma_{22}$ in the X_2 direction.

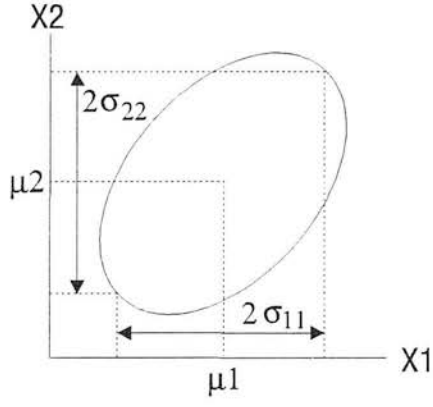

Fig. 7.4 The bivariate normal distribution (after James 1985) takes the form of an elliptical area. The ellipse defines the 95.44% probability of any value of X_1 and X_2 occurring within 2 standard deviations (Sokal and Rohlf 1981).

The off-diagonal terms, σ_{12} and σ_{21}, are equal and measure the 'association' of the two variables. The on-diagonal terms, σ_{11} and σ_{22}, affect the spread in the X_1 and X_2 directions and the off-diagonal terms affect the spread between these two directions. A trivariate normal would cluster in ellipsoidal groups and so on into

higher dimensions. Discriminant analysis assumes that the variables have a normal distribution with equal covariance matrices (James 1985).

When considering two groups and two variables the sample space of the two groups could appear as follows:

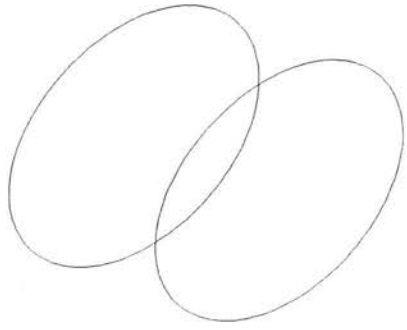

The aim of discriminant analysis is to divide these two groups with a classification function. This function is linear and separates groups using flat surfaces or 'hyperplanes'. In two dimensions a hyperplane is a straight line, in three it is a flat plane, in four it is a volume, and in dimensions higher than four it is not possible to imagine but it possesses many of the properties of the straight line and plane (James 1985).

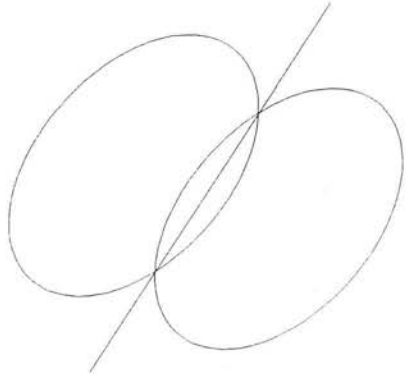

The classification function takes the form of a multiple regression equation:

$$Y = \text{constant} + (\text{coefficient } 1 \cdot \text{variable } 1) + (\text{coefficient } 2 \cdot \text{variable } 2) \text{ etc.}$$

The implicit Y value in the regression equation is one or zero, depending on whether this observation is the correct group or not. Hence, a predicted value near zero indicates that the observation is not in the group, while a value near one indicates a strong possibility that this observation is in the group. There is nothing to prevent these predicted values from being greater than one or less than zero. They are not estimated probabilities.

Program 7M evaluates the functions for each case and assigns the case to a group. A summary table is given along with the percentage of correct classifications. The classification matrix may provide an optimistic estimate of the probability of classification. Therefore, the program also classifies each case into a group with the highest Y value according to classification functions computed from all the data except the case being classified. This is a special case of the general cross validation method in which the classification functions are computed on a subset of cases, and the probability of classification is estimated from the remaining cases. When each case is left out in turn, the method is known as the jack-knife (Lachenbruch and Mickey 1968).

In addition to evaluating the success of the classification function by the percentage of tubers correctly classified as bruised or unbruised, the probability of this classification occurring by chance is evaluated by Wilk's Lambda, the multivariate extension of R-squared. Wilk's Lambda reduces to $1-R^2$ in the two group case. It is interpreted in a way exactly opposite to R-squared. It varies from one to zero. Values near one imply low predictability, while values close to zero imply high predictability.

In this experiment, a successful classification is one in which a large percentage of tubers are correctly classified as bruised as unbruised. The meaning of 'large' is evaluated by obtaining a probability (p) less than 0.001 for Wilk's Lambda, that is, the classification function has a high predictability. A p-value greater than 0.001 implies that the classification could have occurred by chance alone (Dixon 1992).

7.3 Results - Unpeeled tubers

Raw, untransformed spectra from bruised tubers appear to have a lower reflectance than unbruised tubers from 250 to about 800 nm. From 800 to 1850 nm, bruised tubers appear to have a higher reflectance than unbruised tubers (Fig 7.5).

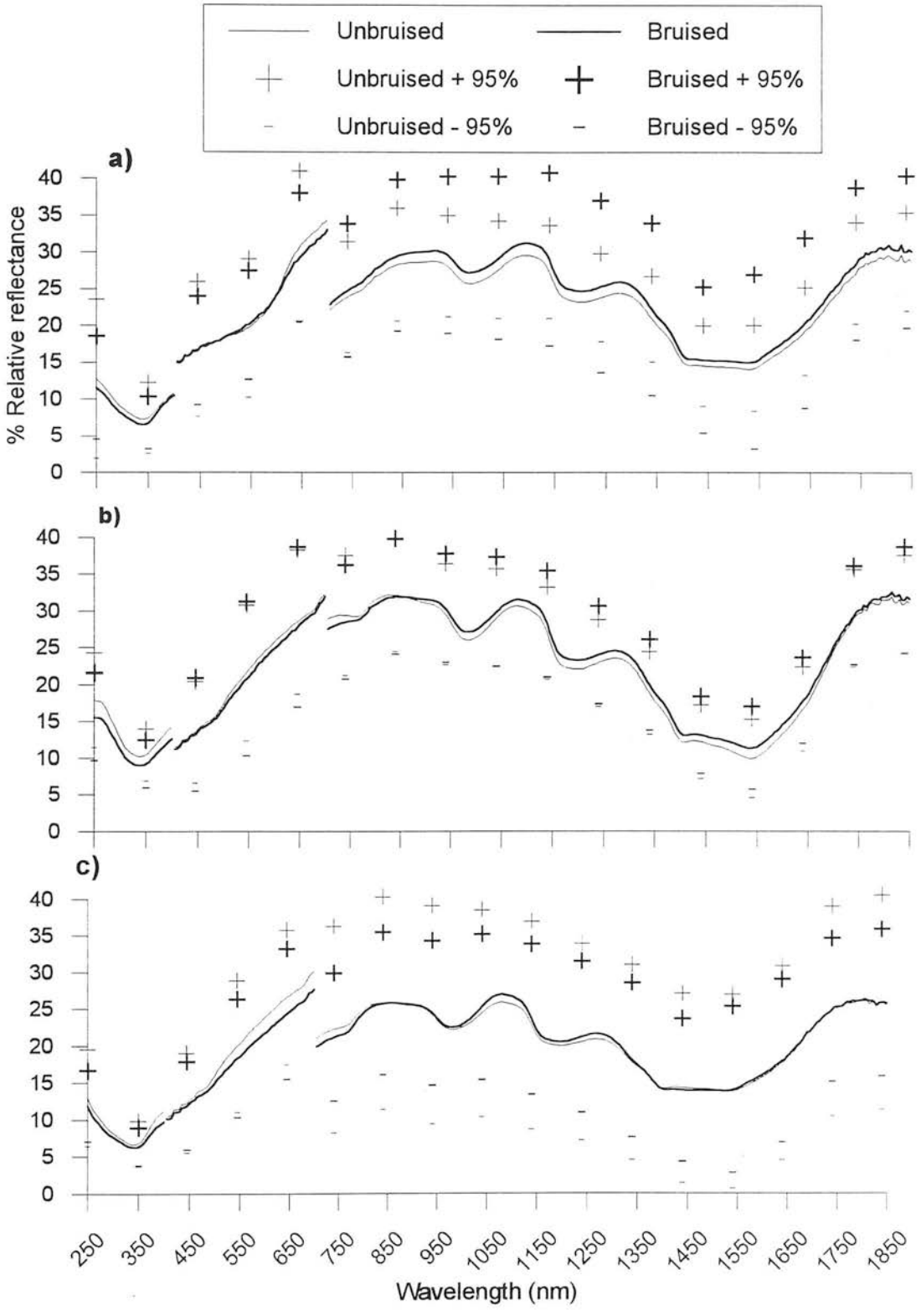

Fig. 7.5 Mean and 95% confidence limits of untransformed spectra from unbruised and bruised unpeeled tubers a) Desiree b) Pentland Dell and c) Record.

There would appear to be differences between untransformed spectra of bruised and unbruised tubers across the whole light spectrum. However, the first derivative spectra reveal few parts of the spectrum where there is a change in slope between bruised and unbruised tubers (Fig 7.6).

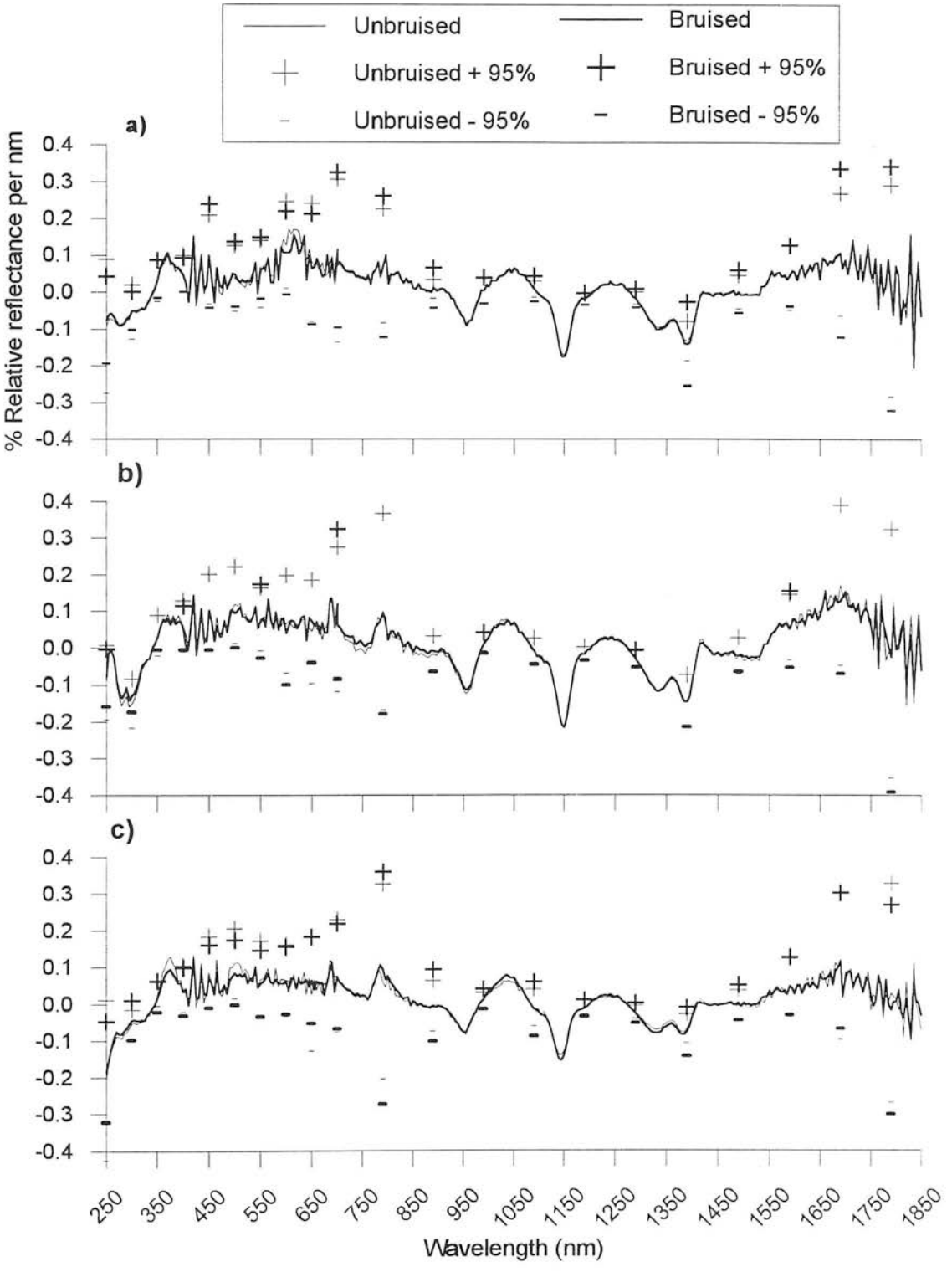

Fig. 7.6 Mean and 95% confidence limits of first derivative spectra from unbruised and bruised unpeeled tubers a) Desiree b) Pentland Dell and c) Record.

Potato variety appears to have an affect on reflected light in the visible light spectrum. The red skin of Desiree gives a lower reflectance at 550 to 650 nm (Fig 7.5). The UV and NIR regions appear to be variety independent.

All varieties showed some shatter bruising with the highest level in Desiree (42%). Record had the most blackspot bruising, followed by Pentland Dell and then Desiree (Table 7.1).

Table 7.1 Percentage of bruised and unbruised tubers.

	Desiree	Pentland Dell	Record
Percentage of unbruised tubers	50	51	51
Percentage of bruised tubers	50	49	49
% Blackspot	58	76	80
% Shatter bruising	42	24	20

Discriminant analysis of the first derivative spectra selected wavelengths that were more variety independent, compared to wavelengths selected from untransformed spectra. These wavelengths were at about 290 nm, 550 to 630 nm, 880 to 840 nm, and 1400 to 1500 nm (Table 7.2). All the first derivative wavelengths selected correspond to changes in slope in the untransformed spectra.

Table 7.2 Wavelengths selected by discriminant analysis to separate unbruised and bruised unpeeled tubers from untransformed and first derivative spectra.

Spectra	Desiree	Pentland Dell	Record	All varieties
UV*				
Untransformed	330, 360	250, 350	none	285
First derivatives	360, 325	290, 350	290	290, 350
Visible*				
Untransformed	700, 635	575	700	700, 485
First derivatives	605, 660, 575	660, 405, 530	670, 605	605, 660, 610, 535, 425, 595, 490
NIR*				
Untransformed	1150, 1720, 950	710, 1780	710, 1780, 990	710, 1060, 1730, 1820
First derivatives	870, 1760, 1740, 1110, 960, 940, 1030, 1560	920, 1700, 1670, 1080, 1370, 1000, 1820, 1750	820, 1610, 1480, 1650	1470, 1370, 1460, 1740, 1780

* Shown in order that discriminant analysis selected wavelengths on basis that F value was >4.

The first derivative spectra generally improved the classification of 'known' tubers (Table 7.3). Analysis of the pooled spectra from all the varieties reduced the percentage classification for all the spectra. Spectra from the NIR gave the best success of classifying a 'known' tuber as bruised or unbruised, followed by the visible and then the UV spectrum.

Table 7.3 Percentage of 'known' unpeeled tubers correctly classified as bruised or unbruised.

Spectra	Desiree	Pentland Dell	Record	All varieties
UV				
Untransformed	86.7	68.1	none	71
First derivatives	82.2	74.5	56.5*	66.7
Visible				
Untransformed	72.5	62*	78.4	72.4
First derivatives	70.6	78	72.5	72.4
NIR				
Untransformed	83	80.4	93	80.1
First derivatives	97.9	87	86	76.5

* the classification is not significant: $p>0.001$ for Wilk's Lambda.

However, when the linear discriminant functions were used on a group of spectra whose classifications were unknown to the program, the classification of 'trial' tubers was only significant for the untransformed NIR spectra from Desiree, Pentland Dell and when spectra from all varieties were pooled (Table 7.4).

Table 7.4 Percentage of 'trial' unpeeled tubers correctly classified as bruised or unbruised.

Spectra	Desiree	Pentland Dell	Record	All varieties
UV				
Untransformed	64.4*	36.2*	none	63.2*
First derivatives	53.3*	53.2*	45.5*	55.1*
Visible				
Untransformed	48.9*	40*	55.1*	54.8*
First derivatives	55*	52*	34.7*	54.7*
NIR				
Untransformed	90.7	77.3	65.9*	71
First derivatives	47.8*	63.6*	54.5*	67.9*

* the classification is not significant: $p>0.001$ for Wilk's Lambda.

7.4 Results - Peeled tubers

From 250 to about 850 nm, bruised tubers appears to have a lower reflectance than unbruised samples. This trend is reversed from about 850 to 1850 nm (Fig. 7.7).

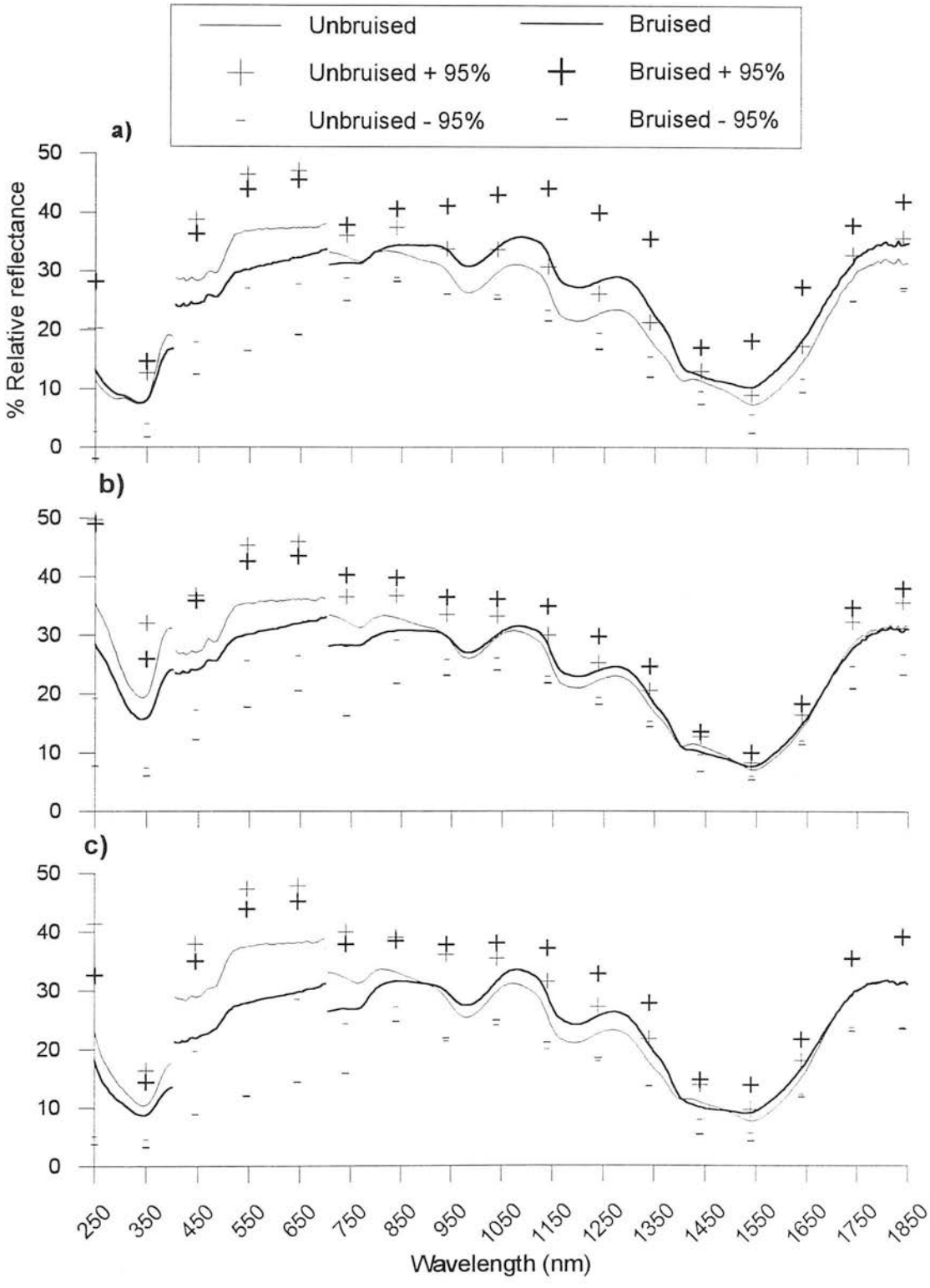

Fig. 7.7 Mean and 95% confidence limits of untransformed spectra from unbruised and bruised peeled tubers a) Desiree b) Pentland Dell and c) Record.

Although there appears to be large differences between untransformed spectra of bruised and unbruised tubers across the range, first derivative spectra reveal differences in only a few wavelength regions (Fig. 7.8).

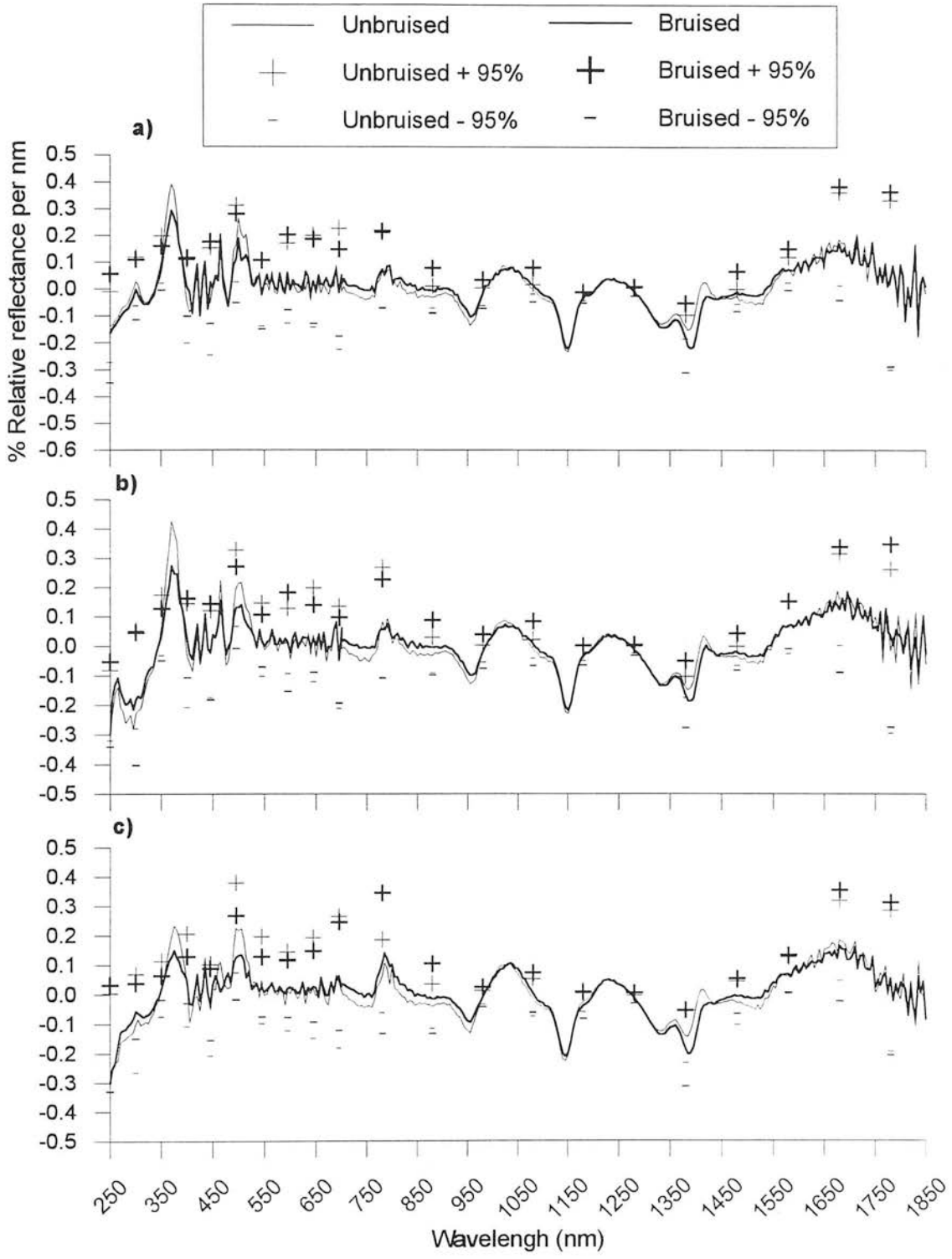

Fig. 7.8 Mean and 95% confidence limits of first derivative spectra from unbruised and bruised a) Desiree b) Pentland Dell and c) Record peeled tubers from 250 to 1850 nm.

Discriminant analysis selected wavelengths from first derivative spectra at about 380 nm, 480 to 510 nm, 635 to 660 nm, 710 to 780 nm, and 1000 to 1200 nm to separate unbruised and bruised tubers (Table 7.5).

Table 7.5 Wavelengths selected by discriminant analysis from untransformed and first derivative spectra to separate unbruised and bruised peeled tubers.

Spectra	Desiree	Pentland Dell	Record	All varieties
UV*				
Untransformed	380, 400, 255	390	275, 355	380, 400
1st derivatives	395, 260, 280, 305, 335	375, 255	345, 350, 375, 330, 400	375, 345, 395
Visible*				
Untransformed	510, 680	535, 695, 470, 400, 495	545, 640, 470	535, 665, 470
1st derivatives	500, 495, 435, 440, 485	505, 500, 410, 435, 415, 595	505, 590, 595, 645, 625, 585, 685, 515, 695	500, 495, 505, 435, 475
NIR*				
Untransformed	980, 1730, 1630	710, 770	710, 790, 1440	710, 740, 810
1st derivatives	740, 1280, 1830, 1640, 1790	840, 1000, 1700, 1560, 1030, 1740, 850, 1670	80, 74, 111, 105	730, 1530, 1430, 970, 850, 740, 1730

* Shown in order that discriminant analysis selected wavelengths.

When these wavelengths were used to discriminate between tubers whose classification was known to the discriminant analysis, the use of first derivative spectra gave a consistently better classification for the UV and NIR spectra. For the visible spectrum, analysis of untransformed spectra gave the best success of classifying a tuber as bruised or unbruised (Table 7.6).

Table 7.6 Percentage of 'known' peeled tubers correctly classified as bruised or unbruised.

Spectra	Desiree	Pentland Dell	Record	All
UV				
Untransformed	86.7	75	76.1	75.5
1st derivatives	91.1	68.8*	82.6	81.3
Visible				
Untransformed	90.2	82.4	90.2	89.5
1st derivatives	73.5	57.1*	57.1*	68*
NIR				
Untransformed	91.5	76.1	95.2	82.2
1st derivatives	95.7	93.5	95.2	86.7

* not significant; $p>0.001$ for Wilk's Lambda.

When the linear discriminant function was used on spectra whose classification was unknown to the discriminant analysis, the interpretation of the results is more complex. For Desiree tubers the best classification was from visible spectra. For Pentland Dell tubers, NIR spectra provided the best classification, and for Record, only the UV spectrum gave any classification results. When all the spectra were pooled, the untransformed visible and NIR spectra gave the best results (Table 7.7).

Table 7.7 Percentage of 'trial' peeled tubers correctly classified as bruised or unbruised.

Spectra	Desiree	Pentland Dell	Record	All varieties
UV				
Untransformed	55.6*	65.2*	79.5	60.7*
First derivatives	60*	82.6	68.2	68.1
Visible				
Untransformed	77.6	69.4	57.1*	74.5
First derivatives	73.5	57.1*	57.1*	68
NIR				
Untransformed	63*	81.8	55.8*	73.7
First derivatives	58.7*	77.3	51.1*	72.9

* not significant; $p>0.001$ for Wilk's Lambda.

7.5 Discussion

Reflectance spectrophotometry has been used to measure the relative reflectance spectra of unpeeled and peeled, unbruised and bruised tubers. These spectra were taken from UV (250 nm) to NIR (1850 nm) wavelengths. The aim was to find wavelengths that were sensitive to cellular changes associated with bruising, and to use these wavelengths to generate equations that could non-invasively and rapidly detect bruising in an unknown sample.

It was found that untransformed reflectance spectra from unpeeled and peeled tubers appear to have a lower reflectance from UV to visible wavelengths, and that this trend is reversed in the NIR. The reason for this reversal is unclear, but in the UV to visible wavelengths a reduction in reflectance would be expected in bruised tubers because of the production of dark coloured melanin.

In unpeeled and peeled tubers there were no obvious differences between unbruised and bruised spectra. However, when the untransformed spectra were converted into first derivatives the changes in spectral slope between unbruised and bruised tubers

were magnified. The first derivatives also reduced errors associated with holding the bifurcated fibre optic at different angles, or disease or soil on the skin.

For unpeeled tubers, the changes in spectral slope between unbruised and bruised tubers appear to be at 290 nm, 500 nm, 600 to 750 nm, 900 nm, and 1400 to 1500 nm. In peeled tubers the differences in slope are more obvious than unpeeled tubers, with changes at about 380 to 400 nm, 475 to 500 nm, 700 to 850 nm and 1350 to 1550 nm. The decrease in slope from unbruised to bruised tubers at these wavelengths were associated with decreases in reflectance in the untransformed spectra.

Discriminant analysis was used to determine the best combination of wavelengths that could separate unbruised and bruised tubers when reflectance spectra from 'known' tubers were analysed. For unpeeled tubers, wavelengths selected from untransformed spectra were dependent on variety, particularly in the visible spectrum. It is possible that the inconsistent classification of unpeeled tubers may have been due to the colour of skin masking the pigments produced in bruised tissue. Wavelengths selected from peeled tubers appeared to be independent of variety for untransformed and first derivative spectra.

Some of the wavelengths selected from first derivative spectra of peeled and unpeeled tubers are similar to known wavelengths of dopachrome and melanin *in vitro* (300, 475 and 640 nm). Absorption bands at 1670 to 1690 nm and 1250 nm are normally assigned to carboxyl groups in melanin (Bellamy 1962) but discriminant analysis of NIR spectra did not select wavelengths in these ranges. Changes in NIR spectra would appear to reflect changes in bruised tissue that are due to cellular processes other than melanin production. Without further biochemical experiments it is not possible to determine what these changes might be.

The classification functions derived by discriminant analysis gave significant classification of a 'known' unpeeled tuber for nearly all untransformed and first derivative spectra. The exceptions were spectra from Record tubers in the UV and untransformed spectra from Pentland Dell tubers in the visible. For peeled tubers, there was a significant classification for all untransformed spectra, and first derivative spectra from the NIR. There was also significant classification of peeled Desiree tubers in the visible and Desiree and Record tubers in the UV.

However, when these classification functions were used on the 'trial' group of spectra, whose classification was unknown to the program, the accuracy of the classification function was reduced. For unpeeled tubers, the only significant

discrimination came from untransformed spectra of Desiree and Pentland Dell tubers in the NIR. For peeled Desiree tubers, the best classification came from visible spectra. For peeled Pentland Dell tubers, NIR spectra provided the best discrimination, and for peeled Record tubers, only the UV spectrum gave any classification results.

The reduction in classification accuracy for the 'trial' tubers, particularly unpeeled tubers, may be due to several reasons:

- The bifurcated fibre optic cable has a small detecting area about 12 mm^2. In unpeeled tubers, because the exact location of a bruise was only known after peeling, the bifurcated cable may have been measuring healthy tissue rather that bruised tissue.

- If there was a gap between the end of the bifurcated cable and the sample, the reflectance from the tuber could have been highly specular. That is, reflectance readings were of the surface rather than the sub-surface tissue.

- Body reflectance is reflected from a sample in a hemisphere. Part of the body reflectance signal could have been lost with a small (12 mm^2) detecting area.

- The presence of soil or disease on the skin of unpeeled tubers affected the reflectance spectra.

If reflectance spectrophotometry is to have a future as a method for non-invasively detecting bruising it has to be capable of detecting bruising in an unknown sample. The results in this chapter suggest that this may be possible in unpeeled tubers, and almost certainly in peeled tubers. However, the method needs to be improved if it is to be a robust technique.

Chapter 8

Detection of bruising in potato tubers using reflectance spectrophotometry with an integrating sphere

8.1 Introduction

One method for increasing the sampling area and reducing the specular component of reflected light is to use an integrating sphere which collects all the diffusely reflected radiation. An integrating sphere is composed of two hemispheres that are mated together to form a spherical cavity. The sphere is machined from or coated with a highly reflective material. Holes or ports in the sphere are used to transmit a collimated beam of light onto a sample at another port (Fig. 8.1).

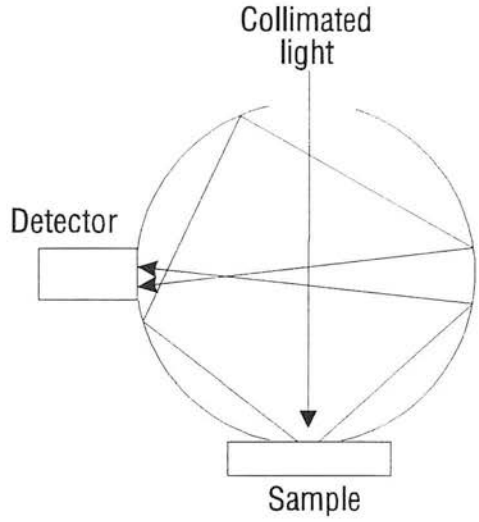

Fig. 8.1 Pathways of light within an integrating sphere (after Labsphere Inc. 1993).

The radiation reflected from the sample consists of a specular and a body reflectance component. The reflected light undergoes multiple reflections on the wall of the sphere, which results in a uniform, spatially integrated radiation distribution within the sphere. A detector placed in a port in the sphere wall measures an output that is completely independent of the angular properties of the input light. The independence of the output of a sphere from the angular properties of the input light, and the uniform internal distribution of light make integrating spheres ideal for many uses (Labshere Inc. 1993).

This chapter describes the use of an integrating sphere to collect spectra of bruised and unbruised tubers in the visible light spectrum in an attempt to increase the sensitivity of the spectrophotometric method.

8.2 Methods

8.2.1 The integrating Sphere

An integrating sphere was machined at the SCAE from a block of Spectralon (Labsphere Inc, UK). Spectralon reflectance material is a thermoplastic resin that can be machined into a wide variety of shapes. The surface of Spectralon gives the highest diffuse reflectance of any known material. The reflectance is generally greater than 99 % over a range from 400 to 1500 nm and greater than 95 % from 250 to 2500 nm.

The internal diameter of the sphere is 110 mm. Light is transmitted from a halogen light source (All Inspection NDT, Ltd, UK) along a fibre optic light guide to a port in the sphere. The fibre optic light guide is held in place by a plug in the port. The inside of the plug is painted matt black to reduce any stray reflections.

The plug contains a 15 mm, focal length 20 mm, bi-convex lens. A light source located at the focal length of a positive lens gives a collimated light beam on the far side of the lens. The collimated light is transmitted to an opposite sampling port. The collimated beam has an area of 18 mm at the sampling port. The sampling port has a diameter of 20 mm. Reflected light from the sample is reflected off the walls of the sphere until it passes along a fibre optic light guide mounted in plug at 90° to the sample port (Fig. 8.2). The fibre optic light guide passes the reflected light component to a Monolight monochromator (6118) and photomultiplier tube.

A reference reading is taken from a block of Spectralon placed over the sample port, before taking a reading of a tuber. A reference reading was taken for every 30 spectra.

Although Spectralon is highly reflective from 200 to 2500 nm, the integrating sphere developed at the SCAE can only analyse spectra from 400 to 800 nm at present. There are several reasons for the restricted range of this integrating sphere.

- Light from the transmitting fibre optic light guide has a transmission angle of approximately 70°. The 15 mm diameter lens captures a small proportion of this light. When the sphere was first tested, a 10 mm diameter lens was used, but the signal needed about 150% gain and was very 'noisy'. With a 15 mm diameter lens, a gain of approximately 7% is used and the signal has very little 'noise'.
- The lens is manufactured from BK 7 glass that attenuates light below 380 nm (Appendix A).

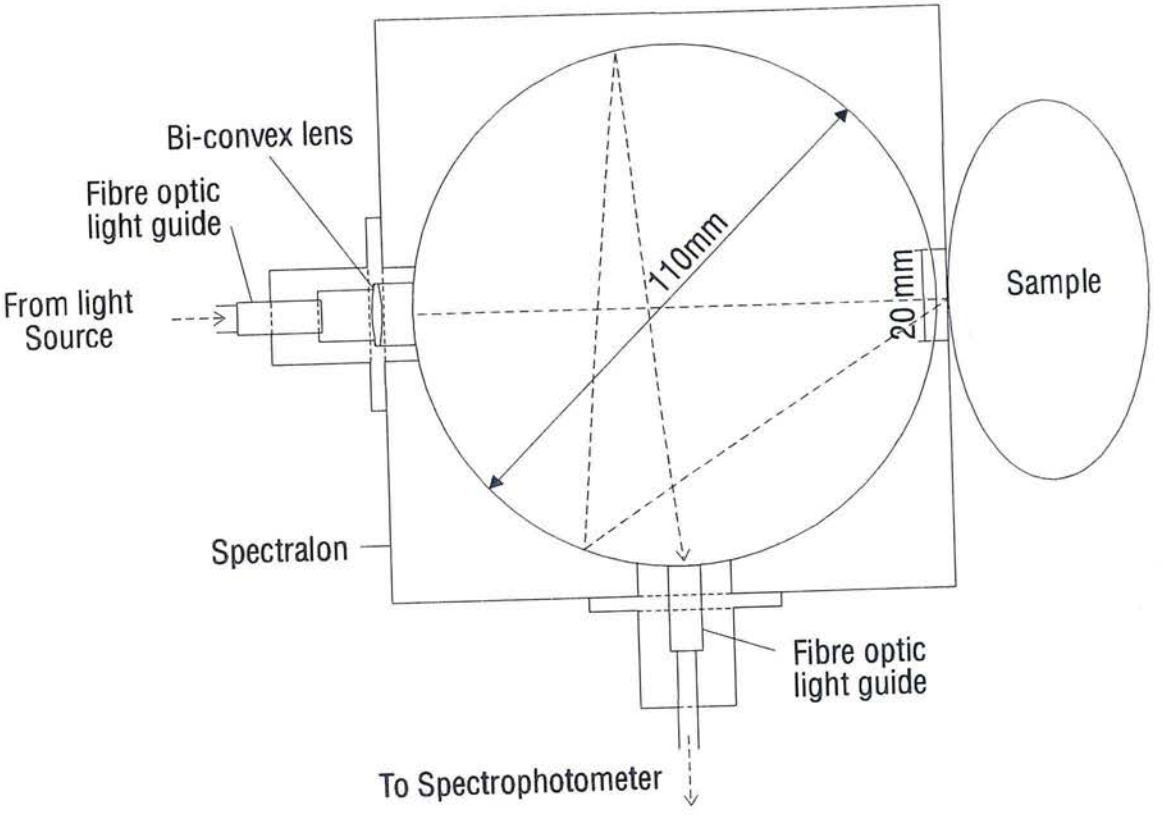

Fig. 8.2 Cross section of the integrating sphere and photograph of experimental set-up.

- The area of the detecting fibre optic is approximately 12 mm^2 which is a small proportion (0.032%) of the total internal area of the sphere.

- The collimated beam of light is not perfectly collimated. There is a 'halo' of light around a bright central 'core'. The core is focused to provide an illuminated area of 18 mm diameter, but part of the halo is reflected off the wall of the sphere. Figure 8.3 shows the percentage of light reflected when there is no reference or tuber at the sampling port.

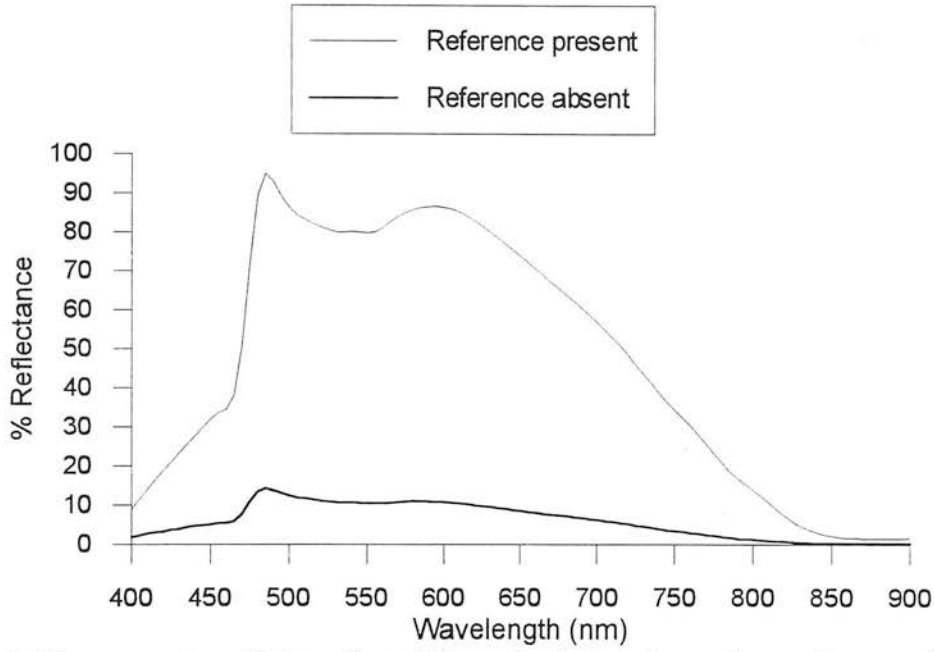

Fig. 8.3 The percentage light reflected from the integrating sphere when a reference of Spectralon material is present or absent.

- A photo multiplier tube is needed to detect the relatively low light signal from the sphere. The photo multiplier is sensitive to light from 200 nm to 900 nm, but has a useful sensitivity from about 250 to 800 nm.

8.2.2 Samples and data analysis

One hundred tubers of each of the varieties Desiree, Pentland Dell and Record were hand dug, washed and stored at 4°C. Tubers were impacted using the SCAE dropper (section 7.2.2) and placed in a hotbox for 16 hours. Spectra were taken of unpeeled and peeled tubers and classified as bruised if there was any discolouration visible after peeling. Spectra were analysed with BMDP discriminant analysis (section 7.2.5). Half of the spectra from bruised and unbruised tubers were used to determine the classification function (denoted as 'known' tubers) and the remainder (denoted as 'trial' tubers) used to determine the success of the classifying a tuber as bruised or unbruised.

8.3 Results - Unpeeled tubers

The mean untransformed spectra of bruised tubers appear to have a slightly lower reflectance than unbruised tubers from 400 to 700 nm for all varieties (Fig. 8.4). Desiree shows less reflectance at 500 to 600 nm due to its red skin.

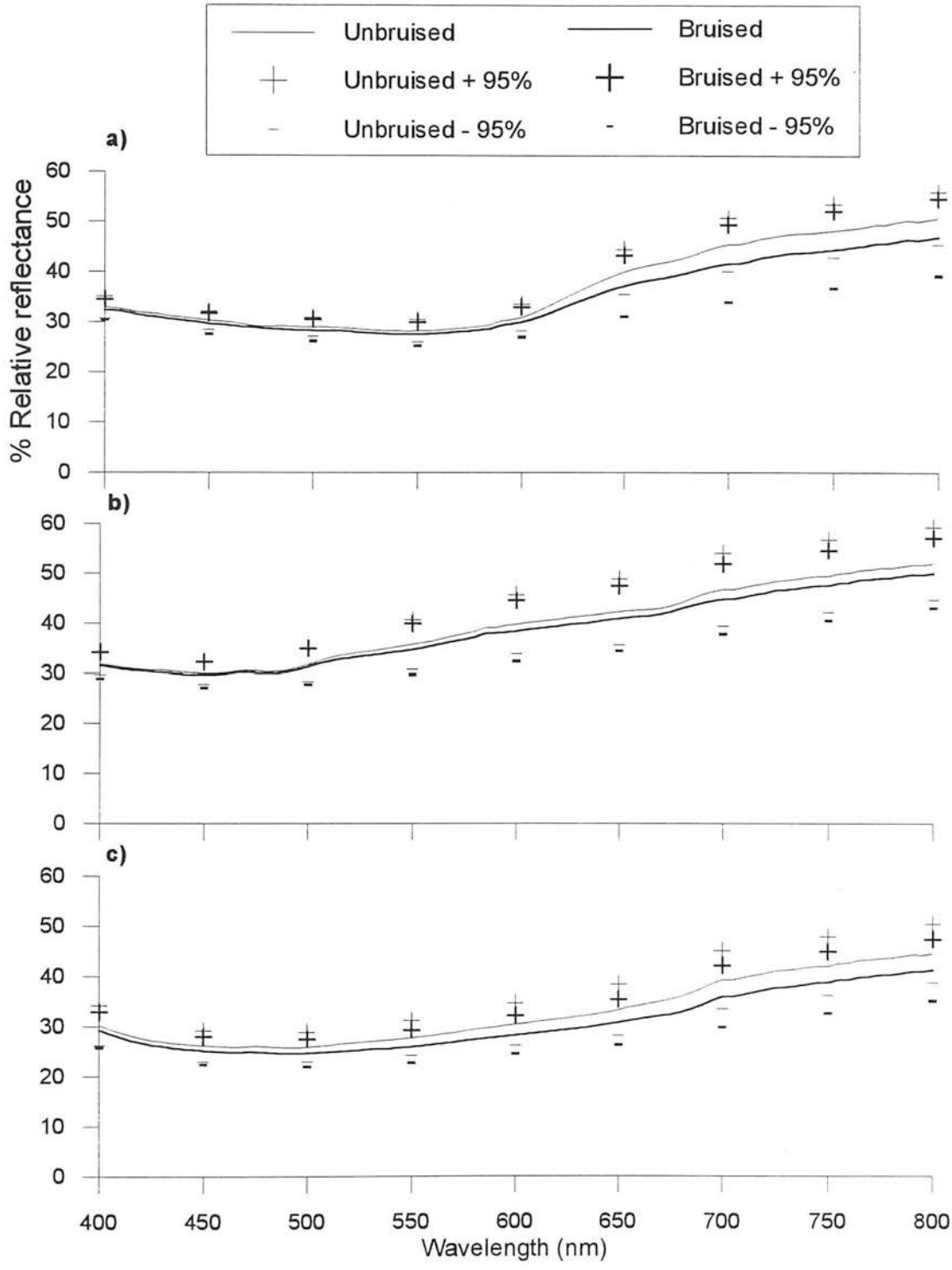

Fig. 8.4 Mean and 95% confidence limits of untransformed spectra from unbruised and bruised unpeeled tubers a) Desiree b) Pentland Dell and c) Record.

The first derivative spectra reveal where the slopes of the spectra differ between bruised and unbruised tubers. For Desiree this is at about 500 and 650 nm. Pentland Dell and Record appear to have the biggest difference at about 680 nm (Fig. 8.5).

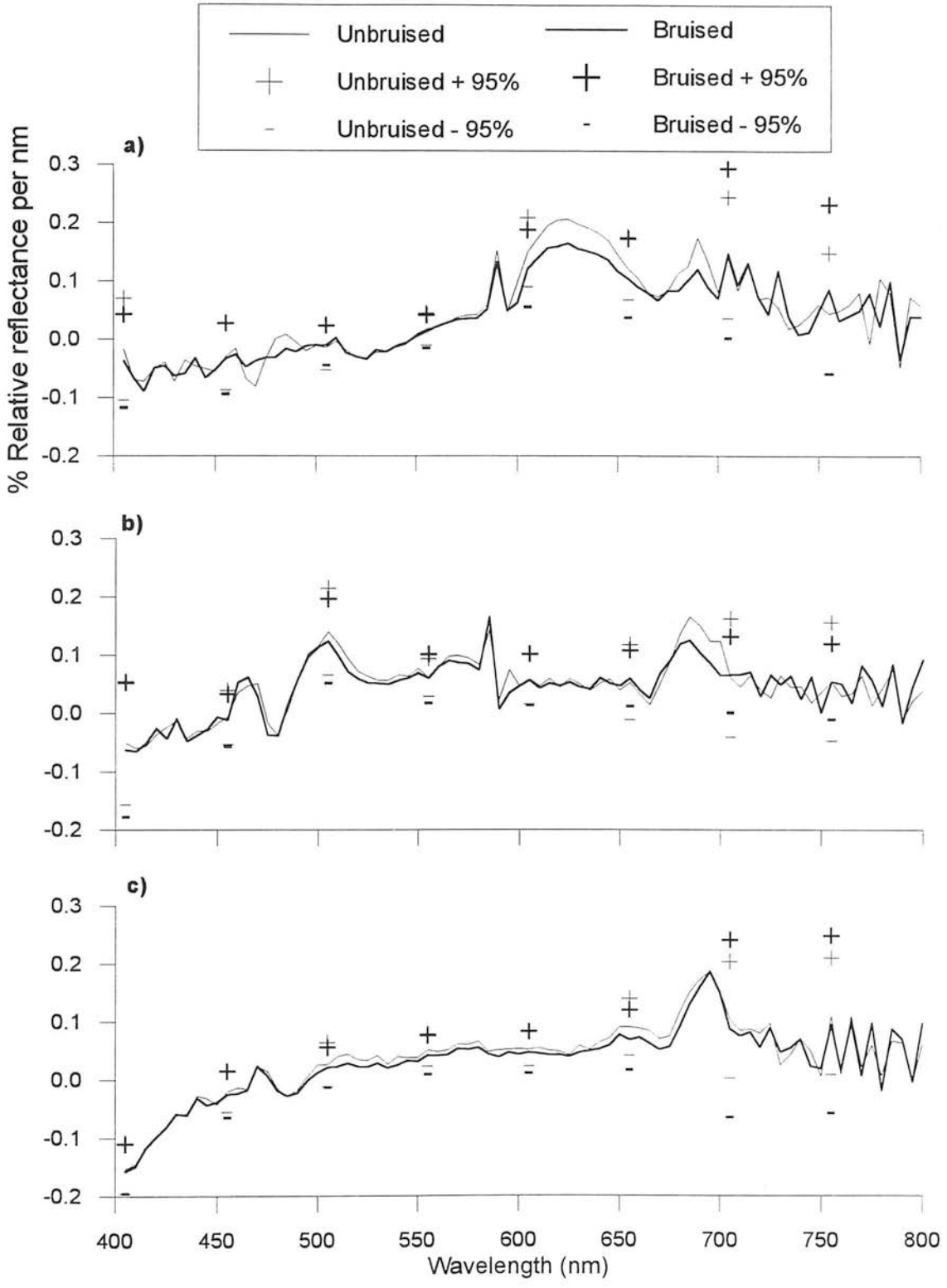

Fig. 8.5 Mean and 95% confidence limits of first derivative spectra from unbruised and bruised unpeeled tubers a) Desiree b) Pentland Dell and c) Record.

All varieties had a high percentage of bruised tubers (52 to 80.2%). Record was the most bruise susceptible (80.2% tubers bruised) and had the highest level of blackspot bruising (95.8%). Desiree was the least bruise susceptible (52% bruising), and Pentland Dell had the highest percentage of shatter bruising (28.8%).

Discriminant analysis of untransformed spectra (Fig. 8.4) selected wavelengths that were dependent on variety to separate unbruised from bruised. Wavelengths selected from first derivative spectra (Fig. 8.5) selected more wavelengths to separate unbruised and bruised tubers and these were independent of variety (Table 8.1).

Table 8.1 Wavelengths selected by discriminant analysis to separate untransformed and first derivative spectra from unbruised and bruised unpeeled tubers.

Spectra	Desiree	Pentland Dell	Record	All
Untransformed	695	none	465, 435	700, 690
First derivatives	490, 610, 625, 540, 510, 530, 410, 520	590, 440, 650, 655	655, 490, 425, 630, 585, 515, 435	590, 490, 695, 655, 635

* Wavelengths (nm) shown in order that discriminant analysis selected variables on basis that F value was greater than 4.

The success of classifying tubers whose classification was known to the discriminant analysis ('known' tubers) was significant ($p<0.001$ for Wilk's Lambda) when first derivative spectra were used (Table 8.2). Analysis of untransformed spectra

When the linear discriminant function was used on tubers whose classification was unknown to the discriminant analysis ('trial' tubers) the best results came from untransformed spectra (Table 8.2). Discrimination of Pentland Dell was not significant for untransformed and first derivative spectra.

Table 8.2 Percentage of unpeeled 'known' and 'trial' tubers correctly classified as bruised or unbruised.

Spectra	Desiree	Pentland Dell	Record	All
'Known'				
Untransformed	66.7*	none	81.6	68.3*
First derivative	91.1	75.6	89.8	73.4
'Trial'				
Untransformed	81.8	none	69.6	71.8
First derivative	61.4*	35.6*	65.2*	41.5*

* not significant: $p>0.001$ for Wilk's Lambda.

8.4 Results - Peeled tubers

Mean untransformed spectra of bruised tubers appear to have a lower reflectance than unbruised tubers from 400 to 700 nm for all varieties (Fig. 8.6).

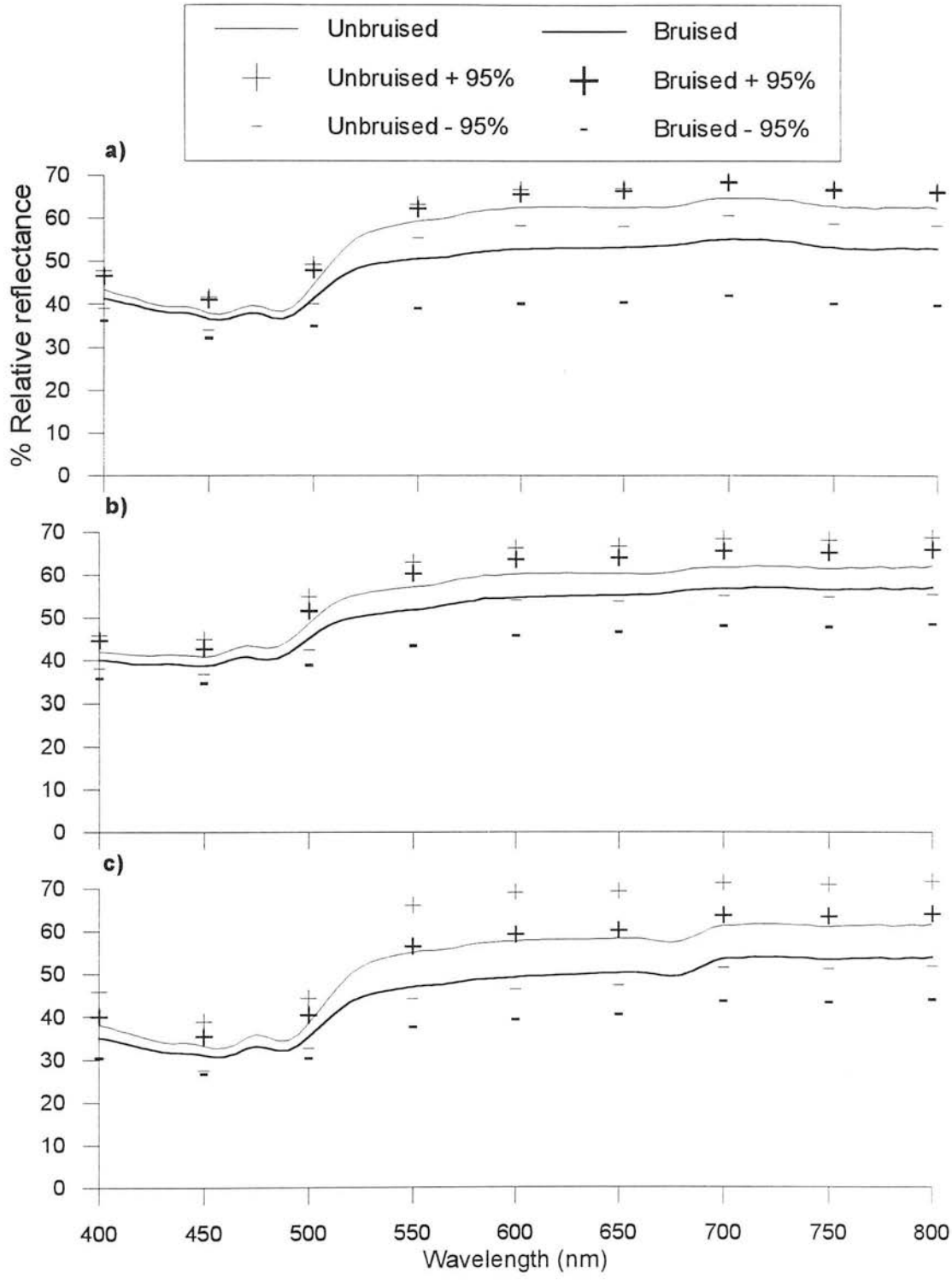

Fig. 8.6 Mean and 95% confidence limits of untransformed spectra from unbruised and bruised peeled tubers a) Desiree b) Pentland Dell and c) Record.

First derivative spectra reveal the greatest change in slope between bruised and unbruised tubers at about 480 to 550 nm for all varieties (Fig. 8.7).

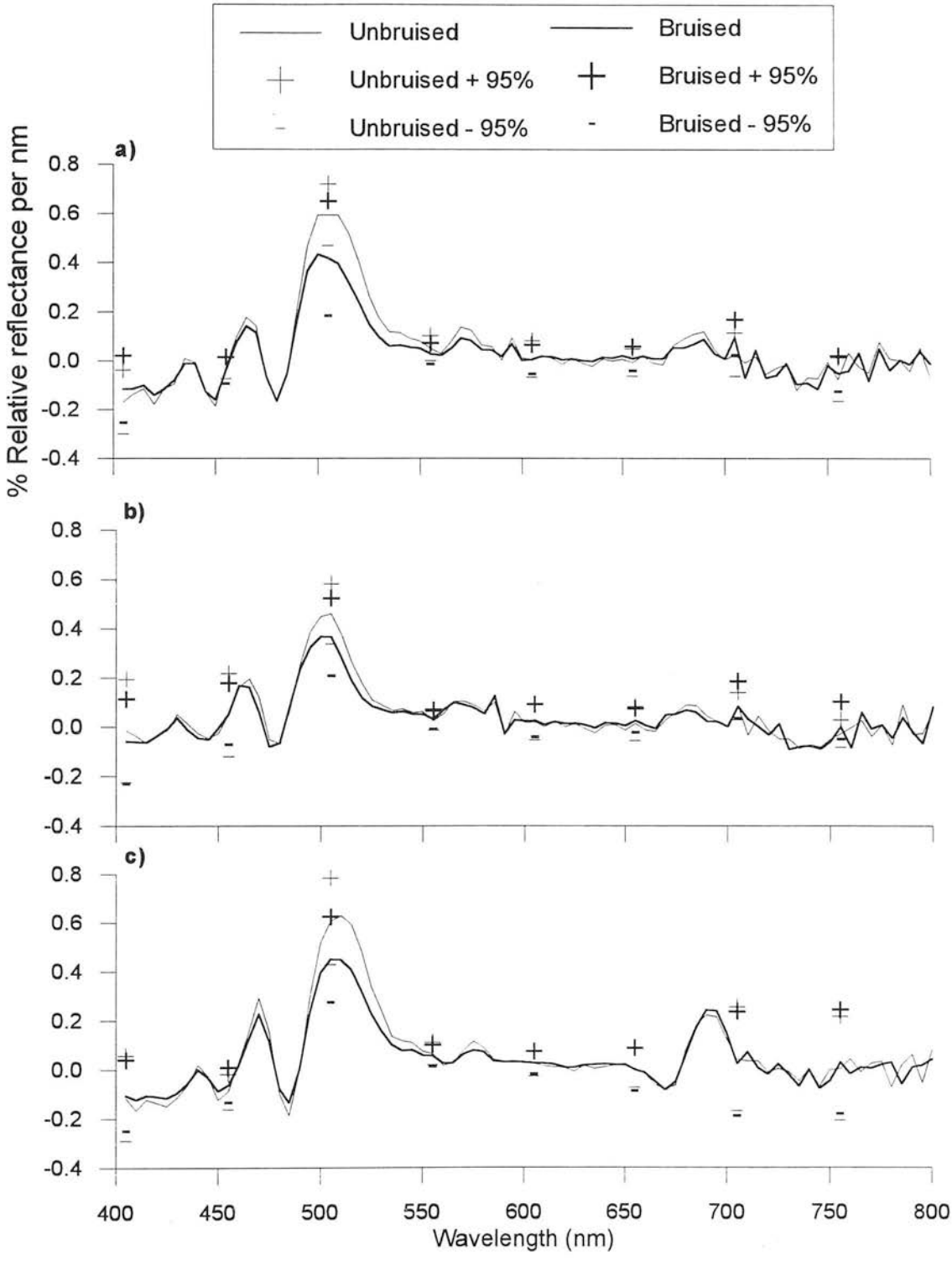

Fig. 8.7 Mean and 95% confidence limits of first derivative spectra from unbruised and bruised peeled tubers a) Desiree b) Pentland Dell and c) Record.

Discriminant analysis selected wavelengths from untransformed spectra that were in the 435 to 505 nm range for all varieties, with Record having additional wavelengths from 590 to 695 nm (Table 8.3).

Table 8.3 Wavelengths selected by discriminant analysis to separate untransformed, first and second derivative spectra from unbruised and bruised *peeled* tubers.

Spectra	Desiree	Pentland Dell	Record	All
Untransformed	590, 665, 500	550, 680	550, 700, 500	555, 505, 650, 490
1st derivatives	515, 680, 420	520, 480, 620, 420, 645	615, 665, 465, 605, 505, 405, 660, 415, 420	510, 635, 680, 425, 645

* Wavelengths (nm) shown in order that discriminant analysis selected variables on basis that F value was greater than 4.

Discriminant analysis gave the best classification of known tubers when first derivative spectra were analysed. However, discrimination of trial tubers was best when untransformed spectra were analysed. When the spectra from all the varieties were analysed together, the best classification of known and trial tubers came from untransformed spectra (Table 8.4).

Table 8.4 Percentage of 'known' and 'trial' peeled tubers correctly classified as bruised and unbruised.

Spectra	Desiree	Pentland Dell	Record	All varieties
'Known'				
Untransformed	87	82.2	89.8	84.3
1st derivatives	91.3	88.9	100	83.6
'Trial'				
Untransformed	72.7	84.4	82.6	79.8
1st derivatives	79.5	68.9*	67.4*	79.1

* not significant: $p>0.001$ for Wilk's Lambda.

8.5 Discussion

An integrating sphere has been used in an attempt to improve the spectrophotometric method. The improvements over using a bifurcated fibre optic cable are as follows.

- All the body reflectance is collected by the sphere. With a bifurcated fibre optic cable some of the body reflectance may have been lost.
- The area of tuber analysed is approximately 314 mm^2. The 12 mm^2 detection area of the bifurcated cable could have missed the bruised area in unpeeled tubers.

- The angle of the sample in relation to the incident light should be more consistent than with a hand held bifurcated cable. This would appear to be the case as the standard deviations of the untransformed spectra are smaller than the corresponding spectra in Chapter 7.

Untransformed spectra of bruised unpeeled and peeled tubers appear to have a lower reflectance than unbruised tubers with a more obvious difference in peeled tubers. In unpeeled tubers, the first derivative spectra are dependent on variety, with changes in slope at approximately 475 nm, 500 nm, 600 nm and 650 nm. First derivative spectra from peeled tubers show a more consistent difference in slope between unbruised and bruised tubers at about 500 nm.

Spectra from unbruised and bruised tubers were split into two groups: 'known' and 'trial' spectra. The spectra from the 'known' group were used by discriminant analysis to select the best combination of wavelengths that separated unbruised and bruised tubers. These wavelengths were then used to generate classification functions that classified the 'known' tubers as bruised or unbruised. For unpeeled tubers, all the first derivative spectra and untransformed spectra of Record had a significant classification result. All the untransformed and first derivative spectra of peeled tubers were classified significantly, with first derivative spectra giving slightly higher percentage of tubers correctly classified as bruised or unbruised.

When the classification functions were used on 'trial' spectra from unpeeled tubers, the only significant discrimination came from untransformed spectra of Desiree, Record and the pooled spectra. When peeled tubers were analysed, all the untransformed spectra were significantly classified along with first derivative spectra of Desiree and the pooled spectra.

Table 8.5 Percentage of *unpeeled* tubers correctly classified as bruised or unbruised. Comparison of spectra collected with bifurcated fibre optic cable and integrating sphere.

	Desiree	Pentland Dell	Record	All varieties
Bifurcated cable				
Untransformed	48.9*	40*	55.1*	54.8*
1st derivatives	55*	52*	34.7*	54.7*
Integrating sphere				
Untransformed	81.8	none	69.6	71.8
1st derivatives	61.4*	35.6*	65.2*	41.5*

* not significant: $p>0.001$ for Wilk's Lambda.

A comparison of these results with 'trial' spectra collected in Chapter 7 with the bifurcated cable reveals that for unpeeled tubers the integrating sphere appears to improve the discrimination of untransformed spectra, except for Record (Table 8.5). With the bifurcated cable none of the untransformed or first derivative spectra were significantly classified.

Discrimination of spectra from 'trial' peeled tubers gave inconsistent results in Chapter 7. Table 8.6 compares the discrimination of spectra collected with a bifurcated cable and the integrating sphere. All the untransformed spectra are significantly classified with spectra collected with the integrating sphere. In comparison, only Desiree and the pooled spectra are significantly classified with a bifurcated cable.

Table 8.6 Percentage of *peeled* tubers correctly classified as bruised or unbruised. Comparison of spectra collected with bifurcated fibre optic cable and integrating sphere.

	Desiree	**Pentland Dell**	**Record**	**All varieties**
Bifurcated cable				
Untransformed	77.6	69.4*	57.1*	74.5
1st derivatives	73.5	57.1*	57.1*	68*
Integrating sphere				
Untransformed	72.7	84.4	82.6	79.8
1st derivatives	79.5	68.9*	67.4*	79.1

* not significant: $p>0.001$ for Wilk's Lambda.

The use of the integrating sphere does appear to give more consistent results than the bifurcated cable, especially for peeled tubers. With unpeeled tubers, the classification of 'trial' spectra is still not consistent. The reason for this inconsistency could be due to surface disease or soil on the skin, or that the skin is attenuating the body reflectance too strongly.

The inconsistent discrimination of trial tubers may also be due to the way that discriminant analysis tries to find linear relationships between unbruised and bruised tubers. If the relationship is non-linear error will inevitably be present. The possibility that non-linear relationships may be present in the reflectance data, will be explored in the next chapter.

Chapter 9

Comparison of discriminant analysis and neural networks for classifying reflectance spectra from bruised and unbruised tubers

9.1 Introduction

Neural networks are inherently useful for the interpretation of non-linear trends in data. The neural network technique is a relatively new computing tool that enables a computer to 'learn' the appearance of a variety of objects and then predict upon new objects presented to it. For example, and in the case presented here, the network was 'trained' with reflectance spectra collected in Chapters 7 and 8 from bruised and unbruised tubers. The algorithms formulated by the neural network were then used to predict the classification of reflectance spectra from trial samples of tubers never 'seen' by the network. The discriminant analysis results obtained for the same data set were used to determine if neural networks can improve the spectrophotometric method.

9.2 Methods

9.2.1 Neural networks

Neural networks identify the underlying organisation pervading a data set. The network learns the similarities between patterns without prior knowledge of the regularities in the data. This is a distinct asset in many applications because it works without conventional programming. Developing a neural network is unlike developing software because the network is trained.

Neural networks offer several advantages over other modelling techniques. They can infer subtle, unknown relationships from data. Networks can also generalise or respond correctly to patterns that are only broadly similar to the original training patterns. Generalisation is useful because the real world is noisy, distorted, and often incomplete. Neural networks are also non linear and while non linear behaviour is common it can be difficult to handle mathematically (Hammerstromn 1993).

Neural nets take their name and the concepts behind their functioning from research into brain cells. A brain cell, or neuron, is connected to a number of other cells via fibres called synapses. The cells receive electrical signals from some and transmit to others. Through these communications the neurons carry out local processing and

can reduce a problem into individually solvable parts. Vast combinations of neurons and synapses produce intelligence.

Neural networks are also composed of neurons and synapses (otherwise known as connections). Connections can be thought of as conductors for signals that can attenuate or amplify the signals passing through them. The associated scaling factor is known as the weight of the connection. A single connection links only two neurons.

Neurons are subdivided into three types; input, output, and hidden. Input neurons accept data from outside the neural net but perform no processing. Hidden neurons are internal to the neural net. Hidden and output neurons perform almost identical processing, but only output neurons transmit data to outside the neural net (Shalkof 1984).

The hidden and output neurons process their inputs in two steps. The first step multiplies every input by its weight, and adds the product to a running total;

$$x = \sum_{i} O_i \cdot w_{ij}$$

where: O is the output of a neuron; i indexes the neurons that feed the jth neuron; w_{ij} is the weight of a connection between the ith and jth neurons.

The second step passes the sum through the following function to produce its result;

$$O_j = \frac{1}{1 + e^{-x}}$$

This transfer function is a steadily increasing S-shaped curve, commonly called a sigmoid function. The attenuation at the upper and lower limbs of the 'S' constrains the raw sums smoothly within the fixed limits of 0 and 1 (Hammerstromn 1993). The function also introduces a non-linearity that further enhances the network's ability to model complex functions (Fig. 9.1).

Neural nets are customised for a particular task through the number of neurons and the weights of their connections. The weights are determined by training the net. The neural net is trained by offering it past experiences and providing it with the correct results. Unlike biological neurons, neural networks have to be told when they are being taught (training) and when they are being asked to provide answers to problems (interrogation).

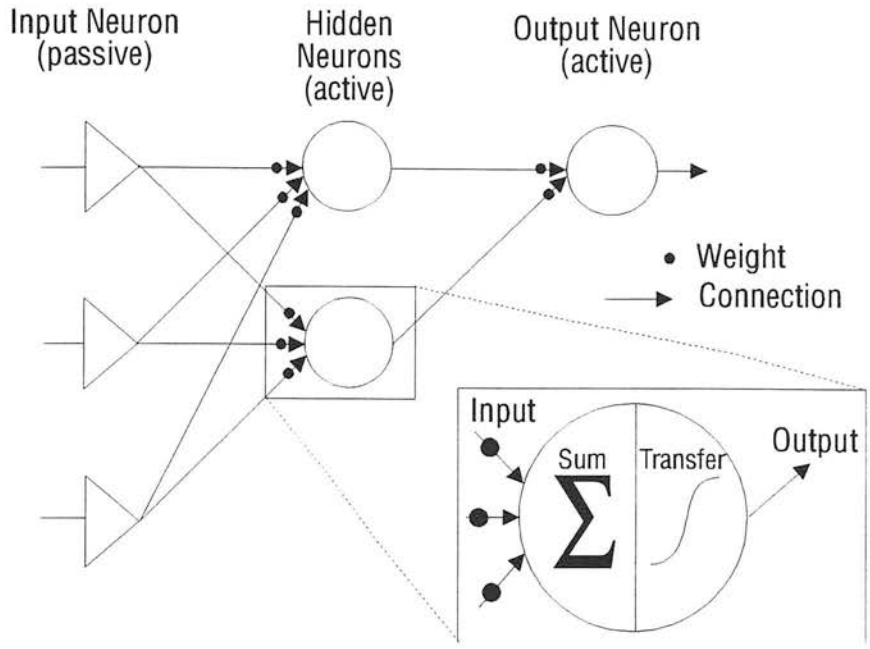

Fig. 9.1 Schematic diagram of a neural network (after Hammerstromn 1993).

The training data contains a series of input patterns labelled with their target output patterns. The training patterns are presented to the neural net and modified at every neuron and connection until an output value is given. Each presentation of a pattern to the net is called an epoch.

If the outputs generated by the network are compared with the expected results, a set of error values can be produced. These error values are squared and then summed to give a single value. This value represents how close a set of connection weights gives the desired result. An algorithm uses the error values to adjust the weights of the connections until the desired associations are learned.

Various algorithms exist but one of the most popular is Back Propagation. The back propagation equation changes the weights of the connections to minimise the sum of squared errors in the network. This minimisation has an intuitive geometric meaning. To see it, all possible sets of weights are plotted against the corresponding sum of squares errors. The result is an error surface shaped like a bowl, whose bottom marks the set of weights with the smallest sum of squares error. Finding the bottom of the bowl, that is, the best set of weights, is the goal during training (Fig. 9.2).

Back propagation achieves this goal by calculating the instantaneous slope of the error surface with respect to the current weights. It then incrementally changes the weights in the direction of the locally steepest path toward the bottom of the bowl. The steeper the slope the faster it jumps, but as the slope flattens out close to the

minimum it makes smaller and smaller changes to the weights. When the error reaches its minimum, the net is said to have converged.

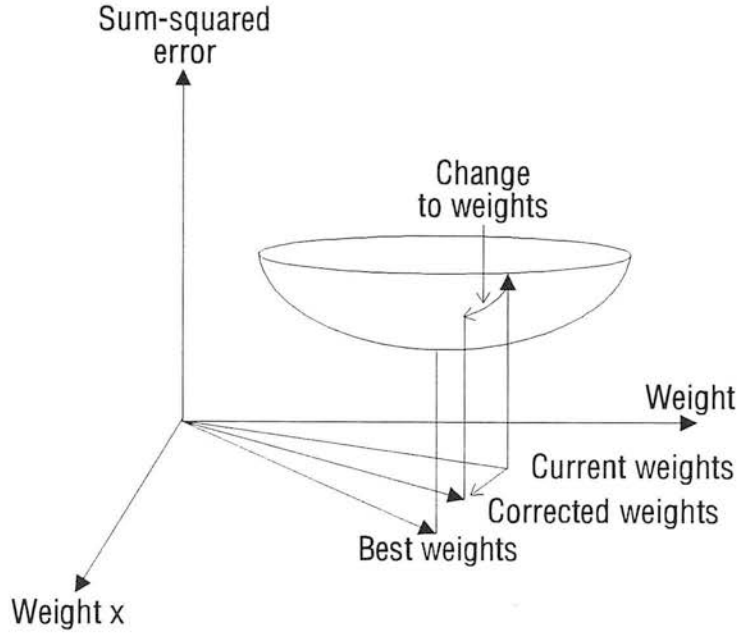

Fig. 9.2 Theoretical error surface (after Hammerstromn 1993)

Real error surfaces can have valleys and many minima. Since back propagation follows the steepest path, the algorithm can train a network into a minimum that it cannot escape. However, in practice, finding the unique global minimum seldom matters. What does matter is finding a set of weights that processes data accurately enough for the application.

The use of neural networks requires some care as they can be over trained to learn the characteristics of a training set without learning what they had in common. A neural network is only useful of it returns appropriate results with data not used to train it, a 'trial' group. Measuring this ability, called generalisation, requires testing the network with the trial data set. There is often a trade-off between accuracy of results and ability to generalise.

9.2.2 Data analysis

Untransformed spectra from the 'known' tuber group presented in Chapters 7 and 8 were used to train a neural net. The net was trained with all the wavelengths, or a subset of wavelengths selected from untransformed spectra by discriminant analysis in Chapters 7 and 8. When a subset of wavelengths was used, additional wavelengths were added to increase the number of selected wavelengths when the discriminant analysis had originally chosen one wavelength. For the UV and visible, this was the

selected wavelength ± 5 nm; for the NIR this was the selected wavelength ± 10 nm. In this way, the accuracy of identifying a tuber with just a few wavelengths could be compared with entire spectrums.

A neural net generated by Neural Computer Sciences scales the relative reflectance values for the 'known' tubers between zero and one. These are the inputs for the net. For the purposes of training the net, it has to be told what the output is for each input. The output was set to zero for unbruised tubers and one for bruised tubers.

The net was trained with a standard back propagation algorithm. Since the error surface represents the network error for all the combinations of weights, movement on the surface implies a modification of the weights as follows:

$$WChange_t = LearnRate \cdot \left(\frac{dE}{dW}\right)_t + \alpha \cdot WChange_{t-1}$$

The last term is a momentum term that includes a proportion of the last weight update in the current one. This has the effect of preventing wild fluctuations due to ripples in the error surfaces. Training proceeds much faster with this term. dE/dW is the rate of change of error with respect to weight for a particular weight. Values of 0.9 were used for α and 0.1 for LearnRate (Neural Desk User's Guide 1992).

The Neural Computer Science software displays the processing state of the network as a graph:

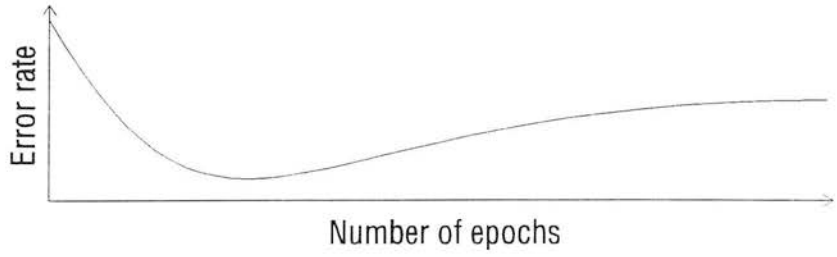

The error rate initially decreases as the number of epochs increase. However, at some point the error rate will level out or rise again. This is the point at which the net is starting to lose its ability to generalise, or overtrain. By testing the net with an independent set of spectra, it is possible to detect the point at which the overtraining starts to occur and stop the training at this point. In general, this point is just before the lowest average error value is reached.

The independent data set used for interrogating the net was the spectra from 'trial' tubers in Chapters 7 and 8. An output value greater then 0.5 was classified as a

bruised tuber, and a value less than 0.5 classed as unbruised. A program written in BASIC (Appendix D) was used to evaluate the percentage of tubers correctly classified as bruised or unbruised.

In addition to giving the percentage of tubers correctly classified, a two-tailed t-test was conducted on the outputs from the interrogation of the net to determine if the classification of the neural net was significant. By way of an example, the following steps were used:

Output values from neural net	Expected values
0.2	0
0.6	0
0.3	0
0.7	1
0.8	1
0.1	1

These values were split into two groups;

Expected value 0 (Unbruised)	Expected value 1 (Bruised)
0.2	0.7
0.6	0.8
0.3	0.1

A two-tailed t-test was then carried out on the two groups with Solo statistical software (BMDP Inc., California) to determine if the means were significantly different. The null hypothesis was that neural nets would find no difference between unbruised and bruised tubers. A p value less than 0.01 for the t-value given by the analysis, was taken as being a significant classification of a tuber as bruised or unbruised by the neural net.

9.3 Results

When all wavelengths were used to train and interrogate a neural net, the percentage of unpeeled tubers correctly classified as bruised or unbruised was significant for UV spectra of Record, visible spectra of Pentland Dell and Record and NIR spectra of Pentland Dell. The main differences between neural nets and discriminant analysis for classifying 'trial' spectra are for UV spectra of Record and visible spectra of Pentland Dell tubers. In both these cases, discriminant analysis failed to classify any tubers as bruised or unbruised, but neural nets did classify them. Discriminant analysis classified visible spectra of Desiree and NIR spectra of Desiree, but neural nets failed to give a significant result.

Table 9.1 Percentage of unpeeled 'trial' tubers correctly classified as bruised or unbruised. Neural net trained and interrogated with all wavelengths.

Spectra	Desiree	Pentland Dell	Record	All varieties
UV				
Disc. analysis	64.4*	36.2*	none	63.2*
Neural net	64.4*	45.6*	72.7	56.3*
Visible: cable				
Disc. analysis	48.9*	40*	55.1*	54.8*
Neural net	57.1*	55.1*	65.3*	56.3*
Visible:sphere				
Disc. analysis	81.8	none	69.6	68.9
Neural net	66.7*	72.7	82.6	72.6*
NIR				
Disc. analysis	90.7	77.3	65.9*	71
Neural net	72.1*	68.2	47.7*	35.1*

* classification was not significant; for discriminant analysis this was $p>0.001$ for Wilk's Lambda, and for neural nets this was a $p>0.01$ for a t-test.

The neural nets correctly classified UV spectra from 'trial' peeled Pentland Dell tubers and visible spectra collected with a bifurcated cable from Record tubers when discriminant analysis found no significant difference. In contrast, discriminant analysis significantly classified visible spectra collected with a bifurcated cable from Desiree tubers, and NIR spectra of the pooled varieties when neural nets found no significant difference (Table 9.2).

Table 9.2 Percentage of 'trial' peeled tubers classified as bruised or unbruised. All wavelengths used to train and interrogate neural networks.

Spectra	Desiree	Pentland Dell	Record	All varieties
UV				
Disc. analysis	55.6*	65.2*	79.5	60.7*
Neural net	57.9*	78.3	72.7	71.1
Visible - cable				
Disc. analysis	77.6	69.4*	57.1*	74.5
Neural net	57.1*	53.6*	71.4	68.0
Visible sphere				
Disc. analysis	72.7	84.4	82.6	79.8
Neural net	79.5	80.0	82.6	84.4
NIR				
Disc. analysis	63.0*	81.8	55.8*	73.7
Neural net	67.4*	75.0	68.2*	65.4*

* classification was not significant; for discriminant analysis this was $p>0.001$ for Wilk's Lambda, and for neural nets this was a $p>0.01$ for a t-test.

Sometimes the net classified all unbruised tubers as bruised, or all bruised tubers as unbruised. When this occurred, the success of classifying a tuber into the right case can be misleading if there are more bruised tubers than unbruised. For example, the tubers collected with the integrating sphere had 72.6% bruising in the sample. If the neural net classified all tubers as bruised, the success of classifying a tuber as bruised or unbruised appears to be 72.6% (Table 9.1). This explains why a classification of result of over 71% is termed non-significant for some of the neural net results. This occurred most frequently with unpeeled tubers and when whole wavelength ranges were analysed.

When selected wavelengths were used (Table 9.3) to train and interrogate a neural net, the time taken for a net to converge was reduced.

Table 9.3 Wavelengths selected by discriminant analysis to separate bruised and unbruised tubers.

Spectra	Desiree	Pentland Dell	Record	All varieties
UV *	330, 360	250, 350	none	285
Vis. cable*	635, 700	575	700	485, 700
Vis. sphere*	695	none	435, 465	690, 700
NIR*	950, 1150, 1720	710, 1780	710, 990, 1780	710, 1060, 1730, 1820

* Additional wavelengths were used to train and interrogate the neural nets. For the UV and visible this was the selected wavelength ± 5 nm, for the NIR it was the selected wavelength ± 10 nm.

When neural nets were trained with a subset of variables, the classification of unpeeled tubers was improved for spectra collected with an integrating sphere from Desiree and pooled varieties, and NIR spectra of Pentland Dell and all varieties. It reduced the classification accuracy of UV spectra of Record tubers, and spectra collected with the integrating sphere from Pentland Dell tubers (Table 9.4). Perhaps the most notable observation is that the classification of spectra collected with an integrating sphere appear to improve the classification of Record and the pooled varieties.

Table 9.4 Percentage of unpeeled 'trial' tubers correctly classified as bruised or unbruised with a neural network trained and interrogated with selected wavelengths.

Spectra	Desiree	Pentland Dell	Record	All varieties
UV				
Disc. analysis	64.4*	36.2*	none	63.2*
Neural net	48.9*	51.1*	none	66.1*
Visible - cable				
Disc. analysis	48.9*	40*	55.1*	54.8*
Neural net	69.4	48*	63.3*	57.4*
Visible sphere				
Disc. analysis	81.8	none	69.6	68.9
Neural net	81.6	none	71.4	78.4
NIR				
Disc. analysis	90.7	77.3	65.9*	71
Neural net	72.1*	79.5	38.6*	68.6

* classification was not significant; for discriminant analysis this was $p>0.001$ for Wilk's Lambda, and for neural nets this was a $p>0.01$ for a t-test.

When neural nets were trained with a subset of variables, the classification of peeled tubers was improved for UV spectra of Desiree and spectra collected with a bifurcated cable from Pentland Dell tubers. It reduced the classification accuracy of UV spectra of Record and the pooled varieties (Table 9.5). It may also be noted that neural nets appeared to improve the classification result for spectra collected with an integrating sphere from Desiree, Record and the pooled varieties.

Table 9.5 Percentage of 'trial' peeled tubers correctly classified as bruised or unbruised. Selected wavelengths.

Spectra	Desiree	Pentland Dell	Record	All varieties
UV				
Disc. analysis	55.6*	65.2*	79.5	60.7*
Neural net	68.9	71.7	65.9*	67.4*
Visible - cable				
Disc. analysis	77.6	69.4*	57.1*	74.5
Neural net	65.3*	71.4	71.4	62.6*
Visible sphere				
Disc. analysis	72.7	84.4	82.6	79.8
Neural net	79.6	83.6	83.7	82.9
NIR				
Disc. analysis	63*	81.8	55.8*	73.7
Neural net	67.4*	70.4	67.4*	67.7*

* classification was not significant; for discriminant analysis this was $p>0.001$ for Wilk's Lambda, and for neural nets this was a $p>0.01$ for a t-test.

9.4 Discussion

Discriminant analysis was used in Chapters 7 and 8 to select wavelengths that best separated spectra from unbruised and bruised tubers and to define a linear relationship that can predict the classification of an unknown case. However, the relationship between reflectance spectra and bruising may not be linear. When non-linearity is present in a sample it can be difficult to model the relationship. Neural networks offer the potential to model non-linear behaviour without programming.

Reflectance spectra from 'known' tubers were used to train neural networks to 'learn' the characteristics of bruised and unbruised tubers. The neural nets were trained with whole wavelength ranges or a subset of wavelengths selected by discriminant analysis. The two different sets of training stimuli were used to assess the value of discriminant analysis for reducing the number of variables. If neural nets can perform with whole ranges of wavelengths then this would simplify the spectrophotometric method.

After a net was trained it was presented with the 'trial' spectra to assess how accurately it could recognise a bruised tuber when the identity was unknown to the net. The comparison of neural nets with discriminant analysis to classify these 'trial' tubers is difficult to interpret. For some spectra, neural nets appeared to improve the classification results, while for others it made it worse. If discriminant analysis did *not* give a significant classification result, the neural nets only managed to give a significant result for a few of these cases. Most notably, these were for UV spectra from unpeeled Record tubers and spectra collected with the integrating sphere from unpeeled Pentland Dell and Record tubers. When discriminant analysis did give a significant classification result, the neural nets often improved slightly on the percentage of tubers correctly classified. However, it is hard to statistically quantify whether neural networks did improve the classification results for these cases.

The use of wavelengths selected by discriminant analysis to train and interrogate neural nets, versus the use of whole wavelength ranges is also complex to interpret. The use of whole wavelength ranges to train a net took longer than with a few wavelengths, but once a net is trained the time taken to interrogate the net is similar for both. However, selecting wavelengths that were sensitive to bruising with discriminant analysis reduced the problem of classifying all tubers as bruised or unbruised. The use of a subset of wavelengths also appeared to increase the percentage of tubers correctly classified in some cases. Perhaps the most obvious improvement was for spectra collected from peeled tubers with the integrating

sphere. Therefore, neural nets benefit from the association with discriminant analysis to reduce the number of variables.

The use of reflectance spectrophotometry as a non-invasive and rapid means of detecting bruising is not consistent enough at present to detect bruising in unpeeled tubers. It was found in Chapter 8 that an integrating sphere overcame some of the disadvantages of a bifurcated fibre optic in the visible part of the spectrum, and that more tubers were correctly classified as a result. However, in Chapter 7 it was found that the only significant discrimination between unbruised and bruised tubers was in the NIR. If the integrating sphere improved the classification of tubers in the visible spectrum, it may be possible to further improve the detection of bruising by using NIR spectra. Further work is needed to investigate NIR spectra collected with an integrating sphere as a method of detecting bruising in unpeeled tubers.

The non-invasive detection of bruising in peeled tubers is a more robust technique. The absence of skin makes the reflectance spectra more consistent and the difference between unbruised and bruised tubers appears to be greater, particularly in the visible part of the spectrum. However, this may be more of theoretical rather than practical interest as it is bruising in unpeeled tubers that go unnoticed through quality control. A possible application for reflectance spectrophotometry would be where tubers are peeled just prior to processing. Sensors could be designed to rapidly monitor wavelengths associated with bruising, and machinery designed to automatically reject bruised tubers.

Chapter 10

Detection of bruising with thermography and scanning laser Doppler imaging

10.1 Introduction

Bruising in potato tubers leads to a rise in respiration (section 2.1.5) which can be detected by measuring the carbon dioxide concentration with an infrared gas analyser (Pisarczyk 1982). Tubers with bruising have a higher respiration rate than unbruised tubers, and so release more carbon dioxide. However, infrared gas analysis cannot pinpoint the location of bruises on tubers. It is known that a rise in respiration can cause a rise in temperature in plant tissues (Straeten *et al.* 1994), therefore, it is possible that a rise in potato tuber respiration may be accompanied by a rise in temperature. If the temperature of bruised tissue could be measured non-invasively then this might be a method for detecting bruised tubers.

Until recently, measurements of thermal changes in bruised tissue have not been measured due to difficulties in obtaining accurate, non-invasive estimates of temperature. However, two recent clinical developments in non-contact thermography appear to have potentially accurate ways of assessing tuber temperature: infra-red (IR) thermography is capable of measuring very superficial, surface values, and microwave thermography (MW) of measuring temperatures from deeper tissues (Land *et al.* 1987). Both are very portable, are sensitive to 0.10 °C and can give readings within two seconds.

Since the thermographic measurements were done in a clinical setting another available technique, laser Doppler imaging (Wardell *et al.* 1993) was employed to assess its potential for bruise detection. This technique is normally used to measure blood flow in the human skin: some of the incident light is Doppler shifted by moving red blood cells and this can be detected, quantified and used to measure blood flow. While this Doppler shifted component is clearly unavailable in the case of the bruised or unbruised potato, there is another component of the signal which has potential relevance, namely, the 'biological zero' which occurs at a low level and is present even without flow. The magnitude of this signal is known to alter with the properties of the underlying tissue (Abbot and Beck 1993) and so it is this signal which might possibly change for unbruised to bruised tissue.

In this chapter, IR and MW thermography, with laser Doppler imaging as a supplement, were used to try to detect bruised sites by a) temperature differences and

b) changes in the magnitude of the biological zero compared with surrounding unbruised skin.

10.2 Methods

10.2.1 Samples

Tubers of the variety Record were hand dug, washed and stored at 4°C. The tubers were impacted with the SCAE dropper (section 7.2.2.) and placed in a hotbox overnight. The tubers were then placed in a thermostatically controlled room at 21°C for 2 hours before measurements of tuber temperature were started.

10.2.2 Infrared (IR) and microwave (MW) temperature measurements

All materials above absolute zero emit thermally generated electromagnetic radiation. In the IR (about 10000 nm) the radiation is emitted from the material a few millimetres deep (Fraser *et al.* 1987). The emission of the radiation is dependent on the conducted energy from below and environmental temperature. By using a longer wavelength in the centimetre region of the electromagnetic spectrum, MW thermography has greater penetration depth and no environmental controls are needed. The exact depth of thermal radiation in the microwave region is difficult to determine as it is affected by the water content of the tissue, but it is thought to be of several centimetres in magnitude (Land *et al.* 1991).

IR and MW thermography were used to measure the temperature of bruised and unbruised tuber tissue. The IR measurements involved using a hand held probe (Biotherm, Chicago, USA) to measure the temperature of tuber tissue with a resolution of 0.10°C. The custom-made MW apparatus (Department of Physics, University of Glasgow) consists of a microwave aerial in contact with the tuber skin and a receiver which amplifies and measures the signal. The body-contact aerial is in the form of a cylinder, 2.8 cm in diameter, 6.5 cm in length, which is connected to the receiver unit through a 1.5 m flexible microwave cable assembly. The receiver operates in the lower microwave frequency region near 3 GHz (Land *et al.* 1991).

10.2.3 Scanning laser Doppler measurements

After the temperature of the unbruised and bruised tuber tissue sites were measured, a laser Doppler scan was taken from the same sites. The laser Doppler scanner (LISCA development AB, Linkoping, Sweden) works on the principle that when a

narrow and monochromatic light beam illuminates a tissue surface, incident photons penetrate the tissue to a depth determined by its optical properties in that region. A fraction of the back-scattered light can be detected by a photodetector and the signal processed to give a signal proportional to the tissue perfusion at that measurement point. By sequentially scanning the tissue with the laser an image of the tissue perfusion at each point can be generated. When the scanning procedure is completed, the system generates a colour-coded perfusion image on a monitor. A perfusion image is built up of data from 4096 measurement sites with a spatial resolution of 2 by 2 mm (Wardell *et al.* 1993).

In the LISCA scanner there are two lasers that can be selected: a helium-neon (He-Ne) laser at 632.8 nm and a NIR laser at 780 nm. In the human skin it is estimated that the sampling depth of the He-Ne laser is 200 to 240 μm depending on the blood content, and that the sampling depth is slightly greater with the NIR laser (Obeid *et al.* 1988). In this experiment, a scan of the tuber tissue was made with both the He-Ne and the NIR laser as a comparison.

10.3 Results

The mean temperature of bruised tuber sites was lower than unbruised sites for IR and MW thermography measurements. However, a two-tailed t-test (BMDP Statistical Software, California) showed that the mean temperatures of bruised and unbruised tubers are not significantly different (Table 10.1).

Table 10.1 Analysis of temperatures from unbruised and bruised sites on unpeeled Record tubers measured with IR and MW thermography.

	Infrared temperatures		**Microwave temperatures**	
	Bruised site	**Unbruised site**	**Bruised site**	**Unbruised site**
Mean	22.810	23.005	25.405	25.72
SD	0.656	0.576	0.696	0.485
t value	-2.052		-1.64	
P value*	0.0541		0.11	

* The probability of obtaining a t value lower than the t value given in this table.

Figure 10.1 shows a colour coded perfusion image with the He-Ne and NIR laser. These tubers had the largest bruised site of all the tubers analysed. The bruised area is within the circle marked on the scan. The difference between bruised and unbruised tubers is not readily apparent.

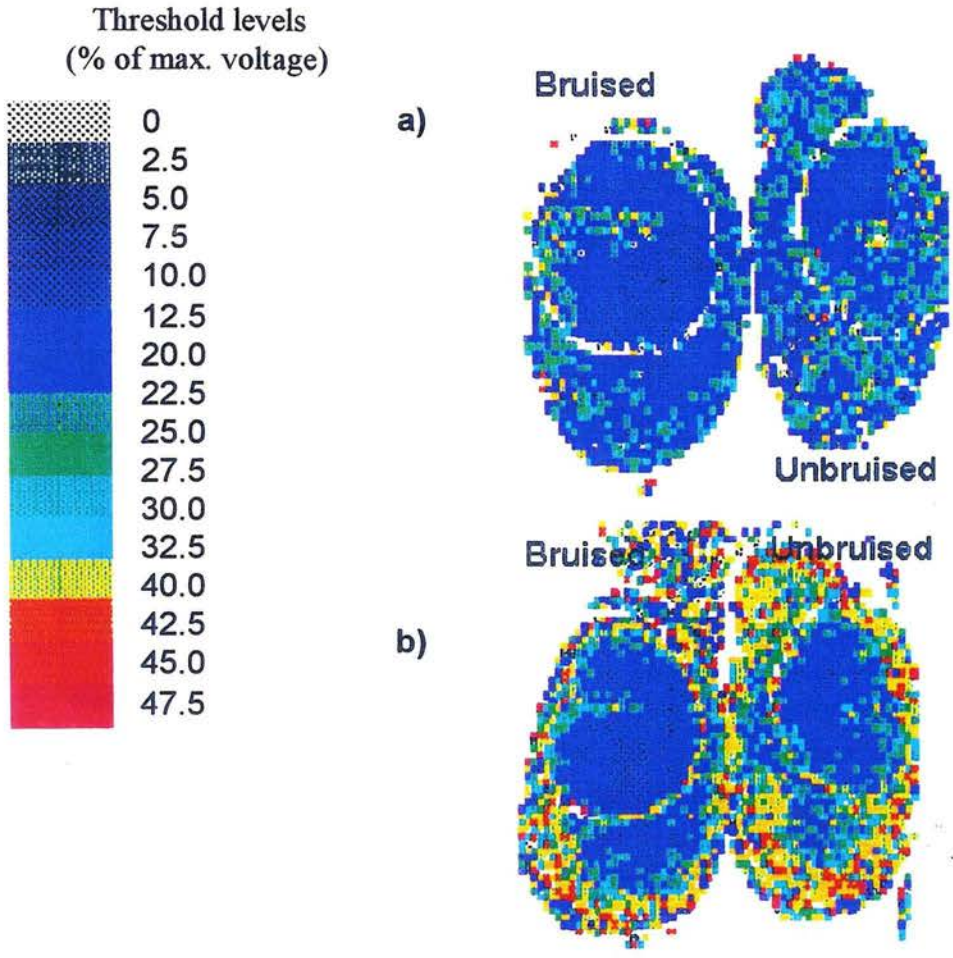

Fig. 10.1 Colour coded perfusion image with a) He-Ne laser and b) NIR laser. The white ring on the images corresponds to a black line drawn around the unbruised and bruised sites.

The scanning laser Doppler gave measurements of tissue perfusion as a voltage. The mean voltages were calculated for an area 11 by 11 pixels in the centre of bruised and unbruised sites. Both the He-Ne and NIR laser gave a lower voltage for bruised sites, but a t-test of the means showed that the difference was not significant (Table 10.2).

Table 10.2 Analysis of perfusion values (voltages) measured with a He-Ne and NIR laser in an area 11 by 11 pixels.

	He-Ne laser		**NIR laser**	
	Bruised	**Unbruised**	**Bruised**	**Unbruised**
Mean	0.74	0.76	0.31	0.34
SD	0.16	0.16	0.09	0.09
Degrees of freedom	28		28	
t value	-7.586		-1.165	
P value	0.454		0.276	

* The probability of obtaining a t value lower than the t value given in this table.

10.4 Discussion

There were no significant differences between the temperatures of bruised and unbruised tuber tissue measured with IR and MW thermography. There are several possible reasons for the lack of significant differences:

- The rise in temperature was too small to be detected with equipment that has a resolution of only 0.10°C.
- Small fluctuations in ambient conditions could easily have affected and confused the IR measurements.
- There is no rise in tuber temperature as a result of bruising, although without more sensitive apparatus this cannot be verified.
- Microwave thermography measures temperatures from tissue greater than 2 or 3 cm deep, and since bruising occurs in the sub-surface tissue it is unlikely that this method is measuring changes in temperature associated with bruising.

In addition to measurements of tuber tissue temperature, the amount of laser light reflected from unbruised and bruised tubers was determined. In some individual tubers, a higher biological zero value could be seen by eye, corresponding to the area of a bruise on the laser Doppler image. However, such rises were small compared to variations in biological zero signal over unbruised tuber tissue and overall no significant increase could be determined. It must be remembered, that the laser Doppler imaging system is calibrated to sensitively detect Doppler shifted light, and that changes to the biological zero, even when accurately detected, are comparatively small.

Chapter 11

Quantification of bruising using reflectance spectrophotometry and colour CCD image analysis system

11.1 Introduction

There is a need for a rapid and non-subjective method for quantifying bruising. In the past researchers have used a reflectometer which measures the total reflectance from a sample (Mapson *et al.* 1963, Pavek *et al.* 1985, Kunkel and Gardner 1986, Dean *et al.* 1993). However, it was found that the measurements were affected by the colour of the bruise and the amount of skin removed to expose the bruise.

It may be possible to improve the reflectometer principle by using reflectance spectrophotometry. Reflectance spectrophotometry measures single wavelengths of light and due to its sensitivity and accuracy it may be possible to quantify bruising in unpeeled tubers. The time needed to evaluate bruising could be significantly reduced if tubers no longer needed to be peeled before quantifying a bruise.

Image analysis techniques were used to accurately measure bruise area for correlation with reflectance measurements. Image analysis involves the capturing of an image with a digital camera, optimising the image, selecting features of interest, and calibrating and measuring the features within the image. The digital camera was also used to determine if it would be a practical method for bruise assessment.

11.2 Methods

11.2.1 Samples and spectra acquisition

One hundred tubers of the variety Record were hand dug, washed and stored at 4°C. Tubers were impacted with the SCAE dropper and placed in a hotbox for 16 hours. Reflectance measurements of unpeeled and peeled tubers were taken with an integrating sphere and spectrophotometer (Chapter 8) from 400 to 700 nm and converted into first derivative spectra. After a tuber was peeled and a reflectance spectrum taken, the area of the bruise was measured with a colour camera connected to a computer. Additional measurements were also made of bruise depth with a Vernier guage and bruise volume calculated using the formula:

$$V = \frac{4}{3} \cdot \text{area} \cdot \text{depth}$$

11.2.2 Image analysis system

The colour camera (KP-C500 series, Hitachi Denshi Ltd., Japan) has an array of 722 x 492 CCD (Charged Coupled Device) picture elements. The CCD colour camera ensures a sharp, clear picture with high sensitivity and without geometric distortion.

The camera was mounted in a stand and a tuber evenly illuminated by four lamps (Philips, UK 75W Photocrescenta PF 603 E/51) placed around an opaque glass diffuser (Fig. 11.1). The focus and iris were adjusted on the camera to ensure the tuber was evenly lit and in focus. A rule was placed alongside the tuber to calibrate measurements of area with the camera.

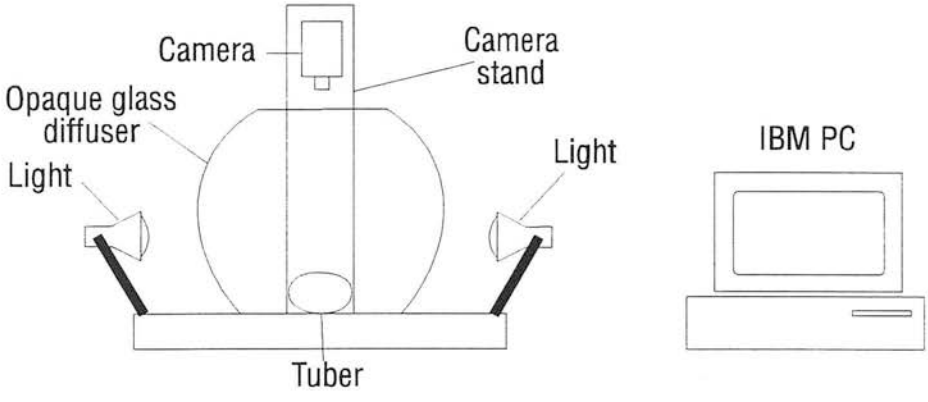

Fig. 11.1 Image analysis set up.

The camera is controlled by MicroScale TC image analysis software (Digithurst Ltd.) and a TC (True Colour) transputer-based framestore image processing card. The transputer handles image capture and processing, relieving the PC processor from tasks at which it is not particularly efficient.

An image of the tuber was first captured (Fig. 11.2) and a rectangular region defined that contained the bruised tissue. Once a region has been defined, all further processing and analysis take place only within that region.

The Microscale TC card holds the captured image as a 720 (horizontal) by 512 (vertical) matrix of picture elements (pixels). Each pixel consists of 24 bits, with 8 consecutive bits representing the brightness level of each of the red, green and blue image planes into which the image is split. In colour mode, the system can work on the whole image colour data, or just the information from one of these planes.

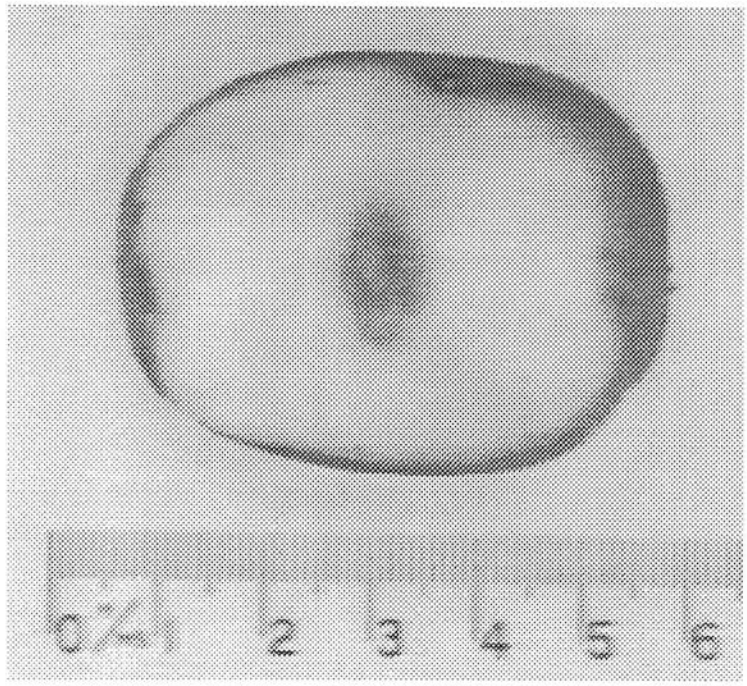

Fig.11.2 Captured image of tuber.

The next step is to select the objects and features of interest in the image, first by thresholding the image, and then by using image editing functions. Pixels are selected from the image to set up the threshold, and MicroScale calculates the maximum and minimum values for each of the red, green and blue components of the current group of chosen pixels. MicroScale then compares all the pixels in the selected region with the threshold values set, and any that fall inside all the constraints are placed in a Binary Map (i.e. are classed as 'detected'). A binary dilate function is then used to join objects that are separated after thresholding, but should not be (Fig. 11.3).

Fig. 11.3 a) Pixels within selected region are selected to set threshold values and then b) any pixels that fall inside the constraints are placed in a Binary Map and a binary dilate function used to join any pixels separated after thresholding.

The fourth step is to calibrate MicroScale measurements by comparing the number of pixels in the image with a known scale. In this experiment, a rule in the image is used to calibrate the MicroScale measurements (Fig. 11.4).

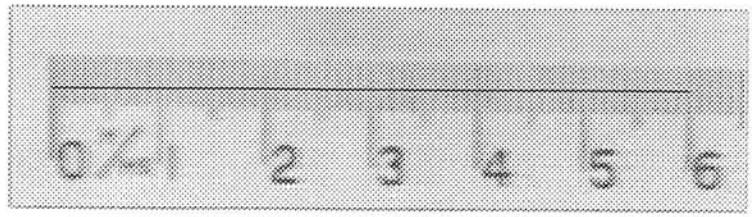

Fig. 11.4 Calibration of MicroScale measurements with a scale in the image.

Once the system has been calibrated, the area of the thresholded region can be evaluated (Fig. 11.5) in units of mm^2.

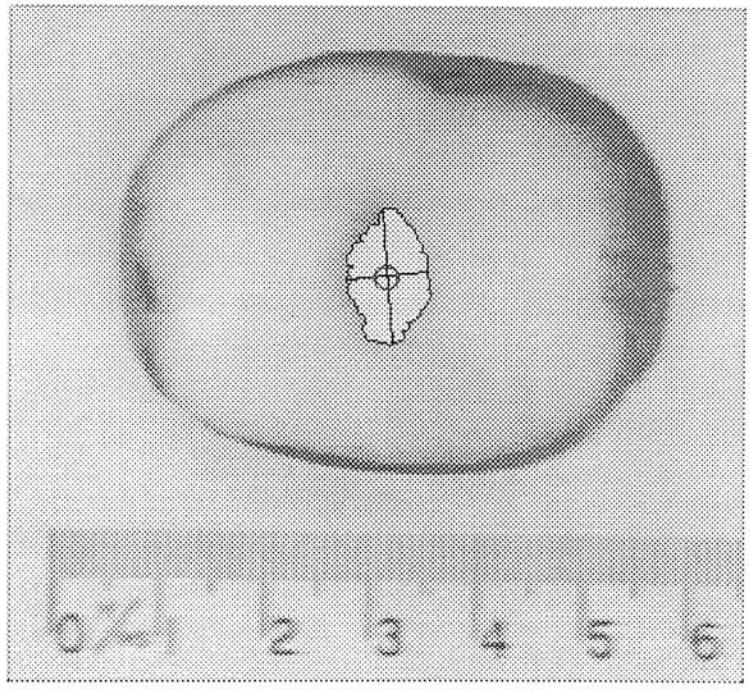

Fig. 11.5 Evaluation of area within the thresholded region.

The process of calibration needs to be carried out once, providing the camera is not moved. The time taken to grab an image, threshold and measure bruise area was about 30 seconds.

11.2.3 Data analysis

Regression Variable Selection (BMDP Statistical Software) was used to find the best set of wavelengths that predict bruise area. The best sets of variables are the ones that give the highest R-square value. The algorithm used by BMDP first finds the best single variable. Then to find the best pair of variables it tries each of the remaining variables and selects the one that adds the most to the R-square value. It then omits the first variable and determines if any other variable would add more to the R-square value. If one is found, it is kept and another search is made through the

list of remaining variables. This switching process continues until no switching will result in a better (higher R-square) subset of variables.

After finding the optimal pair of variables, the program searches for the best three variables in much the same manner. First, the best third variable is found using the optimal two from the last step. Next, each of them is omitted and each remaining variable is tested to determine if it would add more to the R-square. The algorithm continues until no switching improves the R-square.

However, in practice there can be a large number of variables selected with only small improvements in the R-square for each additional variable. Therefore, the number of variables the program could select was limited to seven and from these the selection was further refined by using Multiple Regression Analysis (BMDP Statistical Software). This is achieved by observing the effect each variable has on the overall R-squared value and selecting those with the greatest effect. Multiple Regression Analysis was also used to determine the straight-line relationship among two or more variables. Multiple regression estimates the β_i's in the equation:

$$Y_j = \beta_0 + \beta_1 X_{1j} + \beta_2 X_{2j} + ...\beta_p X_{pj} + e_j$$

Where the X's are the independent variables. Y is the dependent variable. The subscript j represents the observation (row) number. The β's are the regression coefficients. The e is the error, disturbance or residual.

The β's are selected to minimise the sum of the squared e's, otherwise known as least squares regression.

11.3 Results

The image analysis system was capable of measuring bruises as small as 3.9 mm^2 and as large as 157 mm^2. Providing there was a discernible bruise on a tuber, the camera was capable of thresholding and measuring the bruised area (Figs 11.6 and 11.7).

The mean bruise area was 57.9 mm^2 ± 95% confidence limits of 50.6 mm^2. The correlation between bruise area measured by rule (length of bruise multiplied by width) and area measured with digital camera was 0.77. Mean bruise volume was 155.69 mm^3 ± 95% confidence limits of 182.6 mm^3.

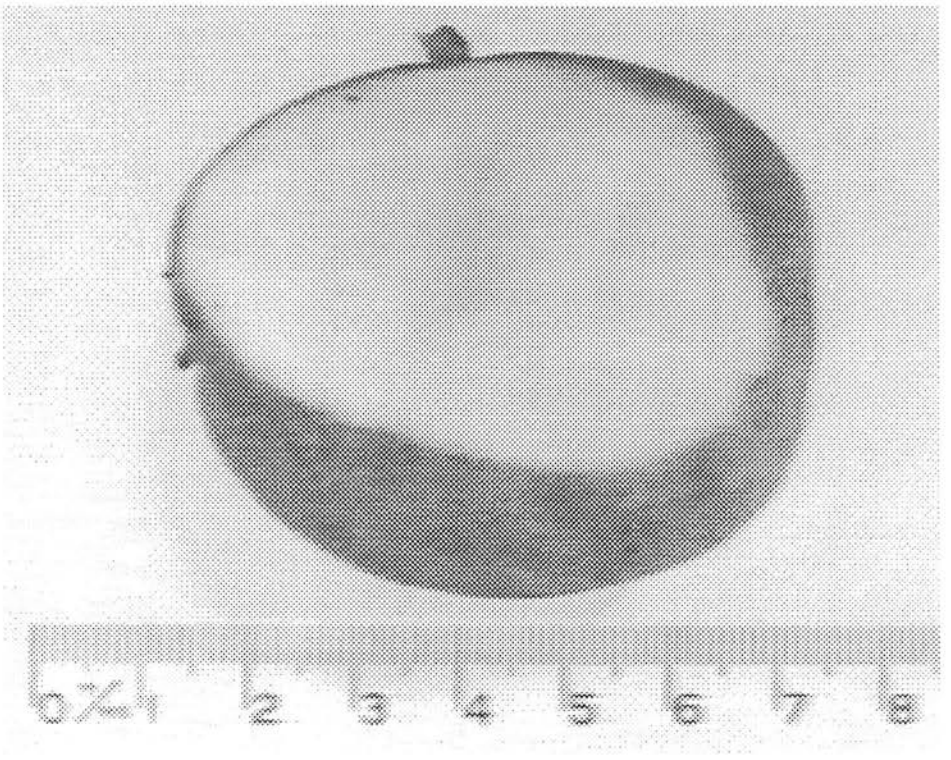

Fig. 11.6 Pale bruise on tuber.

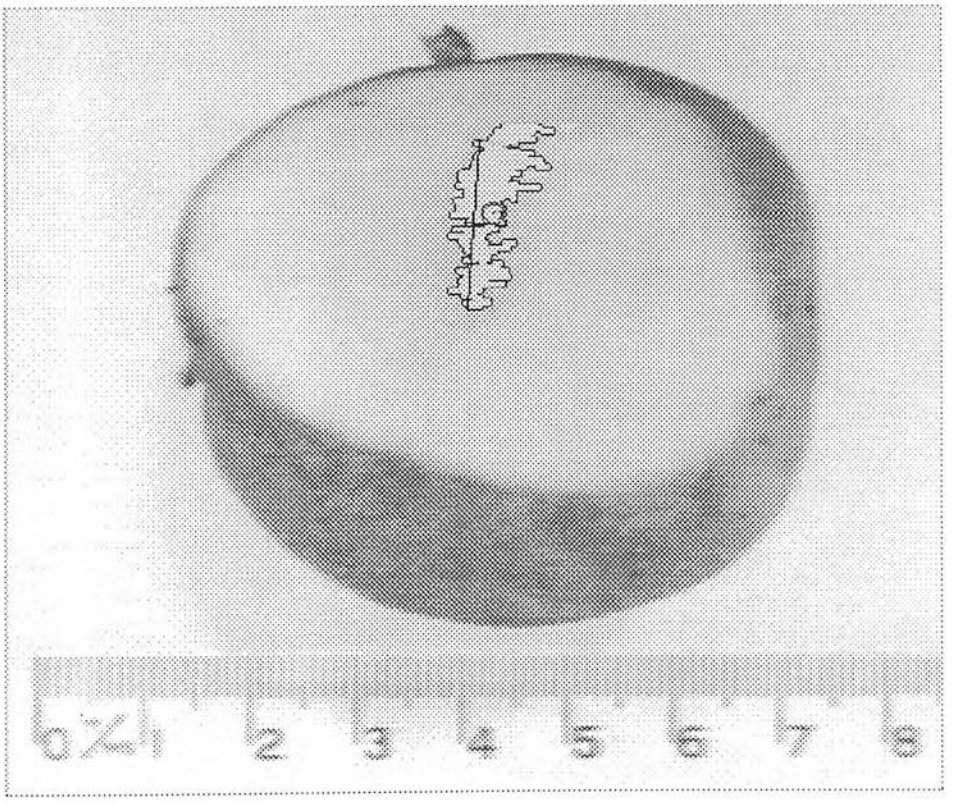

Fig. 11.7 Thresholding of pale bruise and measurement of area.

Correlation coefficient of area versus volume is 0.88. The bruise with the largest and smallest area had the largest and smallest bruise volume (Fig. 11.8).

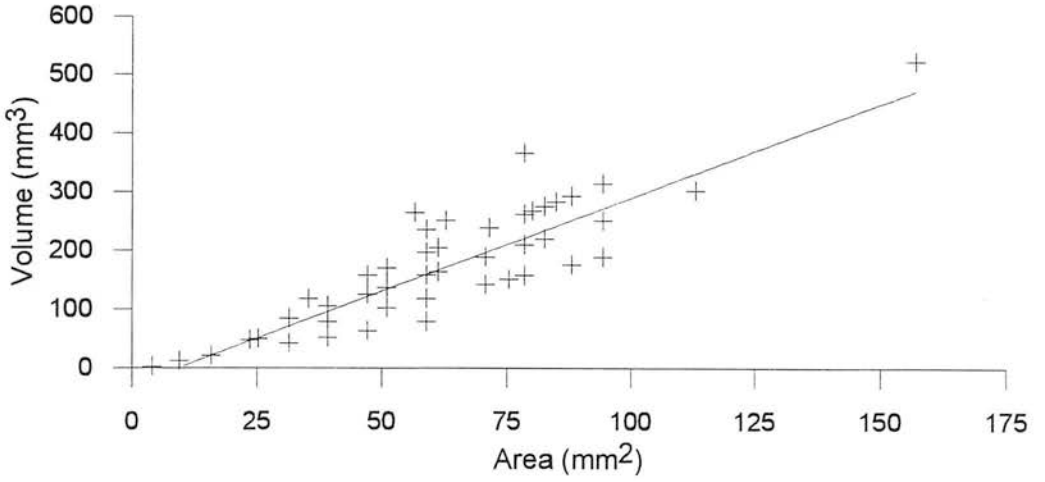

Fig. 11.8 Plot of bruise area against bruise volume.

11.3.1 Unpeeled tubers

The first derivative spectra from unpeeled tubers appear to be erratic with a possible separation between the smallest and largest bruise areas at about 685 nm (Fig. 11.9).

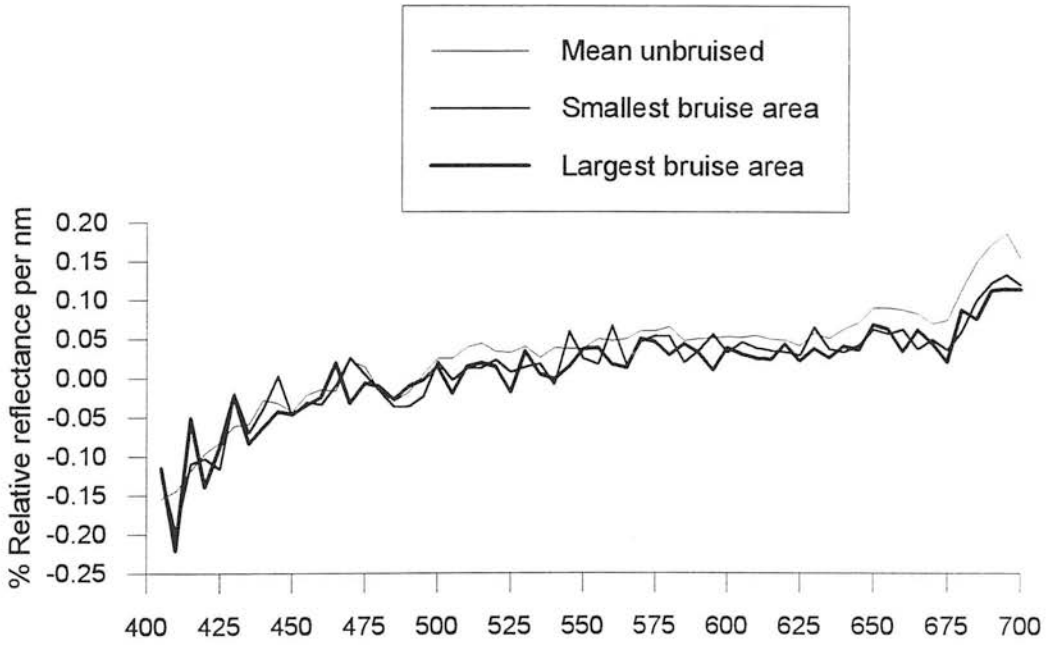

Fig. 11.9 First derivative spectra of unbruised, smallest and largest bruise area from unpeeled Record tubers; 400 to 700 nm.

Regression variable selection identified wavelengths at 440, 445, 545, 550, 575, 580, and 655 nm. The first wavelength selected was 655 nm with an R-square value of 0.13. With seven variables selected the R-square value was 0.41 (Table 11.1).

Figure 11.10 shows the plot of bruise area against the first derivative value at 655 nm.

Table 11.1 Regression variable selection from first derivative spectra of unpeeled Record tubers versus bruise area.

Wavelength (nm)	R-square value
655	0.13
575, 655	0.20
575, 580, 655	0.25
550, 575, 580, 655	0.29
440, 445, 575, 580, 655	0.33
440, 445, 550, 575, 580, 655	0.38
440, 445, 545, 550, 575, 580, 655	0.41

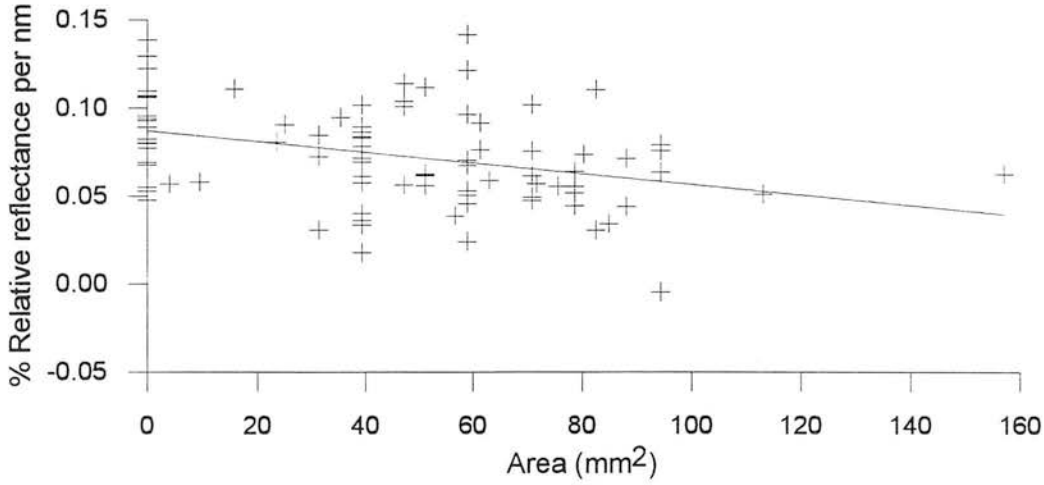

Fig. 11.10 Plot of first derivative at 655 nm from unpeeled Record tubers against bruise area.

Analysis of bruise volume gave an R-square value of 0.39 for seven wavelengths. These wavelengths were very similar to those selected for bruise area, with the addition of wavelengths at about 415 and 515 nm (Table 11.2). Figure 11.11 shows the plot of bruise volume against the first derivative at 575 nm.

Table 11.2 Regression variable selection from first derivative spectra of unpeeled Record tubers versus bruise volume.

Wavelength (nm)	R-square value
575	0.12
575, 580	0.19
575, 580, 655	0.25
415, 575, 580, 655	0.28
415, 515, 575, 580, 655	0.32
415, 445, 515, 575, 580, 655	0.35
415, 440, 445, 515, 575, 580, 655	0.39

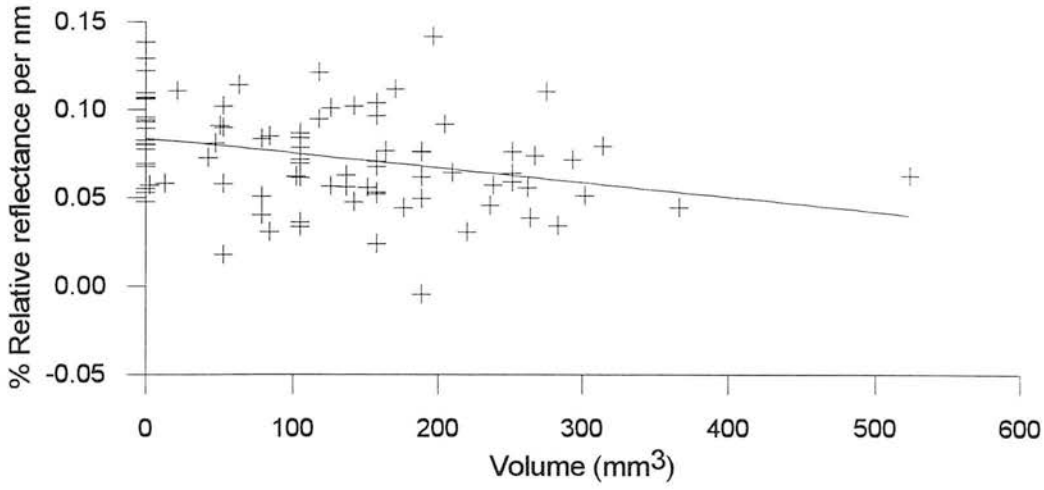

Fig. 11.11 Plot of first derivative at 575 nm against bruise volume.

The wavelengths selected by regression variable selection were reduced to a minimum with multiple regression analysis. For bruise area, six variables were included in the linear regression equation to give an overall R-square value of 0.38. For volume, three variables were included to give an overall R-square value of 0.25. Table 11.3 shows the coefficients for the multiple regression of bruise area and bruise volume.

Table 11.3 Multiple regression analysis of first derivative spectra of unpeeled tubers versus area and volume.

Depend. variable	Ind. variable	βest[1]	Stand Error[2]	t value[3]	Prob. level[4]	Seq. R square[5]	Simp. R square[6]
Area	intercept	94.6	15.4	6.14	0		
	440 nm	-429.5	146.2	-2.94	0.004	0.02	0.02
	445 nm	-442.6	136.5	-3.24	0.002	0.07	0.01
	550 nm	656.6	247.6	2.65	0.009	0.09	0.02
	575 nm	-654.3	175.9	-3.72	0.0004	0.20	0.10
	580 nm	-664.4	190.3	-3.49	0.0008	0.30	0.10
	655 nm	-388.2	109.7	-3.54	0.0007	0.38	0.13
Volume	intercept	350.93	44.1	7.95	0		
	575 nm	-1365.3	538.4	-2.54	0.01	0.12	0.12
	580 nm	-1557.3	582.3	-2.67	0.009	0.19	0.12
	655 nm	-900.9	355.3	-2.53	0.01	0.25	0.09

intercept; the β_0 in the regression equation. [1] The regression coefficients; the β in the multiple regression equation. [2] The standard error of β. An estimate of the precision of the regression coefficient. [3] The t-statistic for testing $\beta=0$ against the alternative $\beta\neq0$. [4] The probability of obtaining a t-value greater than the above in absolute value. [5] The incremental value of R-squared as each independent variable is added to the regression equation. [6] The R-squared value that would be obtained if the regression equation contained only the variable named in the row.

11.3.2 Peeled tubers

First derivative spectra reveal that the greatest change in slope between the smallest and largest bruised area is at 470 nm and 500 to 520 nm (Fig. 11.12).

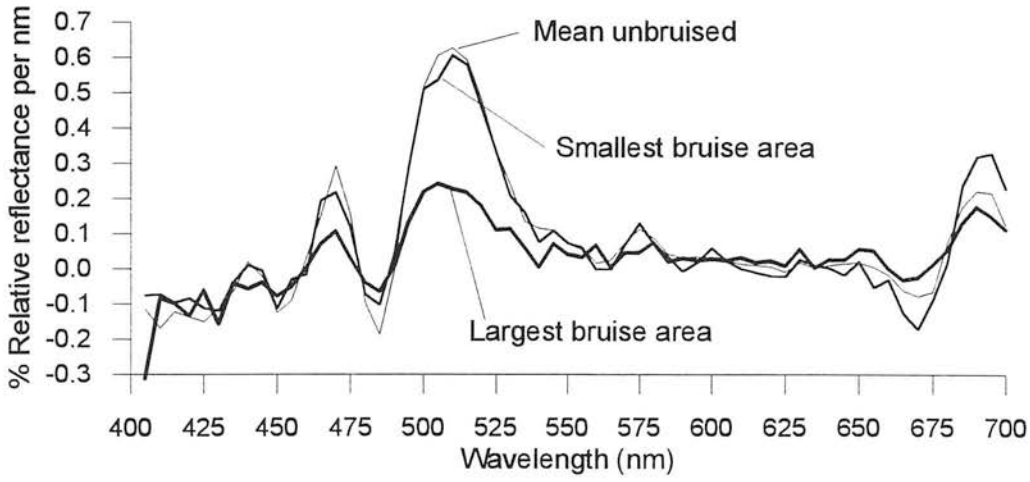

Fig. 11.12 First derivative spectra of unbruised, smallest and largest bruise area from peeled Record tubers; 400 to 700 nm.

Regression variable selection selected wavelengths at 435, 440, 515, 575, 635, 640 and 685 nm for measuring bruise area (Table 11.4).

Table 11.4 Regression variable selection from first derivative spectra of peeled Record tubers versus bruise area.

Wavelength (nm)	R-square value
515	0.48
515, 645	0.51
435, 440, 515	0.55
435, 440, 515, 640	0.58
435, 440, 515, 640, 685	0.61
435, 440, 515, 575, 640, 685	0.62
435, 440, 515, 575, 635, 640, 685	0.64

The R-square value for the first variable selected, 515 nm, was 0.48. Figure 11.13 shows the plot of the first derivative reflectance spectra at 515 nm against bruise area.

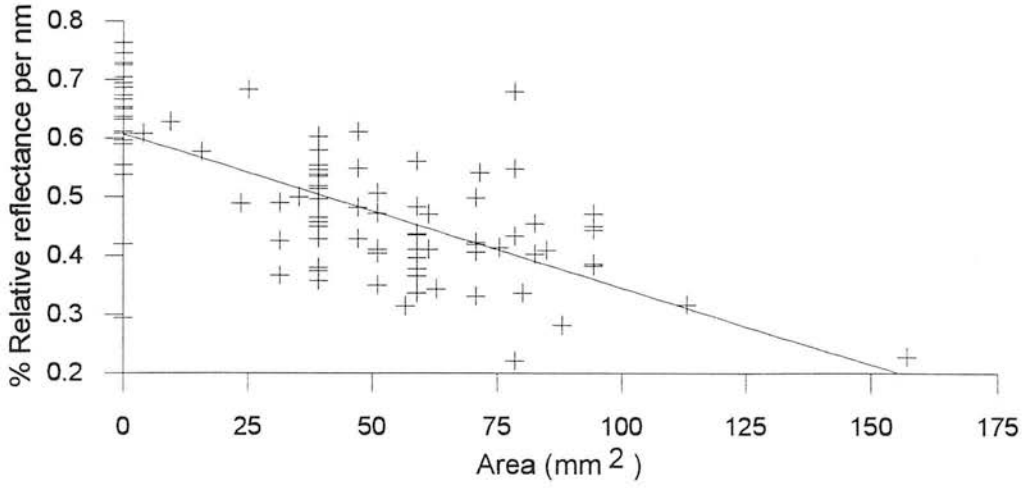

Fig. 11.13 Plot of first derivative at 515 nm from peeled Record tubers against bruise area.

Wavelengths selected for bruise volume were almost identical to those for bruise area, with 510 nm being selected first instead of 515 nm (Table 11.5). Figure 11.14 shows the plot of the first derivative at 510 nm against bruise volume.

Table 11.5 Regression variable selection from first derivative spectra of peeled Record tubers versus bruise volume.

Wavelength (nm)	R-square value
510	0.42
510, 645	0.46
515, 565, 585	0.49
440, 515, 565, 585	0.53
440, 515, 565, 585, 640	0.54
440, 515, 565, 585, 635, 640	0.57
435, 440, 515, 565, 585, 635, 640	0.60

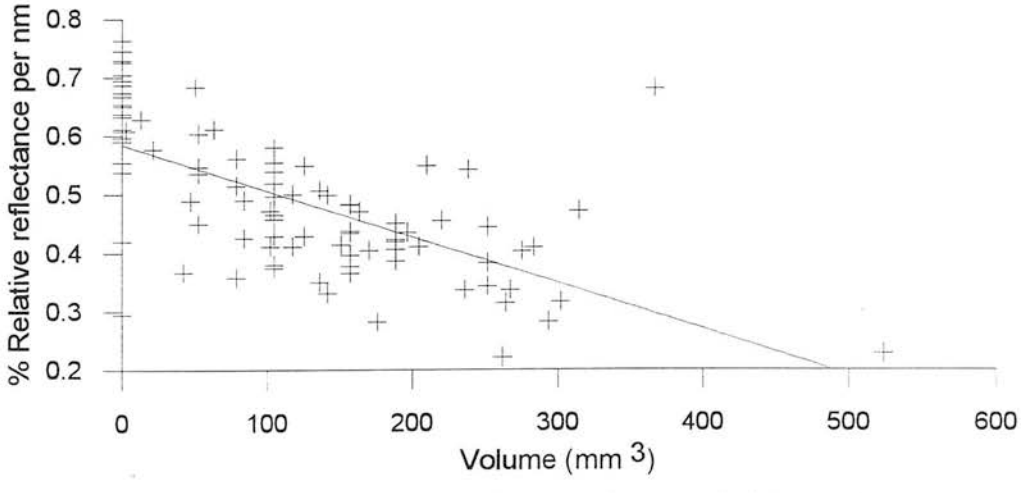

Fig. 11. 14 Plot of first derivative at 510 nm from peeled Record tubers against bruise volume.

Multiple variable regression analysis of the variables selected by variable selection reduced the number of variables to two for bruise area and three for bruise volume. The overall R-squared value for bruise area was 0.51, and 0.48 for bruise volume (Table 11.6).

Table 11.6 Multiple regression analysis of 1st derivative spectra of peeled tubers versus area and volume.

Depend. variable	Ind. variable	βest.[1]	Stand. error[2]	t value[3]	Prob. level[4]	Seq. R square[5]	Simp. R square[6]
Area	intercept	125.12	9.7	12.92	0		
	440 nm	-205.35	88.4	-2.32	0.02	0.13	0.134
	515 nm	-175.2	21.1	-8.31	0	0.51	0.483
Volume	intercept	376.81	33.1	11.36	0		
	440 nm	-642.24	287.9	-2.23	0.03	0.13	0.13
	515 nm	-467.21	70.4	-6.64	0	0.45	0.41
	585 nm	-1130.3	474.5	-2.40	0.02	0.48	0.11

intercept; the β_0 in the regression equation. [1] The regression coefficients; the β in the multiple regression equation. [2] The standard error of β. An estimate of the precision of the regression coefficient. [3] The t-statistic for testing $\beta=0$ against the alternative $\beta\neq0$. [4] The probability of obtaining a t-value greater than the above in absolute value. [5] The incremental value of R-squared as each independent variable is added to the regression equation. [6] The R-squared value that would be obtained if the regression equation contained only the variable named in the row.

11.4 Discussion

The digital camera was capable of measuring a variety of bruise colours and areas with precision. However, the threshold values had to be varied for each tuber making bruise assessment time consuming. There are also possible errors associated with measuring bruise area if the tuber is not at 90° to the camera or if the tuber surface is curved.

First derivative reflectance spectra from unpeeled tubers showed less obvious differences between the largest and smallest bruise areas than from peeled tubers. Statistical analysis of these spectra revealed that for unpeeled tubers reflectance measurements are probably too erratic to be reliably used for bruise assessment. Regression variable analysis and multiple variable regression selected seven wavelengths from first derivative spectra of unpeeled tubers compared to two wavelengths for peeled tubers. The R-square value for correlation of bruise area and these wavelengths was also lower for unpeeled tubers (R square of 0.38) than peeled tubers (R square 0.51).

When bruise volume was correlated with first derivative spectra the R square value was reduced to 0.25 for unpeeled tubers and 0.48 for peeled tubers. Reflectance spectra are more sensitive to bruise area rather than bruise depth. However, providing bruise area is quantified accurately the volume of bruise could be predicted from the linear relationship between bruise area and volume.

Reflectance spectrophotometry can measure bruise sizes faster than the image analysis system, but less accurately. The method might be improved by combining reflectance spectrophotometry with image analysis techniques. Reflectance measurements could determine the threshold values and the camera then used to calculate the bruise area. This method could be used to develop a system for the automatic sorting of tubers which are peeled just prior to processing.

Chapter 12

The effect of temperature on the rate of melanin formation *in vitro*

12.1 Introduction

The rate of melanin formation *in vitro* is controlled by a number of factors. Muneta (1977) showed that the reaction rates for both the enzymatic and non-enzymatic reactions are pH dependent. The enzymatic oxidation of tyrosine, the main phenol involved in the formation of melanin, is very slow at pH 4 and increases rapidly at pH 5. The rate of oxidation is also affected by the levels of tyrosine and polyphenol oxidase (Horowitz and Shen 1952).

Temperature is also likely to be an important factor, but to date the kinetics of the melanin formation in relation to temperature changes have not been studied. Consequently, experiments were devised to monitor the rate of colour change from dopachrome to melanin at different temperatures using transmission spectrophotometry. This involved extracting polyphenol oxidase from potato tubers and adding this to known quantities of the substrate dopa. An orange solution of dopachrome was obtained which was warmed to 20°C, 40°C and 60°C. Transmission spectrophotometry was used to enable single wavelengths to be monitored from 400 to 600 nm as orange dopachrome developed into black melanin.

12.2 Methods

The method of polyphenol oxidase extraction was modified from Muneta (1977). Tubers of the variety Record were hand dug and washed. Approximately 100g potato, 90g ice and 15 ml ascorbic acid solution (2.8 g ascorbic acid in 100 ml water, neutralised to pH 6 with NaOH) were ground in a Moulinex blender for 2 minutes. Ascorbic acid was added to inhibit melanin formation. The mixture was filtered through a Buchner funnel with a Whatman 41 filter paper and Whatman electronic suction pump (Whatman, London, UK). The ground potato residue was washed with 300 ml of distilled water. The filtrate containing most of the polyphenol oxidase was discarded as the products react quickly to give melanin.

The potato residue was then mixed with 150 ml distilled water in a beaker. Ten ml of 0.01M L-dopa were added to 100 ml of residue mixture. The remaining 50 ml of residue mixture was filtered with Whatman GF/A paper and suction pump and kept aside as a reference. The reaction between dopa and polyphenol oxidase in the

residue was allowed to take place for 5 minutes before being filtered with Whatman GF/A paper and suction pump. An orange filtrate of dopachrome was obtained.

Twenty five ml of dopachrome filtrate were added to 25 ml of 0.2 M phosphate/citrate buffers at pH 6.0 (final pH of solution was 6.2). The solution was added to five 1 ml cuvettes. A sixth cuvette contained the reference solution of filtered residue without the addition of dopa. The cuvettes were placed in a temperature regulated holder inside a Beckman DU-65 scanning transmission spectrophotometer (Beckman, Germany). Cuvettes were kept at 20°C, 40°C or 60°C. The spectrophotometer took absorption spectra from 400 to 600 nanometers (nm) in 25 nm steps. A spectral scan was first taken of the reference solution and then from the five cuvettes containing the dopachrome solution. The scan of the reference solution was started 15 minutes after the addition of dopa to allow sufficient time to organise the cuvettes and program the spectrophotometer. Each spectrum took approximately 75 seconds to collect, so the first measurement of a dopachrome solution was approximately 17 min after the addition of dopa. A scan of all six cuvettes was taken at 15 min intervals.

12.3 Results

Figure 12.1 shows the overall pattern of spectral changes determined from cuvette samples.

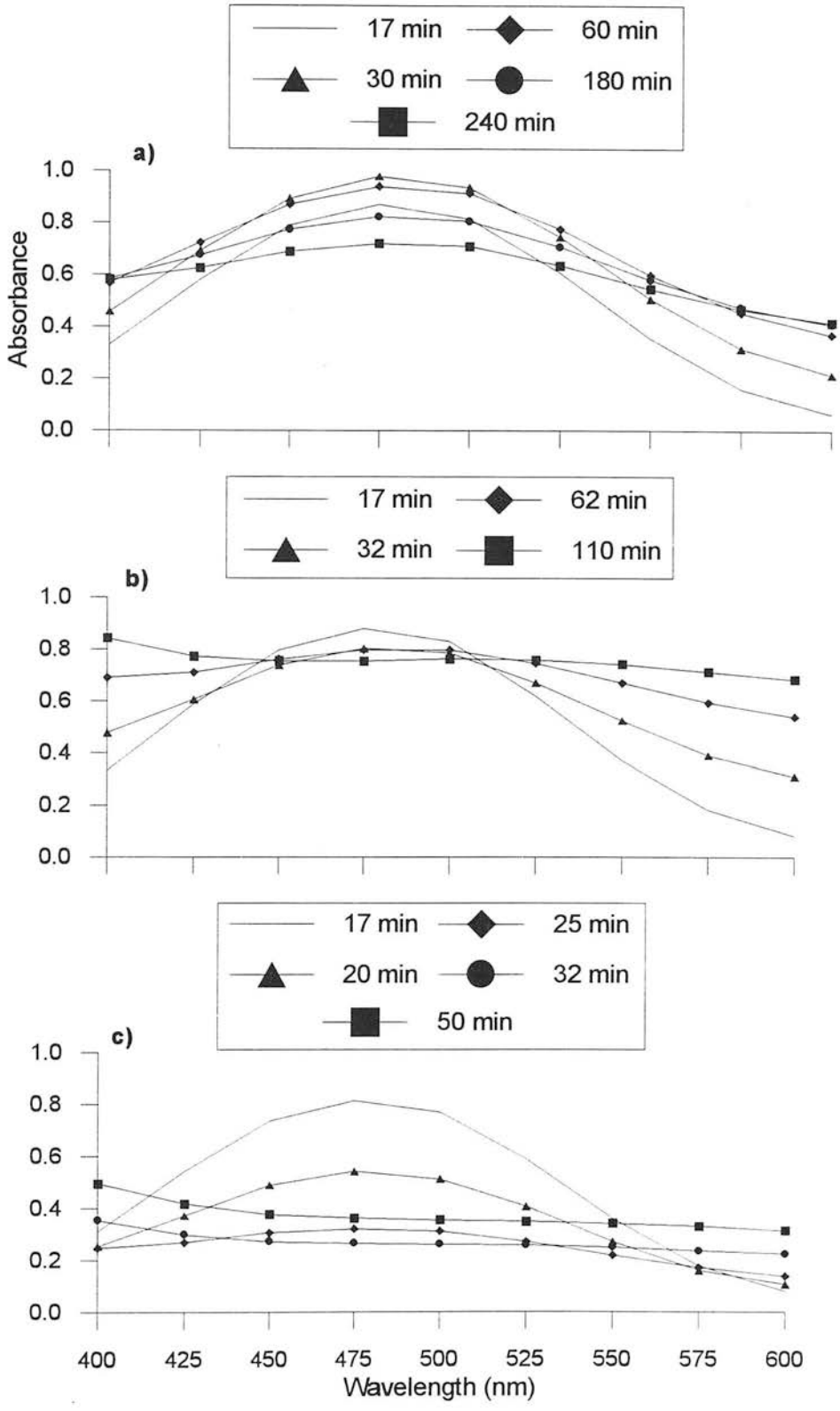

Fig 12.1 Change in absorbance of dopachrome filtrate from 400 to 600 nm at a cuvette temperature of a) 20°C, b) 40°C and c) 60°C.

There is a decrease in the absorption of orange dopachrome at 475 nm. The spectrum is then broadened and absorption starts to rise again as black melanin is created.

Figure 12.1 shows that at 20°C it took over 4 hours for melanin to form. Melanin formation at 40°C was slightly faster at approximately 110 minutes. At 60°C, the change is very rapid and melanin formed after 50 minutes.

Figure 12.2 shows the change in absorbance at 475 nm. It can be seen that at 20°C the absorption rises for about 45 minutes then starts to fall. At 40°C the decrease at 475 nm is immediate and thereafter falls steadily. At 60°C there is a very rapid change and within 50 minutes the absorption has dropped to a minimum and starts to increase again as the whole spectrum rises.

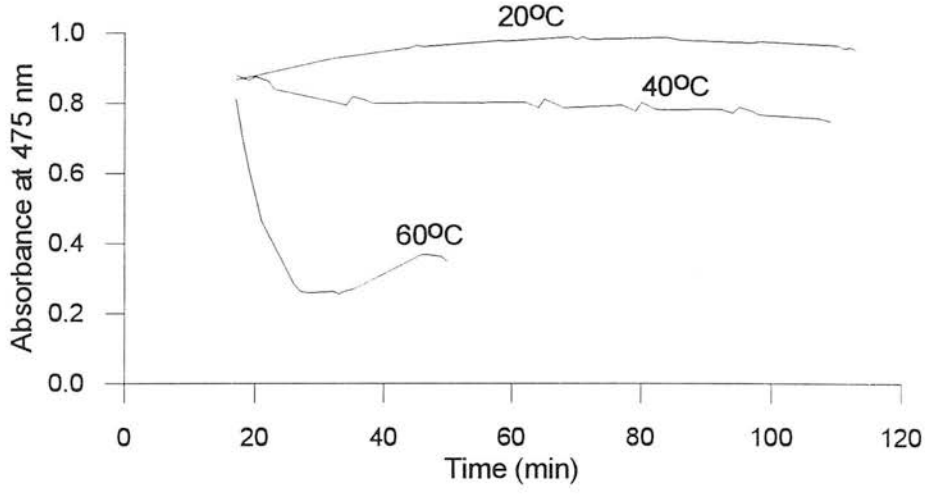

Fig 12.2 Time course of absorption (475 nm) changes at 3 cuvette temperatures 20, 40 and 60°C. The abrupt change at the end of the 60°C trace corresponds to disruption of the spectra as melanin granules precipitate from the cuvette.

12.4 Discussion

The cause of the initial decrease in spectra is the colour change as orange dopachrome (475 nm) is transformed to purple 5,6 dihydroxy-indole (540 nm). As black melanin is created, the spectra are broadened. The irregularity of spectra after this point is due to melanin formation as granules that are precipitated to the bottom of the cuvette. Horowitz and Shen (1952) reported a similar problem when they used a colorimeter to correlate the level of dopachrome with the concentration of polyphenol oxidase in a sample. They found that readings were erratic when melanin began to precipitate and judged them to be valueless for a quantitative comparison.

Precise times taken for melanin to form at a given temperature are difficult to determine, due to variability between samples and melanin precipitating from the solution. The rate of melanin formation is also affected by the concentration of polyphenol oxidase and tyrosine (Horowitz and Shen 1952) and the pH of the solution (Muneta 1977)

The time course in Fig. 12.2 at 475 nm shows that at 20°C dopachrome is still being created before being rearranged to give the purple 5,6 dihydroxy-indole derivative. At 60°C, there is an abrupt end to the series of spectral readings as melanin granules precipitate.

In summary, melanin formation at 60°C was twice as fast as at 40°C, and four times as fast as 20°C. The increased rate of melanin development at 60°C could be one way of accelerating bruise development in tubers. Further work is required to determine if bruise development can be accelerated *in vivo* by raising the temperature of tubers above 40°C.

Chapter 13

The detection of bruise development *in vivo* with reflectance spectrophototometry

13.1 Introduction

While information has been gained about the rate of melanin formation at different temperatures it was not clear if the findings could be applied to whole tubers. Therefore there was a need to develop a method for non-destructive monitoring of bruise development which would have three possible applications.

- Early indicators of bruise development could reduce the time for bruise detection.
- The effect of different atmospheric conditions on bruise development could be determined.
- If bruising development could be monitored in unpeeled tubers this would eliminate the need to peel a tuber to detect bruising.

The method developed used a fibre optic coupling port to connect the Monolight spectrophotometer to the integrating sphere inside a compressed air tank. In this way, reflectance measurements could be made of bruise development under different atmospheric conditions.

13.2 Methods

13.2.1 High pressure compressed air tank

The high pressure compressed air tank (Fig. 13.1) is a horizontal steel cylinder measuring 2 metres long, 500 mm external diameter, internal diameter 400 mm. The tank can hold four plastic trays containing approximately 100 kg of potatoes.

The entrance to the tank is sealed with a gasket and steel door secured with 20 bolts. The bolts are tightened and undone with a compressed air socket driver fed from a tee off the main compressor. A safety cage covers the bolts and has to be opened before the bolts can be undone. The air inside the tank is automatically vented when the safety cage is opened. This also means that the safety cage has to be closed before the tank can be pressurised.

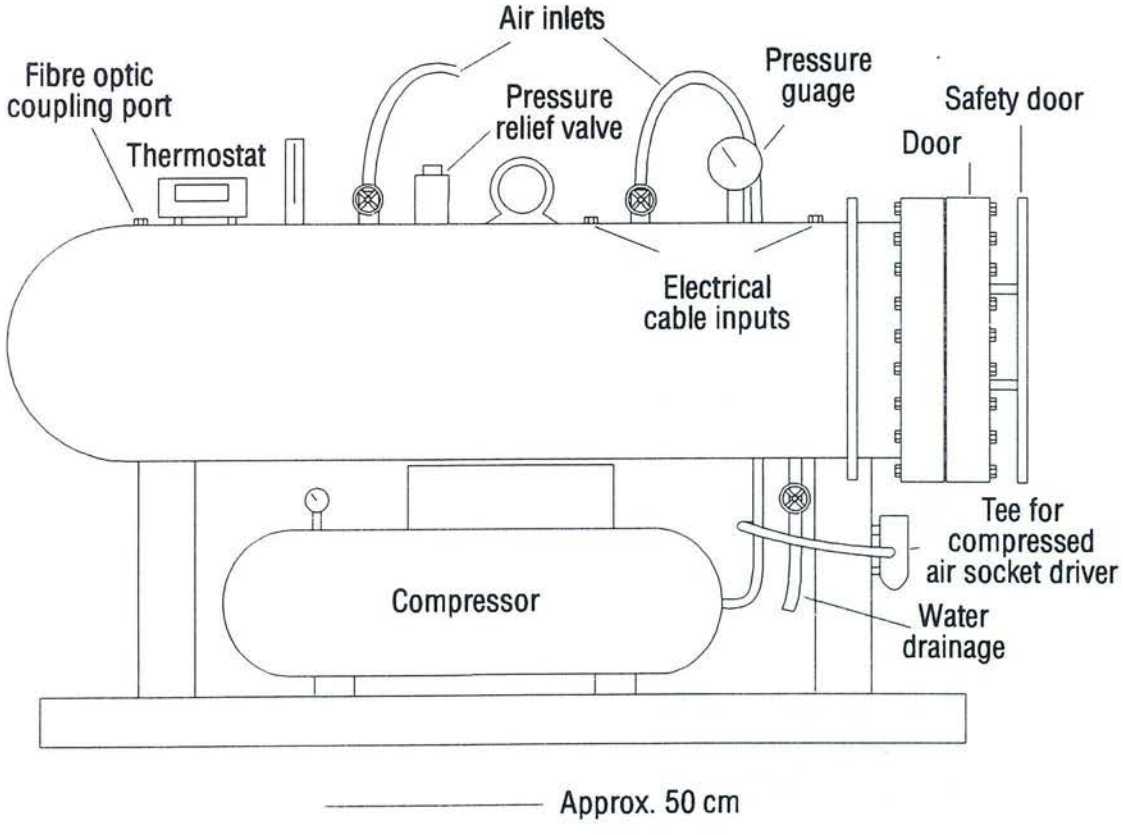

Fig. 13.1 Photograph of and schematic diagram of compressed air tank.

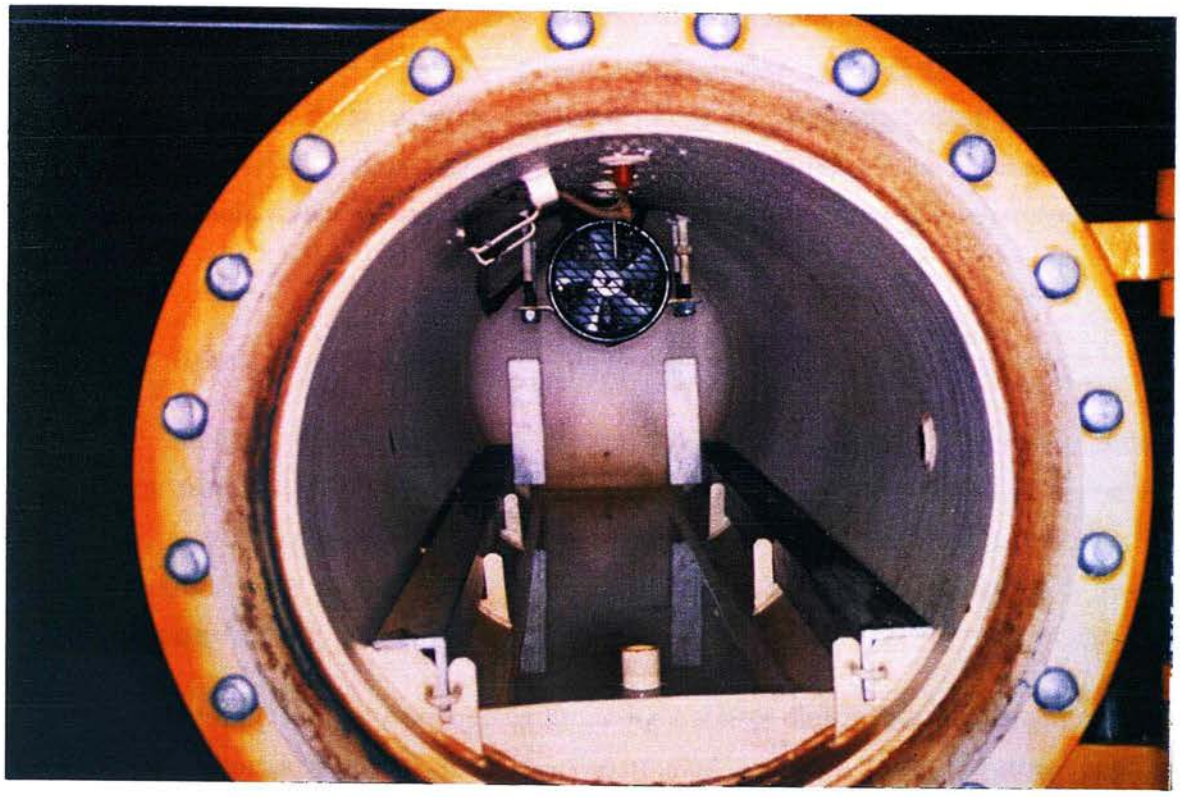

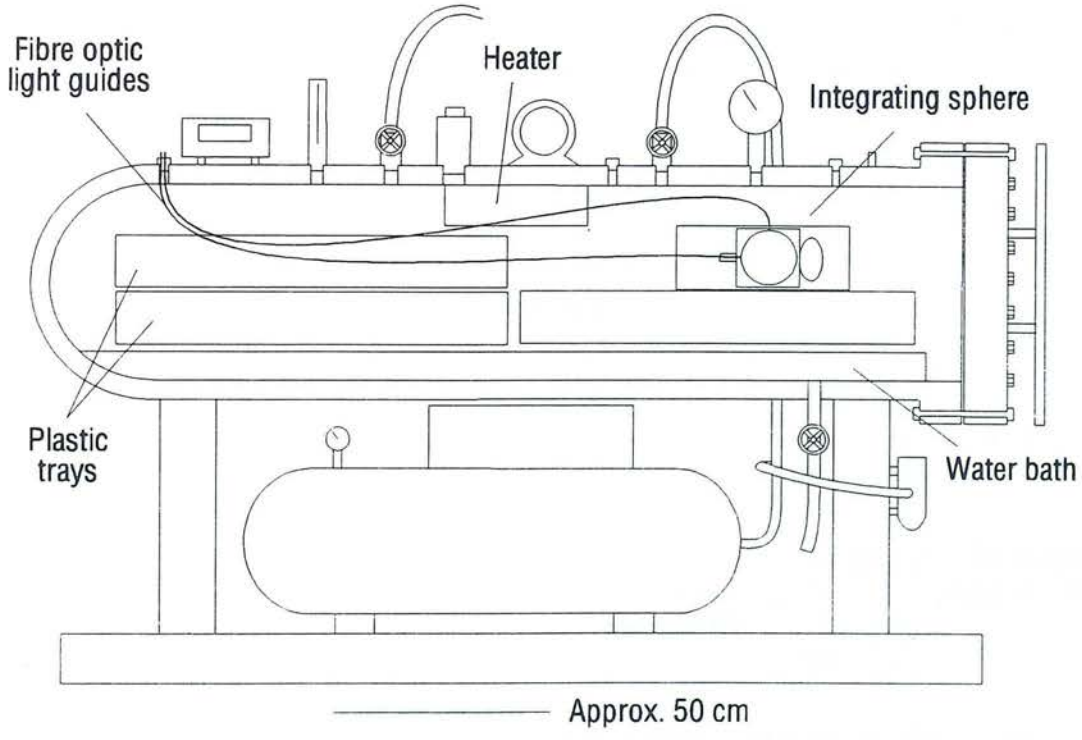

Fig. 13.2 Photograph of inside the tank and schematic diagram of compressed air tank in cross section.

In the floor of the tank is a shallow water bath, 5 cm deep, that increases the relative humidity of the air. A fan heater inside the tank circulates the warmed humidified air, and is controlled by an external thermostat (Fig. 13.2). Compressed air is fed into the tank from two compressors, one of which is mounted at the base of the tank. The first compressor cuts out once the pressure reaches 7 bar, the other cuts out at 10 bar.

13.2.2 Spectra acquisition

The Monolight spectrophotometer (section 5.4.5) was used to automatically collect spectra from 400 to 700 nm every 15 min from the integrating sphere (Chapter 8). The integrating sphere was placed in an aluminium box to enable a tuber to be kept at the aperture with packing. The box containing the sphere was placed on a plastic tray inside the tank.

The integrating sphere is connected to the light source and spectrophotometer with a fibre optic coupling port (Fig. 13.2). The original port used 5 mm diameter coupling spheres (Fig. 13.3) but attenuated the light too strongly to capture a noise-free signal. A new coupling port was designed with an air gap instead of coupling spheres and rubber o-rings to provide a seal. A plate holds the cables in place and ensures an air-tight seal against the rubber o-rings (Fig. 13.3). The new coupling port still attenuated the signal, but with 2000 averages and 15% gain, the signal is stable enough to capture spectral signatures.

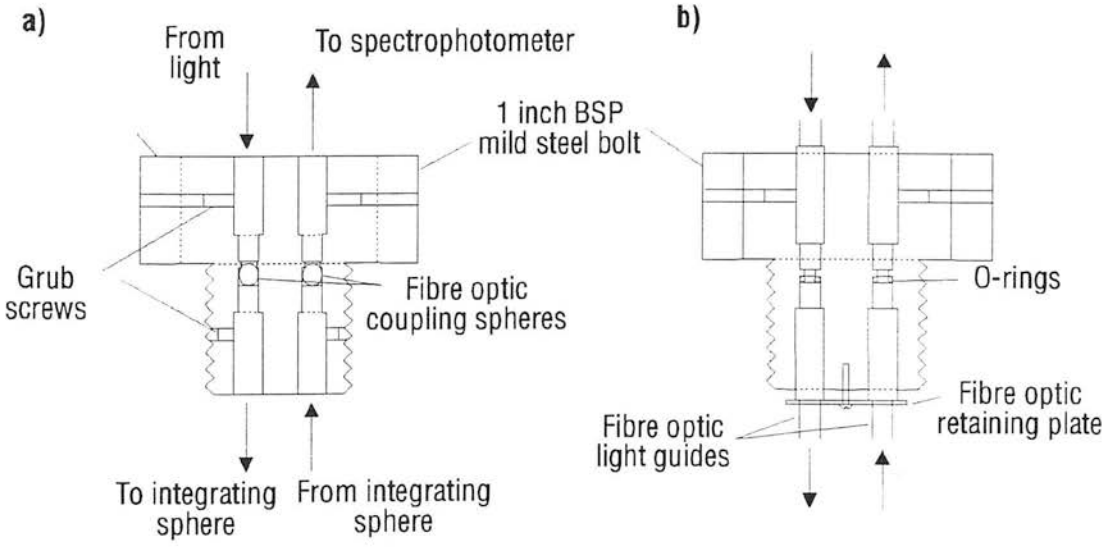

Fig. 13.3 Cross section of fibre optic coupling ports. The one on the left has fibre optic coupling spheres, the one on the right has rubber o-ring seals.

Tubers of the variety Record were hand dug, washed and stored at 4°C. A tuber was impacted with the SCAE dropper (section 7.2.2) and either placed unpeeled or peeled at the aperture of the integrating sphere. The first spectra reading was started and the tank sealed up and pressurised to 10 bar for 6 hours. The reflectance spectra were analysed in untransformed and first derivative formats (section 7.2.5).

13.4. Results

Untransformed spectra from bruised and unbruised, *unpeeled tubers*, show a general rise in reflectance with time. For unbruised tubers there are no obvious changes in any part of the spectrum. In contrast, bruised tubers have a reduced reflectance with time from 550 to 700 nm, and a very slight increase in reflectance at 475 nm (Fig. 13.4).

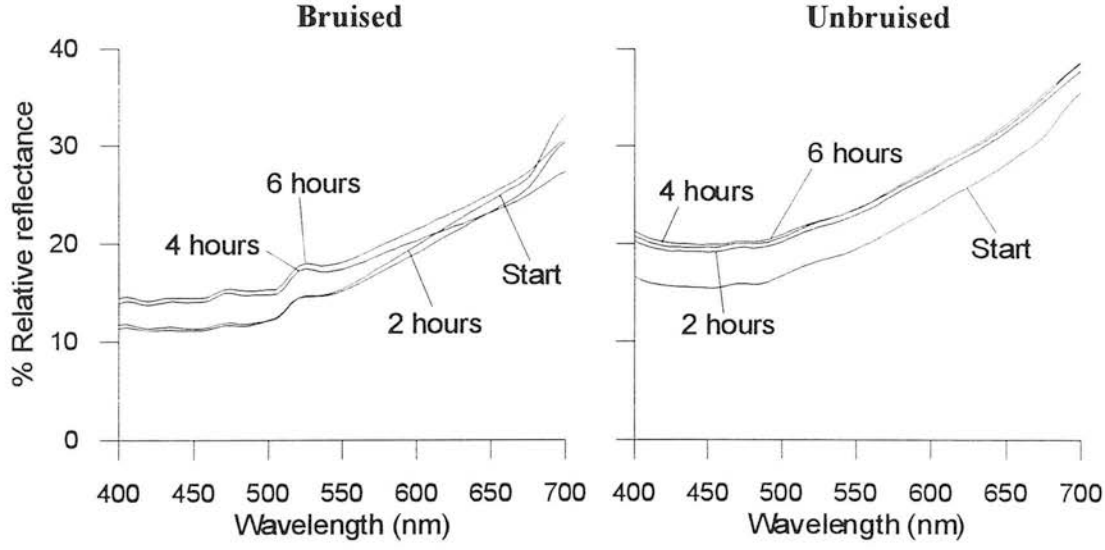

Fig. 13.4 Reflectance spectra from bruised and unbruised *unpeeled* Record tubers every two hours at 10 bar.

When the untransformed spectra are converted to first derivatives, it becomes apparent that while there is a general increase in reflectance with time, there are only a few parts of the spectrum that has a change in slope (Fig. 13.5).

The bruised tuber shows a change in slope at 425 nm, 475 nm, 500 nm and 690 nm. The unbruised tuber has only a change in slope at 690 nm between the start of the experiment and 2 hours, with no difference between the spectra taken at 2, 4 and 6 hours (Fig. 13.5).

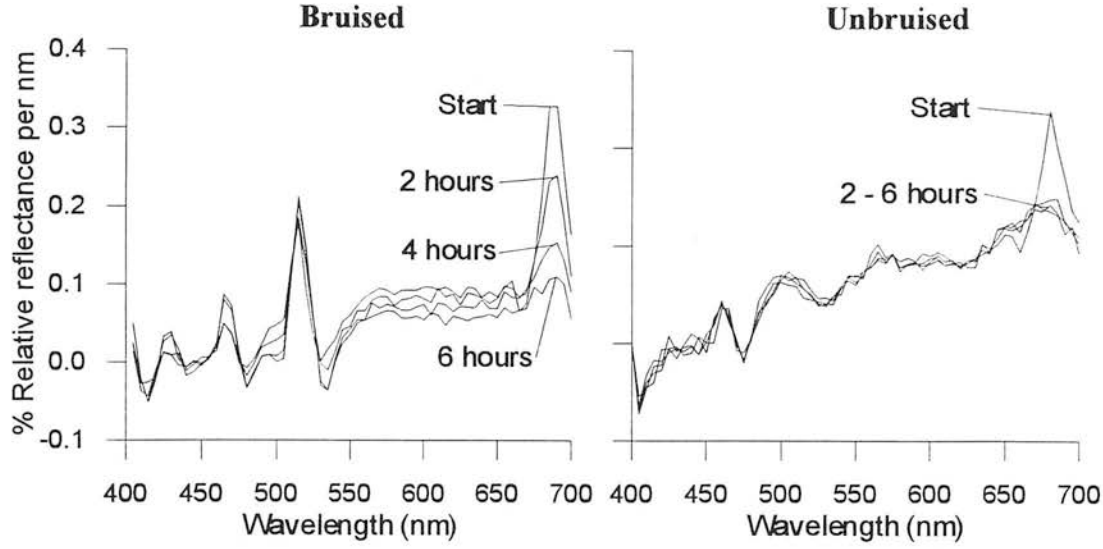

Fig. 13.5 First derivative spectra from bruised and unbruised *unpeeled* Record tubers every 2 hours at 10 bar.

A close-up of the first derivative spectrum between 450 to 500 nm further highlights the differences between the bruised and unbruised tubers (Fig. 13.6). With the bruised tuber there is a change in the first derivative spectrum at 465 and 500 nm that is absent in the unbruised tuber.

Where the first derivative spectrum crosses the x-axis this indicates where a peak in the untransformed spectrum is present. If the slopes either side of the cross-over point is changing then the peak in the untransformed spectrum must be changing too. In this case the first derivative indicates that there is a change in the reflectance at 475 nm in the untransformed spectrum (Fig. 13.4).

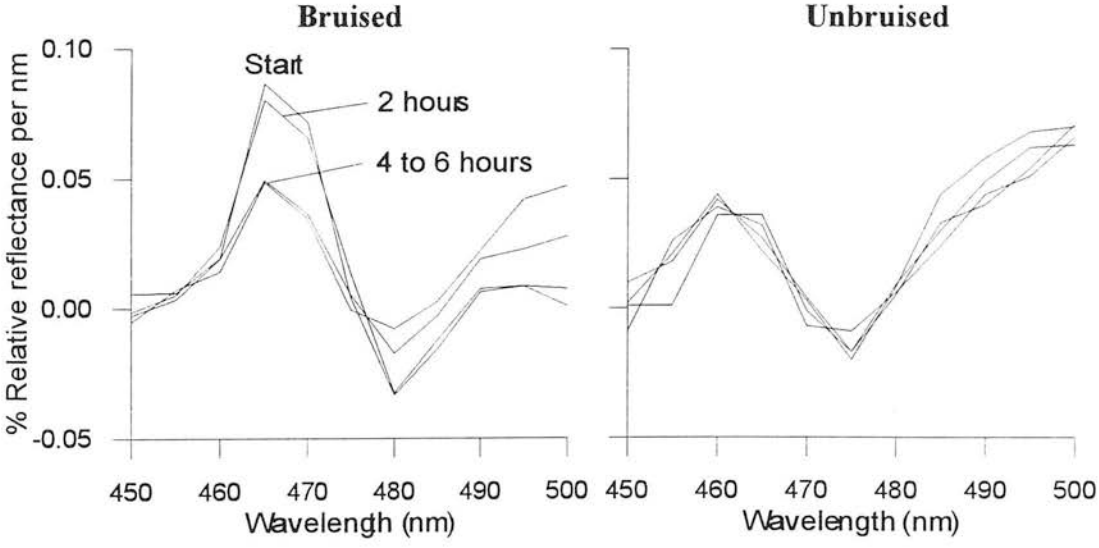

Fig. 13. 6 Close-up of first derivative spectrum from bruised and unbruised *unpeeled* Record tubers from 450 to 500 nm over time.

The difference between bruised and unbruised tubers can be emphasised by showing a plot of the first derivative at 500 and 690 nm with time (Fig. 13.7). In bruised tubers there is a more rapid change at 690 nm compared to 500 nm. In unbruised tubers there is a slight change at 690 nm, but no change at 500 nm.

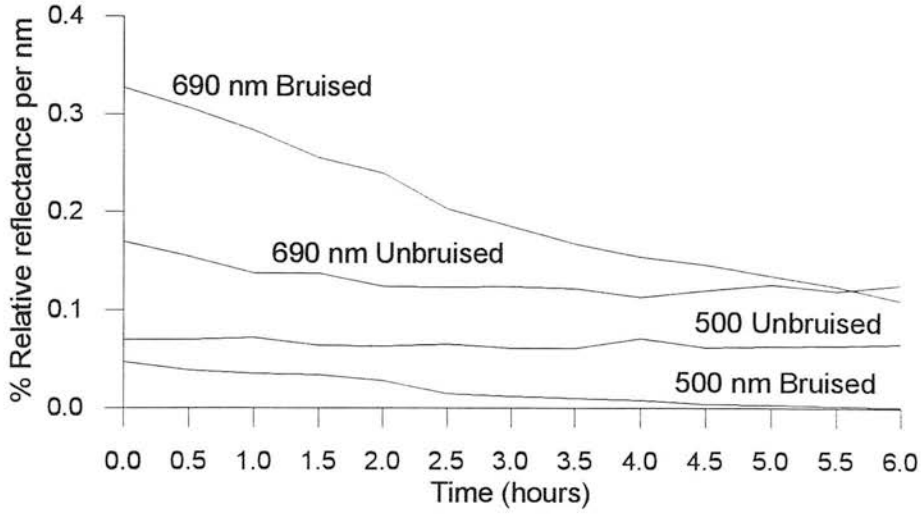

Fig. 13. 7 Change in first derivative spectrum at 500 and 690 nm over time for bruised and unbruised *unpeeled* Record tubers.

Tubers that were bruised and then peeled before taking reflectance spectra showed no difference between bruised and unbruised tubers (Fig. 13.8).

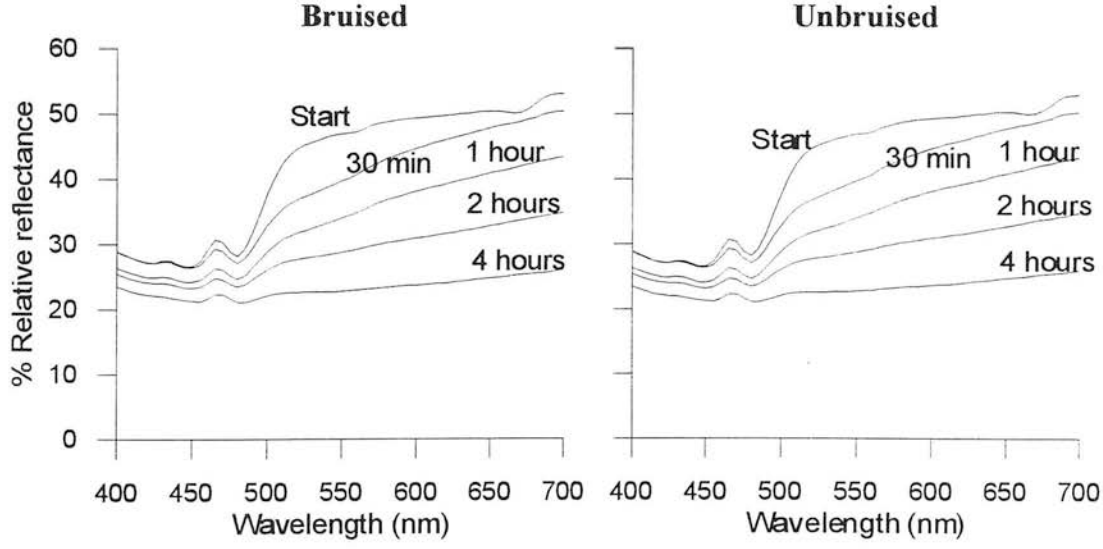

Fig. 13.8 Change in reflectance spectra from bruised and unbruised *peeled* Record over time.

Although there appears to be large changes in the reflectance spectra with time, the first derivative spectra highlight only a few wavelengths where there is a change in slope (Fig. 13.9).

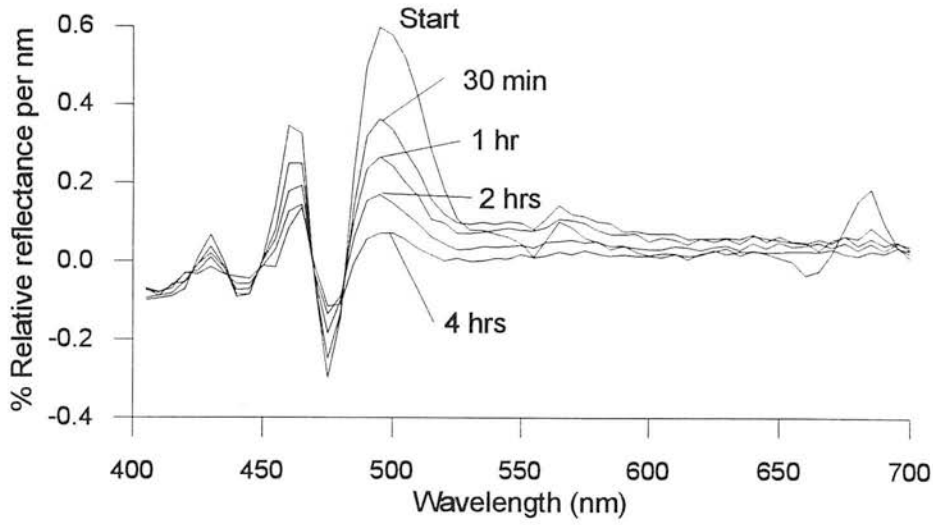

Fig. 13.9 Change in first derivative spectrum from bruised *peeled* Record tuber with time.

The largest change in slope is at 500 nm, with smaller changes at 465 nm and 425 nm. The decrease in slope at 500 nm corresponds to a decrease in reflectance at 475 nm in the untransformed spectrum. A plot of the first derivative at 500 nm with time highlights the changes that are occurring (Fig. 13.10).

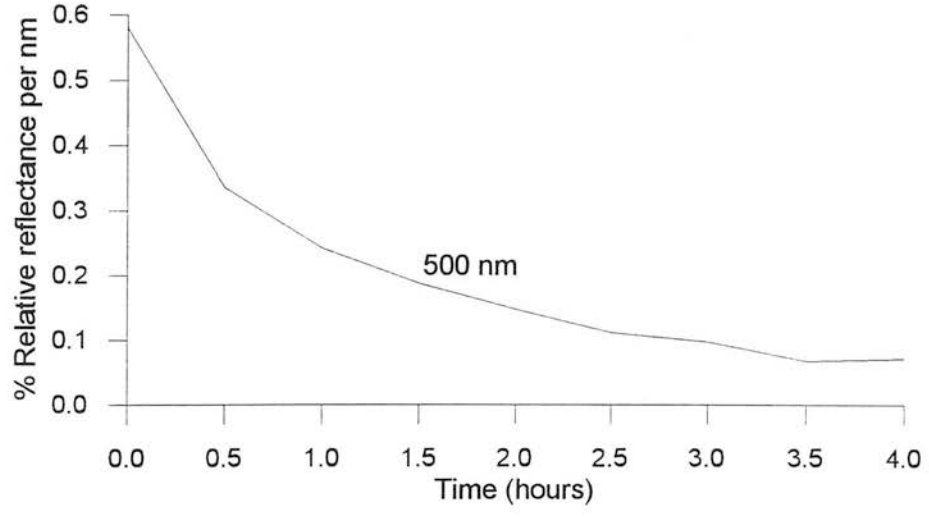

Fig. 13.10 Change in first derivative spectrum at 500 nm from bruised *peeled* tuber with time.

It was observed that when a peeled tuber had been taken from the tank after 4 hours that the surface was a dark grey colour. It was also found that when a tuber was peeled and left in ambient conditions outside the tank that the peeled surface gradually became orange then brown and finally grey. Reflectance spectra from this tuber taken when the orange colour (dopachrome) appeared to be most intense and after a grey colour (melanin) had developed can be seen in Fig. 13.11.

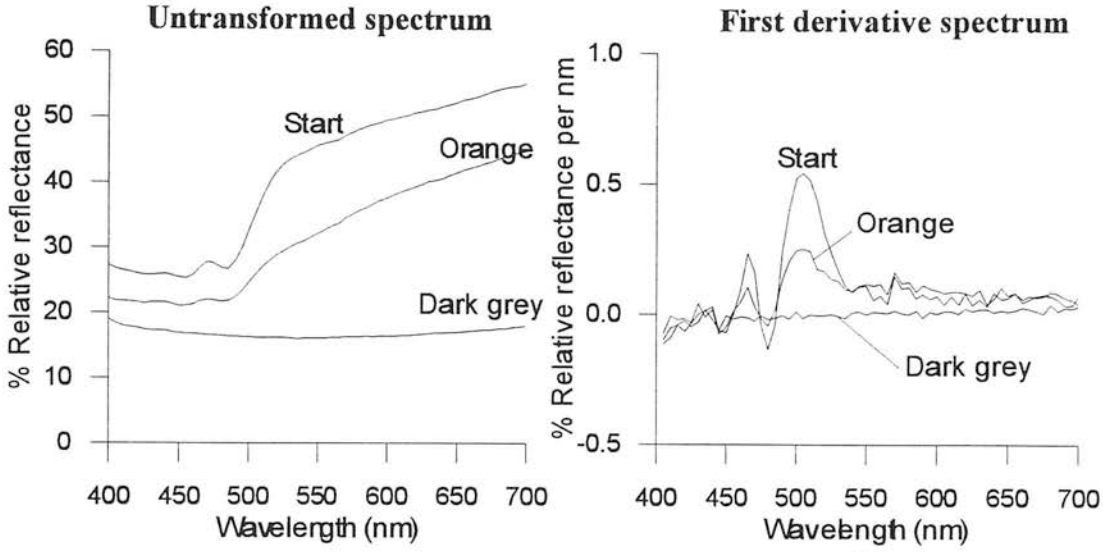

Fig. 13.11 Untransformed and first derivative spectra from peeled surface at different stages of discolouration.

It can be seen that the changes in the reflectance spectra from the peeled tuber under ambient conditions are similar to the changes seen in the peeled tuber in the tank. The decrease at 500 nm in the first derivative corresponds to the production of dopachrome in the tuber followed by the formation of melanin.

13.4 Discussion

Reflectance spectra from unpeeled tubers reveal a difference between bruised and unbruised tubers with time. The differences are not obvious in the untransformed spectra, but the first derivative spectra show there is a change in slope with time at 500 and 690 nm. The change in slope at 500 nm highlights that there is a change in reflectance at 475 nm in the untransformed spectrum. There is also a change at 690 nm in the unbruised tuber that indicates that the change in this part of the spectrum might not be due to the development of bruising. It appears that the unpeeled tubers undergo other changes when they are exposed to the pressurised heated environment.

In peeled tubers there is no difference between bruised and unbruised tubers. When a tuber is peeled the cutting action of the peeler caused the cells to rupture and discolouration processes to begin. The cells damaged by the peeler discolour more rapidly than cells damaged by bruising because they are in direct contact with atmospheric oxygen. The damaged cells on the surface of the tuber therefore mask any discolouration that may occur in the sub-surface tissue.

First derivative spectra from peeled tubers show that the greatest change in slope between reflectance spectra over time is at 500 nm. The change in slope at 500 nm is associated with a decrease in reflectance in the untransformed spectrum at 475 nm.

The change in reflectance at 475 nm observed in unpeeled and peeled tubers is due to the production of dopachrome at this wavelength (Chapter 12). The experiment from a peeled tuber under ambient conditions revealed that dopachrome is visible as an orange colour in intact tubers as well as in a test tube. The dark grey colour is attributable to the production of melanin and appears to have no distinguishing features in the first derivative spectrum.

The early change in reflectance in unpeeled tubers at 475 nm indicates that reflectance spectrophotometry is detecting the initial development of a bruise. Therefore, by looking for a change at 475 nm in unpeeled tubers early signs of bruising can be detected. However, there are several problems associated with this technique.

- Only one tuber can be placed with the sphere at a time. Therefore, it would take a long time to gather sufficient data to assess the effect of different atmospheric conditions on bruise development.

- The development of a bruise is not guaranteed after an impact due to reasons outlined in Chapter 3.

- The skin of a tuber has a variable effect on the reflectance characteristics (Chapters 7 and 8). Without knowing the starting reflectance values it could be difficult to determine if any change had occurred due to bruise development.

The combination of these factors makes the determination of factors affecting bruise development with reflectance spectrophotometry difficult. However, the technique could be adapted using the following method.

- Tubers are impacted and placed in the air tank.

- After a period of time the tubers are removed from the air tank and peeled.

- The spectrophotometer and integrating sphere are used to take reflectance measurements of the impact site on the tuber. Spectra from peeled tubers are more predictable, providing a reading is taken soon after peeling

- Changes in reflectance in the first derivative spectra at 500 nm are used as a measure of the degree of discolouration.

This method will be described and evaluated more fully in the next chapter.

Chapter 14

The use of humidified compressed air to accelerate bruise development in potato tubers

14.1 Introduction

A combination of different air pressures and temperatures were used in the compressed air tank to determine the effect on bruise development. The degree of bruise development was evaluated by measuring the change in first derivative spectra at 500 nm. However, because reflectance measurements are affected by the size of bruise they were augmented with a visual assessment of the colour of bruise, rated on a scale of 1 to 5. Tubers were also placed in a hotbox at 40°C as a comparison to the compressed air tank method.

14.2 Methods

14.2.1 Samples

Tubers of the varieties Desiree, Pentland Dell and Desiree were hand dug, washed and stored at 4°C. Tubers were impacted with the SCAE dropper (section 7.2.2). A sample of 30 tubers were used per temperature and pressure treatment.

14.2.2 Pressures and temperatures

The tubers were placed in the compressed air tank (section 13.2.1) at pressures of 3 bar, 7 bar and 10 bar and a temperature of 40°C. The control for all pressure treatments was held at atmospheric pressure.

Tubers of the variety Desiree, Pentland Dell and Record were placed in the tank at a temperature of 40°C. The tubers were left in each combination of temperature and air pressure for 1, 2, 3 and 4 hours. The recorded time at a given pressure was started once the tank reached that pressure. Record tubers were also placed in the tank at a temperature of 60°C. For comparison other samples of Record were held in a hotbox for a period of 1 to 7 hours.

An automatically recording temperature probe (Temptrak; Hanna Instruments Ltd, Bedfordshire) was used to monitor the temperature inside the compressed air tank, the hotbox and the tubers.

14.2.3 Spectra acquisition

The integrating sphere and Monolight spectrophotometer were used to take reflectance spectra from 400 to 700 nm. Reflectance spectra were taken after the tubers had been removed from the tank and peeled.

14.2.4 Data analysis

The first derivative was calculated from each spectra at 500 nm:

$$\frac{R\lambda 500 - R\lambda 495}{5}$$

where Rλ500 and Rλ495 are the percentage relative reflectance measurements at 500 and 495 nm.

The first derivative at 500 nm was the location of the largest change in slope as a bruise developed (Chapter 13). By measuring the first derivative at 500 nm it was considered to be possible to obtain a non-subjective measurement of bruise development. The first derivative also reduces any error in reflectance measurements caused by holding a tuber at different angles to the integrating sphere.

The reflectance measurements are affected by the size of bruise (Chapter 11) so the colour of bruises on peeled tubers was also evaluated visually on a scale of 1 to 5:

1. Yellow
2. Pale orange
3. Orange
4. Light brown
5. Brown to grey colour coloured bruise.

The classes of bruise colour are designed to give sensitivity to the early development of bruises. Once a bruise becomes brown to grey, the formation of melanin has started and is more difficult to define the different stages of melanin production.

The average and standard deviation of first derivative spectra and visual assessments were taken for bruised tubers only. Unbruised tubers were not included in the analysis because there is no guarantee that the unbruised tubers would have developed into a bruise if left for a longer time in the tank.

A one-way analysis of variance (ANOVA) was conducted with BMDP Statistical software to test if temperature and pressure had a significant effect on the reflectance and visual assessments. The result of an ANOVA is an F-value which is the ratio of

the between group sum of squares and the within group sum of squares. The larger the F-value the more significant the difference between group means. In this analysis a p-value less than 0.05 for the F-value is taken to be a significant difference between group means, that is, the treatment has had an effect.

14.3 Results

14.3.1 Effect of air pressure on bruise development

Appendix E contains tables of results for the effect of pressure and temperature on the reflectance measurements and visual assessments. Some of these results are shown in the form of graphs in this section.

The graphs in this section are for visual and reflectance measurements of blackspot bruise only. However, for Desiree, very few bruises were blackspot bruises, so the graphs show the mean reflectance and visual assessments for shatter and blackspot bruises. It was found that shatter bruises, where the skin is unbroken but the sub-surface tissue is cracked, discoloured at a faster rate than blackspot bruises where there are no cracks in the tissue. It appeared that in shatter bruising the cells are more severely damaged and the cracks may have allowed an easier passage of oxygen to the cells.

The time taken to reach a given pressure can be seen in Fig. 14.1. It took approximately 13 minutes for the tank to pressurise to 10 bar. The time at a given pressure was recorded once the pressure had reached the desired value.

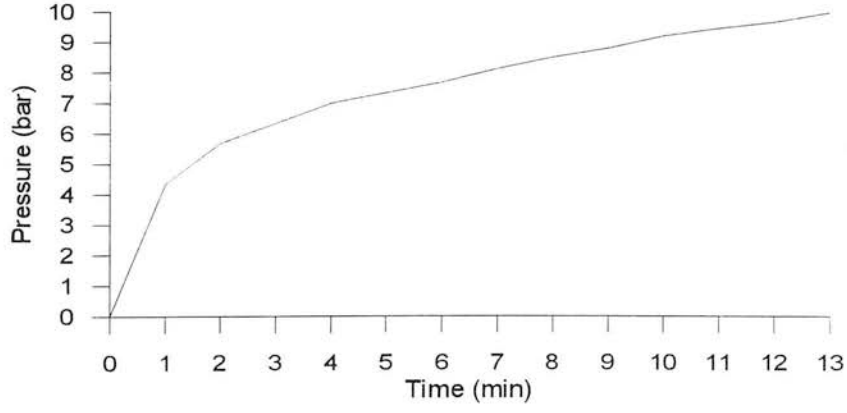

Fig. 14.1 Time taken to reach a given air pressure in the air tank. The first compressor cuts off at 7 bar, the second compressor cuts off at 10 bar.

The effect of air pressure on the mean visual rating of bruised tubers can be seen in Fig. 14.2. An asterisk at a given time shows that air pressure had a significant effect on bruise development as evaluated by a p-value less than 0.05 for one-way ANOVA. The higher the visual assessment the darker the bruise.

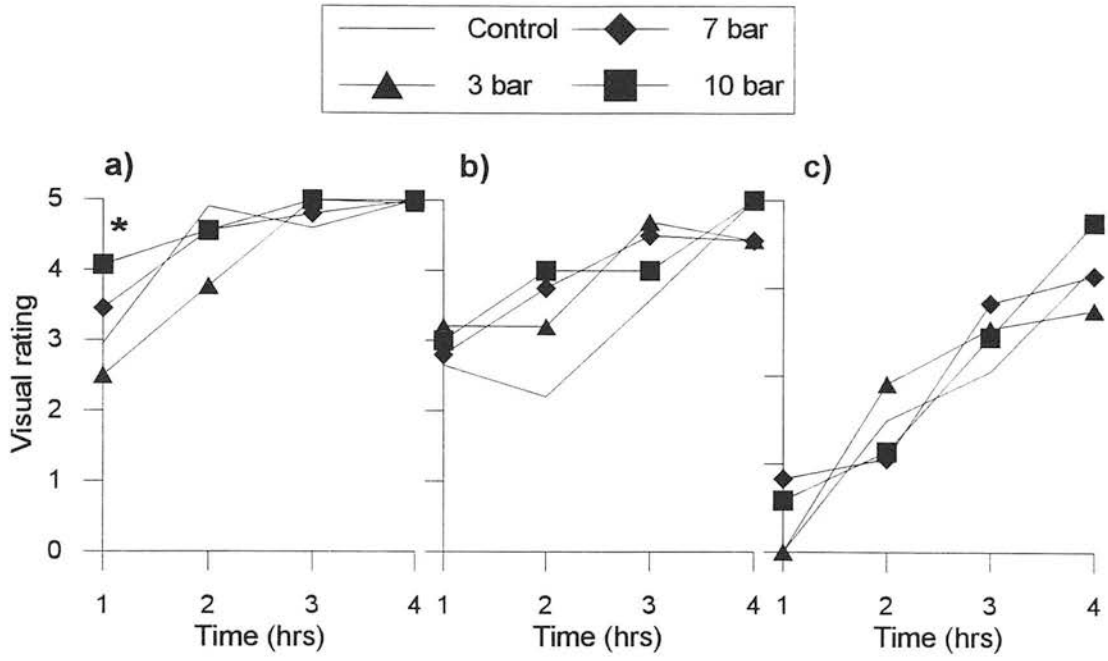

Fig 14.2 Effect of air pressure on mean visual rating of bruise discolouration in a) Desiree, b) Pentland Dell and c) Record tubers. For a) Desiree, the mean discolouration rating is for shatter bruises; for b) Pentland Dell and c) Record the rating is for blackspot bruises. The *higher* the visual rating the darker the bruise.

The bruises become darker over time with Pentland Dell and Desiree appearing to have darker bruises at each time than Record. The only significant effect of air pressure on bruise development is for Desiree after 1 hour where 10 bar gives a darker bruise followed by 7 bar, control and 3 bar. The effect of air pressure on visual assessment is difficult to interpret for all the varieties as the effect appears to be erratic.

The mean visual measurements for atmospheric pressure were subtracted from for the readings for 10 bar, 7 bar and 3 bar to gain a better understanding of the effect of pressure on bruise development. This gave a relative measurement for the effect of air pressure compared to the control. A value greater than 0 indicates that the discolouration was darker than the control. A value less than 0 indicates that the discolouration was lighter than the control (Fig. 14.3).

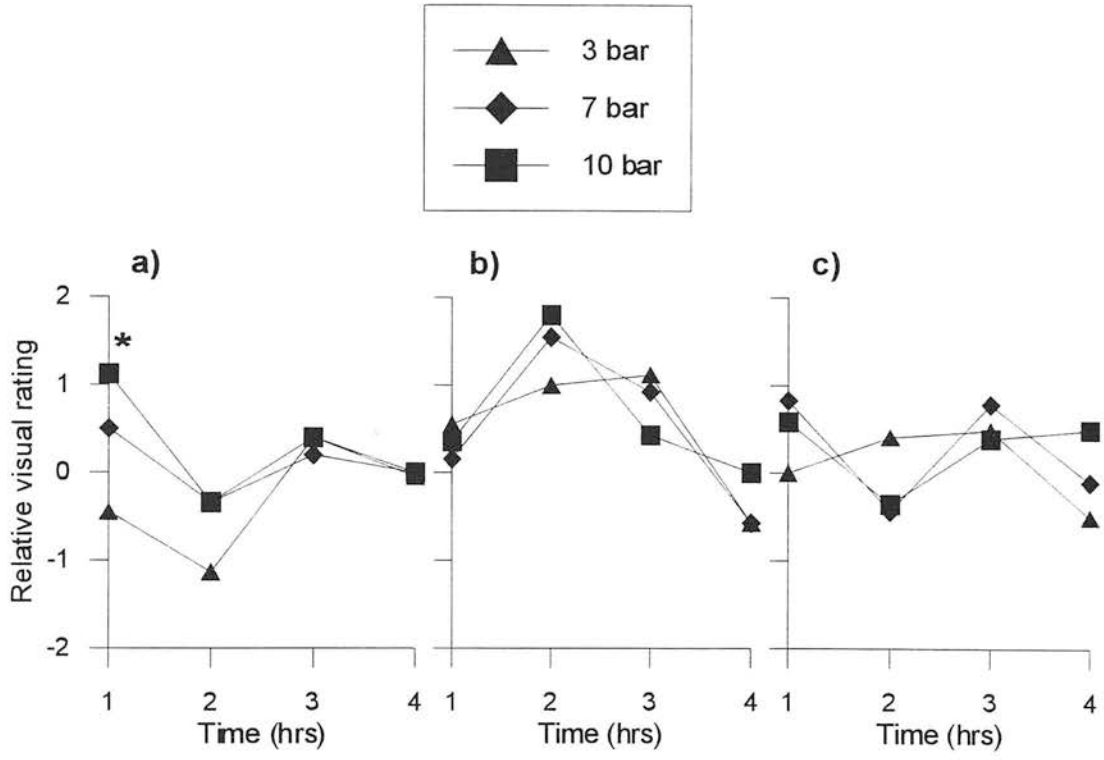

Fig. 14.3 Relative change in visual rating compared to control for a) Desiree, b) Pentland Dell and c) Record tubers. A value *greater than 0* indicates that the treatment gave a higher, but not necessarily significant, bruise discolouration than the control.

The plot of relative visual assessment over time reveals that for Desiree, air pressure gives a darker bruise after 1 hour, but from 2 to 4 hours the bruise colour is similar to the control. Air pressure appears to have an effect on bruise development in Pentland Dell tubers, with darker bruises than the control for 1 to 3 hours, but at 4 hours the bruises are a similar colour to the control. At two hours, it appears that the higher the pressure, the darker the colour of bruised Pentland Dell tubers. Bruised Record tubers also appear to be affected by air pressure from 1 to 4 hours, but the effect is inconsistent. At 1 hour 7 bar appears to give the darkest bruises, at 2 hours it is 3 bar, at 3 hours it is 7 bar and at 4 hours it is 10 bar.

A plot of mean first derivative spectra at 500 nm over time reveal that air pressure had a significant effect on more treatments than the visual assessments (Fig. 14.4). The *lower* the first derivative, the darker the bruise.

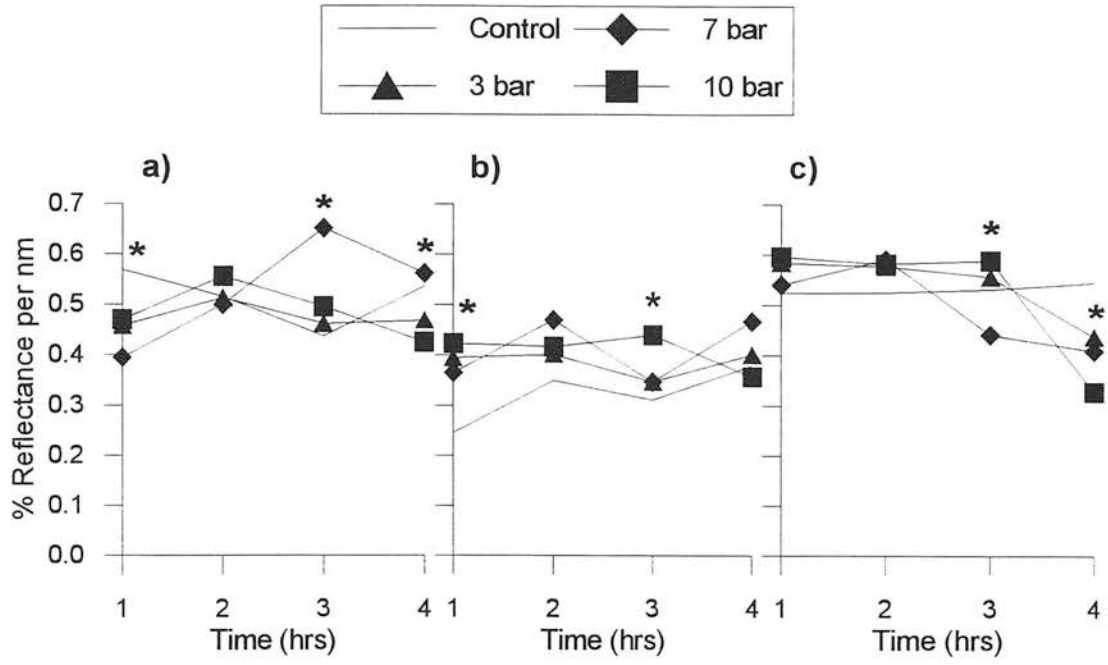

Fig. 14.4 Effect of air pressure on mean first derivative reflectance at 500 nm of a) Desiree, b) Pentland Dell and c) Record tubers. The *lower* the first derivative value, the darker the bruise.

It appears that over time, only Record has an obvious reduction in the first derivative. Desiree and Pentland Dell appear to remain unchanged. However, ANOVA reveals that there is a significant effect of air pressure on reflectance readings at 1, 3 and 4 hours from Desiree tubers. The effect is erratic with air pressure giving a darker bruise at 1 hour but not at 3 hours. There is also a significant effect for the effect of air pressure on Pentland Dell tubers at 1 and 3 hours, but from 1 to 4 hours the control is darker than the pressure treatments. Record tubers have a significant difference between treatments at 3 and 4 hours. At 3 hours, 3 bar is darker than the control, but 7 bar and 10 bar are lighter than the control. After 4 hours, the higher the pressure the darker the bruise.

The mean reflectance measurements for atmospheric pressure were subtracted from for the readings for 10 bar, 7 bar and 3 bar to give a relative change in reflectance to the control. A value less than 0 indicates that the bruises were darker than the control, and a value greater than 0 indicates that the bruises were lighter than the control.

A plot of the relative reflectance over time (Fig. 14.5) reveals that air pressure gave significantly darker bruises than the control for Desiree at 1 and 4 hours. The relative change in reflectance from Pentland tubers shows that the bruises became darker over time, but that the control was darker than the air pressure treatments.

Record tubers also became darker over time with 7 and 10 bar giving significantly darker bruises than the control after 3 and 4 hours.

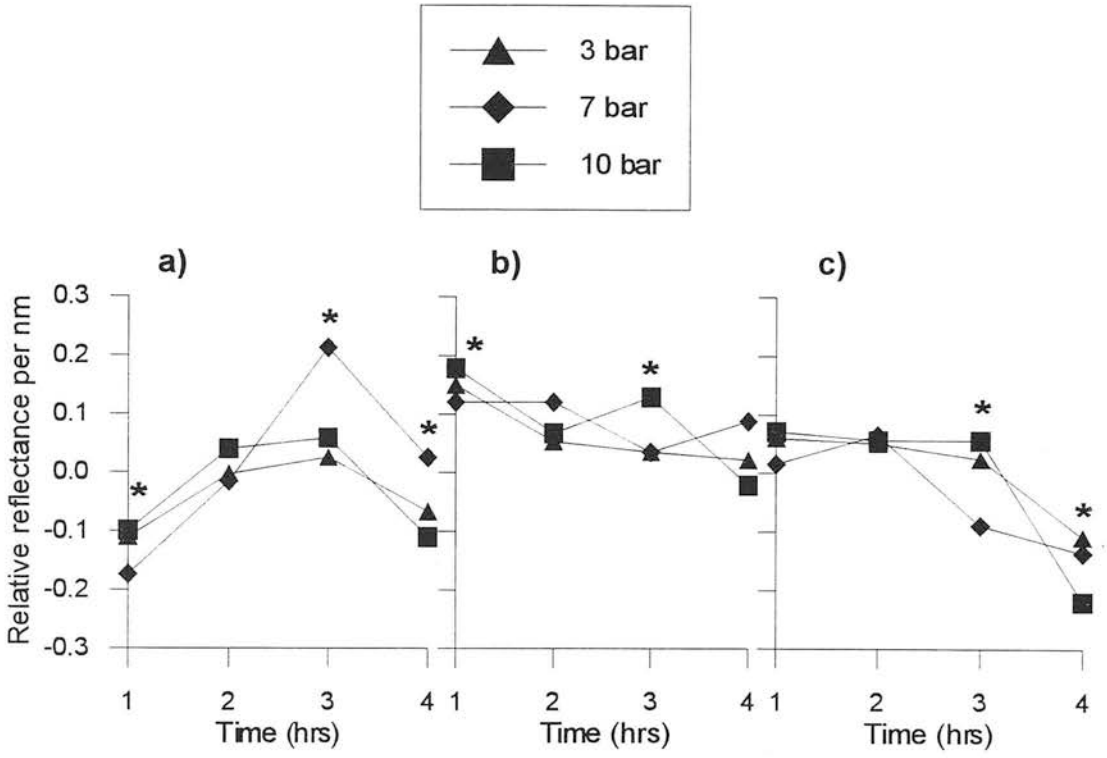

Fig. 14.5 Relative first derivative reflectance at 510 nm compared to control for a) Desiree, b) Pentland Dell and c) Record tubers. A value *less than 0* indicates that the treatment gave a darker discolouration than the control.

A plot of the percentage of tubers displaying no discolouration over time at each of the pressure treatments can be seen in Fig. 14.6. It appears that the longer the tubers are left in the tank, the lower the percentage of tubers showing no discolouration. It also appears, particularly for Record, that the higher the air pressure the lower the percentage of unbruised tubers.

A sample of Record tubers were left in ambient conditions (16°C) for 24 and 48 hours and 7 days as a comparison to the percentage of unbruised tubers in the tank. The percentage of unbruised tubers was approximately 5% for all the tubers left in ambient conditions. Therefore, the percentage of tubers showing no bruising in the tank may be an inaccurate estimate of the amount of bruising in a sample kept in ambient conditions.

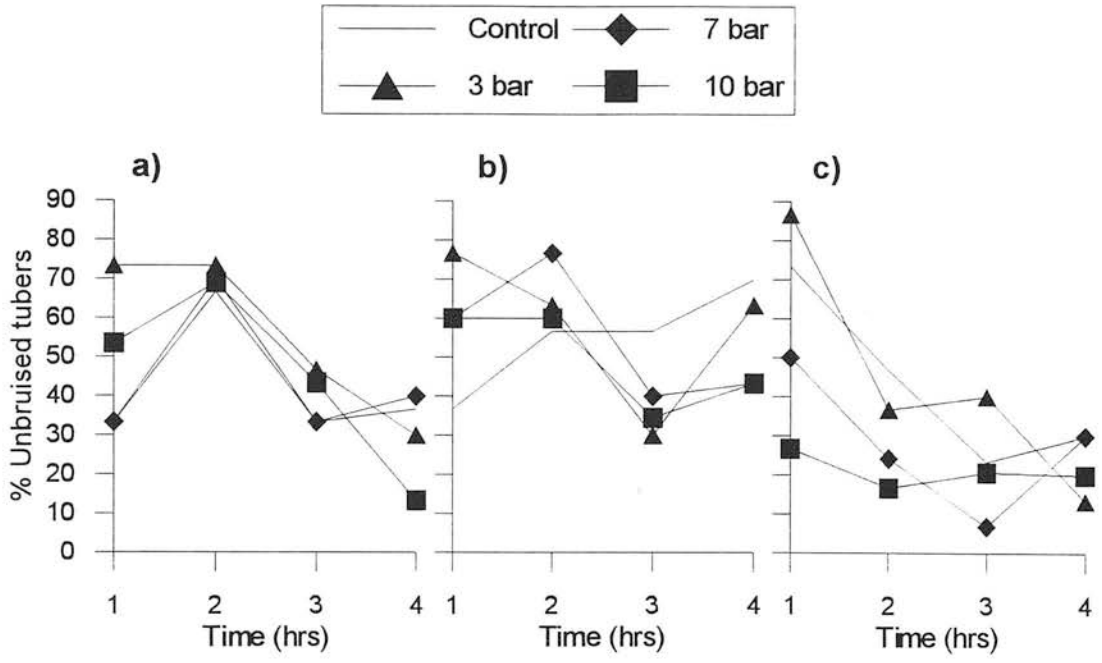

Fig. 14.6 Effect of air pressure on percentage of tubers developing no discolouration in a) Desiree, b) Pentland Dell and c) Record tubers.

14.3.2 Effect of temperature and pressure on bruise development

When tubers were placed at 60°C in the compressed air tank the tuber warmed to a higher temperature and at a faster rate than a similarly sized tuber at 40°C (Fig. 14.7). It took approximately 140 min for the temperature to rise above 40°C when tubers were in the tank at 60°C.

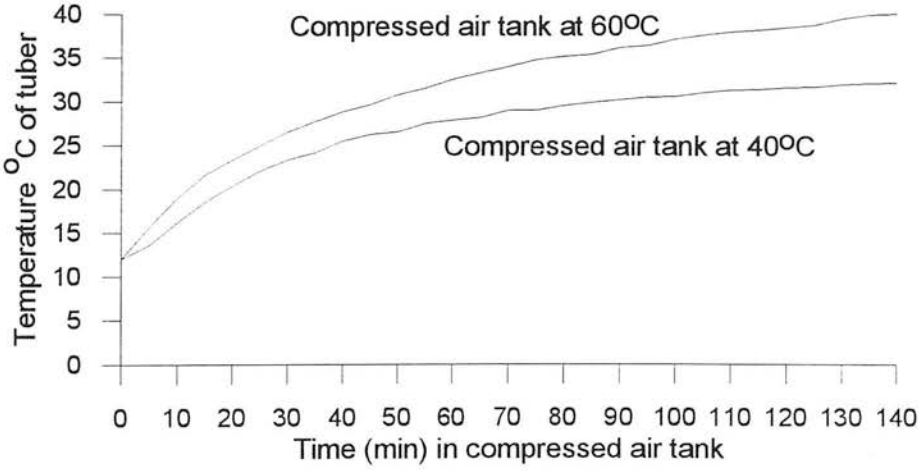

Fig. 14.7 Temperature recorded over time from inside tubers in the compressed air tank at 10 bar and 40 and 60°C.

Tubers were placed in the tank at 60°C at atmospheric pressure and 3, 7 and 10 bar for 1 and 2 hours to determine if the higher temperature could reduce the time for bruise development. The effects of pressure at 60°C on visual and reflectance measurements were inconsistent (Table 14.1). After 1 hour there was no significant

differences between treatments, although for visual assessments pressures of 3, 7 and 10 bar appear to be higher than the control. After 2 hours there was a significant difference between treatments for visual and reflectance measurements. However, for visual assessments the control is almost as dark as at 10 bar and reflectance measurements after 2 hours is lowest for the control.

Table 14.1 Effect of air pressure on mean visual and reflectance measurements at 60°C from bruised Record tubers.

	10 bar	7 bar	3 bar	1 bar
Visual*				
1 hour				
blackspot only	1.77 ± 2.5	1.92 ± 2.7	1.50 ± 2.4	1 ± 0
2 hours				
blackspot only	3.57 ± 3.6	none	1.33 ± 2.0	3.10 ± 3.3
Reflectance*				
1 hour				
blackspot only	0.62 ± 0.07	0.63 ± 0.12	0.66 ± 0.05	0.67 ± 0.05
2 hours				
blackspot only	0.59 ± 0.17	none	0.59 ± 0.10	0.40 ± 0.12

* The higher the visual assessment the darker the bruise. The lower the reflectance measurements the darker the bruise.

When the visual assessments were compared to the results obtained at 40°C, there was a significant difference after 1 hour, with tubers at 60°C having darker bruises than at 40°C. However, after 2 hours there was no significant effect of temperature on visual assessment. A comparison of reflectance measurements at 40 and 60°C showed no significant difference after 1 hour, but there was a significant difference after 2 hours, with tubers at 60°C appearing to have a slightly lower reflectance than at 40°C.

14.3.3 Comparison of compressed air and hotbox on bruise development

A comparison of tuber temperatures recorded inside large and small tubers at 10 bar and in the hotbox can be seen in Fig. 14.8. The temperature of tubers in a compressed air tank appear to increase at a faster rate than in a hotbox. However, after about 120 min, the temperature of all the tubers was very similar.

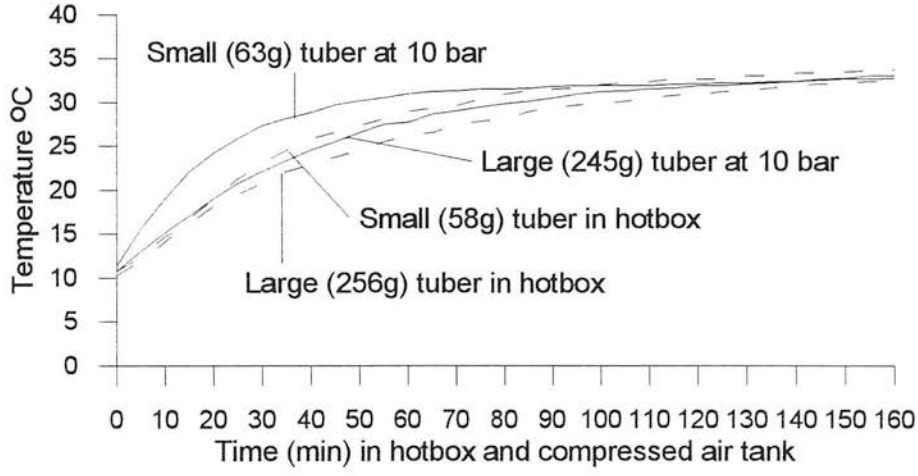

Fig. 14.8 Temperature changes recorded over time in small and large tubers in a hotbox and in a compressed air tank at 10 bar.

A plot of visual and reflectance assessments over time (Fig. 14.9) shows that at 10 bar the bruises are darker for each hour than from the hotbox. However, a plot of visual and reflectance measurements at 1 bar appears to give bruises that are darker or as dark as bruises at 10 bar.

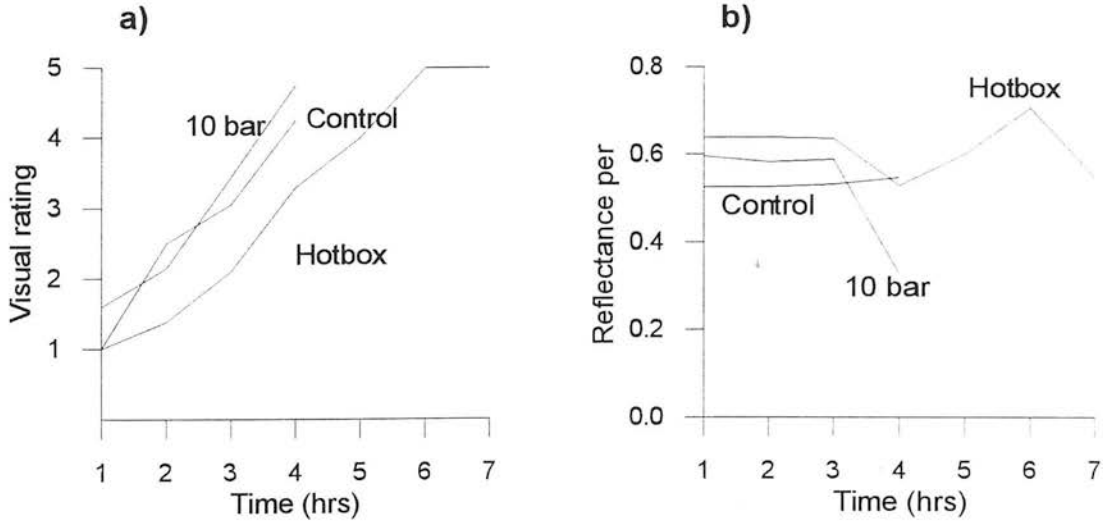

Fig. 14.9 Comparison of hotbox and air pressure at 10 bar and atmospheric pressure on a) visual and b) reflectance measurements.

ANOVA gave a significant difference between visual ratings at 10 bar, atmospheric pressure and the hotbox for each time. There was insufficient data to determine if there was a significant difference between reflectance measurements.

14.4 Discussion

Desiree, Pentland Dell and Record tubers were placed in a high pressure compressed air tank at pressures of 10, 7, 3 and atmospheric pressure for 1 to 4 hours at a temperature of 40°C. Thirty tubers were used per pressure and temperature treatment. After tubers were removed from the tank they were peeled and an assessment made of the bruised area with reflectance spectrophotometry and a visual rating from 1 to 5. The darker the bruise the lower the reflectance measurements and the higher the visual rating. The mean visual and reflectance measurement was taken for blackspot bruises only, except for Desiree which had mostly shatter bruising for all treatments. Unbruised tubers were not included as there was no guarantee that these would have exhibited bruising if left for a longer time in the tank.

The visual and reflectance measurements were analysed with one-way analysis of variance (ANOVA) to determine if air pressure had a significant effect on bruise development. There were very few treatments that gave a statistically significant result ($p<0.05$ for the F value derived from the ANOVA). The effect of air pressure on visual and reflectance measurements is very confusing and statistically inconclusive. Where there was a significant difference between treatments a raised air pressure gave a darker bruise, particularly for Record tubers. However, it was difficult to determine which pressure gave the best bruise development. The reasons for the apparently erratic results could be due to the following points.

- The number of tubers showing a bruise effects the mean and ANOVA. The lower the number if tubers, the less chance there is of finding a statistically significant difference between means, and the more likely a mean is to be affected by outliers.

- Only blackspot bruises were included in the analysis because shatter bruises are darker than blackspot bruises for a similar time in the tank. It would appear that if a tuber had shatter bruising that the cells were more severely damaged and cracks in the cell walls allowed an easier passage of oxygen to them. Desiree had the highest percentage of shatter bruising followed by Pentland Dell and then Record. By excluding shatter bruises, the number of tubers with blackspot was reduced.

- The number of tubers showing a bruise increased with time in the tank. Therefore, the number of tubers with blackspot increased over time and the likelihood of finding a statistically significant result between treatments increased.

- The number of tubers per treatment was limited to thirty for practical reasons. A larger sample size may have given more tubers with blackspot bruising and more statistically significant results. However, measurement of the time that tubers were left in the tank for a particular pressure was commenced once the pressure had been reached. The development time of bruises does not include the time needed to reach that pressure, the time to bolt and unbolt the doors, the time to impact tubers or the time to take reflectance readings. Therefore, the time taken for bruises to develop from the time of impact to reflectance readings could have been an extra 45 minutes. If the sample size had been increased, this extra time would also have increased.

- The large variation in reflectance and visual assessments for a given treatment may have been affected by this extra development time. However, it is known that tubers within a variety vary in their response to impact. This inherent variability cannot be easily explained.

- More replicates per treatment may have increased the number of tubers with blackspot, but. there was only one set of tubers per treatment due to limited time and resources. The aim was to use a range of temperatures, pressures, times and varieties as the effect of high air pressures on bruise development was unknown. In hindsight, the number of treatments could have been reduced or increased.

- Reflectance measurements gave more statistically significant results than the visual assessments, but there was still a large variability within samples. The method might have been improved by developing an algorithm that used more than just the first derivative at 500 nm.

A comparison of Record tubers at 40°C and 60°C gave significant difference between visual ratings after 1 hour, and between reflectance readings after 2 hours. It is not possible to conclusively say that a higher temperature resulted in darker bruises, but it did appear that a higher air tank temperature resulted in a more rapid rise in tuber temperature. It is possible that the quicker a tuber is raised to 40°C, the faster that bruise development will occur.

When the hotbox was used to accelerate bruise development there was a significant difference in visual ratings compared to 10 bar, with bruises in the hotbox being

lighter in colour. However, bruised tubers at atmospheric pressure gave similar bruise development as those in the hotbox. Theoretically there should have been no difference between the tank and the hotbox as they are both at atmospheric pressure and 40°C. It is possible that air circulation was better in the tank than the hotbox thereby improving bruise development. However, due to inherent sampling problems outlined previously, it cannot be conclusively stated that the air tank is better than the hotbox.

Although experiments with the pressure tank and hotbox were inconclusive, it can be said that by looking for an orange to light brown colour in bruised tissue, the time for bruise detection can be reduced. With the compressed air tank, an orange to light brown colour became visible after about 3 hours, and after about 4 hours in the hotbox. This colour of bruise is visible to the human eye and does not need reflectance spectrophotometry to detect it in peeled samples. By training processors and producers to look for a light brown colour bruise instead of a dark grey bruise, the time for bruise detection can be reduced. As the formation of dopachrome always leads to the formation of melanin (Thomas 1955) the volume of orange coloured tissue is identical to the final volume of blue-black coloured tissue.

However, more work needs to be carried out to determine the accuracy of results obtained with the compressed air tank and hotbox, compared to samples kept in ambient or storage conditions. In addition, work needs to be done with samples whose bruise location is unknown to determine how readily dopachrome can be detected by the untrained eye under different lighting conditions.

Chapter 15

Quantification of bruising as percentage of tuber weight lost

15.1 Introduction

There are many different ways of classifying and quantifying bruising (section 4.2) but there is no national or international agreement as to which is best. A standard method would help to ensure that the price obtained for a potato crop was fair and would enable different grades of potatoes to be sold to specific markets, and would allow for results to be compared between different producers. It would also be useful to potato breeders who try to select for varietal characteristics that may be involved in bruise resistance.

Present methods usually involve peeling a tuber to detect a bruise and then assessing the severity of bruise either visually or directly. Depending on the method of assessment, the time taken to for the quantification of bruising in a sample of tubers can be considerable and result in an index that is difficult to interpret.

From the viewpoint of the consumer or processor, bruising results in a loss of time and potato tissue. The bigger the bruise, the greater the proportion of tissue lost. It follows that the severity of bruising may be quantified in terms of percentage tuber volume lost to the processor or consumer. By calculating the percentage of tuber volume lost per peeler stroke in removing a bruise, a new index can be devised. This method would also take into account most types and size of bruise.

To test this idea in practice, the percentage tuber volume lost per peeler stroke was calculated from measurements of peeled slices of the variety Record. The data collected from these slices was used to develop a mathematical model that could predict the percentage tuber volume lost per peeler stroke for any other potato variety. The severity of bruising was then calculated by counting the number of peeler strokes to remove a bruise and multiplying by the tuber volume lost per peeler stroke. The index formed from this method can give the total tuber volume lost in a sample of tubers, or an indication of the severity of bruising on individual tubers.

15.2 Methods

Four hundred tubers of the variety Record were washed and dried. Each tuber was weighed and the length, breadth and depth measured using digital callipers. Peeled slices were taken from one of four zones; the bud end, the stem end, and the locations of the maximum and minimum radius of curvature along the major axis of a tuber (Fig. 15.1). These zones were chosen to represent the extremes of curved surface from which peeled slices might be taken.

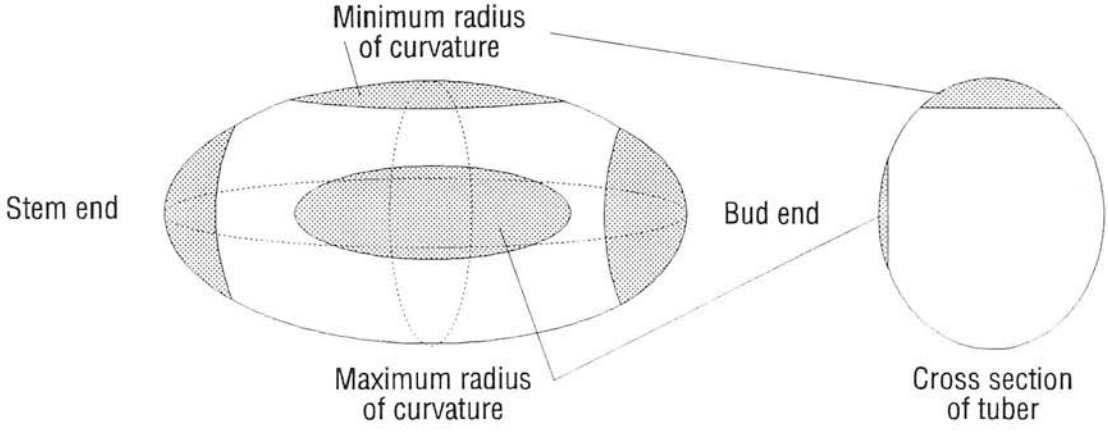

Fig. 15.1 Tuber zones: maximum and minimum radius of curvature and bud and stem end.

From each zone, 10 peeler strokes were taken using a hand held peeler (Prestige Group Ltd.) with a swivelling head (Fig. 15.2). The maximum length, breadth, and depth of each slice were measured using digital callipers, and weighed. For each zone, a total of 1000 slices was taken.

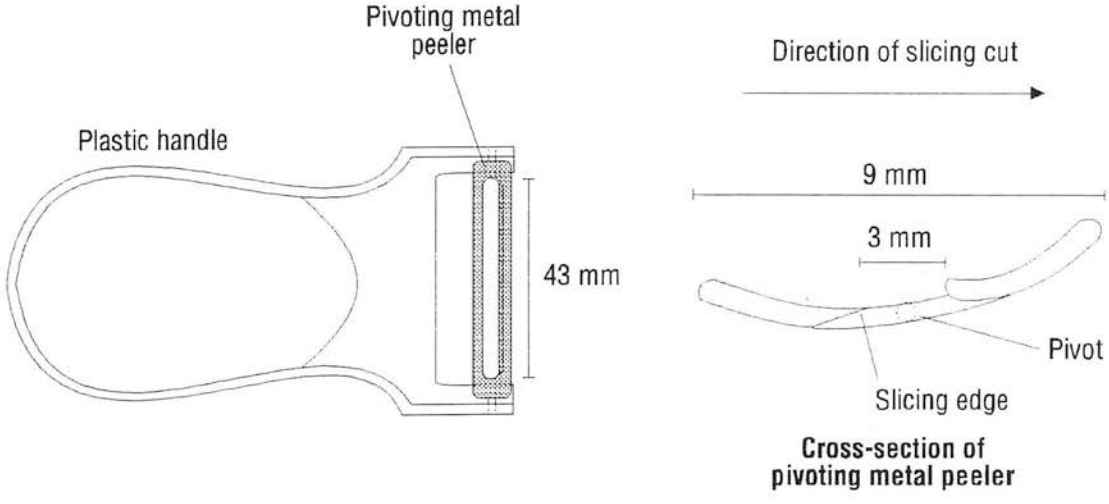

Fig. 15.2 Schematic diagram of potato peeler.

Data collected by Glaseby and McRae (1991) was used to provide the mean weight, length, breadth and depth from nine other varieties. This data set consisted of 10000 tubers from three sources; Yorkshire, the Scottish Borders and Fife.

15.3 Results

Appendix F contains tables of results for the measurements of peel length, breadth and weight removed per peeler stroke for all four zones. These results are shown in the form of graphs in this section.

The mean depth of peel for the first peeler stroke from all zones was 1.5 mm (SD ± 0.44 mm) and 1.2 mm (± 0.36 mm) for the other nine strokes. The average depth for all 10 strokes from all zones was 1.23 mm (± 0.4 mm). However, this is the maximum depth and does not indicate that peel depth can vary within a slice.

Peel length varied considerably within zones. The mean length of peel per peeler stroke was very similar for the maximum and minimum radii of curvature, and was longer than from the stem and bud ends (Fig. 15.3). The difference in peel length between bud and stem ends shows that the tuber is slightly narrower at the stem end.

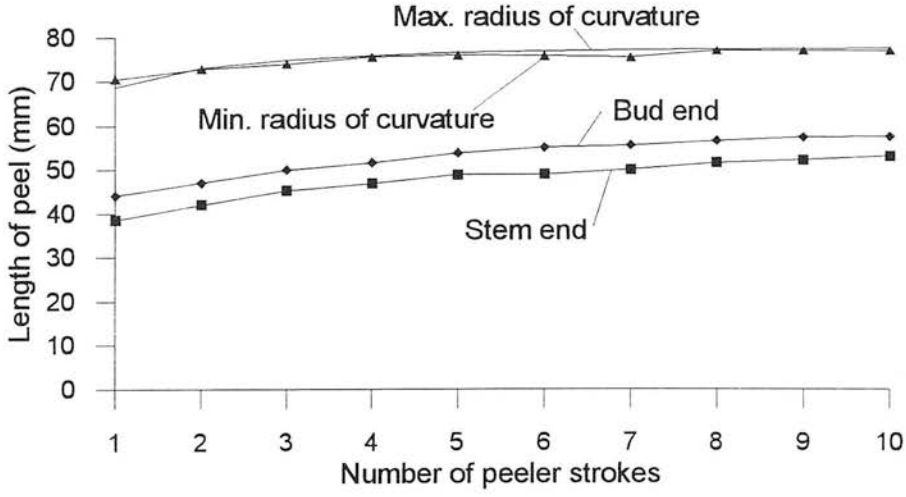

Fig. 15.3 Length of peel per peeler stroke for all zones.

The effect of varying peel length on the percentage of tuber weight removed can be seen in Fig. 15.4. The longer the peeler stroke, the higher the percentage tuber weight removed.

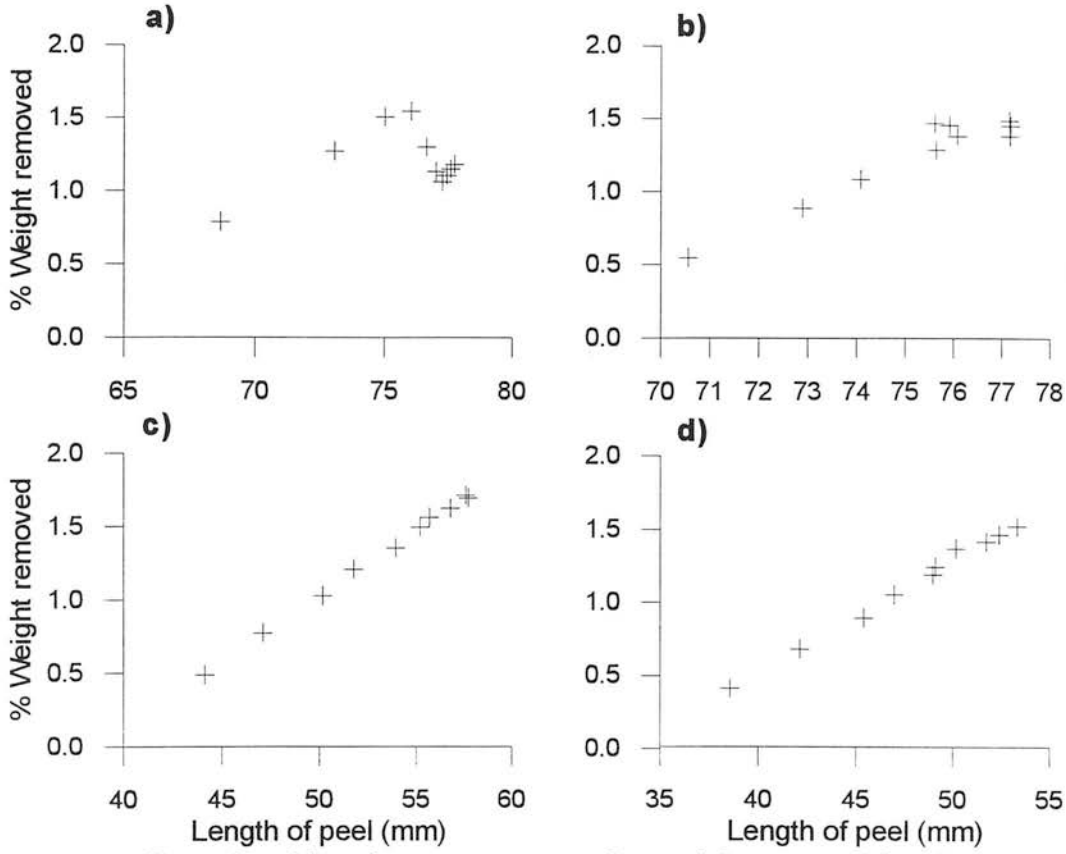

Fig. 15.4 Effect of peel length on percentage tuber weight removed for a) maximum radius of curvature b) minimum radius of curvature c) bud end d) stem end.

The mean percentage tuber weight removed per peeler stroke increases for strokes 1 to 4 then levels off (Fig. 15.5). However, for maximum radius of curvature, percentage volume removed per peeler stroke decreases after the fourth stroke. As peel depth increases in the maximum radius zone, there comes a point where the width of the peeler can no longer encompass the full depth of the tuber. The peeler then has to be angled so that further peeler strokes can be taken. The percentage weight of these successive slices is almost as small as the first peeler stroke, and increases slightly. The trends seen in the maximum radius of curvature can also occur in the other three zones if a tuber is particularly wide.

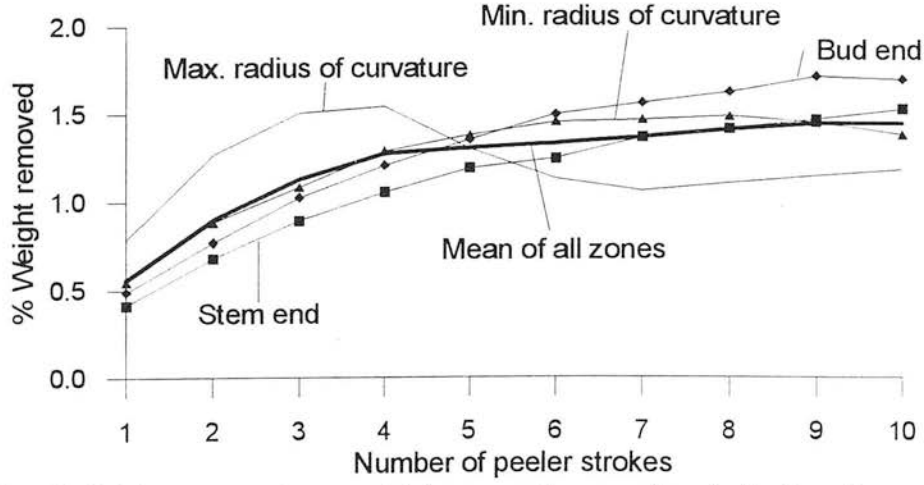

Fig. 15.5 Mean percentage weight removed per peeler stroke for all zones.

The accumulative percentage tuber weight removed per peeler stroke are very similar for stem and bud ends, and minimum radius of curvature (Fig. 15.6). Peeler stroke from the maximum radius of curvature removes more weight than the other three zones, until after the fourth stroke, where it starts to decrease.

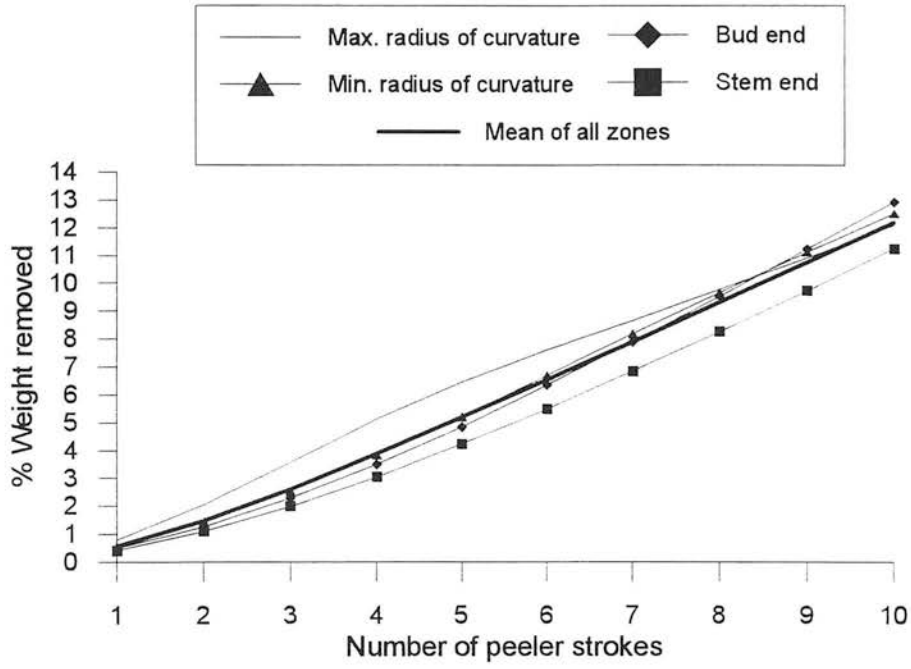

Fig. 15. 6 Mean accumulative percentage tuber weight removed for all zones.

15.3.1 Development of a model to predict the percentage tuber weight removed per peeler stroke for a range of potato varieties

The average weight, length, depth, and width of peel removed per peeler stroke has been determined for the variety Record. However, a mathematical model was needed to determine the percentage tuber volume removed per peeler stroke for a range of potato varieties. The mathematical model developed bases the shape of a tuber on an ellipsoid. An ellipsoid is a surface whose intersection in every plane is an ellipse:

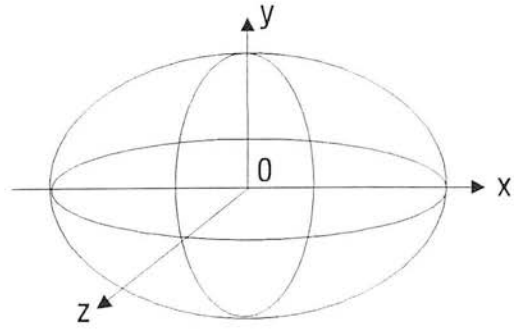

The first step in the model development was to calculate the width of peel for a given depth of peel and length and depth of tuber as chord length across an ellipse (see Appendix G for derivation of formula):

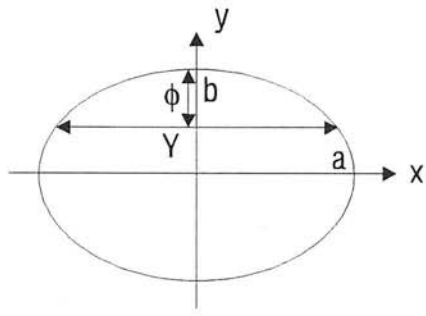

$$Y = 2 \cdot \left[\frac{a}{b} \cdot \sqrt{b^2 - (b - \phi)^2} \right]$$

Where Y = length of chord, a = half major axis, b = half minor axis, ϕ = total depth of slice (a depth of 1.2 mm per peeler stroke was used to calculate chord length for all zones).

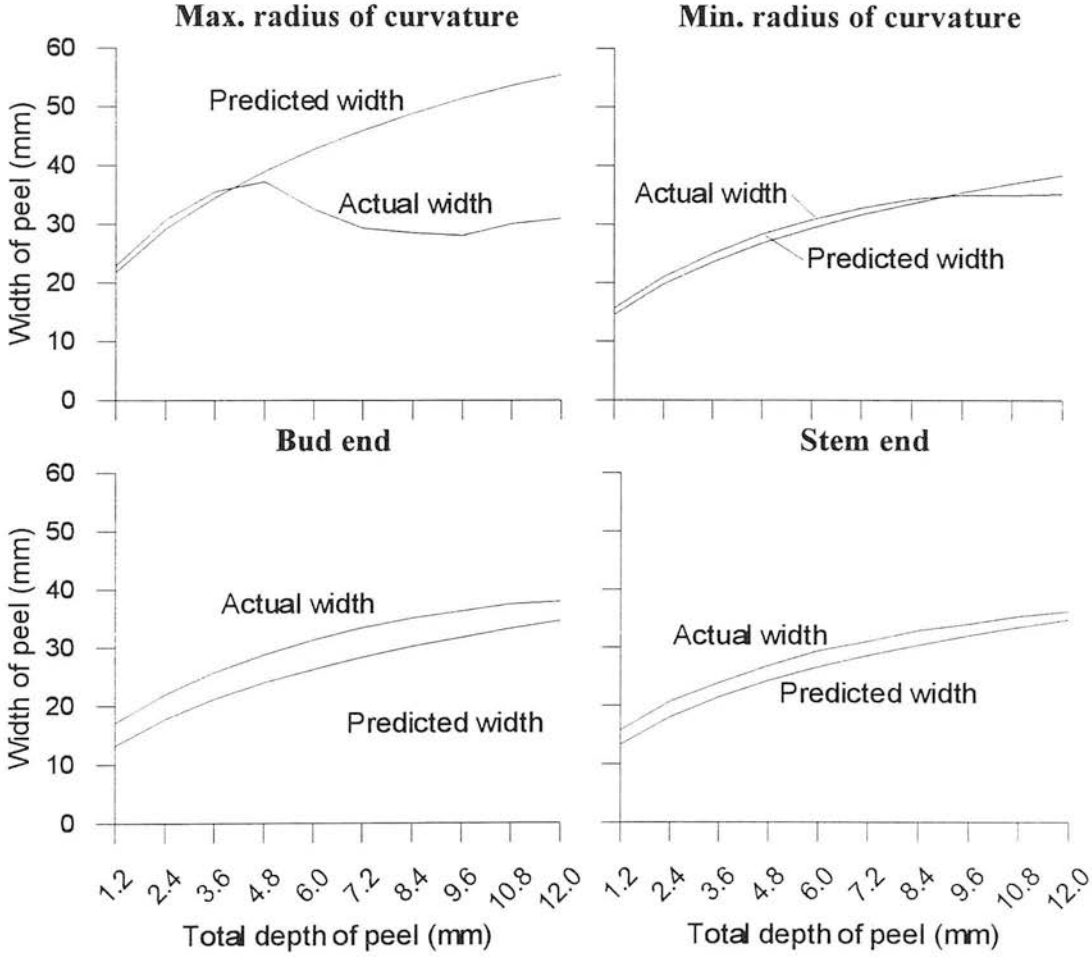

Fig 15.7 Mean width of peel and predicted width for maximum and minimum radius of curvature and bud and stem ends.

In the bud, stem and minimum radius of curvature zones, the predicted width is similar to the actual mean peel width (Fig. 15.7). For the maximum radius of curvature, the first four peeler strokes are very close to the predicted values then

widely diverge. The divergence arises when the predicted width is greater than the width of the peeler. When this occurs the peeler has to be slightly re-angled to take successive slices. This trend can occur in any zone if a tuber is particularly large. The correlation coefficient between width of peel and predicted width was 0.81 for maximum radius of curvature (strokes 1 to 4) 0.86 for minimum radius of curvature, 0.88 for bud end, and 0.89 for stem end.

It was found that peel length does not conform to chord length across an ellipse because peeler strokes are taken around the circumference rather than parallel to the axes. To model peel length, the following equation (see Appendix H for derivation of formula) was used to measure the length of an arc on an ellipse, given the starting and ending angle of the arc about the origin.

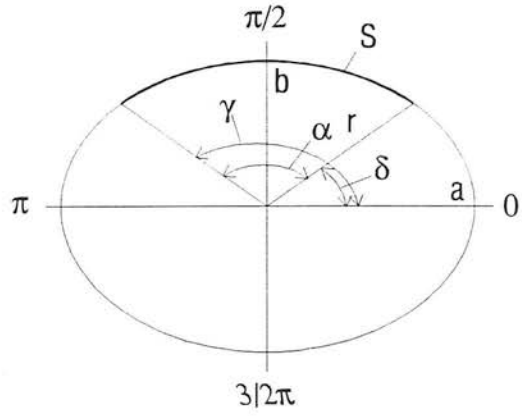

$$S = \int_{\delta}^{\gamma} \sqrt{\left(a^2 \cdot \frac{b^2}{b^2 \cdot \cos(\alpha)^2 + a^2 \cdot \sin(\alpha)^2}\right) + \left(-a \cdot b \cdot \cos(\alpha) \cdot \sin(\alpha) \cdot \frac{-b^2 + a^2}{\left(b^2 \cdot \cos(\alpha)^2 + a^2 \cdot \sin(\alpha)^2\right)^{\frac{3}{2}}}\right)^2} \, d\alpha$$

Where S = length of arc on ellipse, δ = starting angle, γ = ending angle, $\alpha = \gamma - \delta$, a = half major axis, b = (half minor axis - depth of peel; 1.2 mm depth of slice for all peeler strokes).

This equation was used to find the mean starting and ending angles for each peeler stroke, using the mean peel length at a given depth. It was found that the total angle from the first slice to the last slice did not increase linearly. Solo Curve Fitter (BMDP Statistical Software, Inc., California) was used to determine the non-linear relationship between total stroke angle and depth of peel;

$$T = A.\phi^{(B \cdot \phi^C)}$$

Where T = total angle between start and end of peeler stroke, A B and C are coefficients, and ϕ is the depth of slice. See Table 15.1 for coefficients.

Correlation coefficient between length of peel and predicted length was 0.78 for maximum radius of curvature, 0.72 for minimum radius of curvature, 0.6 for stem end, and 0.73 for the bud end.

Table 15.1 Coefficients providing the best fit for non-linear regression between first and last peeler stroke angle; 1.2 mm peeler depth per peeler stroke.

	Max. radius	Min. radius	Bud end	Stem end
Total angle-first stroke (radians)	1.805	1.787	1.414	1.243
Total angle-last stroke (radians)	2.115	2.112	1.986	1.826
A	1.190	1.350	1.765	1.683
B	0.134	0.114	6.514	0.184
C	0.093	0.125	0.041	-0.239

In addition to modelling a potato tuber as an ellipsoid it is assumed that the potato does not vary in density from the pith to the cortex. In this way, a model of percentage tuber volume removed can be converted to percentage tuber weight removed, or vice versa.

To estimate the volume of each slice, the area of peel was taken as an ellipse, and multiplied by the depth of peel. This was then divided by the total volume of the tuber, based on the volume of an ellipsoid. The total percentage tuber volume removed at each peeler stroke, was calculated as:

$$V = \sum_p \left(\frac{\pi \frac{S_p}{2} \cdot \frac{Y_p}{2} \cdot \phi}{\frac{4}{3} \cdot \pi \cdot a \cdot b \cdot c} \right) \cdot 100$$

Where V = total percentage volume removed; p is the number of peeler strokes; a, b and c are half the major and minor axis of an ellipsoid; ϕ = total depth of peel; S_p = length of peel at ϕ; Y_p = width of peel at ϕ.

For the bud and stem ends, using 1.2 mm as the mean peel depth to calculate peel volume, the correlation coefficient between percentage tuber volume removed and predicted values were 0.96 for bud end, and 0.94 for stem end (Fig. 15.8).

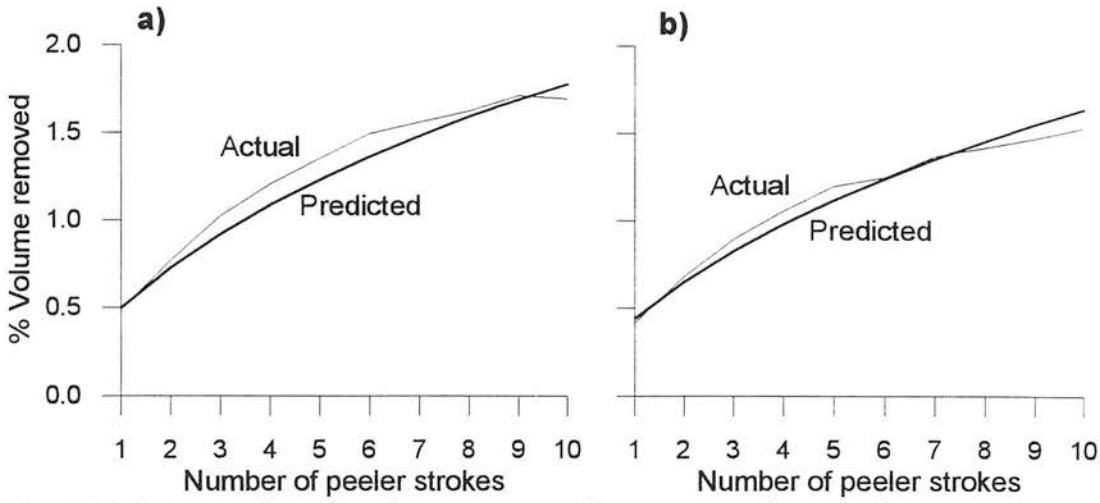

Fig. 15.8 Mean and predicted percentage volume removed per peeler stroke for the a) bud and b) stem ends.

For maximum radius of curvature, using a mean depth of 1.2 mm for all volumes, the correlation coefficient between predicted and actual percentage tuber volume removed was 0.66. The low correlation arises from the model predicting a peel width greater than the width of the peeler after the fourth peeler stroke. To improve the model, a varying depth of slice per peeler stroke was incorporated. This compensates for the problem of removing full widths of peel after the fourth peeler stroke (Fig 15.9).

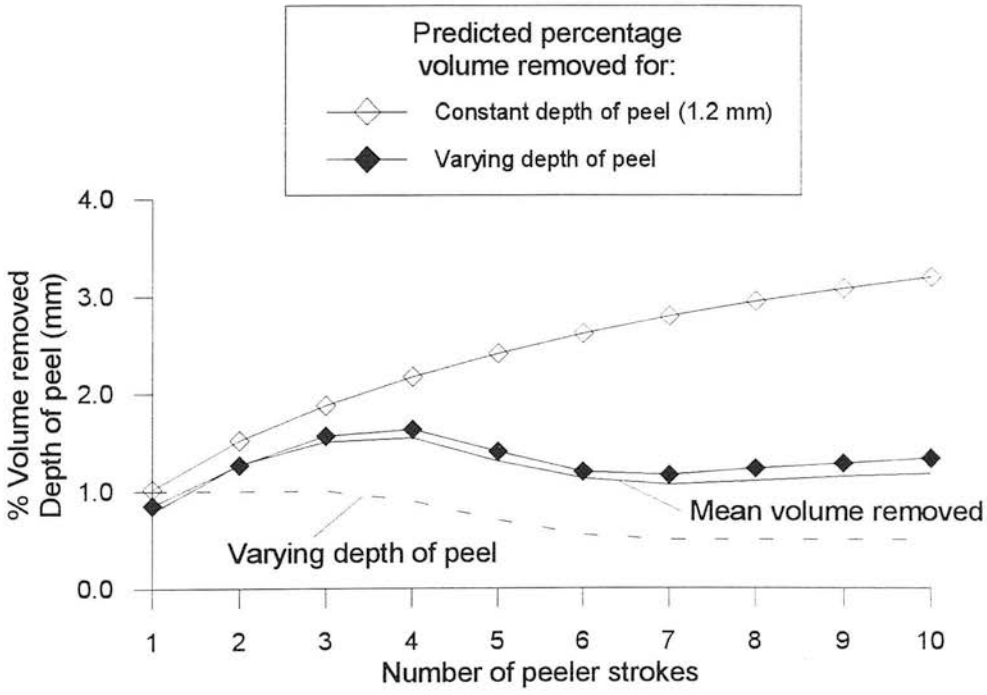

Fig. 15.9 Effect of varying peel depth on predicted percentage tuber volume removed per peeler stroke at the maximum radius of curvature.

The minimum radius of curvature had a correlation coefficient of 0.76 between predicted and actual percentage tuber volume removed per peeler stroke. Figure 15.10 shows that by varying the depth of peel, the correlation is increased to 0.95.

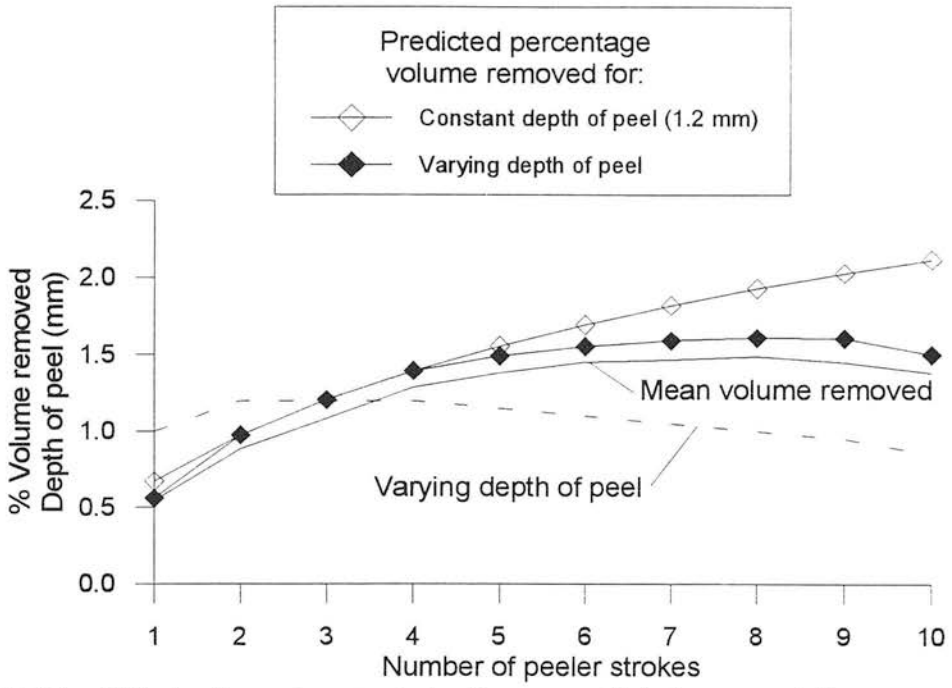

Fig. 15.10 Effect of varying peel depth on predicted accumulative percentage volume removed per peeler stroke at the minimum radius of curvature.

The average predicted percentage tuber volume removed per stroke can be calculated by taking the mean percentage removed from all zones. The correlation coefficient between percentage tuber volume lost and predicted loss is 0.88 (Fig. 15.11).

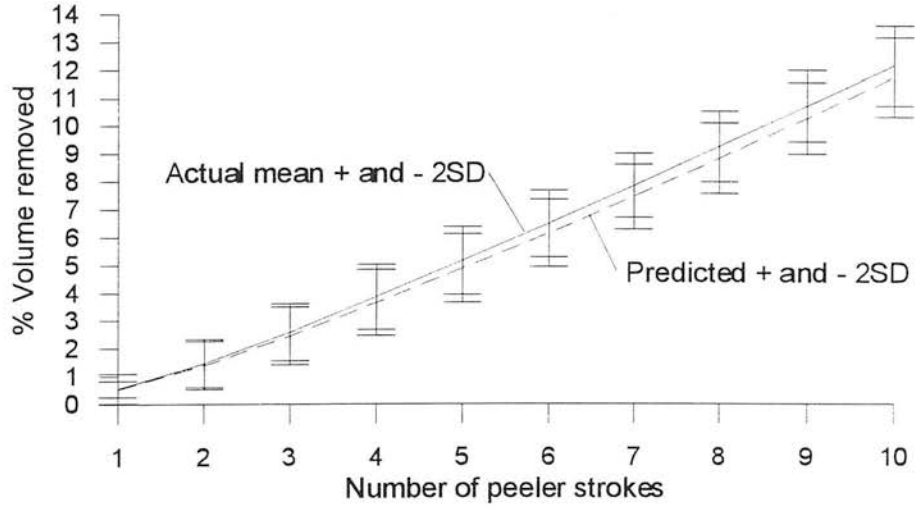

Fig. 15.11 Mean and 95% confidence limits of accumulative percentage tuber volume removed per peeler stroke and predicted loss for all zones.

The model can now be applied to other potato varieties, using the mean length, breadth and depth of tubers (Appendix F) to find the accumulative percentage tuber volume removed per peeler stroke (Table 15.2).

Figure 15.12 plots the two varieties that have maximum and minimum percentage tuber volume removed per peeler stroke. The 95% confidence limits of the actual percentage tuber volume removed per peeler stroke is greater than the predicted

means of the other 10 varieties. Therefore, there is no significant difference between the varieties.

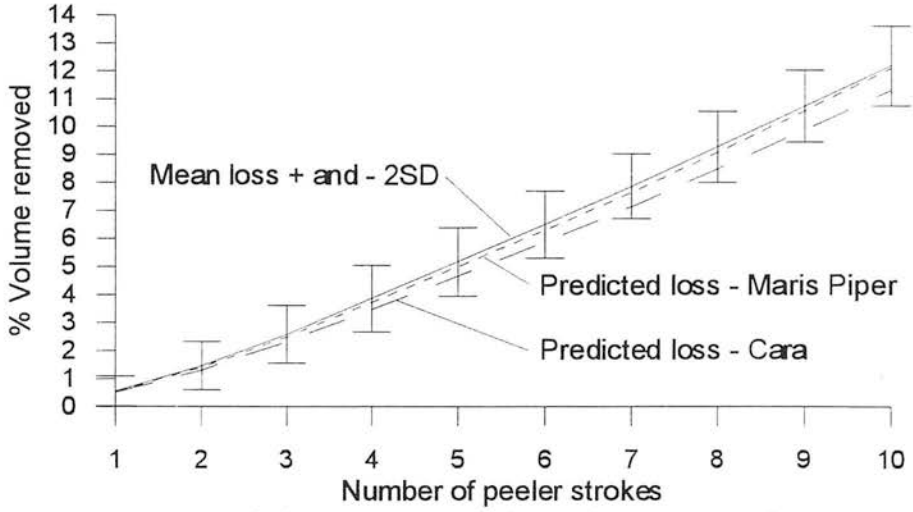

Fig. 15. 12 Mean accumulative percentage tuber volume removed per peeler stroke and the maximum and minimum predicted loss from 10 potato varieties.

The relationship between number of peeler strokes and percentage tuber volume removed is non-linear. To simplify calculations of percentage tuber volume removed, a linear regression line can be fitted with the following relationship;

$$V = 1.25 \cdot p - 1.2$$

Where V = percentage volume lost, p = number of peeler strokes.

The percentage volume removed with the first stroke is smaller than the model (Fig. 15.13). However, if this model is to be used in practice, the first peeler stroke would be discounted as this is used to reveal bruising. If a bruise is found, it is the number of peeler strokes used to removed it that is significant.

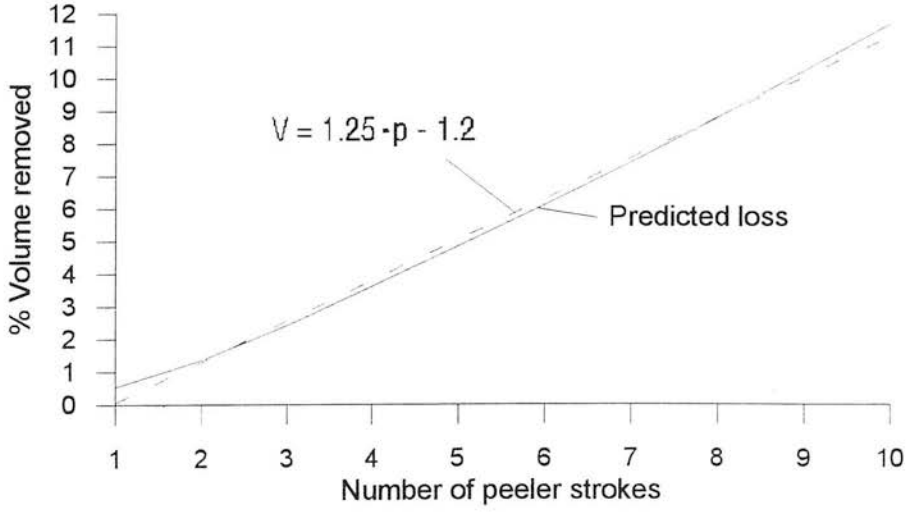

Fig. 15.13 Linear regression of mean predicted accumulative tuber volume removed per peeler stroke of all zones and all varieties.

The linear regression gives an average of 1.25% tuber volume removed with each stroke. This is the approximate percentage tuber volume removed per peeler stroke for any part of a tuber and for any variety. However, if a potato peeler has a mean slicing depth greater or less than 1.2 mm then a linear regression of percentage tuber volume removed with peel depth gives the following equation;

$$V = 1.03 \cdot \phi - 1.1.4$$

Where V = percentage volume removed, ϕ = total depth of slice (mm)

15.3.2 Examples of model in practice

Examples of how this method might be used in practice would be to:

1.
   - Take a random sample of 25 tubers.
   - Peel away skin to reveal bruise.
   - Count the number of peeler strokes to remove bruise.
   - Add up the number of peeler strokes required to remove all the bruises on all tubers.
   - Instead of multiplying by 1.25, which is cumbersome to calculate mentally, the number of peeler strokes could be multiplied by 5 to give a damage index.
   - Alternatively, the actual loss from a sample with a damage index of, for example 350 can be expressed as a percentage by dividing the damage index by 100. This gives the theoretical percentage tuber volume lost due to bruising for a sample of 100 tubers.

2. The method could also give an indication of the different degree of bruising on individual tubers by plotting a histogram of the number of tubers with the number of peeler strokes to remove bruises.

3. The average percentage tuber volume lost could be calculated by multiplying the total number of peeler strokes to remove bruises in a sample, multiply by 1.25 and dividing by the number of tubers in sample.

4. In terms of monetary loss, the average percentage tuber volume lost due to bruising could be multiplied by the price per tonne for the crop, multiplied by the number of tonnes harvested.

Table 15.2 Accumulative percentage tuber volume removed per peeler stroke for all varieties.

Peeler stroke	Record	King Edward	Pentland Ivory	Pentland Hawk	Maris Piper
1	0.56 ± 0.3	0.55	0.5	0.5	0.5
2	1.46 ± 0.5	1.4	1.3	1.3	1.4
3	2.6 ± 0.6	2.5	2.3	2.4	2.5
4	3.9 ± 0.7	3.7	3.5	3.5	3.7
5	5.2 ± 0.7	5.0	4.6	4.7	5.0
6	6.5 ± 0.8	6.3	5.9	5.9	6.3
7	7.9 ± 0.8	7.6	7.1	7.2	7.6
8	9.3 ± 0.8	9.1	8.5	8.5	9.1
9	10.7 ± 0.8	10.5	9.9	9.9	10.6
10	12.2 ± 0.8	12.0	11.3	11.4	12.1

Peeler stroke	Pentland Dell	Pentland Squire	Pentland Crown	Cara	Desiree
1	0.5	0.5	0.5	0.5	0.5
2	1.4	1.4	1.4	1.3	1.4
3	2.4	2.4	2.4	2.3	2.4
4	3.6	3.6	3.6	3.5	3.6
5	4.8	4.8	4.8	4.7	4.9
6	6.1	6.1	6.1	5.9	6.1
7	7.4	7.4	7.4	7.1	7.4
8	8.8	8.8	8.8	8.5	8.8
9	10.3	10.2	10.2	9.9	10.3
10	11.8	11.7	11.7	11.3	11.8

Peeler stroke	All varieties	Actual loss
1	0.5	0.5 ± 0.6
2	1.4	1.4 ± 0.8
3	2.4	2.4 ± 1.0
4	3.6	3.6 ± 1.2
5	4.8	4.8 ± 1.2
6	6.1	6.0 ± 1.2
7	7.4	7.3 ± 1.2
8	8.8	8.7 ± 1.2
9	10.2	10.1 ± 1.2
10	11.7	11.6 ± 1.4

15.4 Discussion

The work described in this chapter involved taking measurements of peel weight, length, breadth and depth for 10 successive peeler strokes from four zones on 400 tubers, variety Record. The zones were minimum and maximum radius of curvature on the longest axis, and bud and stem ends. Measurements were also taken of tuber length, breadth, and depth.

The intention was to use this empirical data to calculate, via a model, a simple index that could be used for a wide variety of potatoes. Although the model appears obscure, in essence it is based on the length, breadth and depth of an ellipsoid, and the depth and length of cut with a potato peeler. It was found that the predictions of peel length, width and volume by the model were closely correlated with the actual data obtained for Record. The model was then applied to the mean tuber dimensions of 9 other potato varieties in Britain. It was found that the predictions of the model were not dependent on potato variety and that an average 1.25% of tuber volume is removed per peeler stroke for all zones on any tuber.

By counting the number of strokes to remove damaged tissue, the total percentage tuber volume lost is easily calculated and a variety of indices can be developed to determine the severity of damage on individual tubers or within a sample. To develop this method further, the potato industry would have to decide the acceptable percentage weight loss for different grades of potatoes. In addition, if there is a need for greater precision then the effect of peeler stroke length will have to be considered as this has the greatest influence on the model.

The model is also influenced by the dimensions of the peeler. A wider peeler blade would have enabled full widths of slices to be taken in all zones, and the model to be simplified. If this method for quantifying damage is adopted by the potato industry, then the peeler would have to be standardised and marketed for the estimation process.

Chapter 16

Overall discussion and conclusions

When a tuber is impacted a cascade of cellular processes is initiated in the sub-surface tissue. These responses are part of the potato's natural defence strategy against pathogens and the healing of damaged tissue. The only change visible to the human eye, and only usually after a tuber is peeled, is the production of the blue-black pigment melanin. The discoloured tissue associated with bruising is considered to be an unacceptable quality in a potato tuber. Bruising caused during harvesting and handling can lead to downgrading of potatoes for the processing industry and quality retail trade.

The financial loss associated with bruising is considerable and a great deal of money has been invested in trying to reduce the problem. Impacts can never be eliminated from the harvesting process because potatoes have to be physically separated from the soil. The forces needed to separate tubers from the soil is dependent on a number of factors such as the type of soil and amount of soil moisture. Harvester settings can be adjusted to vary the forces, but the delay between an impact occurring and the development of a bruise, means they can never be truly optimised. The longer the delay between the time of impact and the development of a bruise, the greater the proportion of a crop that can be harvested with potentially high bruising levels. It is estimated that when operating a two-row harvester, every hour that elapses before bruising is discovered can lead to a loss of over £700.

Unfortunately there is not always a correlation between a tuber receiving an impact and the initiation of a bruise. There are many factors which affect the susceptibility of a tuber to bruising and primarily there is a need to understand the factors that affect this susceptibility. If bruising susceptibility could be manipulated by genetic or environmental means before harvesting, this would reduce the need to monitor harvester settings. However, bruising susceptibility is multi-factorial and it will probably be many years before its elements are fully determined.

Bruised tubers pass unnoticed through quality control to reach the processor or consumer. This may result in lost confidence in the producer or in potato wastage. The need to peel a tuber first to detect bruising makes quality assessment time consuming and therefore costly. At present there are no national or international standards for quantifying bruising. Current methods can be subjective and result in an index that is difficult to interpret. If the assessment of bruising is inaccurate, the

crop could be unnecessarily downgraded leading to financial loss. Consistent bruise indices need to be evolved if different grades of potatoes are to be sold to specific markets, if results are to be compared between producers and if potato breeders world-wide are to properly select for varietal characteristics that may be involved in bruise resistance.

In this thesis, the two main aims were to reduce the time needed to detect bruising and to evaluate and develop a method for quantifying bruising. Reflectance spectrophotometry was chosen as a possible technique to fulfil both these aims. If bruising could be detected without the need for peeling, tubers could be automatically sorted and the effect of different harvester settings assessed more quickly.

The varieties Desiree, Pentland Dell and Record were chosen for all the experiments to study the effect of variety, in particular skin colour and response to impacts. Initial experiments with spectrophotometry involved measuring the transmission characteristics of unpeeled and peeled tubers. It was demonstrated that in peeled tubers the transmitted light can be detected in sections up to about 12 mm thick, and in unpeeled tubers the light could be detected in sections about 6 mm thick. It was hypothesised that if a perfect reflector were present in the tuber that transmitted light would pass through the tissue until it was reflected out of the initial interface. This was taken to be a simplified model of body reflectance and that it could be detected from tissue about 3 mm deep in unpeeled tubers and about 6 mm deep in peeled tubers. Therefore, by measuring body reflectance from potato tubers it should be possible to detect the colour change associated with bruising.

The body reflectance of bruised and unbruised tubers was then measured with a scanning monochromator and bifurcated fibre optic light guides from the UV to NIR. The spectra from unbruised and bruised tubers were divided into two groups: 'known' and 'trial' tubers. Spectra were analysed in untransformed and first derivative format. The use of first derivative spectra highlights where changes in spectral slope are occurring between unbruised and bruised tubers, and reduces errors caused by holding the bifurcated cable at different angles.

Discriminant analysis selected wavelengths from the 'known' tubers that were most sensitive to differences between unbruised and bruised tubers. It was found that spectra from bruised unpeeled and peeled tubers appeared to have a lower reflectance than unbruised tubers from the UV to visible spectrum, and that this trend was reversed in the NIR. A lower reflectance for bruised tubers would have been

expected due to the production of dark coloured melanin, but the reason for the increase in reflectance in the NIR is unclear.

There were no obvious differences between untransformed spectra of bruised and unbruised tubers, but first derivative spectra revealed where changes in spectral slope were occurring that corresponded to a change in reflectance in the untransformed spectra. It was found that some of the wavelengths selected by discriminant analysis from peeled and unpeeled tubers were similar to known wavelengths of dopachrome and melanin *in vitro* (300, 475 and 640 nm). However, the wavelengths selected from unpeeled tubers appeared to be dependent on variety particularly in the visible spectrum. Wavelengths selected in the NIR were not associated with absorption bands for carboxyl groups in melanin. NIR spectra would appear to detect changes in bruised tissue that are due to cellular processes other than melanin production. Without further biochemical experiments it is not possible to determine what these changes might be.

Discriminant analysis then used the wavelengths selected from the 'known' tubers to generate linear classification functions that could predict whether a tuber was unbruised or bruised. Nearly all spectra from 'known' unpeeled tubers were significantly classified, with spectra from the NIR giving the highest percentage (86 to 97.9 %) tubers correctly classified as bruised or unbruised. All spectra from 'known' peeled tubers were significantly classified with the highest percentage correctly classified (93.5 to 95.7%) from NIR spectra.

However, when these classification functions were used to determine the classification of spectra from tubers whose identity was unknown to the program ('trial' tubers) the results were not so optimistic. The only significant classification of unpeeled tubers came from the NIR with 71 to 90.7% correctly classified. With peeled tubers, the results were more complex with significant classifications for one or two, but not all, of the varieties from the UV to NIR. The highest percentage classification was 81.8 % from the NIR followed by 79.5% from the UV.

It was suggested that the inconsistent classification of 'trial' tubers was due to a small sampling area, that not all the body reflectance was being detected and that holding the fibre optic at different angles affected the spectra. In addition, the presence of soil or disease on the skin could also have affected the spectral characteristics of unpeeled tubers. An integrating sphere was then used in an attempt to improve the spectrophotometric method. The integrating sphere collects all the reflectance from a larger sample area and the detected radiation is also independent of the geometry of

the incident light. Due to the inherent light losses in an integrating sphere the spectral range of this apparatus was limited to 400 to 800 nm.

It was found that the integrating sphere gave more consistent and significant classification results than a bifurcated cable. Unpeeled 'known' tubers were classified with 75.6 to 91.1% accuracy, and 69.6 to 81.8% of 'trial' tubers correctly classified. For peeled tubers 88.9 to 100% 'known' tubers were correctly classified and 79.5 to 84.4% of 'trial' tubers correctly classified. However, it was found that the results were still inconsistent in that the highest percentage of unpeeled tubers correctly classified came from the first derivative spectra for 'known' tubers and from untransformed spectra for 'trial' tubers. This trend was reversed for peeled tubers.

The use of neural nets was then investigated as a possible improvement over the way that discriminant analysis tries to separate unbruised and bruised tubers. Neural nets were trained with the spectra collected for the 'known' tubers and interrogated spectra from 'trial' tubers. The nets were trained with entire spectral ranges or wavelengths selected by discriminant analysis from untransformed spectra. It was found that nets trained with a subset of wavelengths trained faster and reduced the likelihood of all tubers being classified as bruised or unbruised. For some 'trial' tubers, neural nets gave a higher percentage of tubers correctly classified, while for others it made it worse. It appeared that if the net was trained and interrogated with spectra that gave good discrimination results, that the net recognised more tubers as bruised or unbruised.

It became apparent that the non-invasive detection of bruising in unpeeled tubers with reflectance spectrophotometry was not consistent enough at present. However, the spectrophotometric method may be improved if the integrating sphere could be adapted to measure wavelengths in the NIR. Spectra collected with a bifurcated cable in the NIR gave the only significant discrimination of 'trial' tubers. The use of an integrating sphere improved the discrimination of tubers in the visible spectrum. Therefore, a similar improvement may be obtained for the NIR.

The use of reflectance spectrophotometry to non-invasively detect bruising in peeled tubers was more robust due to the absence of skin, and the more obvious differences between spectra from unbruised and bruised spectra. Therefore, it may be possible in the future to develop machine vision techniques to automatically detect bruising after tubers are peeled, and before being processed.

The methods of infrared and microwave thermography were then investigated to non-invasively measure possible temperature rises associated with an increase in

respiration in bruised tissue. Scanning laser Doppler imagery was also investigated as a possible tool to detect changes in the biological zero of bruised tissue. It was found that there were no significant differences between unbruised and bruised tissue measured with either of these techniques. The changes in temperature or biological zero in bruised tissue is either non-existent or too small to be measured with these methods at present

Reflectance spectrophotometry was also investigated as a non-invasive and non-subjective method for measuring bruise area and volume. Spectra were taken with the integrating sphere from bruised unpeeled and peeled Record tubers and converted into the first derivative format. After reflectance spectra were acquired the area of bruise was measured from peeled tubers with a colour digital camera. The camera was used to obtain accurate measurements of bruise area for correlation with reflectance spectra and to evaluate it as a possible method for bruise assessment. It was found that the image analysis technique could measure a variety of bruise colours and shapes with precision, but the threshold values had to be adjusted for each tuber making the method time consuming.

Reflectance spectrophotometry can measure bruise area faster but less accurately than the digital camera. Regression Variable Selection was used to select a subset of wavelengths gave the best correlation with bruise area and volume. Multiple linear regression reduced the selected variables to a minimum and defined linear equations for the correlations. Reflectance spectra from unpeeled and peeled tubers were most closely correlated with bruise area. However, the R-squared value for bruise area against bruise volume was 0.88, so if the area is known an approximation of the bruise volume can be reached.

Measurement of bruise area with reflectance spectra from unpeeled tubers had an R-square value of 0.38. From peeled tubers the R-square value was increased to 0.51. The determination of bruise size in unpeeled tubers is difficult due to the variability of the skin and the effect that it has on the attenuation of body reflectance. With peeled tubers the difference in first derivative spectra between large and small bruises is more clearly defined but is affected by the colour of bruise. It may be possible in the future to use reflectance spectrophotometry to determine the threshold levels for image analysis techniques and in this way offer the potential for automatic bruise assessment where tubers are peeled prior to processing.

The effect of temperature on the rate of melanin formation was studied with transmission spectrophotometry. Polyphenol oxidase was extracted from tubers and

added to the substrate DOPA to form the orange pigment dopachrome. Spectral readings were taken of dopachrome (peak absorption at 475 nm) as it was rearranged to form black melanin at temperatures of 20°C, 40°C and 60°C. The spectral characteristics of melanin are difficult to determine *in vitro* as the melanin forms as granules that precipitate to the bottom of the cuvette. It was found that the time taken for dopachrome to form melanin was twice as fast at 60°C compared to 40°C, and four times as fast as 20°C. The increased rate of melanin development at 60°C could be one way of accelerating bruise development in tubers. However, the higher the tuber temperature the greater the risk of de-naturing the polyphenoloxidase (Iritani and Weller 1985).

The effect of temperature and pressure on the development of dopachrome and melanin *in vivo* was studied with reflectance spectrophotometry. Previous experiments with compressed air at the SCAE had demonstrated that a pressure of 3 bar could accelerate bruised development to within 5 hours and that a higher pressure might further reduce this time. As a result, a new high pressure compressed air tank was built to operate at a pressure of 10 bar. The reflectance spectrophotometer was connected with a fibre optic coupling port to the integrating sphere placed inside a high pressure compressed air tank. Reflectance readings were taken every 15 min from bruised unpeeled and peeled tubers while the air pressure was raised to 10 bar.

A change in the first derivative slope occurred at 500 nm for unpeeled and peeled tubers that corresponded to a change in reflectance in the untransformed spectrum at 475 nm. In unpeeled tubers the change in slope occurred over about 6 hours and in peeled tubers about 2 hours. In unbruised unpeeled tubers there was no change in slope over time at 500 nm, but in unbruised peeled tubers the change was identical to bruised peeled tubers. It appeared that cells ruptured by the peeler on the tuber surface discoloured at a faster rate and masked any discolouration associated with cells damaged due to an impact.

When reflectance measurements were taken of a peeled tuber outside the tank under ambient conditions the surface turned from white to pale orange, to orange to brown and finally grey. A change in spectral slope at 500 nm was measured which corresponded to the unseen changes in the compressed air tank. The orange pigment corresponds to dopachrome and the grey colour to melanin.

While bruise development could be monitored in unpeeled tubers the method could not be used to assess the effect of different atmospheric conditions on bruise development. This was due to being able to place only one tuber at a time in the

integrating sphere, the development of a bruise did not always occur, and the initial starting reflectance value was variable. The method was modified by peeling a sample of tubers after they had been in the pressure vessel and measuring the first derivative reflectance spectra at 500 nm from the bruised area. In addition to measuring the reflectance of bruised tuber, a visual assessment was made of the bruise on a scale of 1 to 5. A value of 1 equated to a very pale bruise and a value of 5 to a dark brown to grey coloured bruise. The visual assessment is subjective but is not affected by the size of bruise as reflectance measurements are.

Samples of 30 tubers for the varieties Desiree, Pentland Dell and Record were impacted and placed in the compressed air tank at pressures of 10 bar, 7 bar 3 bar and atmospheric pressure for 1, 2, 3 and 4 hours at 40°C. In addition, Record tubers were placed in the air tank at a temperature of 60°C and placed in a hotbox as a comparison to the compressed air method.

Unbruised tubers were excluded from the analysis as there was no guarantee that a bruise would have developed if left for a longer time in the air tank. Shatter bruises were also excluded from Pentland Dell and Record tubers as cracks in the sub surface tissue made them discolour much faster than blackspot bruises. Bruises on Desiree were almost exclusively shatter bruises so these were included in the analysis.

Bruises from all varieties became darker over time, with Desiree becoming darker more quickly than Pentland Dell and Record tubers due to the presence of shatter bruising. The visual and reflectance measurements were variable for each treatment and there were few significant differences (evaluated by one-way ANOVA) between pressures on the rate of bruise development. Where there was a significant difference between pressures, the optimum pressure for bruise development varied. In general it may be said that pressure appeared to increase the rate of bruise development but statistically it could not be categorically stated that the higher the pressure the darker the bruise. Several possible reasons were proposed for the lack of statistically significant results. The main reason being the low number of tubers with blackspot bruises, even when the number of bruised tubers increased with time. There is also a large variability in response to bruising which cannot be easily explained due to the multitude of factors that can affect bruise susceptibility.

A temperature of 60°C appeared to increase the rate of bruise development but again the statistics were inconclusive. It would seem that a higher air tank temperature raised the temperature more quickly to 40°C and it may be the case that the sooner the tuber temperature is raised to 40°C the faster the bruise development.

The hotbox appeared to give a slower rate of bruise development than the compressed air tank at 10 bar, but pressure at atmospheric pressure also gave as dark a bruise as 10 bar. Although experiments with the pressure tank and hotbox were inconclusive, it can be said that by looking for an orange to light brown colour in bruised tissue, the time for bruise detection can be reduced. With the compressed air tank, an orange to light brown colour became visible after about 3 hours, and after about 4 hours in the hotbox. This colour of bruise is visible to the human eye and does not need reflectance spectrophotometry to detect it in peeled samples. By training processors and producers to look for a light brown colour bruise instead of a dark grey bruise, the time for bruise detection can be reduced. It is important to note that the volume of bruised tissue does not change over time, only the colour. Therefore, information about the severity of bruising can also be achieved by looking for dopachrome.

A new way of quantifying bruising was developed by taking measurements of peeled slices from the variety Record. The length, width, depth and weight of peel removed per peeler stroke was measured for 10 consecutive peeler strokes from four zones on a tuber. A mathematical model was then developed to predict the percentage of tuber volume removed per peeler stroke that could be applied a range of varieties. The predictions of the model were very similar to the actual results obtained and there was no significant difference between varieties. An average of 1.25% of the tuber volume is removed per peeler stroke for all four zones. By counting the number of peeler strokes to remove bruised tissue and multiplying by 1.25, an estimate of the percentage tuber volume lost as a result of bruising can be obtained for individual tubers or for a sample. The index accounts for any size and shape of bruise and does not rely on categorising the severity of bruising.

The mathematical model is affected by the design of peeler. If this index were adopted by the potato industry the peeler would have to be standardised for the estimation process. In addition, the industry would have to decide acceptable limits of tuber volume loss for grading potatoes.

Chapter 17

Summary and future research proposals

The following points summarise the advancements made so far in developing methods of rapid bruise detection and formulation of robust bruise indices.

- Reflectance spectrophotometry can non-invasively and rapidly detect bruising in peeled tubers, but is less consistent with unpeeled tubers.

- Bruise development can be monitored in unpeeled and peeled tubers. The production of pre-cursor pigments in bruised tissue can be used as markers for early bruise development and reduce the time for bruise detection. These pigments are visible to the human eye.

- Non-invasive detection of bruising in unpeeled tubers with infrared and microwave thermography or scanning laser Doppler imagery is not sensitive enough at present to detect changes in bruised tissue.

- Temperature and air pressure accelerate bruise development. The optimum air pressure cannot be categorically stated due to statistical sampling problems. However, by looking for dopachrome, an orange pre-cursor pigment to melanin, the time taken for bruise detection can be reduced to approximately half the time it takes for a dark grey bruise to develop. This time is about 3 hours in the compressed air tank and 4 hours in the hotbox.

- Reflectance spectrophotometry can give an approximate measure of bruise area and volume in peeled tubers, but is not as precise as image analysis techniques. Measurements of bruise area and volume in unpeeled tubers are not consistent.

- A new bruise index based on the percentage of tuber volume removed per peeler stroke can accommodate any size and shape of bruise, and results in an easily interpreted index.

Future developments from this work could involve the following investigations.

- Adapt spectrophotometric method to measure wavelengths from unpeeled tubers in the NIR with the integrating sphere.

- Develop spectrophotometric method as a non-contact method for detecting bruised tubers.

- The detection of dopachrome as a way of reducing the time for bruise detection needs to be evaluated in practice on samples whose bruise location is unknown.

- The compressed air tank method could be modified for practical use by making the tank small enough to hold just a small sample of tubers. In this way the cost of making the apparatus could be reduced and safety factors simplified. It could also make access to the pressure vessel easier.

- The percentage of tubers exhibiting bruising in a hotbox or compressed air tank may be an under or over estimate of the actual percentage of bruising in a sample kept in store or at ambient conditions. This needs further investigation.

- If the new bruise index is adopted by the potato industry the design of peeler and standards for acceptable percentage volume losses due to bruising would need to be agreed.

Appendix A

Comparison of the light transmission properties of different types of commonly used optical materials, 10 mm thick (after Melles Griot Inc. 1990)

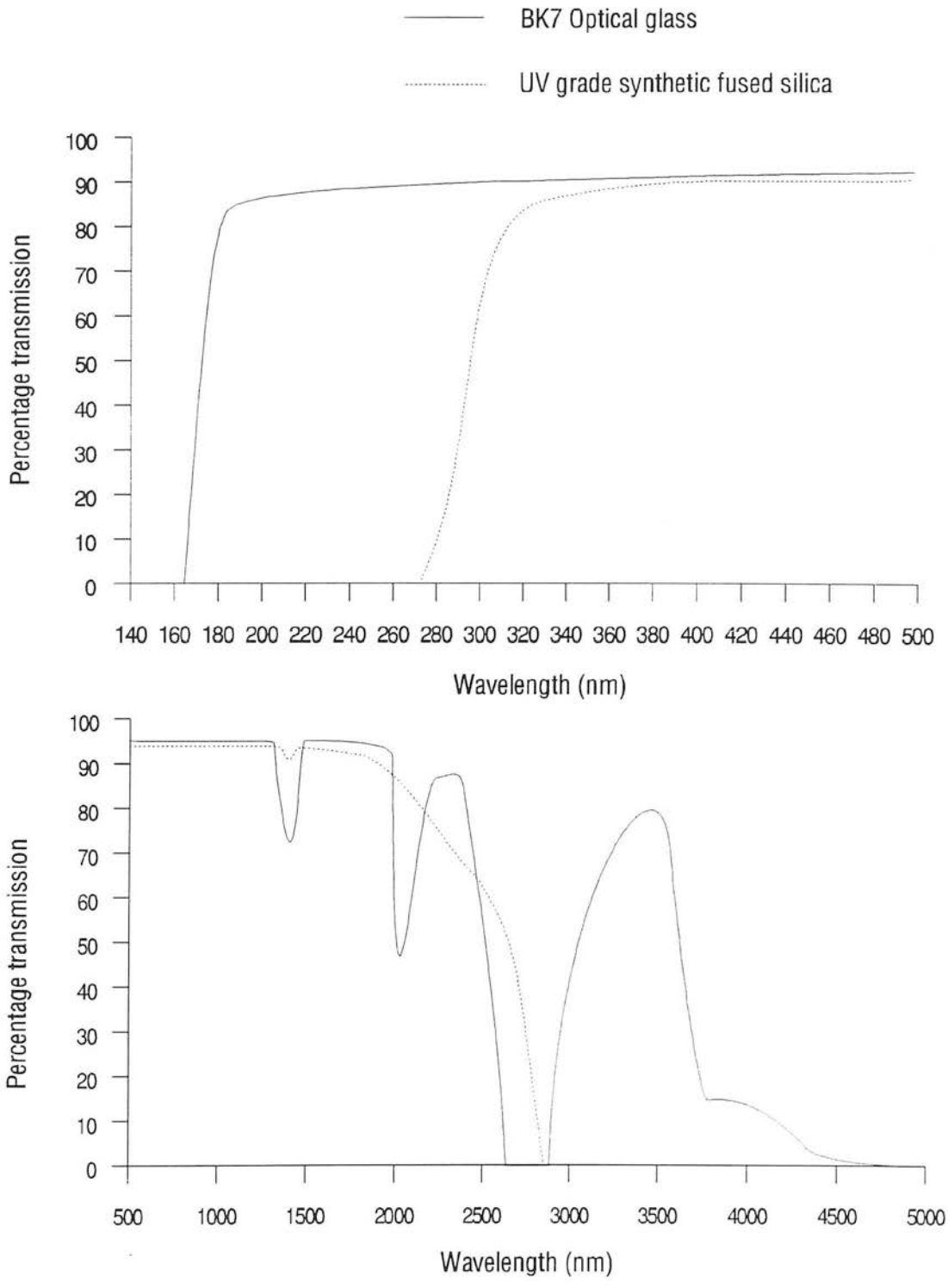

Appendix B

BASIC program for placing 20 text files into spreadsheet format and calculation of first derivative spectra in Chapters 7 and 8

```
restart: CLS
CLEAR
h$ = ".TXT"
root$ = "c:\"

'prompt for location of text files
count = 1
PRINT "Name of directory with text files, or q to quit";
INPUT source$
IF source$ = "q" OR source$ = "Q" THEN SYSTEM
source$ = root$ + source$
PRINT
PRINT "Do you want a list of text files every time the program runs, y or n";
reask: INPUT l$
IF l$ = "n" OR l$ = "N" THEN skip = 0
IF l$ = "y" OR l$ = "Y" THEN skip = 1
PRINT
PRINT "Is location of *.csv files to be the same as the *.txt files, y OR n";
ask: INPUT output$
IF output$ = "n" THEN GOTO question
IF output$ = "y" THEN output$ = source$
GOTO start
question:
PRINT
PRINT "Name of directory for output";
INPUT output$
output$ = root$ + output$

'prompt for text file sequence and start of main loop
start: CHDIR source$
CLS
IF skip = 0 THEN GOTO start2
FILES "*.txt"
start2: PRINT "Files to combine into spreadsheet format, or q to quit";
INPUT f$
IF f$ = "q" THEN SYSTEM
PRINT "Start of file sequence ";
INPUT s$
s = VAL(s$)
PRINT "End of file sequence ";
two: INPUT e
IF e < s THEN GOTO two
IF e > 100 THEN GOTO two
```

```
'look at first text file to determine spectral parameters
g$ = f$ + s$ + h$
OPEN "i", #1, g$
FOR g = 0 TO 9
INPUT #1, y(g)
NEXT g
CLOSE #1
'starting wavelength
sw = y(1)
'last wavelength
lw = y(2)
'wavelength increment
wi = y(4)
'number of data in file minus headings
d = ((lw - sw) / wi) + 9

' calculations to determine the number of output files
fill = ((e - s) + 1)
IF fill <= 20 THEN sp = 1
IF fill > 20 AND fill <= 40 THEN sp = 2
IF fill > 40 AND fill <= 60 THEN sp = 3
IF fill > 60 AND fill <= 80 THEN sp = 4
IF fill > 80 AND fill <= 100 THEN sp = 5

'Allocation of program memory
DIM a(((sp * 20) + e), d)
'number of files names is equal to last file number
DIM d$(e)
DIM a$(e)
CLS

'prompt for output file information
CHDIR output$
IF count = 1 THEN GOTO skip
FILES "*.csv"
skip: PRINT "Name of spreadsheet file ";
INPUT comb$
PRINT
PRINT "Do you want to covert data to 1st derivatives, y or n ";
INPUT der$
IF der$="n" then der=1
CHDIR source$

' text file names are stored into an array for later recall
FOR t = s TO e
IF t > 9 AND t < 20 THEN a$(t) = CHR$(49)
IF t > 19 AND t < 30 THEN a$(t) = CHR$(50)
IF t > 29 AND t < 40 THEN a$(t) = CHR$(51)
IF t > 39 AND t < 50 THEN a$(t) = CHR$(52)
```

```
IF t > 49 AND t < 60 THEN a$(t) = CHR$(53)
IF t > 59 AND t < 70 THEN a$(t) = CHR$(54)
IF t > 69 AND t < 80 THEN a$(t) = CHR$(55)
IF t > 79 AND t < 90 THEN a$(t) = CHR$(56)
IF t > 89 AND t < 100 THEN a$(t) = CHR$(57)
IF t <= 9 THEN b$ = CHR$(48 + t)
IF t > 9 AND t < 20 THEN b$ = CHR$(38 + t)
IF t > 19 AND t < 30 THEN b$ = CHR$(28 + t)
IF t > 29 AND t < 40 THEN b$ = CHR$(18 + t)
IF t > 39 AND t < 50 THEN b$ = CHR$(8 + t)
IF t > 49 AND t < 60 THEN b$ = CHR$(-2 + t)
IF t > 59 AND t < 70 THEN b$ = CHR$(-12 + t)
IF t > 69 AND t < 80 THEN b$ = CHR$(-22 + t)
IF t > 79 AND t < 90 THEN b$ = CHR$(-32 + t)
IF t > 89 AND t < 100 THEN b$ = CHR$(-42 + t)

'formation of input file names into an array for later recall
d$(t) = f$ + a$(t) + b$ + h$
NEXT t

'formation of output file names into an array for later recall
FOR l = 1 TO 5
sprd$(l) = comb$ + CHR$(48 + l) + ".csv"
NEXT l

'each file is opened and the spectral data is input into an array for later recall
FOR x = s TO e
OPEN "i", #1, d$(x)
LOCATE 12, 1
PRINT d$(x)
FOR y = 0 TO d
IF EOF(1) THEN GOTO six
INPUT #1, a(x, y)
a(x, 8) = x
NEXT y
six: CLOSE #1
NEXT x

'conversion of data into first derivatives
IF der=1 THEN GOTO savedata
FOR x=s TO e
FOR y=8 To d
a(x,y)=(a(x,y+1)-a(x,y))/wi
a(x,8)=x
a(x,9)=0
NEXT x
NEXT y
```

```
' output of spectral data into spreadsheet format
savedata:FOR l = 1 TO sp
x = (((20 * l) - 19) + s) - 1
LOCATE 13, 1
CHDIR output$
PRINT sprd$(l)
OPEN sprd$(l) FOR OUTPUT AS #2
FOR y = 8 TO d
wa = sw + ((y - 9) * wi)
IF y = 8 THEN wa = 0
IF l >= 2 THEN GOTO jumpy
PRINT #2, USING "####.###,  "; wa; a(x, y); a(x + 1, y); a(x + 2, y); a(x + 3, y); a(x
+ 4, y); a(x + 5, y); a(x + 6, y); a(x + 7, y); a(x + 8, y); a(x + 9, y); a(x + 10, y); a(x +
11, y); a(x + 12, y); a(x + 13, y); a(x + 14, y); a(x + 15, y); a(x + 16, y); a(x + 17, y);
a(x + 18, y); a(x + 19, y)
GOTO looopy
jumpy: PRINT #2, USING "####.###,  "; a(x, y); a(x + 1, y); a(x + 2, y); a(x + 3, y);
a(x + 4, y); a(x + 5, y); a(x + 6, y); a(x + 7, y); a(x + 8, y); a(x + 9, y); a(x + 10, y);
a(x + 11, y); a(x + 12, y); a(x + 13, y); a(x + 14, y); a(x + 15, y); a(x + 16, y); a(x +
17, y); a(x + 18, y); a(x + 19, y)
looopy: NEXT y
BEEP
CLOSE #2
NEXT l
CHDIR source$

'reset dimensioned arrays and goto start of main loop
ERASE a
ERASE d$
ERASE a$
count = count + 1
GOTO start
```

Appendix C

Program instructions for BMDP Program 7M, Stepwise Discriminant Analysis in Chapters 7 and 8

```
/input file is 'c:\athesis\chapter2\visible\dynamic\dellup.dat'.
variables=63.
cases=100.
reclen=502.
format = free.
/variable names = trialb,allbrus,'400','405','410','415','420','425','430','
435','440','445','450','455','460','465','470','475','480','485','490','
495','500','505','510','515','520','525','530','535','540','545','550','
555','560','565','570','575','580','585','590','595','600','605','610','
615','620','625','630','635','640','645','650','655','660','665','670','
675','680','685','690','695','700'.
use=1, 3 to 63.
/group variable=trialb.
codes(trialb)=0,1,3,4.
names(trialb)=unbruised,bruised,trialbruised,trialunbrus.
use=unbruised,bruised.
/disc jack.
tol=0.01.
no step.
/print no step.
no point.
/plot.
no canon.
/end.
```

Appendix D

BASIC program for comparing output of neural nets with expected results in Chapter 9

```
start: CLS
DIM a(350)
DIM b(350)
FILES "*.txt"

'prompts for user information
PRINT "Enter file name with correct results, or q to quit ";
WHILE INKEY$ <> "":WEND
INPUT corr$
IF corr$ = "q" THEN END
corr$ = corr$ + ".txt"
PRINT "Enter neural desk output file ";
WHILE INKEY$ <> ""
WEND
INPUT pred$
pred$ = pred$ + ".txt"
PRINT "Number of spectra ";
WHILE INKEY$ <> ""
WEND
INPUT l
l = l - 1

'input correct data from text file into an array
OPEN "I", #1, corr$
FOR s = 0 TO l
IF EOF(1) THEN GOTO one
INPUT #1, a(s)
NEXT s
one: CLOSE #1

'input data from neural network into an array
OPEN "i", #2, pred$
FOR s = 0 TO l
IF EOF(2) THEN GOTO two
INPUT #2, b(s)
NEXT s
two: CLOSE #2

'scale neural network data as 0 or 1
FOR s = 0 TO l
IF b(s) > .5 THEN b(s) = 1
IF b(s) <= .5 THEN b(s) = 0
NEXT s
corrb = 0
```

```
wrongb = 0
corrub = 0
wrongub = 0
brus = 0
unbrus = 0

'calculation of classification matrix
FOR s = 0 TO l
IF b(s) = 1 AND a(s) = 1 THEN corrb = corrb + 1
IF a(s) = 1 THEN brus = brus + 1
IF b(s) = 0 AND a(s) = 1 THEN wrongb = wrongb + 1
IF b(s) = 0 AND a(s) = 0 THEN corrub = corrub + 1
IF a(s) = 0 THEN unbrus = unbrus + 1
IF b(s) = 1 AND a(s) = 0 THEN wrongub = wrongub + 1
NEXT s
per = ((corrb + corrub) / (brus + unbrus)) * 100
CLS

'print result of analysis
PRINT "File is "; corr$; "  Number of spectra "; l + 1
PRINT
PRINT "Classification Matrix "
PRINT
PRINT "Total No. UB "; unbrus; " Total No. B "; brus
PRINT ""
PRINT "Unbruised "; corrub; ; wrongub
PRINT ""
PRINT "Bruised "; wrongb; ; corrb
PRINT
PRINT "% Correctly Classified "; per
PRINT
PRINT "Press any key to continue ";
INPUT k
CLS
GOTO start
```

Appendix E

Results for Chapter 14; effect of air pressure and temperature on bruise development measured with reflectance spectrophotometry and a visual rating

Note: for visual ratings the higher the value the darker the bruise. For reflectance measurements, the lower the reflectance value the darker the bruise.

Effect of air pressure on visual ratings ± 2SD from peeled Desiree tubers at 40°C.

	10 bar	7 bar	3 bar	1 bar
1 hour				
all bruises	4.07 ± 1.99	3.45 ± 1.37	2.50 ± 1.85	2.95 ± 0.45
blackspot	4	none	none	none
2 hours				
all bruises	4.55 ± 2.67	4.55 ± 2.67	3.76 ± 3.71	4.90 ± 0.63
blackspot	none	3.00 ± 5.66	1.60 ± 2.68	none
3 hours				
all bruises	5 ± 0	4.80 ± 1.79	5 ± 0	4.60 ± 1
blackspot	5 ± 0	3.00 ± 5.65	5	none
4 hours				
all bruises	5 ± 0	5 ± 0	4.95 ± 0.43	5 ± 0
blackspot	5 ± 0	5 ± 0	4.80 ± 0.89	none

Effect of air pressure on first derivative ± 2SD from peeled Desiree tubers at 40°C.

	10 bar	7 bar	3 bar	1 bar
1 hour				
all bruises	0.47 ± 0.3	0.39 ± 0.15	0.46 ± 0.17	0.57 ± 0.18
blackspot	0.65	none	none	none
2 hours				
all bruises	0.56 ± 0.16	0.50± 0.22	0.51 ± 0.21	0.52 ± 0.18
blackspot	none	0.44 ± 0.49	0.54 ± 0.11	none
3 hours				
all bruises	0.50 ± 0.16	0.65 ± 0.23	0.46 ± 0.26	0.44 ± 0.18
blackspot	0.56 ± 0.08	0.62 ± 0.04	0.44	none
4 hours				
all bruises	0.43 ± 0.19	0.56 ± 0.22	0.47 ± 0.21	0.54
blackspot	0.59 ± 0.13	0.62 ± 0.14	0.53 ± 0.14	0.26

Percentage of Desiree tubers unbruised, shatter bruise and blackspot.

	10 bar	7 bar	3 bar	1 bar
1 hour				
% unbruised	53.4	33.3	73.3	33.3
% shatter	43.3	66.7	26.7	66.7
% blackspot	3.3	0	0	0
2 hours				
% unbruised	68.9	70.0	73.3	66.7
% shatter	31.1	23.3	40.0	33.3
% blackspot	0	6.7	16.7	0
3 hours				
% unbruised	43.3	33.3	46.7	33.3
% shatter	50.0	60.0	50.0	66.7
% blackspot	6.7	6.7	3.3	0
4 hours				
% unbruised	13.3	40.0	30.0	36.7
% shatter	80.0	43.3	53.3	63.3
% blackspot	6.7	16.7	16.7	0

Effect of air pressure on mean visual ratings ± 2SD from peeled Pentland Dell tubers at 40°C.

	10 bar	7 bar	3 bar	1 bar
1 hour				
all bruises	3.33 ± 2.31	3.17 ± 3.30	3.28 ± 2.51	2.89 ± 2.48
blackspot only	3.0 ± 2.62	2.80 ± 3.28	3.20 ± 2.97	2.64 ± 2.55
2 hours				
all bruises	4.33 ± 3.11	4.00 ± 2.80	3.73 ± 2.84	3.00 ± 2.95
blackspot only	4.00 ± 3.70	3.50 ± 3.46	3.33 ± 3.72	2.20 ± 3.28
3 hours				
all bruises	4.35 ± 2.70	4.61 ± 1.96	4.76 ± 1.78	3.07 ± 2.90
blackspot only	4.00 ± 3.46	4.50 ± 2.33	4.70 ± 2.21	3.57 ± 2.27
4 hours				
all bruises	4.41 ± 2.65	4.70 ± 1.97	4.64 ± 2.41	4.90 ± 0.70
blackspot only	4.11 ± 3.53	4.43 ± 3.02	4.43 ± 3.02	5.00 ± 0

Effect of air pressure on mean first derivative spectra at 500 nm ± 2SD from peeled Desiree tubers at 40°C.

	10 bar	7 bar	3 bar	1 bar
1 hour				
all bruises	0.43 ± 0.08	0.41 ± 0.13	0.38 ± 0.20	0.24 ± 0.11
blackspot only	0.42 ± 0.09	0.37 ± 0.06	0.39 ± 0.22	0.24 ± 0.12
2 hours				
all bruises	0.39 ± 0.17	0.44 ± 0.16	0.41 ± 0.12	0.38 ± 0.13
blackspot only	0.42 ± 0.16	0.47 ± 0.18	0.40 ± 0.17	0.35 ± 0.08
3 hours				
all bruises	0.42 ± 0.14	0.34 ± 0.17	0.35 ± 0.12	0.34 ± 0.13
blackspot only	0.44 ± 0.14	0.35 ± 0.18	0.35 ± 0.14	0.31 ± 0.11
4 hours				
all bruises	0.36 ± 0.17	0.42 ± 0.24	0.41 ± 0.12	0.35 ± 0.14
blackspot only	0.36 ± 0.18	0.47 ± 0.15	0.40 ± 0.13	0.38 ± 0.15

Percentage of Pentland tubers showing no discolouration (unbruised) shatter bruising and blackspot bruising.

	10 bar	7 bar	3 bar	1 bar
1 hour				
% unbruised	60.0	60.0	76.7	36.7
% shatter	13.3	23.3	6.7	16.7
% blackspot	26.7	16.7	16.6	46.6
2 hours				
% unbruised	60.0	76.7	63.3	56.7
% shatter	13.3	10.0	20.0	26.7
% blackspot	26.7	13.3	16.7	16.6
3 hours				
% unbruised	34.5	40.0	30.0	56.7
% shatter	34.5	20.0	26.7	20.0
% blackspot	31.0	40.0	43.3	23.3
4 hours				
% unbruised	43.3	43.4	63.3	70.0
% shatter	26.7	33.3	13.3	13.3
% blackspot	30.0	23.3	23.4	16.7

Effect of air pressure on mean visual ratings ± 2SD from peeled Record tubers at 40°C.

	10 bar	7bar	3 bar	1 bar
1 hour				
all bruises	1.86 ± 2.49	1.62 ± 2.05	2.75 ± 3.0	2.12 ± 3.1
blackspot only	1.59 ± 2.01	1.28 ± 0.94	1.0	1 ± 0
2 hours				
all bruises	2.46 ± 2.50	2.33 ± 2.63	2.74 ± 2.50	3.20 ± 2.77
blackspot only	2.14 ± 1.97	2.06 ± 2.18	2.91 ± 2.30	2.50 ± 3.28
3 hours				
all bruises	3.68 ± 2.34	3.92 ± 2.33	3.88 ± 2.63	3.14 ± 2.64
blackspot only	3.44 ± 2.29	3.83 ± 2.33	3.54 ± 2.70	3.05 ± 2.71
4hours				
all bruises	4.91 ± 0.57	4.40 ± 2.46	4.32 ± 2.43	4.71 ± 0.92
blackspot only	4.75 ± 0.92	4.14 ± 2.81	3.75 ± 2.97	4.25 ± 1.0

Effect of air pressure on mean first derivative spectra at 500 nm ± 2SD from peeled Record tubers at 40°C.

	10 bar	7bar	3 bar	1 bar
1 hour				
all bruises	0.59 ± 0.15	0.54 ± 0.3	0.58 ± 0.12	0.52 ± 0.09
blackspot only	0.59 ± 0.17	0.58 ± 0.3	0.64	0.56 ± 0.04
2 hours				
all bruises	0.58 ± 0.20	0.59 ± 0.16	0.58 ± 0.11	0.52 ± 0.14
blackspot only	0.59 ± 0.18	0.58 ± 0.14	0.59 ± 0.10	0.52 ± 0.13
3 hours				
all bruises	0.59 ± 0.17	0.44 ± 0.18	0.55 ± 0.20	0.53 ± 0.16
blackspot only	0.59 ± 0.18	0.44 ± 0.18	0.59 ± 0.15	0.53 ± 0.17
4hours				
all bruises	0.33 ± 0.22	0.42 ± 0.17	0.44 ± 0.21	0.55 ± 0.17
blackspot only	0.36 ± 0.23	0.41 ± 0.16	0.45 ± 0.23	0.62 ± 0.16

Percentage of Record tubers showing no discolouration (unbruised) shatter bruising and blackspot bruising at 40°C.

	10 bar	7 bar	3 bar	1 bar
1 hour				
% unbruised	26.7	50.0	86.7	73.3
% shatter	13.3	23.3	10.0	13.3
% blackspot	60.0	26.7	3.3	13.4
2 hours				
% unbruised	16.7	24.1	36.7	46.7
% shatter	10.0	13.8	23.3	33.3
% blackspot	73.3	62.1	40.0	20.0
3 hours				
% unbruised	20.7	6.9	40.0	23.3
% shatter	17.2	6.9	13.3	10.0
% blackspot	62.1	86.2	46.7	66.7
4 hours				
% unbruised	20.0	30.0	13.3	30.0
% shatter	50.0	20.0	40.0	56.7
% blackspot	30.0	50.0	46.7	13.3

Effect of air pressure on mean visual ratings ± 2SD from peeled Record tubers at 60°C.

	10 bar	7bar	3 bar	1 bar
1 hour				
all bruises	2.50 ± 3.2	2.74 ± 3.5	2.92 ± 3.6	1.2 ± 0.89
blackspot only	1.77 ± 2.5	1.92 ± 2.7	1.50 ± 2.4	1 ± 0
2 hours				
all bruises	4.44 ± 2.6	5 ± 0	2.5 ± 3.6	3.61 ± 2.9
blackspot only	3.57 ± 3.6	none	1.33 ± 2.0	3.10 ± 3.3

Effect of air pressure on mean first derivative spectra at 500 nm ± 2SD from peeled Record tubers at 60°C.

	10 bar	7bar	3 bar	1 bar
1 hour				
all bruises	0.62 ± 0.09	0.61 ± 0.12	0.62 ± 0.66	0.60 ± 0.31
blackspot only	0.62 ± 0.07	0.63 ± 0.12	0.66 ± 0.05	0.67 ± 0.05
2 hours				
all bruises	0.55 ± 0.17	0.53 ± 0.23	0.60 ± 0.09	0.38 ± 0.11
blackspot only	0.59 ± 0.17	none	0.59 ± 0.10	0.40 ± 0.12

Effect of air pressure on mean visual ratings ± 2SD from peeled Record tubers at 20°C.

	10 bar	7bar	3 bar	1 bar
2 hour				
all bruises	1.30 ± 1.9	2.64 ± 2.78	2.59 ± 3.1	2.0 ± 3.1
blackspot only	1.37 ± 2.1	2.64 ± 2.78	1.33 ± 2.0	1.6 ± 2.7
4 hours				
all bruises	2.71 ± 2.1	2.80 ± 2.67	4.04 ± 1.57	3.17 ± 2.87
blackspot only	2.73 ± 2.4	3.63 ± 3.34	3.94 ± 1.60	2.80 ± 3.0
6 hours				
all bruises	4.19 ± 3.2	3.63 ± 3.34	3.05 ± 3.50	3.43 ± 2.06
blackspot only	3.78 ± 3.7	3.67 ± 3.43	2.83 ± 3.65	3.10 ± 2.40

Effect of air pressure on mean first derivative spectra at 500 nm ± 2SD from peeled Record tubers at 20°C.

	10 bar	7bar	3 bar	1 bar
2 hour				
all bruises	0.51 ± 0.13	0.44 ± 0.12	0.56 ± 0.16	0.31 ± 0.12
blackspot only	0.52 ± 0.14	0.44 ± 0.12	0.57 ± 0.16	0.31 ± 0.13
4 hours				
all bruises	0.55 ± 0.17	0.73 ± 0.11	0.31 ± 0.11	0.38 ± 0.11
blackspot only	0.54 ± 0.19	0.73 ± 0.11	0.31 ± 0.10	0.38 ± 0.10
6 hours				
all bruises	0.52 ± 0.17	0.47 ± 0.15	0.60 ± 0.15	0.73 ± 0.74
blackspot only	0.55 ± 0.16	0.47 ± 0.15	0.59 ± 0.15	0.14 ± 0.10

Effect of hotbox on mean visual and reflectance values ± 2SD from peeled Record tubers.

	Visual rating	Reflectance reading
1 hour		
all bruises	1.22 ± 3.22	0.62 ± 0.11
blackspot only	1 ± 0	0.65 ± 0.09
2 hours		
all bruises	2.54 ± 3.55	0.61 ± 0.13
blackspot only	1.37 ± 2.12	0.64 ± 0.08
3 hours		
all bruises	2.42 ± 2.56	0.57 ± 0.22
blackspot only	2.10 ± 2.33	0.63 ± 0.11
4 hours		
all bruises	3.57 ± 3.07	0.48 ± 0.23
blackspot only	3.29 ± 3.14	0.53 ± 0.16
5 hours		
all bruises	4.71 ± 1.71	0.52 ± 0.18
blackspot only	4.0 ± 3.10	0.60 ± 0.16
6 hours		
all bruises	4.05 ± 2.79	0.66 ± 0.27
blackspot only	3.87 ± 3.10	0.70 ± 0.15
7 hours		
all bruises	4.27 ± 3.16	0.50 ± 0.16
blackspot only	3.54 ± 4.04	0.55 ± 0.13

Appendix F

Depth, length,width and weight of tubers from 10 potato varieties (Glaseby and McRae 1991) and peel depth, length, width and weight removed per peeler stroke for the variety Record

Mean weight, length, breadth and depth of tubers from 10 potato varieties.

Variety	Mean weight (g)	Mean length (mm)	Mean breadth (mm)	Mean depth (mm)
Record ± 2SD	148.7±128.8	78.6 ±31.6	48.1 ± 16.6	62.5 ± 8.3
[1]King Edward	130.7	77.2	47.3	59.8
[1]Pentland Ivory	143.9	78.6	52.0	62.5
[1]Pentland Hawk	147.9	82.0	49.8	60.6
[1]Maris Piper	131.8	75.8	47.7	60.3
[1]Pentland Dell	139.9	86.1	46.3	56.1
[1]Pentland Squire	140.6	76.2	50.4	60.7
[1]Pentland Crown	147.4	78.8	48.2	61.5
[1]Cara	149.5	79.8	50.6	62.6
[1]Desiree	132.0	80.5	47.3	59.2
[1]All Varieties	141.5	79.0	48.7	60.5

[1]95% confidence limits not available.

Average depth of peel (mm) ± 2 SD measured per peeler stroke from each zone.

Peeler stroke	Max. radius mean ± 2SD	Min. radius mean ± 2SD	Bud end mean ± 2SD	Stem end mean ± 2SD
1	1.46 ± 0.45	1.43 ± 0.33	1.54 ± 0.49	1.56 ± 0.41
2	1.23 ± 0.36	1.26 ± 0.36	1.29 ± 0.45	1.33 ± 0.36
3	1.18 ± 0.38	1.21 ± 0.36	1.26 ± 0.40	1.29 ± 0.36
4	1.18 ± 0.43	1.22 ± 0.34	1.23 ± 0.34	1.24 ± 0.31
5	1.23 ± 0.41	1.18 ± 0.34	1.19 ± 0.30	1.23 ± 0.31
6	1.19 ± 0.44	1.17 ± 0.34	1.22 ± 0.31	1.21 ± 0.31
7	1.21 ± 0.40	1.14 ± 0.36	1.21 ± 0.33	1.21 ± 0.29
8	1.24 ± 0.43	1.16 ± 0.32	1.20 ± 0.32	1.18 ± 0.29
9	1.19 ± 0.34	1.11 ± 0.36	1.20 ± 0.30	1.17 ± 0.29
10	1.17 ± 0.37	1.12 ± 0.34	1.17 ± 0.34	1.16 ± 0.29

Average length of peel (mm) ± 2 SD measured per peeler stroke from each zone.

Peeler stroke	Max. radius mean ± 2SD	Min. radius mean ± 2SD	Bud end mean ± 2SD	Stem end mean ± 2SD
1	68.3 ± 31.2	70.6 ± 29.3	44.1 ± 16.4	38.5 ± 17.4
2	72.6 ± 30.2	72.9 ± 30.4	47.1 ± 15.6	42.1 ± 17.2
3	73.7 ± 30.6	74.1 ± 32.8	50.1 ± 17.4	45.4 ± 19.2
4	74.6 ± 35.6	75.6 ± 33.6	51.7 ± 17.6	46.9 ± 16.0
5	76.2 ± 33.8	76.1 ± 32.0	53.9 ± 16.4	48.9 ± 16.4
6	76.3 ± 33.0	75.9 ± 33.4	55.1 ± 15.4	49.1 ± 16.2
7	77.4 ± 35.0	75.6 ± 31.4	55.7 ± 16.8	50.1 ± 17.0
8	76.4 ± 31.4	77.2 ± 33.8	56.8 ± 18.2	51.7 ± 16.8
9	77.2 ± 32.0	77.2 ± 33.8	57.6 ± 16.2	52.4 ± 17.2
10	76.0 ± 32.2	77.2 ± 35.6	58.2 ± 18.6	53.3 ± 15.8

Average width of peel (mm) ± 2 SD measured per peeler stroke from each zone.

Peeler stroke	Max. radius mean ± 2SD	Min. radius mean ± 2SD	Bud end mean ± 2SD	Stem end mean ± 2SD
1	22.9 ± 6.7	15.7 ± 5.1	17.1 ± 8.5	15.8 ± 7.0
2	30.8 ± 7.1	21.0 ± 5.6	22.0 ± 8.8	20.6 ± 7.7
3	35.5 ±6.3	25.0 ± 7.5	25.7 ± 8.9	23.9 ± 7.4
4	37.2 ± 10.3	28.3 ± 6.8	28.7 ± 8.3	26.8 ± 7.5
5	32.5 ± 16.9	30.8 ± 7.7	31.3 ± 8.2	29.3 ± 7.5
6	29.4 ± 15.3	32.7 ± 9.8	33.4 ± 7.8	30.9 ± 7.3
7	28.5 ± 12.0	34.4 ± 9.4	35.1 ± 7.9	32.9 ± 7.6
8	28.1 ± 10.6	35.0 ± 9.9	36.3 ± 7.8	34.0 ± 7.0
9	30.1 ± 10.6	35.0 ± 11.2	37.5 ± 6.4	35.4 ± 7.2
10	31.0 ± 9.8	35.3 ± 10.9	37.9 ± 8.2	36.2 ± 7.2

Average percentage weight removed ± 2SD per peeler stroke from each zone.

Peeler stroke	Max. radius mean ± 2SD	Min. radius mean ± 2SD	Bud end mean ± 2SD	Stem end mean ± 2SD	All zones mean ± 2SD
1	0.8 ± 0.4	0.5 ± 0.6	0.5 ± 0.4	0.4 ± 0.4	0.6 ± 0.4
2	1.3 ± 0.6	0.9 ± 0.8	0.8 ± 0.6	0.7 ± 0.6	0.9 ± 0.8
3	1.5 ± 0.8	1.1 ± 1.2	1.0 ± 0.8	0.9 ± 0.8	1.1 ± 1.0
4	1.5 ± 0.8	1.3 ± 1.6	1.2 ± 1.0	1.0 ± 1.0	1.3 ± 1.2
5	1.3 ± 1.0	1.4 ± 1.8	1.3 ± 1.0	1.2 ± 1.0	1.3 ± 1.2
6	1.1 ± 1.0	1.4 ± 1.4	1.5 ± 1.0	1.2 ± 1.0	1.3 ± 1.2
7	1.1 ± 1.2	1.5 ± 0.8	1.6 ± 1.2	1.4 ± 1.2	1.4 ± 1.2
8	1.1 ± 1.2	1.5 ± 1.2	1.6 ± 1.4	1.4 ± 1.2	1.4 ± 1.2
9	1.1 ± 1.4	1.4 ± 1.0	1.7 ± 1.4	1.5 ± 1.2	1.4 ± 1.2
10	1.2 ± 1.4	1.4 ± 1.0	1.7 ± 1.4	1.5 ± 1.4	1.4 ± 1.4

Average accumulative percentage weight ± 2SD removed for all zones.

Peeler stroke	Max. radius mean ± 2SD	Min. radius mean ± 2SD	Bud end mean ± 2SD	Stem end mean ± 2SD	All zones mean ± 2SD
1	0.8 ± 0.4	0.5 ± 0.6	0.5 ± 0.4	0.4 ± 0.4	0.6 ± 0.6
2	2.1 ± 0.6	1.4 ± 0.8	1.2 ± 0.6	1.1 ± 0.6	1.5 ± 0.8
3	3.6 ± 0.8	2.5 ± 1.2	2.3 ± 0.8	2.0 ± 0.8	2.6 ± 1.0
4	5.1 ± 0.8	3.8 ± 1.6	3.5 ± 1.0	3.0 ± 1.0	3.9 ± 1.2
5	6.5 ± 1.0	5.2 ± 1.8	4.8 ± 1.0	4.2 ± 1.0	5.2 ± 1.2
6	7.6 ± 1.0	6.7 ± 1.4	6.3 ± 1.0	5.5 ± 1.0	6.5 ± 1.2
7	8.6 ± 1.2	8.2 ± 0.8	7.9 ± 1.2	6.8 ± 1.2	7.9 ± 1.2
8	9.8 ± 1.2	9.7 ± 1.2	9.5 ± 1.4	8.3 ± 1.2	9.3 ± 1.2
9	10.9 ± 1.4	11.1 ± 1.0	11.2 ± 1.4	9.7 ± 1.2	10.7 ± 1.2
10	12.1 ± 1.4	12.5 ± 1.0	12.9 ± 1.4	11.2 ± 1.4	12.2 ± 1.4

Appendix G

Derivation of formula to calculate chord length across an ellipse for use in Chapter 15 towards the determination of peel width per peeler stroke

The standard equation of an ellipse is:

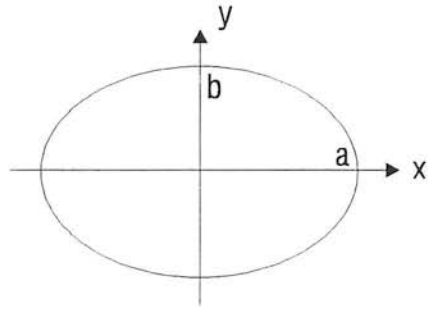

$$\frac{y^2}{b^2}+\frac{x^2}{a^2}=1$$

where the x-axis is the major axis, a the major semiaxis, b the minor semiaxis, center in the origin.

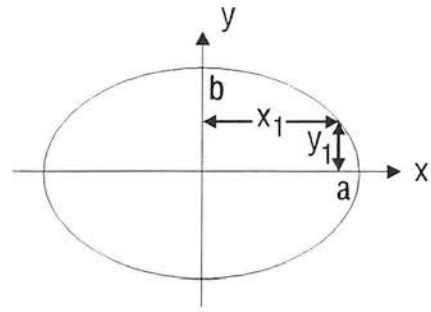

Length of line x_1 at height y_1 can be calculated by first rearranging the standard equation of an ellipse:

$$\frac{x_1^2}{a^2}=1-\frac{y_1^2}{b^2}$$

$\frac{b^2}{b^2}$ is used to substitute 1 in the above equation to give a common denominator:

$$\frac{x_1^2}{a^2}=\frac{b^2-y_1^2}{b^2}$$

Therefore:

$$x_1^2=\frac{a^2}{b^2}\cdot\left(b^2-y_1^2\right)$$

and from this:

$$x_1=\frac{a}{b}\cdot\sqrt{\left(b^2-y_1^2\right)}$$

However, chord length is twice the length of x_1 so:

$$2 \cdot x_1 = 2 \cdot \left[\frac{a}{b} \cdot \sqrt{\left(b^2 - y_1^2 \right)} \right]$$

Therefore the length of chord at any given peel depth is:

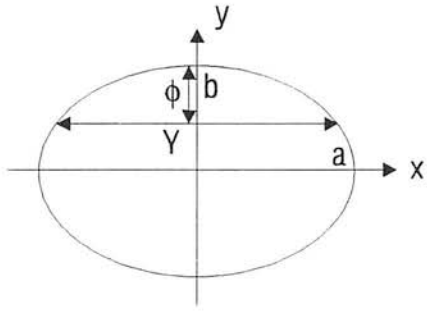

$$Y = 2 \cdot \left[\frac{a}{b} \cdot \sqrt{b^2 - (b - \phi)^2} \right]$$

Where Y = length of chord, a = half major axis, b = half minor axis, ϕ = total depth of slice (a depth of 1.2 mm per peeler stroke was used to calculate chord length for all zones).

Appendix H

Derivation of formula to calculate the length of arc on an ellipse for use in Chapter 15 towards the determination of percentage volume removed per peeler stroke

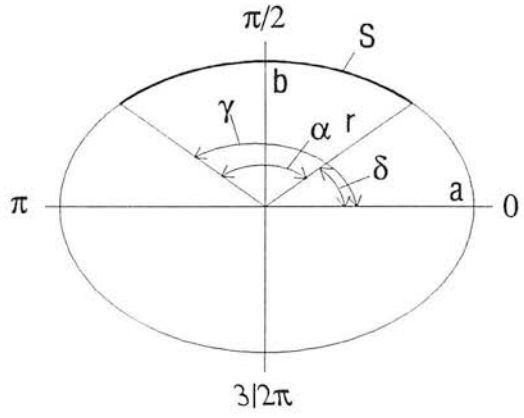

The starting angle of arc S is δ, the ending angle is γ. The angle of arc is given as α, which is γ minus δ.

$$\text{length of arc} = \int_{\delta}^{\gamma} \left(r^2 + \frac{dr}{d\alpha} \right) d\alpha$$

The equation of an ellipse with major axis 2a and minor axis 2b is:

$$\frac{x^2}{a^2} + \frac{y^2}{b^2} = 1$$

This equation can be expressed in terms of polar co-ordinates:

$$\frac{\cos^2 \alpha}{a^2} + \frac{\sin^2}{b^2} = \frac{1}{r^2}$$

from this:

$$r = \sqrt{a^2 \cdot \frac{b^2}{\left(b^2 \cdot (\cos\alpha)^2 + a^2 \cdot (\sin\alpha)^2 \right)}}$$

the differential of the radius with respect to the angle is:

$$\frac{dr}{d\alpha} = -a \cdot b \cdot \cos\alpha \cdot \sin\alpha \cdot \left(-b^2 + a^2\right) \cdot \frac{1}{\left(b^2 \cdot 2 \cdot \cos(\alpha)^2 - a^2 + a^2 \cdot \cos(\alpha)^2\right)^{\frac{3}{2}}}$$

therefore length of arc given by:

$$\int_{\delta}^{\gamma} \left(r^2 + \frac{dr}{d\alpha}\right) d\alpha$$

is given by:

$$S = \int_{\delta}^{\gamma} \sqrt{\left(a^2 \cdot \frac{b^2}{b^2 \cdot \cos(\alpha)^2 + a^2 \cdot \sin(\alpha)^2}\right) + \left(-a \cdot b \cdot \cos(\alpha) \cdot \sin(\alpha) \cdot \frac{-b^2 + a^2}{\left(b^2 \cdot \cos(\alpha)^2 + a^2 \cdot \sin(\alpha)^2\right)^{\frac{3}{2}}}\right)^2} \, d\alpha$$

I would like to thank Mr. Bill Lamond for his help in deriving this formula using Mathcad 5.0 (Microsoft Corporation).

References

Abbot, N.C. and Swanson Beck, J. (1993). Biological zero in laser Doppler measurements in normal ischaemic and inflamed skin. Int J Microcirc Clin Exp 12:89-98.

Allen, H.A. and Fieldmesser, J. (1971). Nematicidal activity of α-chaconine as fungitoxic compounds in extracts of Irish potato tubers. Phytopathology 58:776-81.

Andrews, D.L., Beames, B., Semmers, M.D. and Park, W.D. (1988). Characterisation of the lipid acyl hydrolase activity of the major potato (*Solanum tuberosum*) tuber protein, patatin, by cloning and abundant expression in a baculovirus vector. Biochem J 252:199-206.

Anon. (1977). Fertiliser in relation to quality and damage susceptibility. Annual Report for 1976/1977. Norfolk Agricultural Station 69:14-16.

Anon. (1982). The national potato awareness campaign. A joint project by the Potato Marketing Board and the Agricultural Development and Advisory Service, Oxford.

Artschwager, E. (1924). Studies on the potato tuber. J Agric Res 27:809-835.

Baumgartner, M., Keller, E.R. and Schwendimann, F. (1983). An investgation into the stability and instability of the 'blue reaction' in potato by an examination of tuber characteristics. Potato Res 26(1):17-30.

Beaver, G. and DeVoy, M. (1985). A rapid test for identifying blackspot bruising of potatoes. Paper No. 85-6015 .

Belknap, W.R. and Rickey, T.M. (1990). Physiological and stress- induced chanfer in potato tuber gene expression. In: The Molecular and Cellular Biology of the Potato (Vayda, M.E. and Park, W.D.J. eds.). Biotechnology in Agriculture No. 3. Wallingford, UK; C.A.B. International.

Belknap, W.R., Rickey, T.M. and Rockhold, D.R. (1990). Blackspot bruise dependent changes in enzyme activity and gene expression in Lemhi russet potato. Am Potato J 67(5):253-266.

Bellamy, L.J. (1962). The infrared spectra of complex molecules. 2nd Edn., Methuen, London.

Birth, G.S. (1960). A nondestructive technique for detecting internal discolouration in potatoes. Am Potato J 37(2):53-60.

Birth, G.S. (1976). How light interacts with foods. In Quality Detection in Foods J.J. Gaffney (ed.). Am Soc Agric Eng, St. Joseph, Mich.

Birth, G.S. and Law, S.E. (1977). Interaction between light and natural materials: laboratory demonstrations. Russell Agricultural Research Centre, Athens, Ga.

Blahovec, J., Patocka, K., Celba, J. and Mica, B. (1983) simple testing of the mechanical properties of potato tubers. Zemedelska Technika 29(2):81-96.

Bland, W.L., Tanner, C.B. and Maher, E.A. (1987). Vapour conductance of wounded potato tuber tissue. Am. Potato J 64(4):197-204.

Blight, D.P., Hamilton, A.J. (1974). Varietal susceptibility to damage in potatoes. Potato Res 17: 261-270.

Bostock, R.M., Kluc, J.A. and Laine, R.A. (1981). Eicospentaenic acid and arachiodonic acids from *Phytophthora infestans* elicit fungitoxic sesquiteropenes in the potato. Science 212:67-69.

Boyd, A.E.W. (1951). The internal blackening of potatoes caused by bruising. J Hort Sci 26:148-156.

Brown, G.K., Segerlind, L.J. and Summitt, R. (1974). Near-infrared reflectance of bruised apples. Trans Am Soc Agric Engrs 17(1):17-19.

Bu'Lock, J.D. and Harley-Mason, J. (1951). Melanin and its precursors. Part III. New syntheses of 5,6 dihydroxyindole and its derivatives. J Chem Soc 2248-2252.

Burton, C.L. and Schlute-Pason, N.L. (1987). Carbon dioxide as an indicator of fruit impact damage. Hortsci 22(2):281-282.

Burton, W.G. (1989). The potato. Third Edition. Longman Scientific and Technical.

Bushway, R. and Ponnampalam, R. (1981). α Chaconine and α solanine content of potato products and their stability during several modes of cooking. J Agric Food Chem 29:814-817.

Chen, P., McCarthy, M.J. and Kauten, R. (1989). NMR for internal quality evaluation of fruits and vegetables. Trans Am Soc Agric Eng 32(5):1737-1753.

Cheng, Y. and Haugh, C.G. (1994). Detecting hollow heart in potatoes using ultrasound. Trans Am Soc Agric Engng 37(1): 217-222.

Cole, C.S. (1975). Variation in dry matter between and within potato tubers. Potato Res 18:28-37.

Collin, G.H. (1961). The effect of mineral nutrition and varietal characteristics on blackspot. PhD thesis, Cornell Univ. 255pp.

Combrink, N.J.J. and Prinsloo, K.P. (1976). Tuber characteristics and practices affecting the resistance of potato tubers to mechanical damage. Agroplantae 8(2):41-45.

Corsini, D., Stark, J. and Pavek, J. (1988). The asssociation of tuber protein with blackspot resistance. Am. Potato J 65(8):475.

Corsini, D.L., Pavek, J.J. and Dean, B. (1992). Differences in free and protein-bound tyrosine among potato genotypes and the relationship to internal blackspot resistance. Am Potato J 69(7):423-435.

Coxon, D.T., Jones, P.G. (1981). A rapid screening method for the estimation of total glycolalkaloids in potato tubers. J Sci Food Agric 32:366-370.

Cutter, E.G. (1977). Structure and development of the potato plant Chapt . 3 in The Potato Crop (P.M. Harris ed). Chapman and Hall, :London, 70-152.

Dean, B. and Kolattukudy, P.E. (1977). Biochemistry of suberisation. Plant Physiol 59:48-54.

Dean, B.B., Jackowiak, N., Nagle, M., Pavek, J. and Corsini, D. (1993). Blackspot pigment development of resistant and susceptible *Solanum tuberosum* L., genotypes at harvest and during storage measured by three methods of evaluation. Am Potato J 70(3):201-217.

Dixon, W.J. ed. (1992). BMDP statistical software manual. University of California Press.

Duncan, H.J. (1973). Rapid bruise development in potatoes with oxygen under pressure. Potato Res 16(4): 306-310.

Dwelle, R.B. and Stallknecht, G.F. (1976). Rates of internal blackspot bruise development in potato tubers under conditions of elevated temperatures and gas pressures. Am Potato J 53:235-245.

Dwelle, R.B. *et al.* (1977). Effects of soil potash treatent and storage temperature on blackspot bruise development in tubers of four *Solanum tuberosum* cultivars. Am Potato J 54(4):137-146.

Finney. D.J. (1975). An introduction to statistical science in agriculture. Blackwell Scientific Pubns. Oxford.

Finney, E.E., Hall, C.W. and Mase, G.E. (1964a). Theory of linear viscoelasticity to damage of potatoes. Potato Res 17:261-270.

Finney, E.E., Hall, C.W. and Thompson, N.R. (1964b). Influence of variety and time upon the resistance of potatoes to mechanical damage. Am Potato J 41:178-186.

Fortunati, E. and Bianchi, V. (1990). Plasma membrane damage detected by nucleic acid leakage. Molec Toxicology 2(1):27-38.

Fraser, S., Land, D. and Sturrock, R.D. (1987). Microwave thermography-an index of inflammatory joint disease. British J. of Rheumatology 26:37-39.

Fukushima, E. and Roeder, B.W. (1981). Experimental pulse NMR: a nuts and bolts approach. Reading, MA: Addition-Wesley Publ. Co.

Gall,H., Lamprecht,P., and Fechter, E. (1967). First results with the rebound pendulum in assessing the susceptibility of potato tubers to damage. Eur Potato J 10:272-285.

Glasbey, C.A. and McRae, D.C. (1991). Analysis of riddle size, numerical distribution, weight, dimensions and derived surface areas of ten potato cultivars. Confidential Report. Scottish Centre of Agricultural Engineering.

Gubb, I., Callow, J.A., Faulks, R.M. and Jackson, M.T. (1989). The biochemical basis for the lack of enzymatic browning in the wild potato species *Solanum hjertingii* Hawkes. Abstract. Am Potato J 66:522.

Gunasekaran, S., Paulsen, M.R., and Shove, G.C. (1985). Optical methods for non destructive quality evaluation of agricultural and biological materials. J Agric Engng Res 32: 109-241.

Hahn, F., Muir, A.Y. (1993). Discriminant analysis of Brassicas and weeds. Dept Note 59, Scott Centre Agric Engng, Penicuik.

Hammerstrom, D. (1993). Working with neural networks. IEEE Spectrum 46:53.

Hartmans, K.J., and van Es, A. (1974). Investigations into the underlying causes of susceptibility to internal blackspot in potatoes. I. Microscopic investigation into the nature of the damage to tuber tissue during bruising using scanning electron microscopy. Publ NO. 272; 19pp. Institut voor Bewaring en Verwerking van Landbouw producten, Wageningen.

Hecht, E. (1989). Optics. Addison-Wesley Publishing Company, Inc. USA.

Hemmat, A. (1987). Stress/strain analysis and internal bruising in potato tubers. PhD Thesis. Silsoe College.

Hesen, J.C., and Kroesbergen, E. (1960). Mechanical damage to potatoes I. Eur Potato J 3:30-46.

Hoff, J.E. (1971). Potato protein crystals. Hort Sci 6:90.

Holland, H.L. and Taylor, G.J. (1979). Transformations of steroids and the steroidal alkaloid solanine by *Phytophthora infestans.* Phytochemistry 18:437-40.

Horne, A.S. (1913). Contributions from the Wisely laboratory XVI. Bruise in potatoes. J Roy Hort Soc 38:40-50.

Horowitz, N.H and Shen, S.C. (1952). Neurospora tyrosinase. J Biol Chem 197:513-522.

Howard, F.D., Yamaguchi, M. and Knott, J.E. (1962). Carbon dioxide as a factor in the susceptibility of potatoes (*Solanum tuberosum* L.) to blackspot from bruising, Proc. 16th Int Hort Congr 584-90.

Hudson, D.E. (1975). The relationship of cell size, intracellular space and specific gravity to bruise depth in potatoes. Am Potato J 52:9-14.

Hughes, J.C. (1974). Factors influencing the quality of ware potatoes. 2. Environmental factors. Potato Res 17:512-547.

Hughes, J.C. (1980a). Potatoes: I. Factors affecting susceptibility to damage. Span 23:65-67.

Hughes, J.C. (1980b). Role of tuber properties in determining susceptibility of potatoes to damage. Ann appl Biol 96:344-345.

Hughes, J.C. (1981). Special report No. 5: Mechanical damage in potatoes. AFRC Food Research Institute, Norwich, Biennial Report 1979 & 1980.

Hughes, J.C. and Grant, A. (1985). The relationship between physical properties of tubers measured during pendulum impact tests and tuber fracture damage. Potato Res 28:203-221.

Hughes, J.C., Grant, A. and Faulks, R.M. (1975). Susceptibility of tubers to internal damage (blackspot). Potato Res 18:338.

Hunter, J.H. and Reeves, A.F. (1983). Respiration increase as an objective measurement of relative susceptibility to bruise damage in breeding clones. Am Potato J 60(10):811.

Ilker, R., Spurr, A.R. and Timm, H. (1977). Ethylene pretreatment and blackspot of potato tuber, *Solanum tuberosum*; histochemistry and histology of wound healing. Z Planzenphysiol Bd 83 (5):55-68.

Iritani, W.M. and Weller, L.D. (1985). Enhancement of blackspot development by the hot water soak method. Washington Potato Conf Proc 1-6.

Isherwood, F.A. (1973). Starch-sugar interconversion in *Solanum tuberosum*. Phytochemistry 12:2579-2591.

Jacob, W.C. (1959). Studies on internal blackspot in potatoes. Mem Cornell Univ Agric Exp Sta 368.

James, M. (1985). Classification algorithms. Collins, Great Britain.

Javanaud, C. (1988). Applications of ultrasound to food systems. Ultrasonics 26:117-123.

Jefferies, R.A., Heilbronn, T.D. and McKerron, D.K.L. (1989). Estimating dry matter concentration from accumulated thermal time and soil moisture. Potato Res 32:411-417.

Johnson, E.F. and Wilson, J.B. (1969). The effect of soil temperature at harvest on the bruise resistance of potatoes. Am. Potato J 46:75-81.

Johnson, G. and Shaal, LA (1957). Accumulation of phenolic substances and ascorbic acid in potato tuber tissue upon injury and their possible role in disease resistance. Am Potato J 34:200-209.

Kahl, G. (1974). Metabolism in plant storage tissue slices. Bot Rev 40:263-314.

Keijbets, M.J.H. and Pilnik, W. (1973). Some problems in the analysis of pectin in potato tuber tissue. Potato Res 17:169-177.

Kida, Y., Honda, N., Uchida, M., Kunisada, Y. and Fukuda, M. (1991). Changes in ascorbic acid content and several enzyme activities concerning synthesis and metabolism of ascorbic acid in potatoes during storage. J Japanese Soc for Food Sci and Tech 38(2):160-165.

Killick, R.J. and Macarthur, A.W. (1980). The relationship between bruising and specific gravity in some potato varieties. Potato Res 23(4):457-461.

Kuczynski, A., De Baerdemaeker, J. and Oszmianski, J. (1994). An optical reflectance method for studying the enymic browning reaction in apple. Int Agrophysics 8: 1-5.

Kunkel, R., Holstad, N. and Butala, H. (1973). Fertilisation and the blackspot proplem in Washingtons Columbia Basin. Am Potato J 50:339.

Kunkel, R. and Gardner, W.H. (1965). Potato tuber hydration and its effects on blackspot of Russet Burbank potatoes in the Columbia Basin. Am Potato J 42:109-124.

Kunkel, R., Gardner, W.H. and Holstad, N.M. (1986). Improvement of techniques for potato blackspot evaluation and some errors associated with measurements. Am Potato J 63:13-23.

Kunkel,R. Weaver, M.L. and Holstad, N.M. (1970). Blackspot of Russet Burbank potatoes and the carbon dioxide content of soil and tubers. Am Potato J 47:105-117.

Labsphere, Inc. (1993). Celebrating 100 years of integrating sphere technology. Lapshere, North Sutton, UK.

Lachenbruch, P. and Mickey, R.M. (1968). Estimation of error rates in discriminant analysis. Technometrics 10:1-11.

Land, D.V., Brown, V.J. and Fraser, S.M. (1991). Clinical testing of combined thermal and microwave radiometric tissue modelling. J Photographic Sci 39:166-169.

Lerner, A.B. and Fitzpatrick, T.B. (1950). Biochemistry of melanin formation. Physiol Rev 30:91-126.

Lesham, Y.Y. (1987). Membrane phosphoplipid catabolism and calcium activity in control of senescence. Physiologia Plantarum 69:551-559.

Lewosz, J. and Lojkowska, E. (1985). Relationship between electrolytes release from potato tuber caused by wounding or by the enzymes of *Erwinia carotovara* ssp. *atroseptica* and susceptibility to microbial decay and mechanical damage. Ziamniak. 25-47. Bonin, Poland; Instytut Ziemnik.

Li, P.H. (1985). Potato physiology. Academic Press Inc. Orlando, Florida.

Lojkowska, E. (1988). Lipid composition and post wounding degradation in potato slices from cultivars differing in susceptibility to autolysis. Potato Res 31:541-549.

Love, S., Thompson-Johns, A., Werner, B.K. and Baker, T.P. (1994). RBM134: a mutant of Russet Burbank susceptible to blackspot bruise. Am Potato J 71(6):411-416.

Lulai. E.C., Sowokinos, J.R. and Knoper, J.A. (1986). Translucent tissue defects in *Solanum tuberosum* L. II. Alterations in lipolytic acyl hydolase, lipoxygenase, and morphology of mitochondria and chloroplasts. Plant Physiol 80:424-428.

Maas, E.F. (1966). A simplified potato bruising device. Am. Potato J. 43: 424-426.

Mapson, L.W., Swain, T., Tomalin, A.W. (1963) Influence of variety, cultural conditions and temperature of storage on enzyme browning of potato tubers. J Sci Food Agric 14: 673-684.

Martin, M.L., Delpuech, J.J. and Martin, G.J. (1980). Practical NMR spectroscopy. London: Heyden & Son Ltd.

Mason, H.S. (1948). The chemistry of melanin III. Mechanism of the oxidation of dihydroxyphenylalanine by tyrosinase. J. Biol Chem 172:83-99.

Mason, H.S. (1967). The structure of melanin. Advan Biol Skin 8:293-312.

McGuire, R.G. and Kelman, A. (1986). Calcium in potato tuber cell walls in relation to tissue maceration by *Erwinia carotovora* pv. *atroseptivca*. Phytopathology. 76(4):401-406.

McIlroy, D.C. (1976). Biochemical and physical aspects of bruising in potatoes. PhD dissertation. London University.

McIlroy, D.C. (1980). Electron microscope studies of bruised and unbruised potato tuber tissue. Ann Appl Biol 96:384.

McRae, D.C., Carruthers, J. and Porteous, R.L. (1976). The effect of drop height on damage sustained by some main crop potato varieties. Dept Note SIN/202, Scottish Centre of Agric Engng, Penicuik.

McRae, D.C. and Fleming, J. (1994). Potato damage - where it occurs and how to avoid it. Third Edn. Potato Marketing Board.

Meijers, C.P. and Kleijburg, P. (1973). Determination of the susceptibility of potatoes to internal blackspot, the accuracy of the method and the influence of tuber temperature. Bedrijfsontwikkeling. 4(6):579-584.

Melles Griot (1990). Optics guide 5. Melles Griot Inc., Cambridge, England.

Melrose, H. (1991). Accelerated detection of potato bruises using high humidity, compressed air. Dep. Note 36, Scott. Centre of Agric. Engng, Penicuik.

Melrose, H. and McRae, D.C. (1985). Bruise assessment in potato tubers using tetrazolium chloride. Dep. Note SIN/437, Scott. Centre of Agric. Engng, Penicuik.

Melrose, H. and McRae, D.C. (1987). Rapid development of bruises in potatoes by means of a humidified pressurised oxygen tank. Dep. Note SIN/491, Scott. Centre of Agric. Engng, Penicuik.

Meyer, N.L., Phelps, R.L., Kleinschmidt, G., Beaver, R.G., and DeVoy, M.L. (1985). The economic importance of bruising to Idaho potatoes in transit. Paper Am Soc Agric Eng No. 85-6022.

Mohsenin, N.N. (1984). Electromagnetic radiation properties of foods and agricultural products. Gordon and Breach Science Publishers, NY.

Mondy, N. I. (1983). Effect of isopropyl-N-3-chlorophenyl carbamate (CIPC) on the potato quality. Proc. 6th Int. Congress of Food Sci and Tech 1:115-116.

Mondy, N.I. and Mueller, T.O. (1977). Potato discolouration in relation to anatomy and lipid composition. J Food Sci 42:14.

Mondy, N.I., Mobley, E.O. and Gedde-Dahl, S.B. (1967). Influence of potassium fertilisation on enzymic activity, phenolic content and discolouration of potatoes. J Food Sci 32:378-81.

Morris, S.C. and Lee, T.H. (1984). The toxicity and teratogenicity of Solanaceae glycoalkaloids particularly those of the potato (*Solanum tuberosum*): a review. Food Tech in Aus 36:118-124.

Muir, A.Y., Porteous, R.L. and Wastie, R.I. (1982). Experiments in the detection of incipient diseases in potato tubers by optical methods. J Agric Engng Res. 27(2):131-138.

Mulder, E.G. (1949). Mineral nutrition in relation to the biochemistry and physiology of potatoes 1. Effect of nitrogen, phosphorous, magnesium and copper nutrition on the tyrosinase activity with particular reference to blackening of the tubers. Plant and Soil 2:59-121.

Mulder, E.G. (1956). Effect of the mineral nutrition of potato plants on the biochemistry and physiology of the tubers. Neth. J. Agric. Sci. 4: 333-356.

Muneta, P. (1977). Enzymatic blackening in potatoes; influence of pH on dopachrome oxidation. Am Potato J 54:387-392.

Murfitt, R.F.A. and Obobi, A.A. (1980). Delayed bruises development in potato tubers. Ann appl Biol 96:341-387.

Neuraldesk user's guide (1992) Neural Computer Sciences.

Nicolaus, R.A. and Piattelli, M. (1965). Progress of natural black pigments. Ren Accad Sci Fis Mat 32(3):83-97.

Nilsson, S.B., Hertz, C.B. and Falk, S. (1958). On the relation between turgor and tissue rigidity. II. Theoretical calculations on model systems. Physiologica Pl. 11:818-837.

Noble, R. (1984). The development of internal bruising in potato tubers following mechanical injury. PhD. thesis, Cranfield Institute of Technology, Silsoe College.

Noble, R. (1985). Prediction of susceptibility of potato tubers to internal bruising by using a pendulum mounted accelerometer. Potato Res 28:285-294.

O'Haver, T.C. (1979). Potential clinical applications of derivative and wavelength modulation spectrometry. Clinical Chem 25(9):1548-1553.

Obeid, A.N., Boggett, D.M., Barnett, N.J., Dougherty, G. (1988). Depth discrimination in laser Doppler skin blood flow measurements using different lasers. Med & Biol Eng & Comput 26:415-419.

Ohad, I., Friedberg, I., Ne'eman, Z.,Schramm, M. (1971). Biogenesis and degradation of starch I. The fate of the amyloplast membrane during maturation and storage of potato tubers. Plant Physiol 47:465-477.

Olsson, K. (1986) The influence of genotype on the effects of impact damage on the accumulation of glycoalkaloids in potato tubers. Potato Res 29(1):1-12.

Ophuis, B.G., Hesen, J.C. and Kroesbergen, E. (1958) The influence of the temperature during handling on the occurence of blue discolourations inside potato tubers. Eur Potato J 1:48-65.

Oriel Corporation, USA (1994). Oriel product guide. Volume 2: Light sources, monochromators and spectrographs, detectors and detection systems, fibre optics.

Pavek, J., Corsini, D. and Nissley, F. (1985). A rapid method for determining blackspot susceptibility of potato clones. Am Potato J 62:511-517.

Pavek, J., J., Brown, C.R., Martin, M.W. and Corsini, D.L. (1989). Inheritance of resistance to blackspot in potato. Abstract. Am Potato J 66:539.

Pena-Cortes, H., Sanchez-Serrano, J.J., Mertens, R., Willmitzer, L., Prat, S. (1989). Abscisic acid is involved in the wound-induced expression of the proteinase inhibitor II gene in potato and tomato. Proc Natl Acad Sci USA.

Perombelon, M.C.M. and Kelman, A. (1980). Ecology of the soft rot Erwinias. Ann Rev Phytopathology 18:361-387.

Peterson, C.L. and Hall, C.W. (1975). Dynamic mechanical properties of the Russet Burbank potato as related to temperature and bruise susceptibility. Am Potato J 52:289-311.

Peterson, C.L., Hall, C.W. (1974). Thermorheological simple theory applied to the Russet Burbank potato. Trans. Am. Soc. Agric. Eng. 546-556.

Pisarcyzck, J.M. (1982). Field harvest damage affects potato tuber respiration and sugar content. Am Potato J 59:205-211.

Pitt, R.E., Davis, D.C. (1984). Finite element analysis of fluid-filled cell reponse to external loading. Trans. Am. Soc. Agric. Eng. 27(6): 1976-1983.

Poovaiah, B.W. and Reddy, A.S.N. (1987). Calcium messenger system in plants. Critical reviews in plant sciences. 6(1):47-103.

Porteous, R.L., Muir, A.Y. and Wastie, R.I. (1981). The identification of diseases and defects in potato tubers from measurements of optical spectral reflectance. J Agric Engng Res 6(2):104-111.

Potato Producers Association (1994). Research priorities. 6 Catherine St., London, UK.

Pratt, H.K. and Goeschl, J.D. (1969). Phyiological roles of ethylene in plants. Ann Rev Plant Physiol 20:541-584.

Pratt, M.A. (1980). Definition of damage terms. Ann appl Biol 96:341-387.

Racusen, D. (1984). Lipid acyl hydrolase of patatin. Can J Bot 62:1640-1644.

Raven, P.H., Evert, R.F. and Curtis, H. (1981). Biology of plants. 3rd Edn. Worth Publishers, Inc., USA.

Rees Intruments Ltd. (1992). Monolight application note number 1. Godalming, Surrey, UK.

Reeve, R.M. (1968). Preliminary histological observation on internal blackspot in potatoes. Am Potato J 45:157-167.

Reeve, R.M., Hautala, E. and Weaver, M.L. (1969a). Anatomy and compositional variation within potatoes I. Developmental histology of the tuber. Am Potato J 46:361-373.

Reeve, R.M., Hautala, E., Weaver, M.L. (1969b). Anatomy and compositional variation within potatoes II. Phenolics, enzymes and other minor components. Am. Potato J. 46: 374-386.

Reid, M.S. and Pratt, H.K. (1972). Effects of ethylene on potato tuber respiration. Plant Physiology J 39:116-121.

Reid, W.S. (1976). Optical detection of apple skin, bruise, flesh, stem and calyx. J Agric Engng Res 21(3):291-296.

Richardson, M. (1977). The proteinase inhibitors of plants and micro-organisms. Phytochem. 16:159-169.

Rickey, T.M., Snyder, G.W. and Belknap, W.R. (1989). Changes in the steady-state transcript levels of potato tubers in response to impact injury and exogenous ethylene treatment. Plant. Physiol 89(4):61.

Rogers-Lewis, D.S. (1980). Methods of reducing damage in maincrop potatoes. Ann appl Biol 96:345-349.

Rogers-Lewis, D.S. and Jarvis, R.H. (1977) Comparison of two methods of assessing internal bruising in potatoes. Exp Husbandry 32:65-67.??

Roztropowicz, S. and Czernik, L. (1985). The ranking of potato varieties on the basis of resistance of tubers to mechanical damage (determined by the laboratory sorter method) as related to the number of peridermal cell layers. Biuletyn Instytutu Ziemniaka 33:35-38.

Sanchez-Serrano, J.J., Amati, S., Kell, M., Pena-Cortes, H. and Prat, S. (1990). Promoter elements and hormonal regulation of poiternase inhibitor II gene expression in potato. In: The Molecular and Cellular Biology of the Potato (Vayda, M.E., Park, W.D.J. eds). Biotechnology in Agriculture No. 3. Wallingford, U.K.; C.A.B. International.

Sanchez-Serrano, J.J., Keil, M., O'Connor, A., Schell, J. and Willmitzer, L. (1987). Wound-induced expression of a potato proteinase inhibitor II gene in transgenic tobacco plants. EMBO J 6:303-306.

Sarkar, N. and Wolfe, R.R. (1983). Potential of ultrasonic measurements in food quality evaluation. Trans Am Soc Agric Eng 26:624-629.

Schalkoff, R.J. (1984). Pattern recognition: statistical, structural and neural approaches. John Wiley and Sons, Inc., New York.

Schippers, P.A. (1968). The influence of rates of nitrogen and potassium application on the yield and specific gravity of four potato varieties. Eur Potato J 11:23-33.

Shekhar, V.C., Iritani, W.M. and Magnuson, J. (1978). Starch-sugar interconverion in *Solanum tuberosum* L. II. Influence of membrane permeability and fluidity. Am Potato J 55:663-670.

Sherif, S.M., Segerlind, L.J. (1977). Contact stresses in a spherical body composed of a nearly incompressible material. Trans. Am. Soc. Agric. Eng. 76.

Shortley, G. and Williams, D. (1971). Elements of physics. Eaglewood Cliffs, New Jersey: Prentice Hall, Inc.

Shotton, F.E. (1978). Effect of level of potassium fertiliser on internal bruising of potato tubers. Potato Marketing Board Potato Physiology Meeting. March 14.

Sinden, S.L., Deahl, K.L. and Aulenbach, B. (1974). Glycoalkaloids as a component of potato flavour. Am. Potato J 51:298.

Singleton, V.L. (1972). Common plant phenols other than anthocyanins, contributions to colouration and discolouration. In the Chemistry of Plant Pigments ed Chichester, C.O. Publ. Acadamic Press, New York, 143-192.

Skrobacki, A., Halderson, J.L., Pavek, J.J. and Corsini, D.L. (1989). Determining potato tuber resistance to impact damage. Am Potato J 66:401-415.

Sokal, R.R. and Rohlf, F.J. (1981). Biometry: the principles of statistics in biological research. W.H. Freeman and Co. N.Y.

Solomos, T. and Laties, G.G. (1975). Mechanism of ethylene and cyanide action in triggering the rise in respiration in potato tubers. Plant Physiol 55:73-78.

Sommewald, U., Sturm, A., Chrispeels, M. and Wilmitzer, L. (1989). Targeting and glycosylation of patatin, the major potato tuber protein in leaves of transgenic tobacco. Planta 179:171-180.

Sowokinos, J.R., Orr, P.H., Knoper, J.A., and Varns, J.L. (1987). Influence of potato storage and handling stress on sugars, chip quality and integrity of the starch (amyloplast) membrane. Am Potato J 64:213-226.

Specht, A. (1981). Beschädigungen an der kartoffel vermeiden (potato damage at harvest time). Auswertungs und Informationsdienst für Ernährung, Landwirtschaft und Forsten (AID) e.V., Konstantinstr. 123, 53179 Bonn Edition 78.

Stark, B.K., Corsini, D.L., Hurley, P.J. and Dwelle, R.B. (1985). Biochemical characteristics of potato clones differing in blackspot susceptibility. Am Potato J 62:657-666.

Straeten, D.V.D., Sharkov, G., and Montagu, M.V. (1994). Fever in plants: thermogenic responce of tobacco to exogenous salicylate. Organ of the European Association of Thermology 4(1):10-17.

Swiniarski, E. and Ladenberger, D. (1970). The sugar content of pototo tubers grown in different rates of nitrogen application. Potato Res 13:114-118.

Tabachuk, V.I. (1953) An investigation into the susceptibility of the potato tuber to damage on impact. Leningradskii selkhoz Inst Zap 7:90-99. NIAE Translation 130.

Talburt, W.F., Schwimmer, S. and Burr, H.K. (1975). Structure and chemical composition of the potato tuber. In W.F. Talburt and O. Smith (eds) pp 11-42.

Thomas, M. (1955). Melanins. In: Modern methods of plant analysis. Vol 4 Tracey, M.V. ed, Peach, K. Publ Springer Verlag. Berlin. 661-676.

Thornton, R. (1979). Potato tuber condition and the harvester operation. Chipper Snacker. Nov. 41-42.

Thornton, R.E. and Timm, H. (1990). Influence of fertiliser and irrigation management on tuber bruising. Am Potato J 67:45-54.

Thornton, M.K., Workman, M. (1987). Changes in ascorbic acid content of blackspot resistant and susceptible potatoes following bruising. Hortsci 2(3):455-456.

Timm, H. (1989). Reducing blackspot bruise under high temperature and dry soil conditions. Proc. Univ of Idaho winter commodity schools. 21:215-218.

Timm, H., Yamaguchi, M., Highes, D.L. and Weaver, M.L. (1976). Influence of ethylene on blackspot of potato. Am Potato J 53:49-56

Vertregt, N. (1968). Relation between blackspot and composition of the potato tuber. Eur Potato J 11:34-44.

Voeste, D. (1990). Further investigations into maximum normal strain and internal bruising of potato tubers. PhD thesis. Silsoe College.

Volbracht, O. and Kuhnke, V. (1956). Mechanical damage to potatoes. Der Kartoffelbau 4:74-77.

Voogd, C.D. (1963). De invloed van bodem em bemesting op de chemische semenstelling van de aardappelknol. Literatuuroverzicht van het IBVL, Wageningen, pp. 10.

Wardale, D.A. and Galliard, T. (1977). Further studies on the subcellular lacalisation of lipid-degrading enzymes. Phytochemistry 16:333-338.

Wardell, K., Jakobsson and Nilsson, G.E. (1993). Laser Doppler perfusion imaging by dynamic light scattering. IEEE Trans Biomed Engng 40(4):309-316.

Weaver, M.L., Brown, R.C., Steen, H.A. (1968) The association of copper with tyrosinase activity and internal discolouration (blackspot) in Russet Burbank potatoes. Am Potato J 45:132-138.

Weber, J., Grassert, V., Effmert, B. (1980). Investigation of the relationship between blackspot bruise and tissue characters of the potato tuber. Potato Res 23(3):311-317.

White, R.P., Munro, D.C. and Sanderson, J.B. (1974). Nitrogen, potassium and plant spacing effects on yield, tuber size, specific gravity and tissue nitrogen, phosphorous and potassium in Netted Gem potatoes. Can J Plant Sci 54:535-539.

Wilson, W.D., Jarvis, M.C., Duncan, H.J. (1987). Rapid bruise development using the tetrazolium test. Agricultural Chemistry Department, University of Glasgow.

Woodwards, L and Jackson, M.T. (1985). The lack of enzymic browning in wild potato species Longipedicellota and their crossability with *Solanum tuberosum*. Z Pflanzenzuchtg 94:278-287.

Workman, M. and Holm, D.G. (1984). Potato clone variation in blackspot and soft rot susceptibility, redox potential, ascorbic acid, dry matter and potassium. Am Potato J 61:723-733.

Wu, M.T. and Salunke, D.K. (1976) Changes in glycoalkaloid content following mechanical injuries to potato tubers. J Am Soc Hort Sci 101(3):329-331.

Wu, M.T. and Salunke, D.K. (1978). Difference in light and wound induced biosynthesis of α-solanine and α-chaconine in potato tubers. Biologia Plantarum 20:149-151.

Yamaguchi, M, Timm H. and Spurr, AR (1964) Effects of soil temperature on growth and nutrition of potato plants and tuberisation, composition and periderm structure of tubers. Proc Am Soc Hort Sci 84:412-423.

Zhang, F., Britton, M.G., Townsend, J.S. (1989). Potato bruise prediction by finite element method. Paper, Am. Soc. Agric. Eng. No. 89-6056.